

N O T I C E

THIS DOCUMENT HAS BEEN REPRODUCED FROM
MICROFICHE. ALTHOUGH IT IS RECOGNIZED THAT
CERTAIN PORTIONS ARE ILLEGIBLE, IT IS BEING RELEASED
IN THE INTEREST OF MAKING AVAILABLE AS MUCH
INFORMATION AS POSSIBLE

(NASA-CR-159771) ADVANCED PROPULSION SYSTEM
FOR HYBRID VEHICLES Final Report
(AiResearch Mfg. Co., Torrance, Calif.)
213 p HC A10/MF A01 CSCL 13F

N80-26212

Unclas
63/85 23513

DOE/NASA/0091-80/1
NASA CR-159771
AIRESEARCH 79-16430

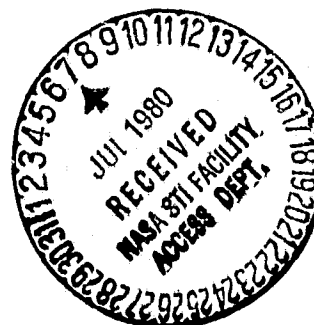
ADVANCED PROPULSION SYSTEM FOR HYBRID VEHICLES

L. V. Norrup and A. T. Lintz
AiResearch Manufacturing Company of California
The Garrett Corporation

January 1980

Prepared for
NATIONAL AERONAUTICS AND SPACE ADMINISTRATION
Lewis Research Center
Cleveland, Ohio 44135

for
U.S. DEPARTMENT OF ENERGY
Conservation and Solar Applications
Office of Transportation Programs



NOTICE

This report was prepared to document work sponsored by the United States Government. Neither the United States nor its agent, the United States Department of Energy, nor any Federal employees, nor any of their contractors, subcontractors or their employees, makes any warranty, express or implied, or assumes any legal liability or responsibility for the accuracy, completeness, or usefulness of any information, apparatus, product or process disclosed, or represents that its use would not infringe privately owned rights.

DOE/NASA/0091-80/1
NASA CR-159771
AIRESEARCH 79-16430

**ADVANCED PROPULSION SYSTEM
FOR HYBRID VEHICLES**

L.V. Norrup and A.T. Lintz
AiResearch Manufacturing Company of California
The Garrett Corporation
Torrance, California 90509

January 1980

Prepared for
National Aeronautics and Space Administration
Lewis Research Center
Cleveland, Ohio 44135
Under Contract DEN 3-91

for
U.S. DEPARTMENT OF ENERGY
Conservation and Solar Applications
Office of Transportation Programs
Washington, D.C. 20545
Under Interagency Agreement EC-77-A-31-1044

PREFACE

The Electric and Hybrid Vehicle Research, Development, and Demonstration Act of 1976 (Public Law 94-413) authorized a Federal program of research and development designed to promote electric and hybrid vehicle technologies. The Department of Energy (DOE), which has the responsibility for implementing the act, established the Electric and Hybrid Vehicle Research, Development, and Demonstration Program within the Office of Transportation Programs to manage the activities required by Public Law 94-413.

The National Aeronautics and Space Administration (NASA) was authorized under an interagency agreement (Number EC-77-A-31-1044) with DOE to undertake research and development of propulsion systems for electric and hybrid vehicles. The Lewis Research Center was made the responsible NASA center for this project. The study presented in this report is an early part of the Lewis Research Center program for propulsion system research and development for hybrid vehicles.

ORIGINAL PAGE IS
OF POOR QUALITY

III PRECEDING PAGE BLANK NOT FILMED

TABLE OF CONTENTS

	<u>Page</u>
SUMMARY	1
INTRCDUCTION	3
Background	3
Program Objectives	3
Program Tasks	3
PART A: TASK I, PARAMETRIC STUDIES	
CONCEPTS FOR TASK I PARAMETRIC STUDIES	7
STUDY GOALS, REQUIREMENTS, GROUND RULES, AND DEFINITIONS	12
Design Goals	12
Design Requirements	12
Study Ground Rules	15
Study Definitions	24
TASK I ANALYTICAL METHODOLOGY	25
Discussion of Propulsion System Concepts	25
Task I Scope and Format of the Results	26
Task I Parametric Study Modeling Procedures	26
Review of Propulsion System Concepts	29
Analytical Modeling	31
Hardware Performance Maps	56
Cost and Weight Analysis Procedures	72
TASK I ANALYTICAL RESULTS	79
Task I Hybrid Propulsion System Parametric Results	79
Task I Flywheel MES/Heat Engine Parametric Results	85
Task I Heat Engine Comparison	85

TASK I RECOMMENDATIONS	92
PART B: TASK II, DESIGN TRADEOFF STUDIES	
TASK II DESIGN TRADEOFF STUDY METHODOLOGY	93
Revised Vehicle Characteristics	93
Revised System Concept Definition	94
Power and Energy Management Tradeoffs	96
Scope of Task II Analysis	101
COST AND PERFORMANCE TRADEOFFS	103
Prime Electric Range and Fuel Economy	103
Annual Fuel Usage	105
Life-Cycle Cost	107
Fuel Usage and Cost Comparison	107
Cost Benefit Comparisons	110
COST OPTIMIZATION TRADEOFFS	112
Cost Benefit Comparison	112
Final System Performance	112
PERFORMANCE SENSITIVITY STUDIES	122
Electric Motor Sensitivity	122
Heat Engine Sensitivity	123
Fuel and Electricity Cost Sensitivity	127
Test Cycle Sensitivity	128
Performance Goal Sensitivity	128
PART C: TASK III, CONCEPTUAL DESIGN	
TASK III CONCEPTUAL DESIGN ACTIVITY	137
DESCRIPTION OF CONCEPTUAL DESIGN	138
WEIGHT AND COST SUMMARY	150

SYSTEM OPERATION AND CONTROL	152
Starting Sequence	152
Acceleration	152
Steady-state Operation	153
Coasting	155
Deceleration and Braking	155
EFFECTS OF HEAT ENGINE OPERATING MODES	156
Cold Operation	156
Engine wear	156
Cold-Engine Sludge	158
Operating Tests	159
PART D: DISCUSSION OF RESULTS AND RECOMMENDATIONS	
DISCUSSION OF RESULTS	163
CONCLUSIONS AND RECOMMENDATIONS	165
REFERENCES	167
BIBLIOGRAPHY	169
APPENDIX A: TASK I PARAMETRIC STUDY RESULTS	A-1
APPENDIX B: WORK PLAN	B-1

SUMMARY

The objective of this study was to evaluate a number of hybrid propulsion systems for application in several different mission/vehicle types. The program was divided into three major tasks during which the various system configurations were parametrically evaluated and compared, design tradeoffs performed, and a conceptual design produced.

The objectives of Task I were to examine and compare five propulsion system concepts in five different types of vehicle, weigh their relative merits, and recommend two propulsion configurations for a more detailed design tradeoff evaluation. The propulsion systems studied included heat engine/battery hybrids, heat engine/battery/flywheel hybrids, and a pure heat engine/flywheel system. The mission/vehicle types studied were a 2-passenger commuter car, 4-passenger local sedan, 6-passenger intercity sedan, 8-passenger van, and a 50-passenger city bus.

Each vehicle/propulsion system concept was analyzed using common ground rules and analytical procedures so that relative comparisons could be made. These Task I comparisons led to the selection of two candidate propulsion system concepts for further detail study. A five-passenger family sedan was also selected as the recommended vehicle.

In Task II, design tradeoffs were made on the two candidate propulsion systems to find the optimum component characteristics for meeting all performance goals. Comparisons were made in terms of fuel usage, electric range, and acquisition and life-cycle costs. The most cost effective system was chosen and optimized to further reduce costs and fuel usage.

The final propulsion system selected to be conceptually designed in Task III had the following principal features: spark ignition gasoline engine (65 kW), brushless dc permanent-magnet motor (20 kW), variable frequency inverter (40 kW), continuously variable traction transmission, ISOA lead-acid battery pack (386 kg), and a transaxle.

The final propulsion system was sized to meet all the performance goals established in the study for the five-passenger sedan, including acceleration from 0 to 90 km/hr in 12 s and sustained 90 km/hr climb on a four-percent grade. This propulsion system features two automatic operational modes, i.e., an electric mode and a heat engine mode. Mode determination is based on the state-of-charge of the battery. In the electric mode the battery is load-levelled by the heat engine during periods of high power demand such as those which occur when the vehicle is accelerating. During periods of low power demand, such as those encountered during steady-state operation, the battery supplies all the power. In the heat engine mode the roles are reversed; i.e., the heat engine is load-levelled by the battery during high power demand periods and supplies all the power during steady-state operation. In both modes, regenerative braking energy is absorbed by the battery.

The performance, cost, and design features of the final propulsion system are summarized as follows:

Vehicle test weight, kg	2032
Battery weight, kg	386
Propulsion system weight, kg	414
Maximum acceleration, 0 to 90 km/hr, s	12
Maximum speed, km/hr	105
Prime electric range, km	218
Battery usage, percent depth of discharge	80
Fuel usage, km/liter	30
Extended range (engine mode)	limited by fuel capacity
Fuel usage on special test cycle, km/liter	14
Fuel usage at constant 90 km/hr, km/liter	18
Propulsion system life-cycle cost, \$/km	0.054
Propulsion system acquisition cost, \$	3214
Annual fuel usage, liter	590

INTRODUCTION

The program described in this report was initiated to identify and evaluate advanced hybrid propulsion systems for a spectrum of mission vehicles. Hybrid vehicles are of interest because their use will reduce petroleum consumption. Today about half of the petroleum consumed in the United States is used for transportation. The introduction of hybrid vehicles could significantly shift the transportation energy base to other sources such as coal, nuclear, and solar.

Background

In 1976 the Electric and Hybrid Vehicle Program was established within the Energy Research and Development Administration (ERDA), now the Department of Energy (DOE). In September Congress passed the Electric and Hybrid Vehicle Research, Development, and Demonstration Act of 1976 (Public Law 94-413). This act is intended to accelerate the integration of electric and hybrid vehicles into the nation's transportation system and to stimulate growth in the electric and hybrid vehicle industry.

Program Objectives

There are two overall program objectives:

- Determine vehicle type/propulsion arrangement/propulsion components that minimize the nation's use of liquid petroleum.
- Design the selected propulsion system/vehicle in such a way that when compared with its equivalent conventional counterpart, the hybrid system has:
 - (a) Competitive acquisition cost
 - (b) Lower life-cycle cost (10 years)

All propulsion system design concepts were based on propulsion components that could be developed by 1983.

Program Tasks

The program effort is discussed in this report in terms of the three principal tasks:

- Task 1--Parametrical investigation of 15 vehicle type/hybrid propulsion system concepts in terms of acquisition and life-cycle costs, electric ranges, and petroleum usage. Included in this investigation were two battery types and three heat engine types. This work resulted in the recommendation of two propulsion systems and one mission/vehicle designation for further study and definition.

- Task II--Performance of design tradeoff studies of the two candidate systems on the basis of cost and fuel savings to select the one that is most cost effective. Included in the system selection was the battery type. The selected system was optimized to maximize its cost benefit to the consumer.
- Task III--Preparation of a conceptual design of the selected system, documenting weight, performance, design features, method of operation, and acquisition and life-cycle costs.

Task I, parametric studies.--Five mission/vehicle designations were included in the parametric investigations:

- Two-passenger commuting
- Four-passenger family use (local)
- Six-passenger family use (intercity)
- Eight-passenger van (variable route)
- Fifty-passenger city bus (variable route)

Three different basic propulsion system types were combined with the identified vehicles to form the Task I study matrix. The propulsion system types that were evaluated are:

- Hybrid
- Hybrid with mechanical energy storage (MES)
- Mechanical energy storage/heat engine only

All the hybrid and hybrid-with-MES propulsion concepts were evaluated using an improved state-of-the-art (ISOA) lead-acid battery and an advanced nickel-zinc battery. The basic heat engine for the study was a spark-ignition gasoline type. It was used with all systems. In addition, a naturally aspirated diesel engine and an advanced gas turbine engine were substituted into selected vehicle/propulsion system arrangements for comparison with the basic engine. The flywheel MES/heat engine propulsion system concepts were treated independently of the other two propulsion system types. This special type system was evaluated in the heavier vehicles of the study (the intercity sedan, van, and bus) to parametrically determine wall-plug (electric) range vs flywheel storage capacity.

The effect of power sharing between the battery and flywheel MES (i.e., load-leveling the battery) was examined as part of the parametric work to determine its impact on propulsion system costs and energy efficiency.

Each vehicle/propulsion system concept was designed to meet the specified performance goals that were established for the individual vehicles as part of the contract. In addition to maintaining constant vehicular performance, a structural growth factor of 1.3:1 was used to determine each new vehicle test weight as a function of parametric changes in the propulsion systems. The vehicle/propulsion system concepts were evaluated over a modified SAE 227a schedule D cycle to determine their electric ranges, fuel usage, and life cycle costs.

Task II, design tradeoff studies.--Design tradeoff studies were performed on the two candidate propulsion systems that were selected from the Task I study. One system was a pure hybrid type and the other was a hybrid with fly-wheel MES type. Both systems have parallel power paths between the heat engine and battery. The mission/vehicle was designated as a five-passenger family sedan with performance requirements that are in line with currently available automobiles.

The systems were evaluated using both lead-acid and nickel-zinc batteries. Power sharing between the heat engine and battery was introduced into the study.

The tradeoffs were performed by varying battery weight, power sharing split, and heat engine size. The systems were ranked in terms of a cost benefit definition that was developed for the study. A single system (including battery type) was selected to be optimized.

Information was generated in terms of electric range, annual fuel usage, and acquisition and life-cycle costs. Electric range and fuel usage were also predicted using the federal urban and highway driving cycles for the optimized system.

Sensitivity studies were performed on the optimized system to determine the effects of engine operation (on-off or continuous), engine type (spark-ignition or diesel), petroleum costs (gasoline and diesel), and electricity costs. In addition, a cursory investigation was made on the effects of varying one of the performance goals, such as the 0- to 90-km/hr acceleration time. The effect of changing the basic driving cycle of the study was also examined in terms of costs, electric range, and annual petroleum usage.

Task III, conceptual design.--The propulsion components for the optimized system were geometrically defined, their performance was specified, and conceptual design drawings were made that included an installation drawing. A method of operation was prepared that included a definition of the power and energy management schedule. A summary of the propulsion system costs, weights, and performance data is a part of the design description.

This document also presents a discussion of the effects of on-off operation on the durability of a spark-ignition heat engine.

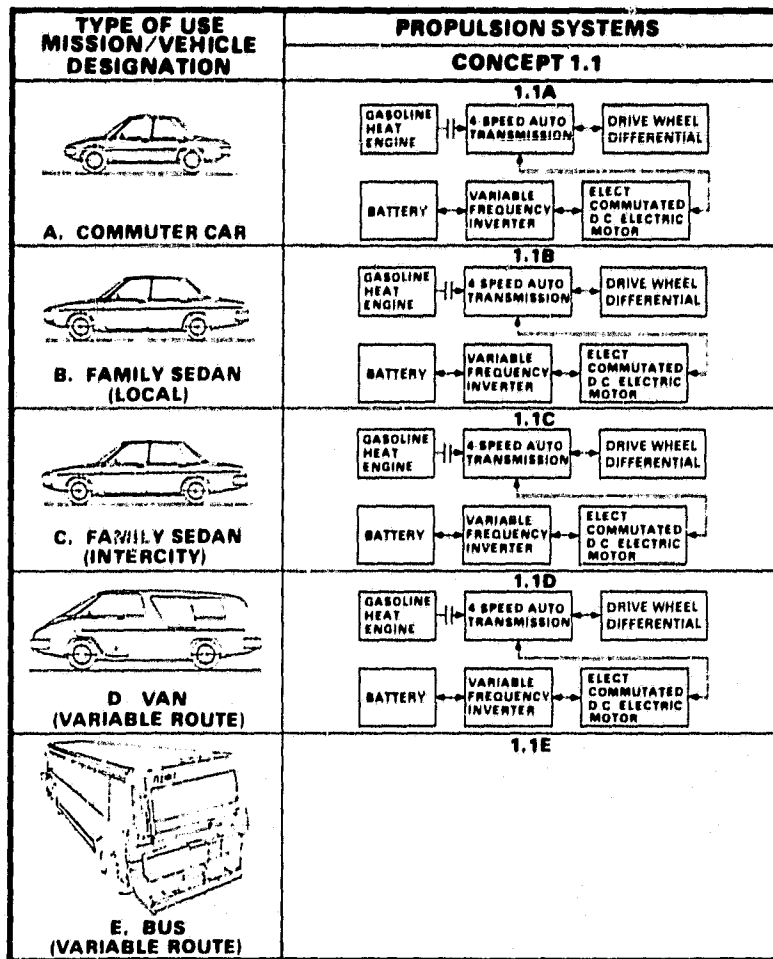
PART A
TASK I, PARAMETRIC STUDIES

PRECEDING PAGE BLANK NOT FILMED

CONCEPTS FOR TASK I PARAMETRIC STUDIES

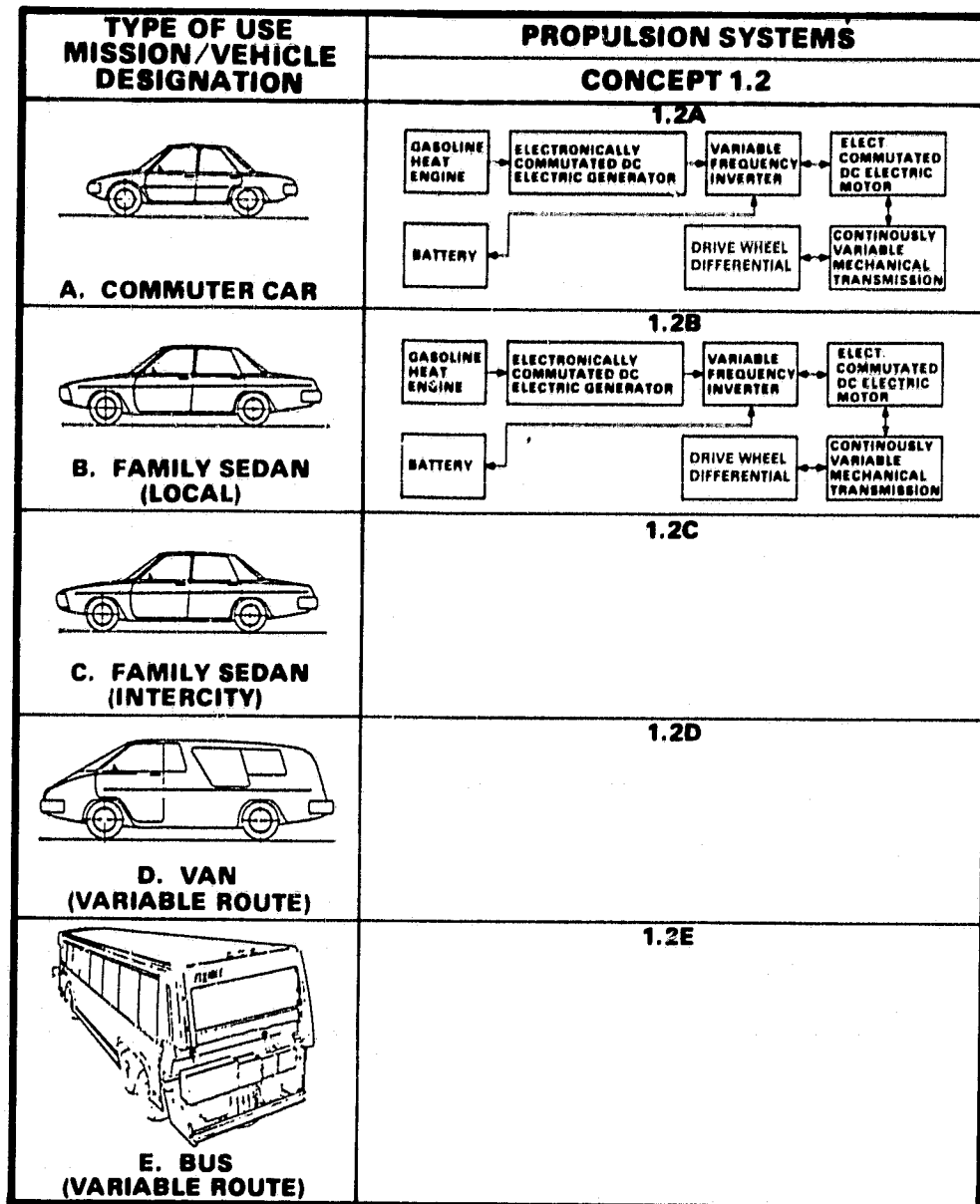
The Task I work is described in the following subsections. Included is the information used to perform the Task I effort as well as a description of the analytical work, results, and conclusions.

To complete the Task I effort, AIRsearch performed parametric studies on a total of five propulsion system concepts that were configured to comply with the contract ground rules and requirements. The propulsion concepts were combined with the five contract-specified mission/vehicles to arrive at the matrix of vehicular systems shown in figs. 1 through 5. The fifteen identified vehicle/propulsion system combinations were parametrically examined to determine the best candidates to carry into the Task II effort for further analysis and refinement.



S-45305

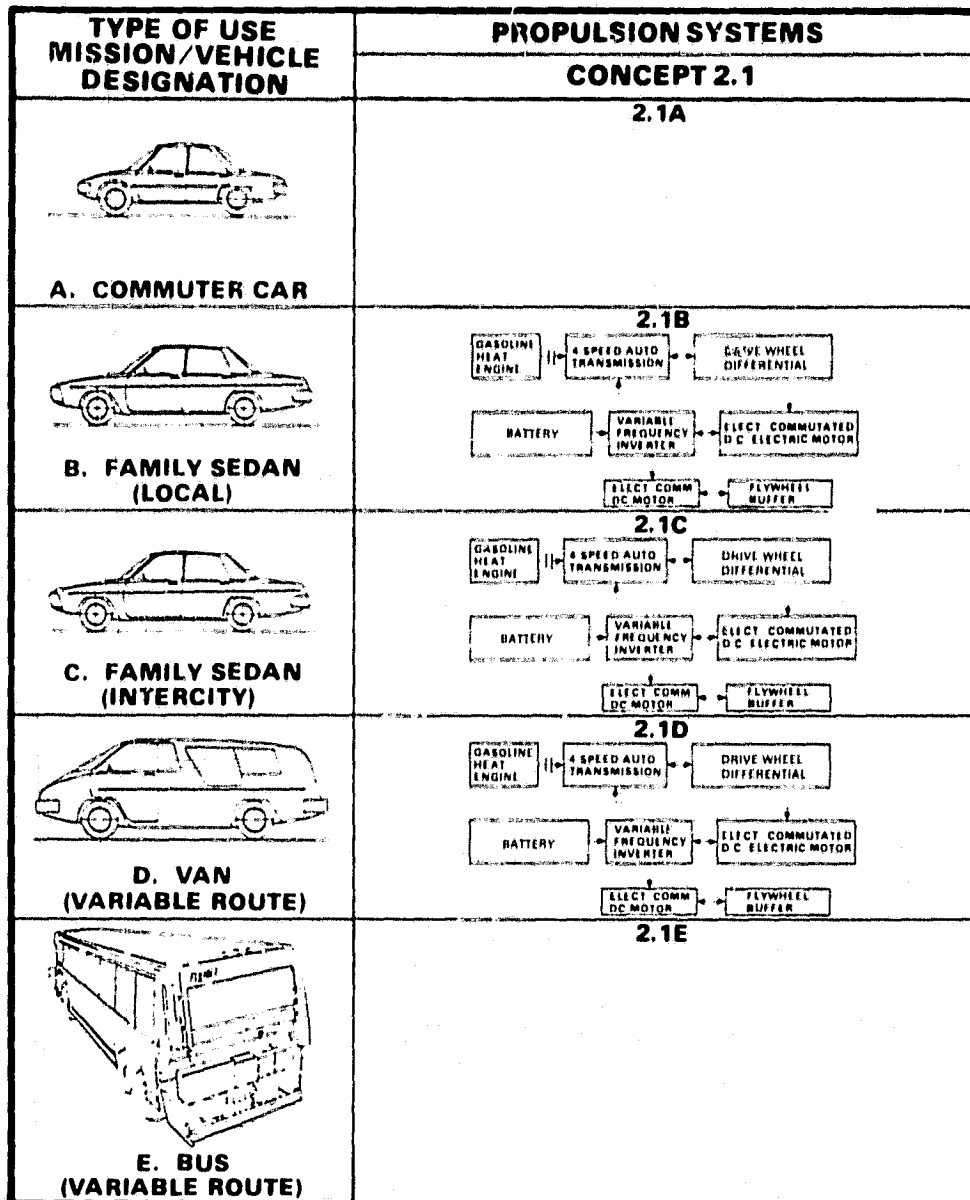
Figure 1.--Hybrid propulsion system concept 1.1.



S.45306 -A

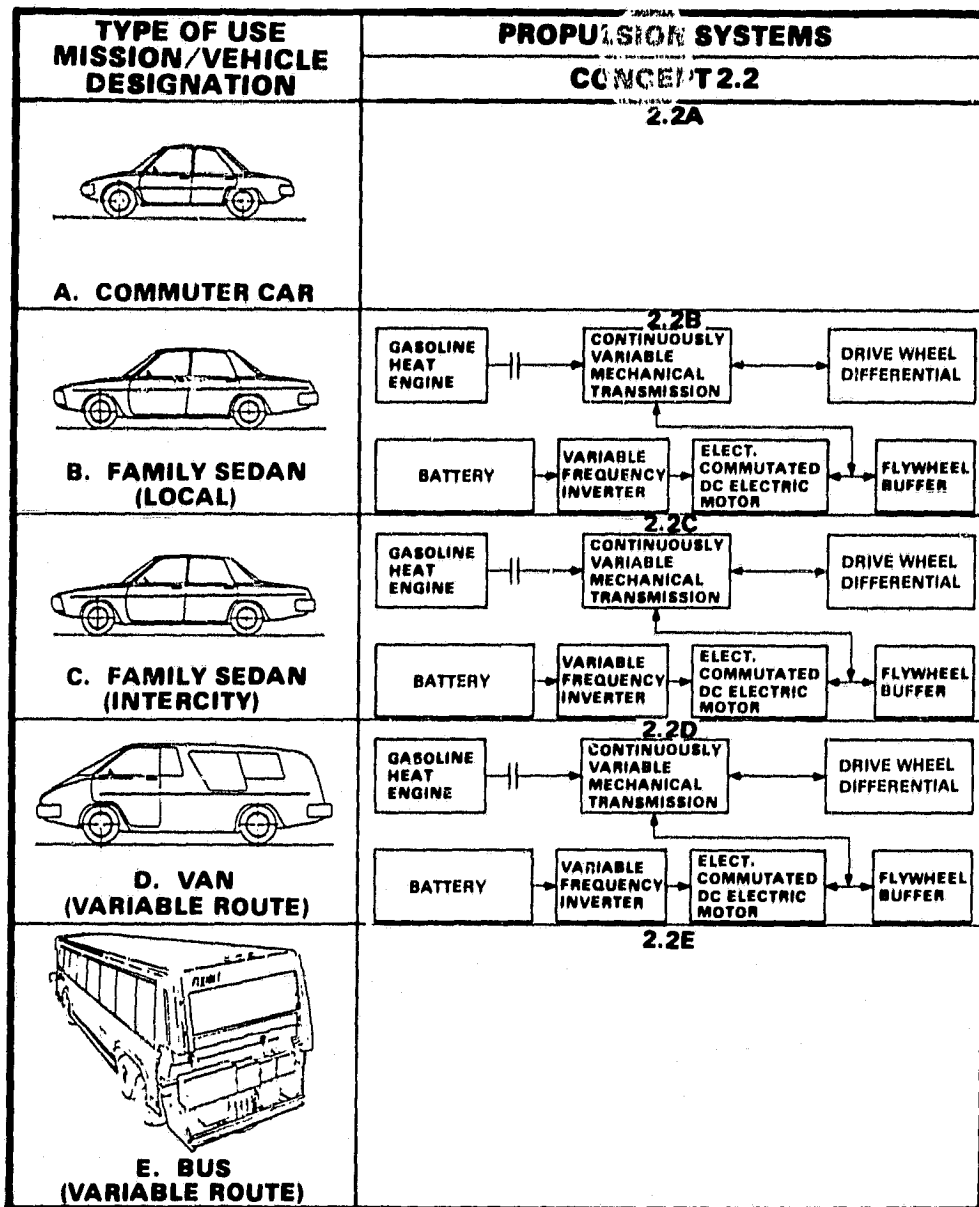
Figure 2.--Hybrid propulsion system concept 1.2.

ORIGINAL PAGE IS
OF POOR QUALITY



S 45307 -A

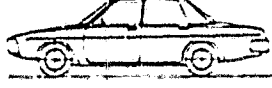
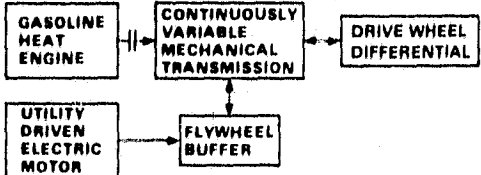
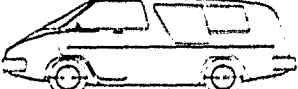
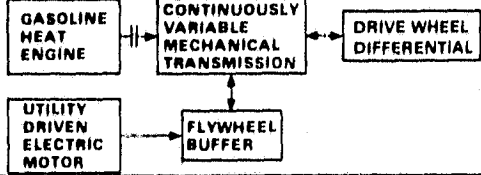
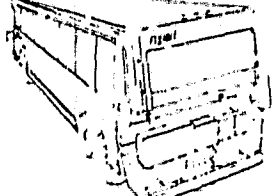
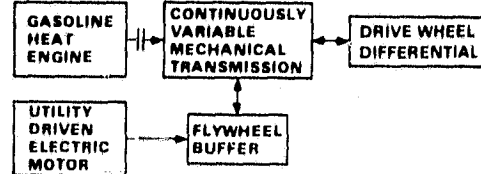
Figure 3.--Hybrid propulsion system concept 2.1 (with mechanical energy storage).



S-45308 -A

Figure 4.--Hybrid propulsion system concept 2.2
(with mechanical energy storage).

ORIGINAL PAGE IS
OF POOR QUALITY

TYPE OF USE MISSION/VEHICLE DESIGNATION	PROPULSION SYSTEMS CONCEPT 2.3
 A. COMMUTER CAR	<p style="text-align: center;">2.3A</p>
 B. FAMILY SEDAN (LOCAL)	<p style="text-align: center;">2.3B</p>
 C. FAMILY SEDAN (INTERCITY)	<p style="text-align: center;">2.3C</p> 
 D. VAN (VARIABLE ROUTE)	<p style="text-align: center;">2.3D</p> 
 E. BUS (VARIABLE ROUTE)	<p style="text-align: center;">2.3E</p> 

S-45309-A

Figure 5.--Propulsion system concept 2.3 (with mechanical energy storage and heat engine power).

STUDY GOALS, REQUIREMENTS, GROUND RULES, AND DEFINITIONS

A number of goals, requirements, and ground rules were imposed by the statement of work and subsequent agreements to constrain the latitude of the investigations. These constraints were applied throughout the contracted work.

Design Goals

The advanced hybrid propulsion systems considered in this study were configured to conform to the basic ground rules and requirements that are specified in the following subsections, with the objective of meeting the goals listed below when incorporated into the identified mission/vehicles.

Cost goal.--A major goal of this work was to provide a hybrid propulsion system design characterized by little or no initial and life-cycle cost penalty to the consumer in comparison with conventional vehicles of similar utility. As a reference point the life-cycle-cost goal for mission/vehicle B in figs. 1 to 5 is \$0.05/km (\$0.08/mi). This is the cost of the propulsion system with the primary energy storage device and the fuel and electric energy.

Propulsion energy efficiency and vehicle range goals.--The major goal of this contract was to reduce petroleum consumption and minimize total propulsion energy usage but still provide the range and basic performance of a conventional vehicle. Quantitative goals were not specified; however, in Tasks I and II, the calculation of vehicle yearly fuel and electricity use, energy requirements as a function of range, and energy distributions in the propulsion system are predicted. This information will assist in setting future goals.

Vehicle performance goals.--AIResearch was instructed to attempt to design all vehicle/propulsion system combinations (figs. 1 to 5) such that the performance goals listed in table 1 could be met. AIResearch interpreted these goals, with NASA concurrence, as requirements, and thus all configurations will meet them. The specified requirements apply at an ambient temperature of 20°C (68°F) and for a new traction battery.

A basic goal for all reference vehicles is that their range be limited only by the quantity of on-board fuel.

Design Requirements

The design requirements described below were imposed on all the vehicle/propulsion system combinations that were studied.

Reference mission/vehicle design constraints.--Table 2 lists the contractual design constraints that were specified for each of the designated mission/vehicles.

TABLE 1.--VEHICLE PERFORMANCE GOALS

Type of use Mission/vehicle designation	Commuting A	Family use (local) B	Family use (intercity) C	Van (variable route) D	City bus (variable route) E
Min. top speed on level road, km/hr (mph)	105 (65)	105 (65)	105 (65)	96 (60)	80 (50)
Max. accel. time:					
0 to 50 km/hr (0 to 31 mph), s	6	5	5	6	12
0 to 90 km/hr (0 to 56 mph), s	15	12	12	15	--
40 to 90 km/hr (25 to 56 mph), s	12	10	10	12	--
Gradeability of speed for specified distance:					
2% grade, 90 km/hr (56 mph), km (mi)	1.0 (0.62)	1.5 (0.93)	1.5 (0.93)	1.5 (0.93)	--
8% grade, 70 km/hr (43 mph), km (mi)	0.3 (0.19)	0.5 (0.31)	0.5 (0.31)	0.5 (0.31)	0.2 (0.12)
15% grade, 25 km/hr (16 mph), km (mi)	0.2 (0.12)	0.3 (0.19)	0.3 (0.19)	0.3 (0.19)	15% max. gr
Min. ramp speed attainable from a stop on uphill 6% grade in 300 m (984 ft), km/hr (mph)	80 (50)	80 (50)	90 (56)	80 (50)	--
Min. sustained speed up 4% grade, km/hr (mph)	90 (56)	90 (56)	90 (56)	90 (56)	70 (44)

TABLE 2.--BASIC DESIGN CONSTRAINTS

Type of use Mission/vehicle designation	Commuting A	Family use (local) B	Family use (intercity) C	Van (variable route) D	City bus (variable route) E
Payload:					
Number of passengers	2	4	6	8	50
Cargo, kg (lb)	30 (66)	0 (0)	100 (220)	500 (1100)	225 (500)
Total, kg (lb)	166 (366)	272 (600)	508 (1120)	1043 (2300)	3629 (8000)
Carriage characteristics:					
Weight without propulsion*, kg (lb)	400 (1100)	680 (1500)	1200 (2650)	1400 (3100)	5000 (11 000)
Aerodynamic coefficient, $C_D A$, M^2 (ft ²)	0.56 (6.0)	0.56 (6.0)	0.60 (6.5)	1.7 (18.3)	6.0 (65)
Tire rolling res. coef.		$0.008 + 1 \times 10^{-5}v$	$+ R \times 10^{-5}v^2$	$(v \text{ km/hr})$	
Tire rolling radius, m (ft)	0.27 (0.89)	0.29 (0.95)	0.31 (1.02)	0.34 (1.12)	0.518 (1.70)
Accessory load (maximum), W	500	600	600	600	15 000

*Propulsion includes primary energy storage.

**Special test cycle (STC): modified SAE J227a scheduled D.

Propulsion energy sources.--The advanced hybrid propulsion system must use at least two sources of propulsion energy:

- (1) Wall-plug electrical energy, storable within the vehicle
- (2) Gasoline or diesel fuel

The device that stores or contains the wall-plug energy on board the vehicle is called the primary energy storage system. This system will be chargeable using wall plug electricity in the following ways:

- (1) On-board charging system that uses a 60-Hz, 120- or 240-VAC, 15-A and/or 30-A supply outlet.
- (2) Off-board charge system that receives its power from a 60-Hz, single-phase, 240-VAC or 208-VAC, 60-amp supply outlet.

Required level of technology.--The level of technology required for work under this contract is defined as advanced, and it conforms to the following definitions:

- (1) Advanced technology: A product, system, or process that is conceptualized and is predicted to be achievable through the application of applied research followed by engineering development with the hardware being available at the end of fiscal year 1983.
- (2) Technology utilization: The conceptual propulsion system design shall emphasize technology that can take advantage of our country's domestic raw material resources. The concept must not exchange our present problem of a domestic petroleum shortage for some other potential material supply crisis beyond our national control.

Control characteristics.--The operation of the advanced propulsion system (response time, driveability, and complexity) should be similar to that of a conventional propulsion system/vehicle.

Reference battery characteristics.--The battery characteristics defined in table 3 were used. The state-of-the-art (SOA) lead-acid battery is listed for reference only and was not used. The characteristics of the improved state-of-the-art (ISOA) lead-acid battery and of the nickel-zinc battery were used for all work involving the use of batteries for primary energy storage. The characteristics for the ISOA battery and the nickel-zinc battery are goals established by the DOE for battery development to be completed in 1981.

Propulsion system emissions.--Although the prime objective of the work is the reduction of petroleum consumption, such reduction must be accomplished within the framework of acceptable pollutant emission levels as defined by those Federal statutory standards applicable to this work.

TABLE 3.--BATTERY CHARACTERISTICS

Parameter	Battery Types		
	Lead-acid		Nickel-zinc
	SOA	ISOA	
Specific energy, W-hr/kg	25 ¹	40 ¹	80 ^{1,2}
Specific power, W/kg	90 ³	100 ³	150 ^{3,4}
Cycle life ⁵	300	800	500
Cost ⁶ , \$/kW-hr	50	50	75
Energy efficiency	>0.6	>0.6	>0.7

- (1) At a 3-hr discharge rate and an 8-hr charge rate.
- (2) Rated at 100 percent discharge.
- (3) Peak from battery, 15 s average.
- (4) At 80 percent discharged state.
- (5) Number of discharges to 80 percent depth of discharge from rated capacity. Duty cycle is 4 to 8 hr charge, 2 to 4 hr discharge rate.
- (6) Price delivered to auto dealer with a production of 10 000 vehicle units per year. Dealer markup is 30 percent above his cost.

Safety.--All applicable Federal motor vehicle safety standards were applied to the study work.

Maintenance and reliability.-- The maintenance and reliability will be equivalent to that of a 1977 conventional vehicle of a similar mission/vehicle type.

Environmental capability.--The propulsion system will be operable over an ambient temperature range from -29°C (-20°F) or less to +52°C (+125°F) or more.

Availability.--The propulsion system will not contain technology so advanced that it could not be available for inclusion in an engineering model of the propulsion system in 1983.

Study Ground Rules

In addition to the previously stated goals and requirements, a set of ground rules was also established by NASA.

Special test cycle.--The specific petroleum fuel consumption and the specific wall plug recharge energy consumption were predicted as a function of distance traveled for each of the vehicle/propulsion system combinations identified in figs. 1 to 5. The calculations assumed a fully charged primary energy storage system and a full tank of fuel at the start of the mission. The continuous execution of the special test cycle described in fig. 6 was used for mission/vehicles A, B, C, and D. For mission/vehicle E (variable route bus), the SAE standard procedure J227a, Cycle C, was used.

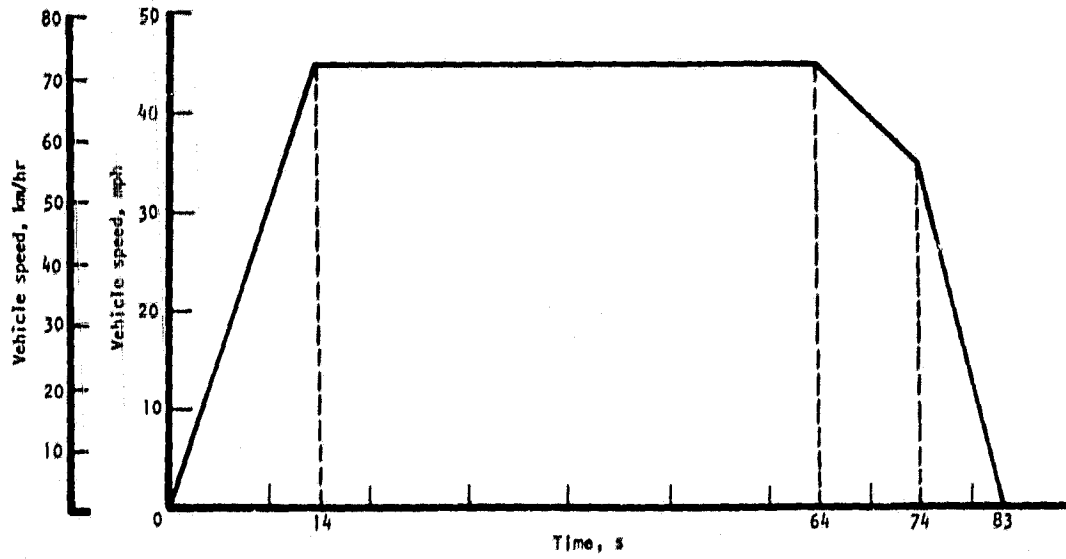
Annual energy usage.--Table 4 specifies a daily range frequency distribution for one year. The specified distribution was used to calculate the fuel and electricity usage on a yearly basis for the vehicle/propulsion system combinations except for the city bus. For days with less than an 80-km range, the special test cycle (STC) shown in fig. 6 was assumed. For days with 80-km range or more, 10 percent of the distance was assumed to be driven over the STC, and 90 percent of the distance was assumed to be driven at a steady speed of 90 km/hr (56 mph). For the city bus, the daily range was assumed to be constant and SAE J227a, schedule C, was used.

TABLE 4.--DAILY RANGE FREQUENCY FOR ONE YEAR

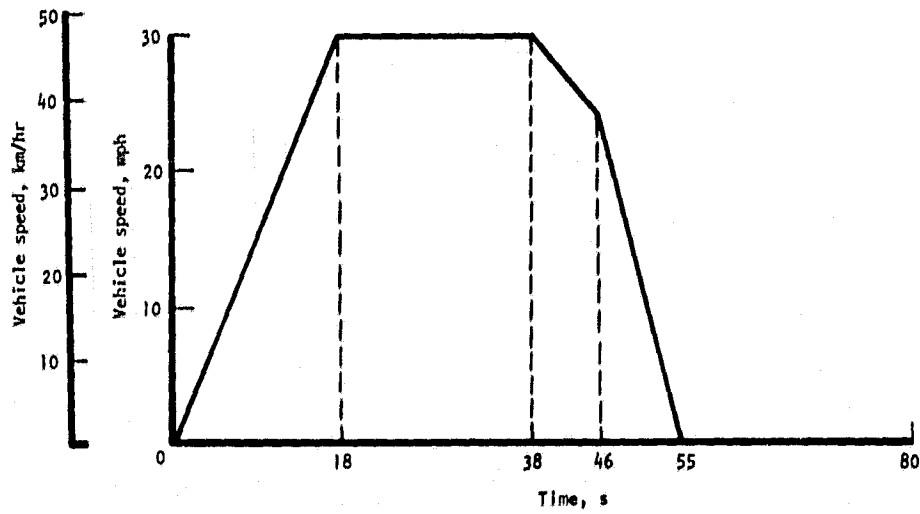
Daily range,		No. of days of the year	Total range,	
km	(mi)		km	(mi)
0	(0.0)	16	0	(0)
10	(6.2)	130	1300	(808)
30	(18.6)	85	2550	(1585)
50	(31.1)	57	2850	(1771)
80	(49.7)	54	4320	(2685)
130	(80.8)	12	1560	(970)
160	(99.4)	7	1120	(696)
500	(311.0)	3	1500	(932)
800	(497.0)	1	800	(497)
Totals		365	16000	(9944)

Weight prediction methods.--The parametric representation of weight and the mission/vehicle specific weight constants that were defined by NASA are displayed in tables 5 and 6, respectively. The weights of the propulsion system elements were determined independently. A weight growth factor of 30 percent was used to adjust each vehicle's curb weight as the propulsion system weight, and battery weight was varied from a calculated reference.

Battery performance.--The curves for battery performance (fig. 7) and cycle-life (fig. 8) were provided by NASA to be used as input data for this study.



Special Test Cycle (Mod, SAE J227a, schedule D)
used to evaluate mission/vehicles A,B,C, and D



SAE J227a, schedule C
used to evaluate mission/vehicle E

S-44093-A

Figure 6.--Driving cycles.

TABLE 5.--PARAMETRIC REPRESENTATION OF WEIGHT

Symbol	Definition	Formula
$W_{PL, \max.}$	Maximum design payload	--
W_{TL}	Test payload	--
W_F	Fixed weight	--
W_G	Gross vehicle weight	$W_G = W_S + W_{PL} + W_P + W_F$
W_C	Curb weight	$W_C = W_G - W_{PL, \max.}$
W_T	Test weight	$W_T = W_C + W_{TL}$
W_S	Structure and chassis weight	$W_S = 0.23 W_G$
W_P	Propulsion weight	Determined by contractor

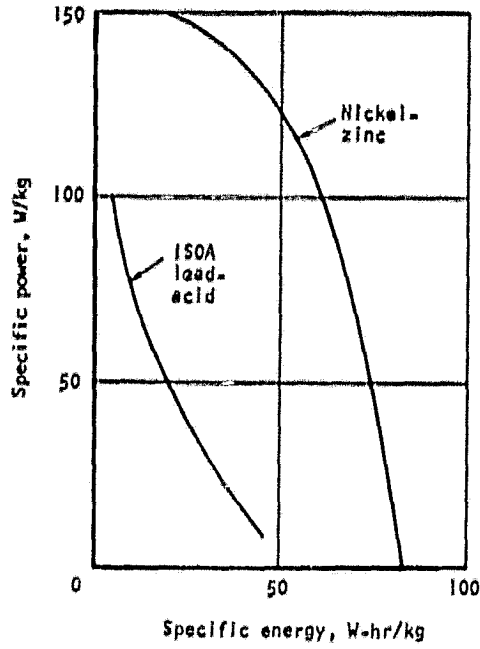
TABLE 6.--MISSION/VEHICLE SPECIFIC WEIGHT CONSTANTS

Constant	Units	Mission/vehicle				
		A	B	C	D	E
$W_{PL, \max.}$	kg (lb)	166 (366)	272 (600)	508 (1120)	1043 (2300)	3629 (8000)
W_{TL}	kg (lb)	83 (183)	136 (300)	254 (560)	522 (1150)	1815 (4000)
W_F	kg (lb)	204 (450)	408 (900)	612 (1350)	816 (1800)	5200 (11 464)

Life-cycle-cost calculations.--The following life-cycle-cost guidelines were provided by NASA as part of the contract:

- (1) Costs shall be calculated only for the propulsion system plus the battery. Therefore other vehicle costs, insurance, and taxes are not included.
- (2) Use 1976 dollars.
- (3) Acquisition cost is the sum of the OEM cost (manufacturing cost plus corporate level costs such as general and administrative, required return on investments of facilities and tooling, cost of sales,...) of components plus the cost of assembling the components plus the dealer markup (assume 17 percent).
- (4) Annual production is 100 000 units.

ORIGINAL PAGE IS
OF POOR QUALITY



5-45279

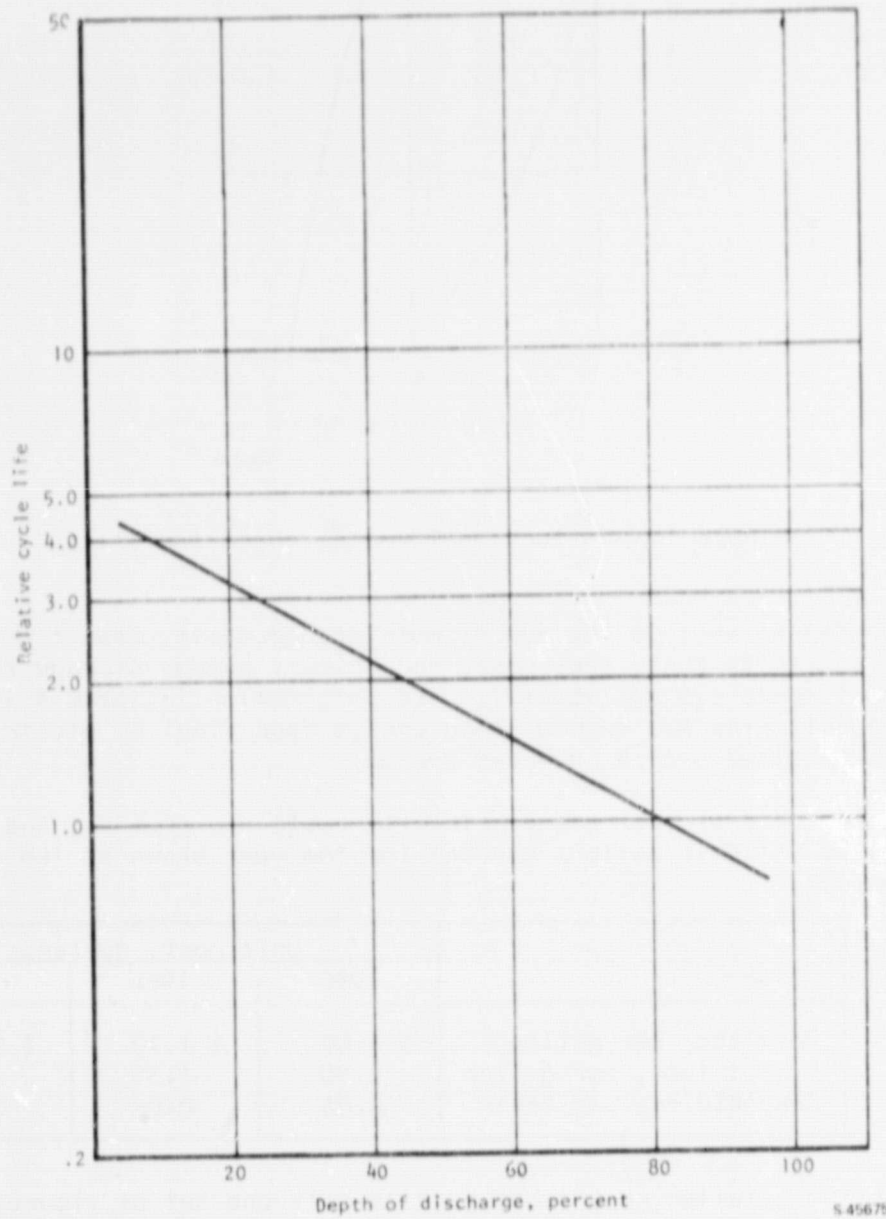
Figure 7.--Battery performance characteristics.

- (5) Operating cost is the sum of maintenance costs, repair costs, electricity cost, fuel cost, and primary energy storage replacement costs (if applicable). The information in table 4 is used to determine how much of each energy type (fuel or electricity) is required over a one-year period.
- (6) Three sets of fuel and electricity costs are provided and are assumed to be valid in dollars current for the year shown at the top of each column:

Item	Unit cost, dollars		
	1980	1985	1990
Gasoline, per gallon	\$ 1.00	\$ 1.50	\$ 2.00
Diesel fuel, per gallon	0.90	1.35	1.80
Electricity, per kW-hr	0.05	0.06	0.07

If the detailed work scope permits only one set of figures to be used, the 1985 column should be used. Otherwise, all three columns of figures may be used for a sensitivity study of the effect of energy costs.

- (7) Vehicle lifetime is 10 years and 160 000 km (100 000 mi).



S 45675

Figure 8.--Cycle-life characteristics.

- (8) A constant noninflating dollar is assumed. No inflation factor is included in the discount rate since it is assumed that personal disposable income tracks inflation.
- (9) A two percent discount rate for personal cars shall be used, as it represents only time preference (opportunity cost). For commercial vehicles (D and E in figs. 1 to 5), a discount rate of ten percent shall be used.
- (10) Cost of finance is not included in this procedure, since it is assumed that the discounted present value of the sequence of total payments would approximately equal the original purchase price.
- (11) All expenses are assumed to be costed at the end of each year. Year 'Zero' is reserved for those costs that must be incurred before the vehicle is operated.
- (12) Scrap/salvage value is 10 percent.
- (13) In determining the life of propulsion system components (such as a primary energy storage system), assume that the vehicle is driven 16 000 km (10 000 mi) per year. For the city bus (mission vehicle E), assume 32 000 km (20 000 mi) per year service. Assume the trip distribution for the mission/vehicles as listed (on a yearly basis) in table 4. The component life shall be determined based on these trip distributions, field environmental effects, and the degradations due to the actual conditions imposed on the components by the rest of the system and vehicle.
- (14) The calculation of life-cycle cost shall follow the format shown on worksheets 1 and 2 (see figs. 9 and 10, respectively), using the following instructions:
 - (a) The purchase price is entered on the appropriate line of the life-cycle-cost worksheet as a year "Zero" cost.
 - (b) Operating costs: electricity, fuel, maintenance and repair, and primary energy storage system replacement costs (if any) are copied from the operating cost worksheet to the same position on the life-cycle-cost worksheet.
 - (c) Discount factor = $(1/(1 + i)^t)$ is computed for each year (where t = year 0 to 10 and i equals the discount rate).
 - (d) For each year, the discount factor times the cost gives the present value of the cost for that year. These are summed to provide the discounted present value of the life-cycle cost.
 - (e) The value computed in step (d) is divided by the total distance driven to provide the life-cycle cost per km and is expressed in cents per km.

OPERATING COST WORKSHEET

YEAR	1	2	3	4	5	6	7	8	9	10
COSTS IN CENTS PER KILOMETER										
Distance Dependent Costs										
Maintenance										
Engine System										
Electric										
Battery										
Energy Buffer										
A TOTAL										
Repair										
Engine System										
Electric										
Auxiliaries										
Transmission										
D TOTAL										
Electricity										
Fuel										
E TOTAL										
F TOTALS A+D+E										
G DISTANCE EACH YEAR										
H TOTAL DOLLARS (F/100) x G										
Battery Replacement										
YEAR TOTALS										
TOTAL OPERATING COST =										
OPERATING COST PER KILOMETER =										

S-46677

Figure 9.--Operating cost worksheet.

LIFE CYCLE COST WORKSHEET

	YEAR	"0"	1	2	3	4	5	6	7	8	9	10
1	PURCHASE PRICE											
2	FUEL											
3	ELECTRICITY											
4	REPAIR + MAINTENANCE											
5	BATTERY REPLACEMENT											
6	SYSTEM SALVAGE (MINUS)											
7	BATTERY SALVAGE (MINUS)											
8	TOTAL											
9	DISCOUNT FACTOR											
10	PRESENT VALUE (8 x 9)											
11	PRESENT VALUE OF LIFE CYCLE COST (SUM OF 10)											
12	PRESENT VALUE OF LIFE CYCLE COST PER KILOMETER DRIVEN (11/TOTAL KM)											

S-45678

Figure 10. ---Life-cycle-cost worksheet.

Study Definitions

The definitions listed below apply for the work performed in this study.

Hybrid vehicle.--A complete self-propelled vehicle system whose propulsion energy is derived from two or more external energy sources, one of which is electrical.

Hybrid propulsion system.--The aggregation of all components that comprise the power train, plus accessory drives and auxiliaries, including the battery charger and primary energy storage system, but excluding tires.

Power train.--The aggregation of all components that comprise the drive train, the power plant, vehicle drive axle, and all secondary energy storage elements.

Power plant.--The basic power-producing unit (or units) that utilize an external energy source (or sources) to generate the propulsive power required to propel a vehicle (excludes auxiliaries and accessories).

Energy buffer.--A device that stores energy temporarily and supplies some or all of the stored energy in a controlled way on demand. The form of the input or output energy may be chemical, electrical, mechanical, etc.

Drive train.--An aggregation of components that transmit power from the vehicle power plant to the drive axle (i.e., transmission, differential, clutch system, torque converter, gearing, etc.)

Carriage.--The complete "curb" configuration of a vehicle less the propulsion system and any electromechanical storage batteries.

Life-cycle cost.--The cost per km of production hardware over its operating life. Included in life-cycle cost are acquisition cost, operating cost, scrap or salvage value discounted to reflect the time value of money.

Engineering development.--The effort that normally follows applied research and is directed toward the application of established technical knowledge, using engineering principles and practices, for the purpose of evolving, via an iterative process of design, fabrication, and test evaluation, a new product, system, or process.

ORIGINAL PAGE IS
OF POOR QUALITY

TASK I ANALYTICAL METHODOLOGY

This section of the report contains a discussion of the five propulsion system concepts, Task I scope, information on the initial sizing of the vehicle/propulsion systems, a description of the digital computer program for the propulsion concepts with their associated mission/vehicles, hardware performance maps, and cost analysis procedures.

Discussion of Propulsion System Concepts

The vehicle/propulsion system concept combinations are shown in figs. 1 through 5. The propulsion concepts were agreed upon during a series of NASA/AiResearch technical meetings. Essentially, there are 5 mission/vehicles and 5 propulsion system concepts, which have been combined to form the 15-element Task I study matrix, as was shown in figs. 1 through 5.

The five vehicle types are representative of current vehicles with the possible exception of the commuter car. The type of propulsion components that were used to perform the Task I parametric studies are shown in table 7. The vehicle/propulsion concepts all use nickel-zinc batteries as the baseline, the spark ignition (SI) gasoline engine (water cooled, naturally aspirated (NA) with smog controls), and an advanced electronically commutated high-speed motor.

TABLE 7.--TASK I PROPULSION COMPONENTS

Component type	Baseline for configurations studied in task I	Components characterized in task I
Heat engine	Spark-ignition, water-cooled, naturally-aspirated, gasoline	(1) Diesel, naturally aspirated (2) Turbine
Electric traction machine	Dc, electronically commutated	---
Battery	Nickel-zinc, 80 W-hr/kg, 150 W/kg	ISOA lead-acid, 40 W-hr/kg, 100 W/kg
Energy buffer	Flywheel mechanical energy storage (MES)	(1) Steel flywheel (2) Composite flywheel
Electric control	Variable frequency inverter	--
Transmission	(1) Electric and discrete ratio (2) Concepts 1.2 and 2.3 use mechanical continuously variable transmission (CVT)	Regenerative continuously variable transmission (CVT)

Task I Scope and Format of the Results

A summary of the Task I scope is shown in fig. 11 along with the format of the results. There are 12 vehicle/propulsion system configurations that are included in the evaluation scope. Each configuration was evaluated using three lead-acid battery weights and three nickel-zinc battery weights. In all cases a structural growth factor of 1.3 was employed when a new vehicle curb weight was being determined for each battery pack weight. The results are determined for presentation, as shown in fig. 11. For each variation in battery type and weight, calculations were made of the prime electric range, driving cycle petroleum usage, annual petroleum usage, propulsion system acquisition cost, and life-cycle cost.

Three heat engine/flywheel, vehicle/propulsion system configurations (2.3C, 2.3D, and 2.3E) were not evaluated in the same manner as the other 12 configurations, because their wall-plug energy is stored in a flywheel instead of a battery pack. For each of these configurations, the electric range was determined as a function of flywheel capacity.

Task I Parametric Study Modeling Procedures

The modeling procedures that were used to guide the preparation of the digital computer evaluation program are basically a set of energy and power management constraints for each type of vehicle configuration. AIResearch experience indicates that the limitations placed on the Task I parametric results due to the specified energy and power management procedures do not effect the relative ranking to such an extent as to cause any reversal in the standings.

One set of procedures applies to those configurations in which both a battery pack and a heat engine are used as energy sources (concepts 1.1 and 1.2). The procedures are as follows:

- (1) Minimum battery is sized to run driving cycle unaided (constant power acceleration).
- (2) Heat engine is sized to perform the steady-state hill climb.
- (3) Battery and heat engine operating together must meet 0- to 90-km/hr acceleration goal. Heat engine size is increased until goal is met (constant power acceleration).
- (4) Battery is used to 80 percent depth of discharge (DOD).
- (5) Battery is load-leveled by heat engine to 80 percent DOD. At 80 percent DOD battery is used only to aid heat engine during high power demand periods.
- (6) Regeneration is into the battery during braking (not to exceed machinery limit).
- (7) Heat engine is off when not needed.

Scope of studies

Concept	Nickel-zinc battery	Lead-acid battery
1.1A	3	3
1.1B	3	3
1.1C	3	3
1.1D	3	3
1.2A	3	3
1.2B	3	3

(No HES)

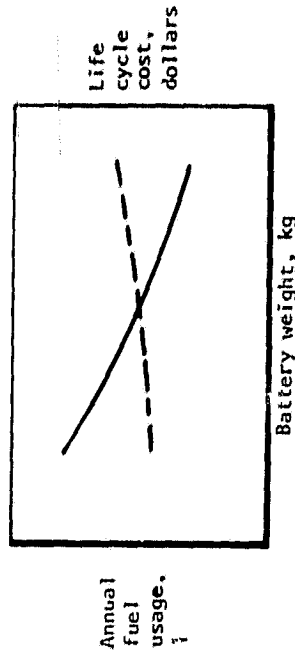
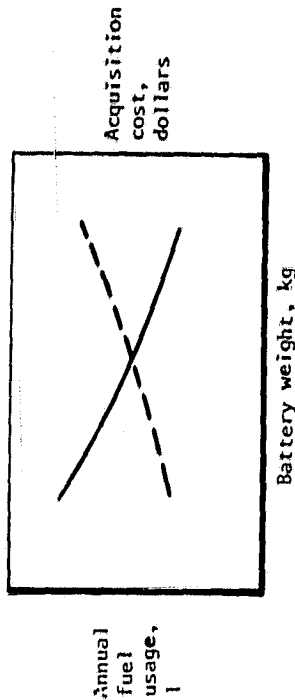
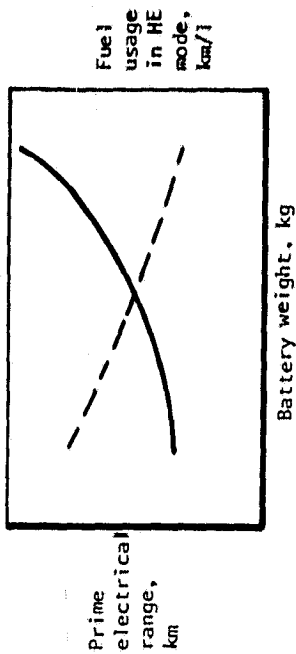
Concept	Nickel-zinc battery	Lead-acid battery
2.1B	3	3
2.1C	3	3
2.1D	3	3
2.2B	3	3
2.2C	3	3
2.2D	3	3

MES, Case (b)
(no power split)

Concept	Nickel-zinc battery	Lead-acid battery
2.1B	3	3
2.1C	3	3
2.1D	3	3
2.2B	3	3
2.2C	3	3
2.2D	3	3

MES, Case (a)
(50/50 power split)

Form of results



5-6378-1

Figure 11.--Task 1 scope and form of results.

- (E) Accessory loads are supplied by the battery until 80 percent DOD; then heat engine is used.

A separate set of procedures is used for those configurations where the battery is the prime energy source, aided by both a flywheel energy buffer and the heat engine (concepts 2.1 and 2.2). The following procedures cover two situations, defined case A and case B. Procedures (1) through (7) apply to both cases; procedure (8) is unique to case B.

Case A.--Minimum battery is sized to run driving cycle unaided (constant power acceleration).

Case B.--Minimum battery is sized to run driving cycle aided by flywheel (50/50 power split; constant power acceleration).

For both case A and case B:

- (1) Heat engine is sized to perform steady-state hill climb.
- (2) Battery and flywheel operating together must meet 0- to 90-km/hr acceleration goal (constant power acceleration).
- (3) Heat engine and flywheel operating together must meet 0- to 90-km/hr acceleration goal.
- (4) Battery is used to 80 percent depth of discharge (DOD).
- (5) Regeneration is into flywheel during braking until it is 100 percent charged.

All excess energy is regenerated into battery (not to exceed machinery capacity).

- (6) Heat engine is off when not needed.
- (7) Accessory loads are supplied by battery until 80 percent DOD; then heat engine is used.

For case B only:

- (8) Battery is load-leveled by flywheel to 80 percent DOD. At 80 percent DOD heat engine and flywheel supply energy (50/50 power split; constant power acceleration).

A final set of procedures is used for those configurations that use a heat engine and a flywheel without a battery (concept 2.3):

- (1) Flywheel supplies all energy until it is 75 percent discharged. Heat engine is turned on to complete remainder of mission.
- (2) Flywheel is fully charged only from wall plug.

- (3) When heat engine is used, flywheel is used as a buffer.
- (4) Energy is recovered during braking by regeneration into the flywheel.

Review of Propulsion System Concepts

For each of the five propulsion system concepts that were evaluated in Task I (shown in figs. 1 through 5), the prime emphasis was placed on arriving at a relative ranking of the vehicle/propulsion system combinations to select the most promising concept. The principal features of these concepts are reviewed in the following paragraphs. The final ranking was based on petroleum energy saved vs the cost savings to the consumer. The consumer costs are determined as propulsion system initial acquisition costs (including batteries) and propulsion system life-cycle costs for a 10-year, 160 000-km life.

A secondary emphasis was placed on parametric investigation of the sensitivity of each vehicle propulsion system configuration to variations in on-board energy storage capacity and storage method. This information provides a data base that can be used to judge similar propulsion arrangements as a function of mission/vehicle designation.

Concept 1.1.--This concept, shown in fig. 1, is an unbuffered configuration and represents the simplest hybrid configuration that is feasible. Both the heat engine and the electrical system are sized as described in the preceding section and then evaluated over the modified SAE J227a, D cycle (fig. 6). In the electrical mode and heat engine mode, the braking energy is regenerated back into the battery.

The generic advantages of this concept are:

- (1) Simplicity
- (2) Low technical risk (minimal development)
- (3) Low weight (except for battery pack)
- (4) Low cost

Concept 1.2.--This concept is an unbuffered approach (fig. 2). This configuration is advantageous because it represents a hybrid derivative of a pure electric propulsion system; i.e., a relatively simple and low-cost gasoline-driven generator is added to achieve longer ranges. Since the gasoline engine must drive through an electrical transmission, however, fuel economy is not good. To improve the heat engine mode economy, the gasoline engine is operated on its maximum (lean mixture) torque line, and the speed is varied to change the available power.

The major advantage of this concept is that it would be relatively easy to provide a small vehicle such as a commuter car with any of the following three drive system options:

- (1) Standard battery pack without a heat engine, which makes the vehicle a low-cost, low-weight commuter
- (2) Large battery pack without a heat engine, which provides a simple vehicle, but with a greater range
- (3) Battery pack plus a heat-engine-driven generator, which would allow extended cruising when needed

The concept was selected as a means to evaluate the impact of the ceramic gas turbine on the fuel economy. In this configuration the gas turbine (and generator) are operated at constant speed to obtain the best efficiency from the gas turbine.

Concept 2.1.--In this concept (fig. 3) the flywheel acts as a buffer for both the electrical and heat engine modes. The heat engine mode is efficient since the speed can be low and, hence, the frictional losses minimal. The electrical mode is also efficient, but the flywheel buffering mode is only of medium efficiency because of the electrical transmission into and out of the flywheel; however, the electrical transmission efficiency can be compensated for because of its flexibility; i.e., it allows the heat engine and traction machine speeds to be decoupled from the flywheel speed.

In principle, this concept is fine, but the practical limitations, i.e., cost and efficiency of the electrical flywheel transmission, limit this concept to special purpose uses.

Minimal technical risk and development costs are the attractions of this concept.

Concept 2.2.--This concept (fig. 4) is essentially a mechanical version of concept 2.1 that uses a continuously variable transmission (CVT) for both the electrical and heat engine modes. The high-speed electrical motor and the flywheel are directly coupled through a fixed-ratio gearset. In the heat engine mode, all three items (flywheel, electric motor, and heat engine) are mechanically geared together. The flywheel energy level, therefore, sets the speed of both the electric-drive motor and the heat engine.

When the availability of a successful and reliable CVT is assumed, this concept looks very attractive, with the following major advantages:

- (1) High drive line efficiencies
- (2) Low weight
- (3) Low cost
- (4) Simple system
- (5) Efficient flywheel drive

ORIGINAL PAGE IS
OF POOR QUALITY

The major limitation of this system is that the flywheel speed sets the speeds of the heat engine and electric traction machine, and this implies that the two propulsion elements may be required to operate in nonoptimum performance regions during the driving cycle. The coupling of the flywheel, engine, and drive motor speeds also results in larger power ratings for the propulsion elements in comparison with concept 2.1.

Concept 2.3.--This concept (fig. 5) substitutes a flywheel energy storage unit for the nickel-zinc battery pack. The flywheel essentially operates in two modes:

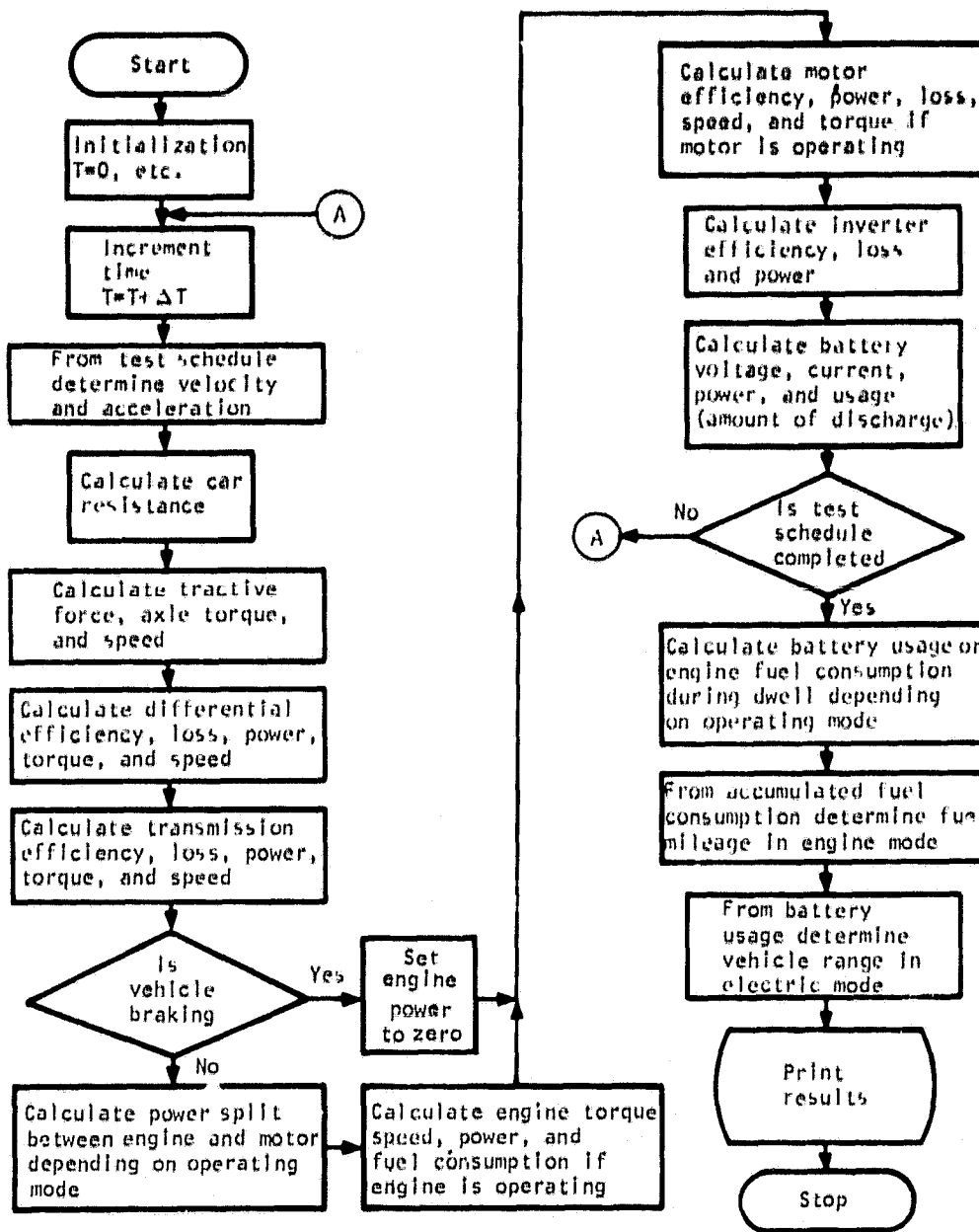
- Mode 1--flywheel energy source
- Mode 2--flywheel buffer

The flywheel is charged by driving the electric motor from external utility system power. This motor is sized as a function of the charging time requirement. Initially the heat engine is not operating, so the clutch is disengaged. The vehicle then operates on the flywheel until it is down to half-speed (18 000 rpm). This condition represents a 75 percent DOD. When the flywheel is depleted to its half-speed point, the engine is started, and the clutch is engaged. The heat engine is geared directly to the flywheel, and therefore its operating speed range is limited. The heat engine mode is the same as that of concept 2.2, which thus produces similar fuel consumption figures. This type of concept shows a major benefit if rapid recharging stations can be conveniently located along a known route every three to five miles. This requirement imposes a restricted route structure on the vehicles.

Analytical Modeling

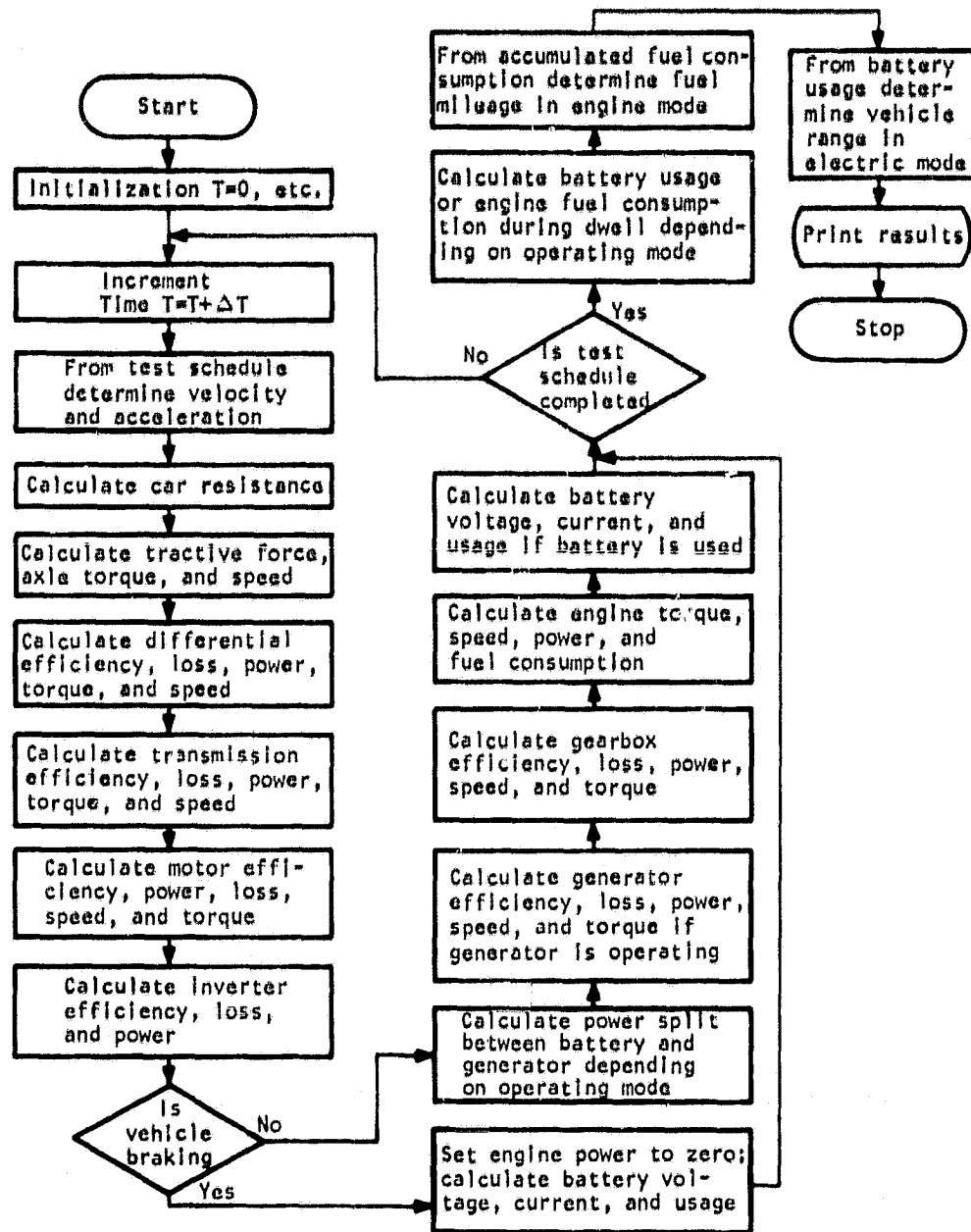
An analytical model of each propulsion system concept was derived and programmed for the digital computer. The basic equations for the rectilinear motion of a rigid body were combined with Newton's second law of motion to establish the basic link between the velocity of the vehicle, as specified by the driving cycle, and the net driving force at the wheels. Analytical descriptions (performance maps) for each major propulsion system component (such as heat engine, battery, and transmission) were incorporated in the programs to determine the response of power train elements to the varying power demands associated with vehicle operation on the specified driving cycle.

Computer simulation descriptions.--General schematic flow charts for the five propulsion concepts are shown in figs. 12 through 19. The arrows indicate the direction and sequence of the data flow. Labeled arrows indicate particular data that is being transferred. The program begins with calculation of the first two velocities of the driving cycle, from which acceleration and average velocity are found. From these results the total force is obtained. From the tire and aerodynamic models, the torque required to overcome the road losses and provide the demanded acceleration is calculated and transmitted through the drive train components. The resulting speed and torque at the heat engine and/or the power demand at the battery terminals define the electrical energy usage and fuel flow at any particular time. These values, assumed constant over each



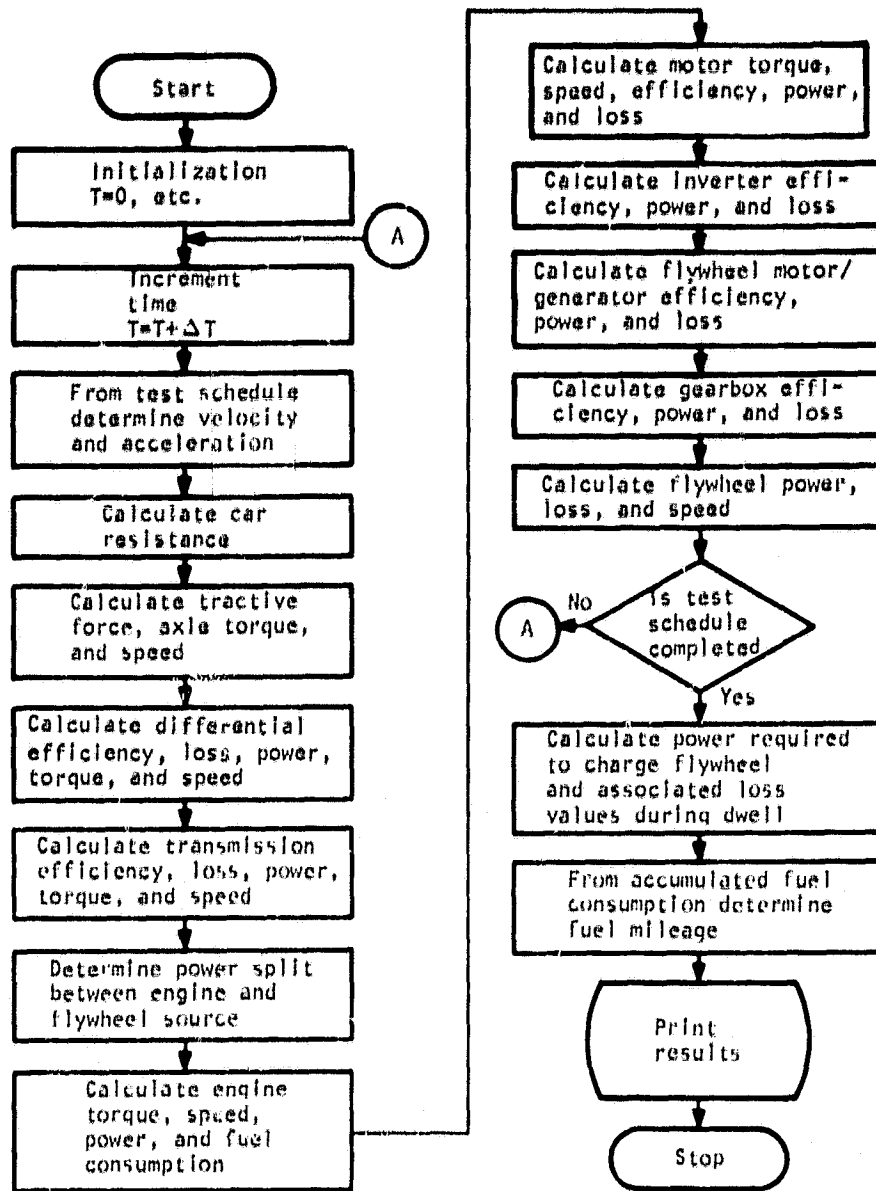
545801

Figure 12.--Methodology flow chart for concept 1.1.



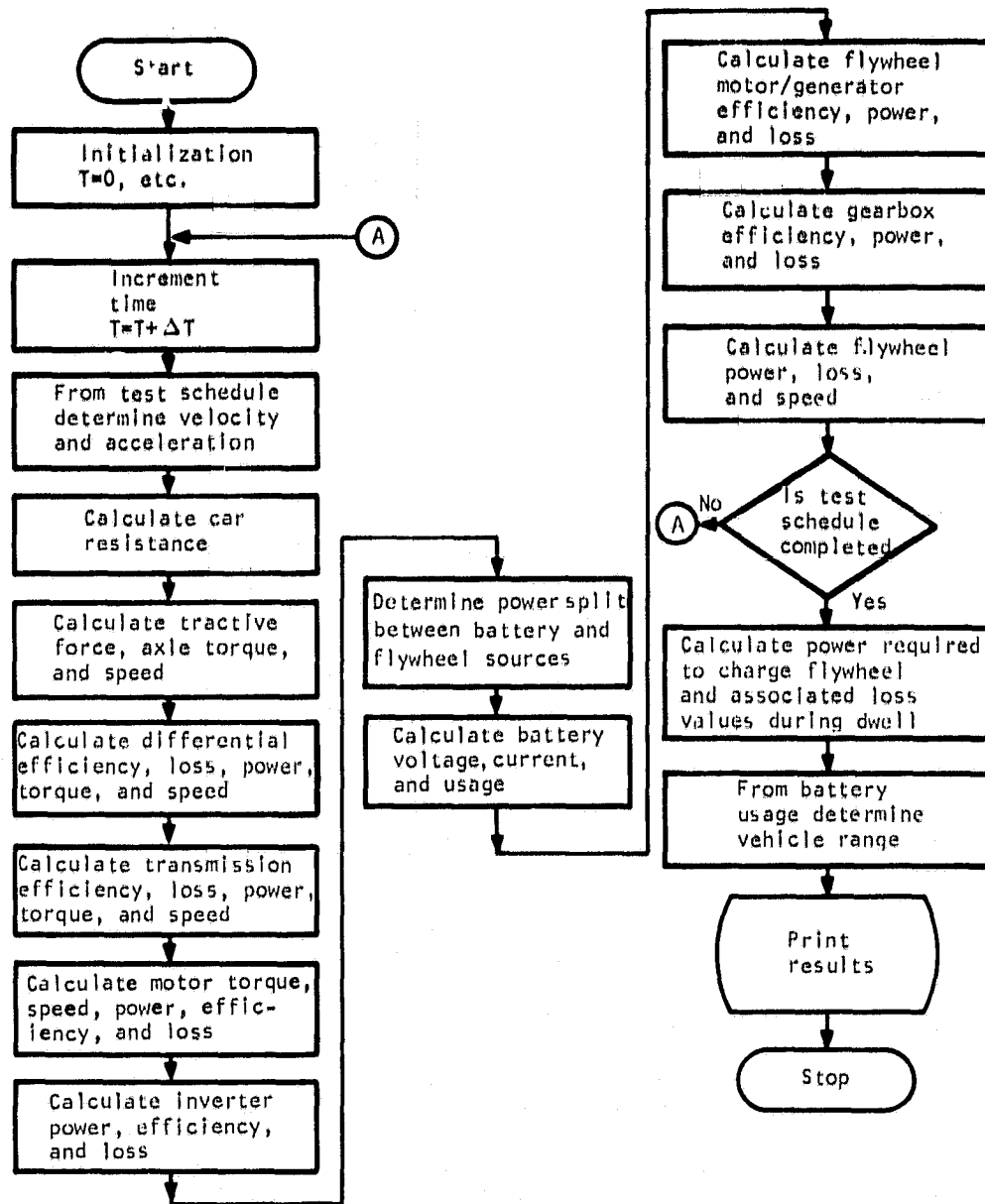
84802

Figure 13.--Methodology flow chart for concept 1.2.



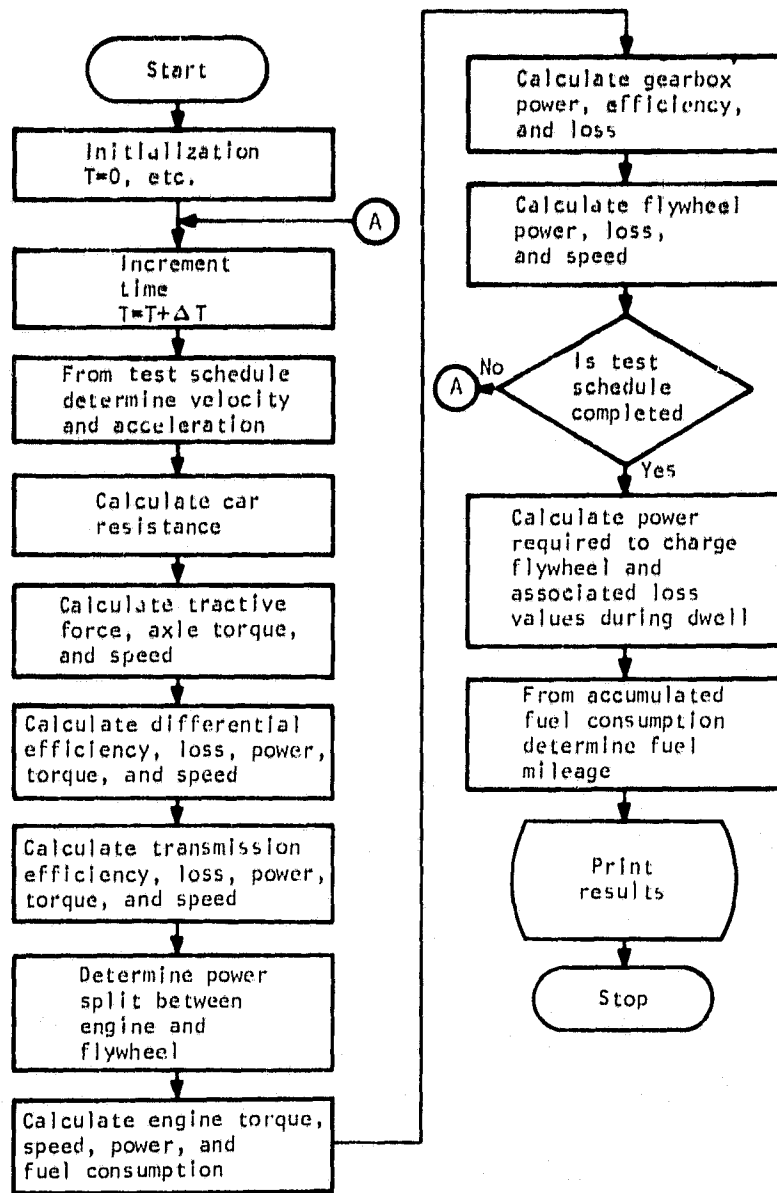
546796

Figure 14.-- Methodology flow chart for concept 2.1, engine mode.



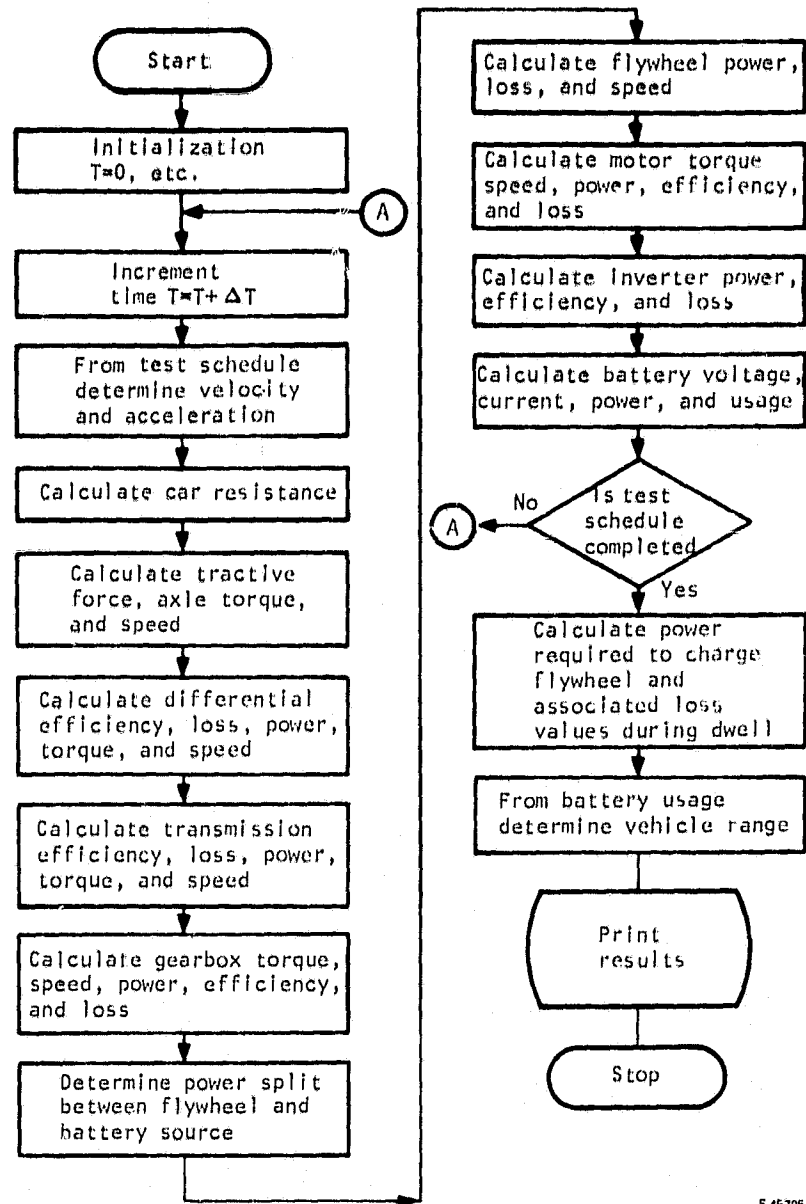
5-45800

Figure 15.--Methodology flow chart for concept 2.1, electric mode.



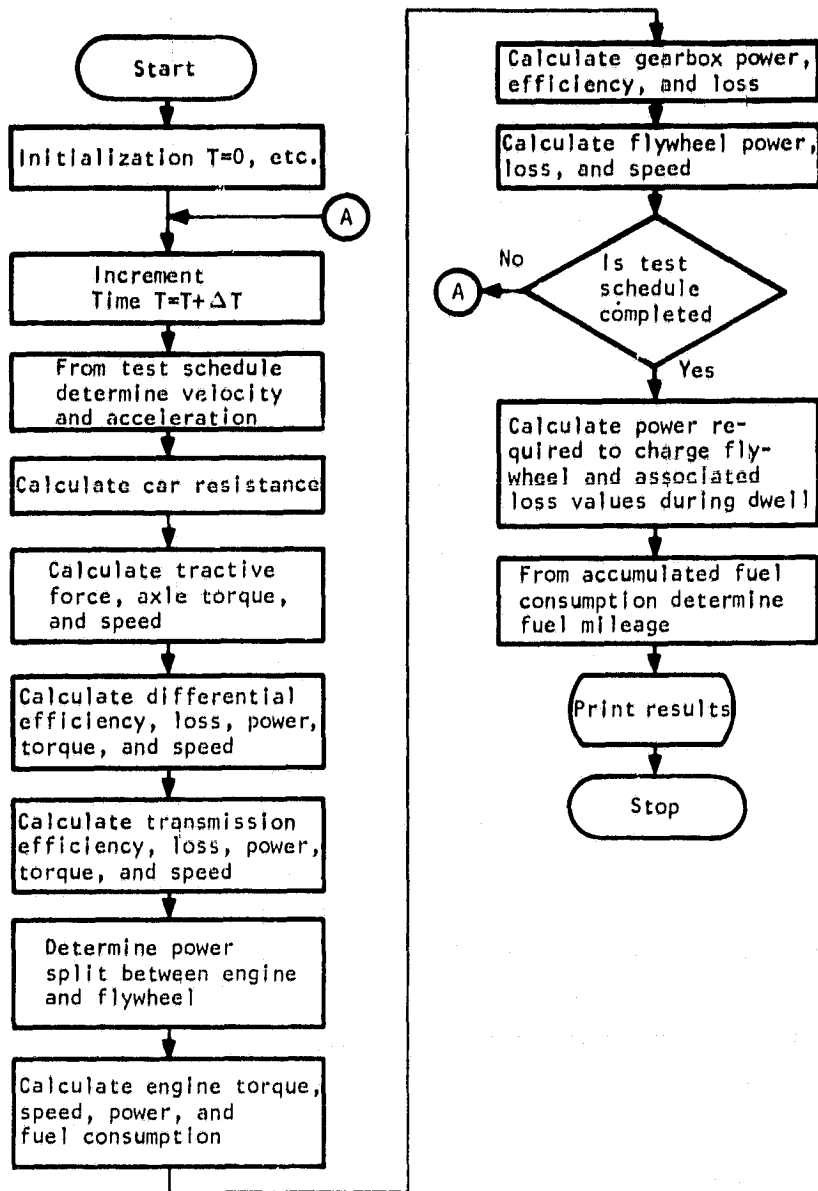
S45799

Figure 16.--Methodology flow chart for concept 2.2, engine mode.



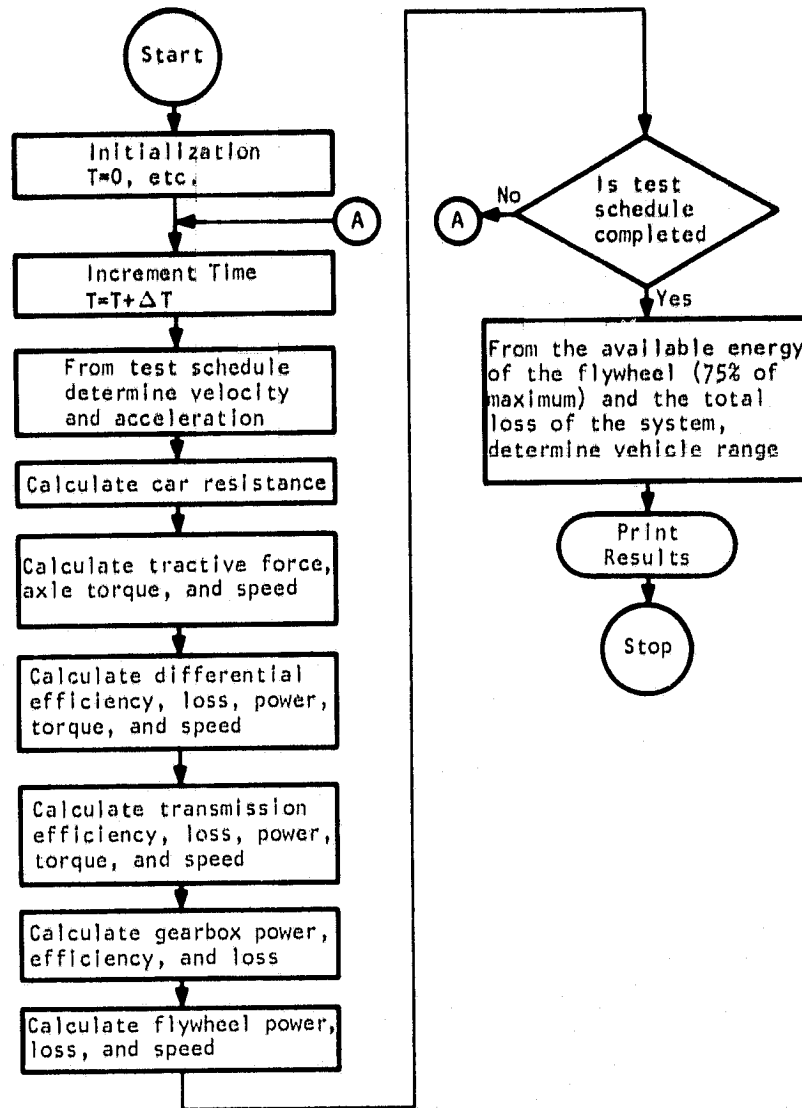
5 46796

Figure 17.--Methodology flow chart for concept 2.2, electric mode.



S 45798

Figure 16.--Methodology flow chart for concept 2.3, engine mode.



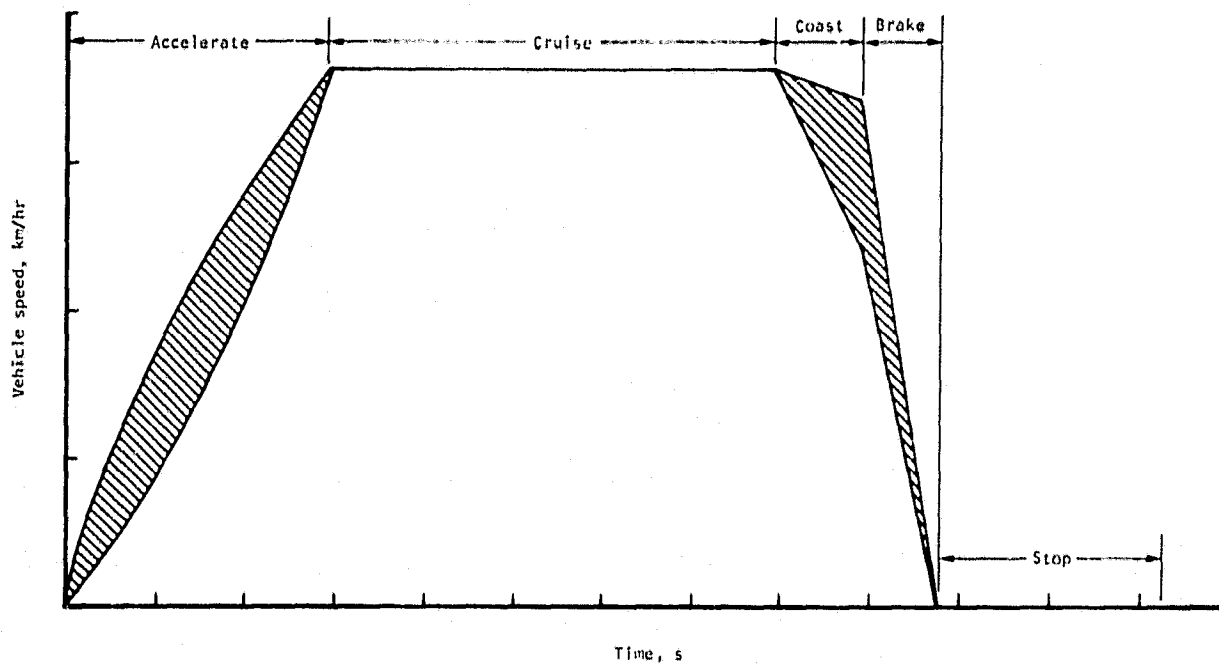
545797

Figure 19.--Methodology flow chart for concept 2.3, flywheel mode.

0.5-s calculation interval, are arithmetically summed to obtain the wall-plug energy and petroleum usage over the driving cycle.

The battery depletion increment, or delta (Δ) DOD, is computed for each sample interval. The DOD's are arithmetically summed to determine the percent of change in state of charge of the batteries at the completion of the driving cycle. The electrical range (battery = 80 percent DOD) is then computed from the distance traveled per cycle and percent change in DOD per cycle.

Each driving cycle profile that was used established velocity vs time in 0.5-s intervals, as required for the program input. The procedure that was used was to set the incremental accelerations so that the required propulsion system power was nearly constant. Fig. 20 depicts the velocity-time profile of a typical test cycle. The shaded areas are drawn to indicate that only the end points of each portion of the cycle are specified. Therefore, the shape of the acceleration portion of the curve can be deliberately varied by controlling the power applied. The speed at the end of the coast period depends on the vehicle drag and loss characteristics. The characteristics of the braking effort can also be varied; one such way is to vary the rate of regeneration to the battery or flywheel.



S 46104

Figure 20.--Typical driving cycle format.

Previous studies (refs. 1 and 2) have shown that vehicle range is definitely affected by the acceleration profile adopted in the driving cycle. If acceleration is accomplished at approximately constant power, the total range is five to ten percent greater than if acceleration is simply constant. Absolutely constant power, however, requires very high acceleration at low speed (fig. 21) which may be beyond the capability of the propulsion system, or beyond the ability of the tires to avoid slipping. Therefore, the acceleration schedule used for the driving cycle was nearly constant power, but lower at the beginning to stay within the capability of the system. The acceleration schedule used for the STC is presented in table 6.

Preliminary machinery sizing (power and operating speeds), propulsion system weights (including battery pack sizes), and vehicle test weights had to be calculated initially to provide the computer programs with the basic input information. The machinery power ratings, such as the heat engine, were approximately determined so that the applicable maps (i.e., performance characteristics representations) could be inserted into the programs. The reason for having more than one performance map for a given piece of machinery is that, in general, parametric scaling of physical systems should be limited to rather narrow bands about known characteristics. For example, the spark-ignition (SI) heat engine is described with four maps, designated A, B, C, and D. Map A describes a 37-kW

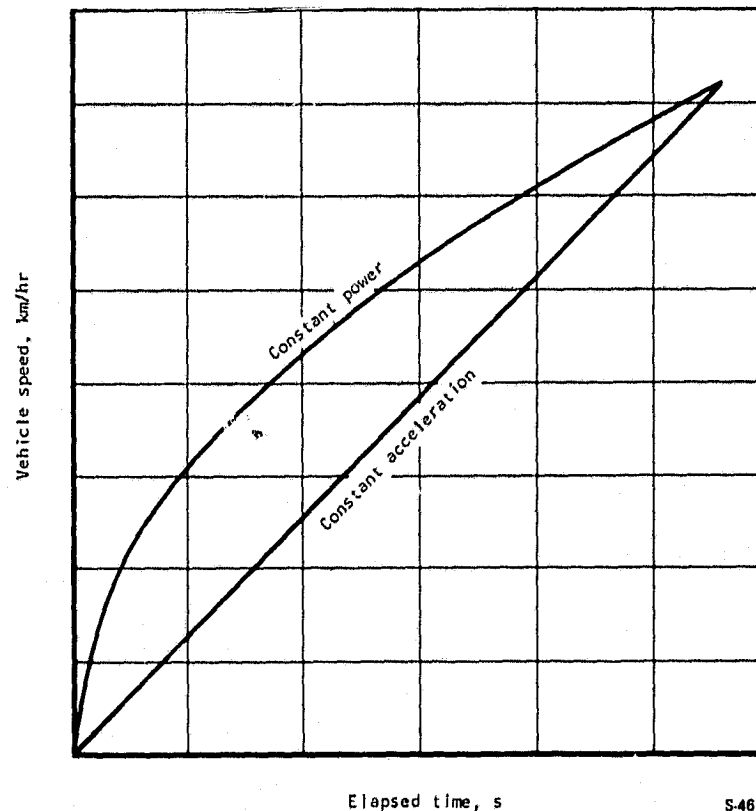


Figure 21.--Velocity schedules for typical driving cycle.

TABLE 8.--ACCELERATION SCHEDULE FOR STANDARD TEST CYCLE

Time, s	Velocity, km/hr
0	0
1	11.8
2	21.1
3	28.5
4	35.9
5	40.8
6	45.3
7	49.4
8	53.3
9	56.8
10	60.3
11	63.5
12	66.6
13	69.6
14	72.4

SI engine. The map was used when an engine of between 30-kW and 48-kW was required. If the propulsion system under parametric investigation required an engine size of greater than 48-kW, Map B was substituted for Map A in the computer program. Map B describes a 56-kW SI engine with a range of validity of 48 to 67 hp. These performance maps are described in a later section.

Battery simulation description.--Both the nickel-zinc and ISOA lead-acid batteries were used in the Task I parametric evaluation. A form of the fractional utilization method was used to calculate the energy usage per cycle and the DOD per cycle for both batteries.

Battery model: The principal measure of battery performance is derived from the specific power vs specific energy curve shown in fig. 7. Curves of this type are obtained by measuring the actual power/energy characteristics of a test cell. The cell is discharged from a 100 percent charge to complete

discharge at a constant power level. Measurement of the total energy expended (power x time) yields one point on the power vs energy chart. A locus of data points taken at various power levels yields the curves shown in fig. 7. Because these curves measure battery discharge characteristics, a model using these curves directly is accurate only for predicting discharge performance. A special interpretation is required to use the conventional power vs energy curve for charging performance that occurs when regenerative braking energy is put into the battery.

In general, the battery was viewed as being made up of two elements (a resistance and a capacity container) as depicted in fig. 22. The resistance has a value in ohms, and the container capacity has a value in W-hr. The reason for modeling the battery as shown is to be able to differentiate between the effectiveness of the batteries during discharging (removing energy) and charging (supplying energy).

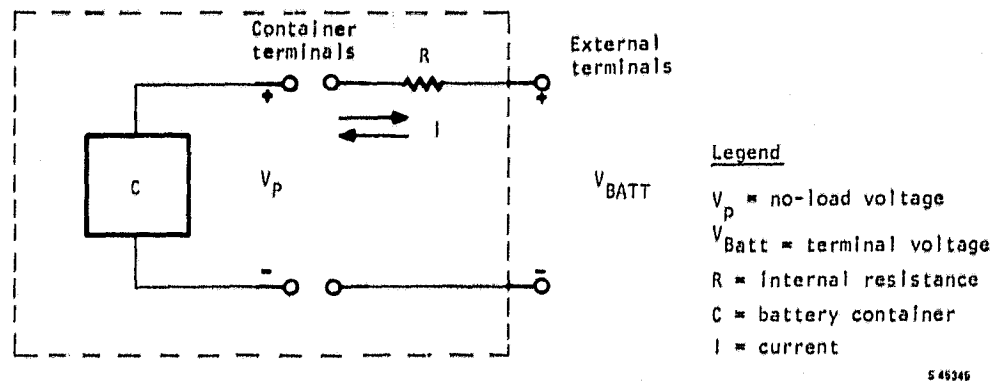


Figure 22.--Battery model.

The important point in comparing charging and discharging characteristics is that the resistance will always represent a loss of energy no matter which way current flows. Suppose the battery is being discharged so that 10 kW is available at the external battery terminals. The battery container must be discharging energy at a higher rate than 10 kW in order to overcome the internal resistance losses. Now suppose the battery is being charged from an external source at a rate of 10 kW. The battery container will not get the full 10 kW, but some lower value because of the internal resistance losses.

For example, during battery discharge the power available to do useful work (at the terminals), as seen in fig. 20, is $V_B I_d$, where V_B is external terminal voltage and I_d is discharge current:

$$V_B I_d = V_p I_d - I_d^2 R$$

The battery power/energy characteristic (fig. 7) may be entered directly with the value of $V_B I_d$ /battery weight (specific power) to determine the total amount of energy available. The term $(V_p I_d - I_d^2 R)$ is implicit in the use of the performance characteristic. The actual power supplied by the container (during discharge) is:

$$V_p I_d = V_B I_d + I_d^2 R,$$

which is greater, by the value of $I_d^2 R$, than what is measured by an external observer.

During battery charging the power available (at the external terminals) to the battery is $V_B I_c$. The question is: "How fast is the battery capacity replenished or charged as a function of power applied at the external terminals and how may the relationship between power and energy be characterized?"

The following reasoning is presented (see fig. 22). In the case where the battery is discharged at a rate that is defined by an external terminal voltage of V_B and a current of I_d , then the voltage is found as:

$$V_B = V_p - I_d R$$

and the discharge power is:

$$V_B I_d = V_p I_d - I_d^2 R$$

Now consider the case where the battery is charged at a rate that is defined by an external terminal voltage of V_B and a current of I_c , for which the voltage is found as:

$$V_B = V_p + I_c R$$

and the charge power is:

$$V_B I_c = V_p I_c + I_c^2 R$$

For the battery container to be affected in the same manner for both charge and discharge implies that the currents must be equal, i.e.,

$$I_d = I_c$$

If the currents are equal and the no-load voltage during the sample interval is constant, then the difference between the charge and discharge external terminal voltages is:

$$V_{Bc} - V_{Bd} = I_c R - (-I_c R) = 2I_c R$$

Then the equivalent power relationship is:

$$V_{Bc} I_c = V_{Bd} I_c + 2I_c^2 R$$

where:

$V_{Bc} I_c$ = equivalent charge power at terminals

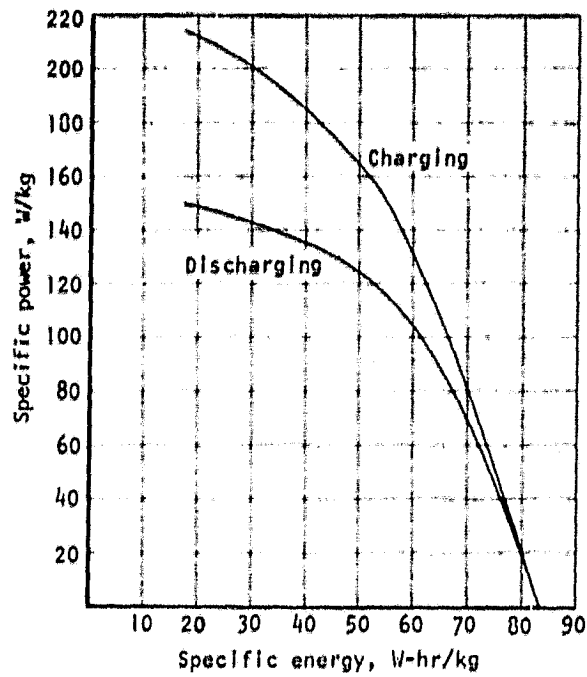
$V_{Bd} I_c$ = discharge power that is related to above charge power

$2I_c^2 R$ = equivalency factor between charge and discharge modes

It is, therefore, postulated that, "The measured power/energy density characteristic of the battery must be reinterpreted to be used to determine the amount of energy actually recovered by the battery as a function of charging power applied at the external terminals." The effect of this reinterpretation is shown in figs. 23 and 24 for the nickel-zinc and the lead-acid batteries, respectively.

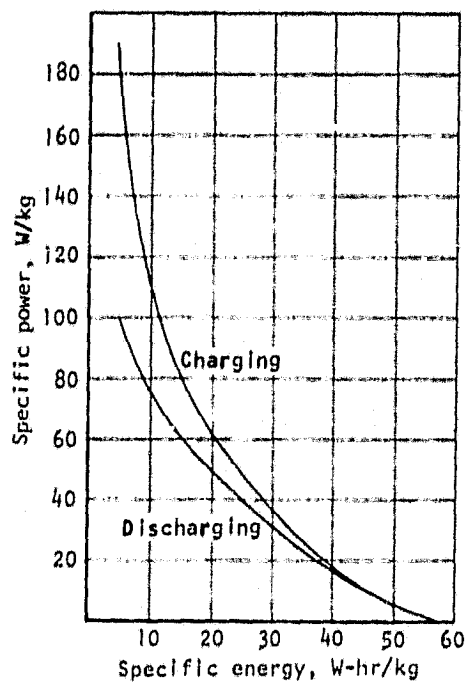
The difference between the battery charging and discharging characteristics are only significant at high specific powers and are due to the internal resistance of the battery. The charging curve is analytically derived by shifting the discharge characteristic by the value of $2I_c^2 R$. The postulated charging performance curve implies that at any given fixed power level and battery weight for which the specific power at the terminals is constant, more energy is required to charge the battery than was available during discharge.

The effect of neglecting the internal resistance of the battery is only apparent when the battery is used in an application where it receives energy by regeneration and is heavily buffered (during peak power periods) by a power source that has a separate energy supply, i.e., a heat engine that uses petroleum. As the electrical energy used (discharge) approaches the electrical energy received (charge by regeneration), the predicted vehicle electrical range becomes mathematically indeterminate.



S 46342

Figure 23.--Power and energy characteristics of the nickel-zinc battery.



S 46341

Figure 24.--Power and energy characteristics of the lead-acid battery.

Battery characteristics: Four characteristics were used to describe both the nickel-zinc and lead-acid batteries in the propulsion system simulation work that was done in this study. The characteristics are:

- (1) Power density vs energy density discharge performance (figs. 23 and 24)
- (2) No-load cell voltage vs depth of discharge (figs. 25 and 26)
- (3) Internal resistance vs battery pack weight (figs. 27 and 28)
- (4) Battery cycle life vs depth of discharge (fig. 29)

The power density vs energy density discharge characteristics for both the ISOA lead-acid and nickel-zinc batteries that are shown in figs. 23 and 24 were supplied by NASA as part of the contract. These characteristics were the primary ones used in the battery performance prediction procedures that are discussed in the next section.

The no-load terminal voltage vs depth-of-discharge characteristics for the two batteries that are shown in figs. 25 and 26 were obtained from the following sources:

- (1) Lead-acid characteristics were developed by AIRsearch from information on an existing ISOA battery, specifically, the high-energy density Eagle-Picher EP200AH (ref. 3).
- (2) Nickel-zinc characteristics were extracted from a Yardney design and cost study report (ref. 4).

The internal resistance characteristics presented in fig. 27 were developed by AIRsearch based on packaging technology and SOA power density. Basic battery pack definitions were previously shown in table 3. The baseline internal resistance for each battery pack (lead-acid and nickel-zinc) was predicted using the data in the table and the fact that the maximum power transfer from the battery to a load, P_{max} , occurs when the battery's internal resistance equals the load resistance. Thus:

$$P_{max} = V_p^2 / 4R$$

For this study the battery pack voltage was held constant at the values shown in table 9. It was decided to maintain the voltage of the battery pack constant for all systems to provide a standard of comparison and to scale total energy capacity in proportion to total weight. It was assumed that a battery could be constructed with the exact proportion of energy capacity and weight needed for each particular application. Therefore, as battery pack weight was varied during the parametric investigations, the internal resistance was changed as follows:

$$R = \frac{\text{Basic batt. wt.}}{\text{New batt. wt.}} \quad (\text{Total internal resistance})$$

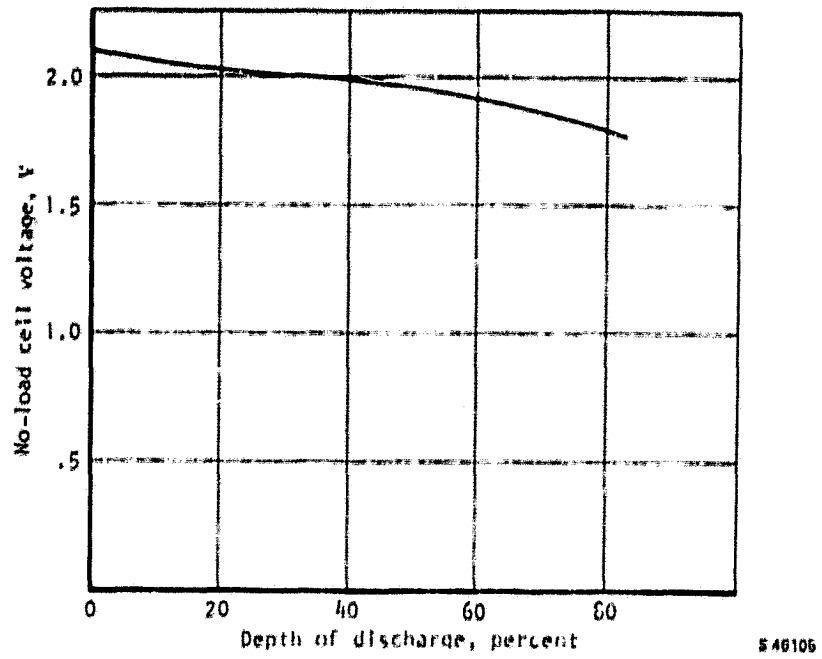


Figure 25.--No-load cell voltage for lead-acid battery.

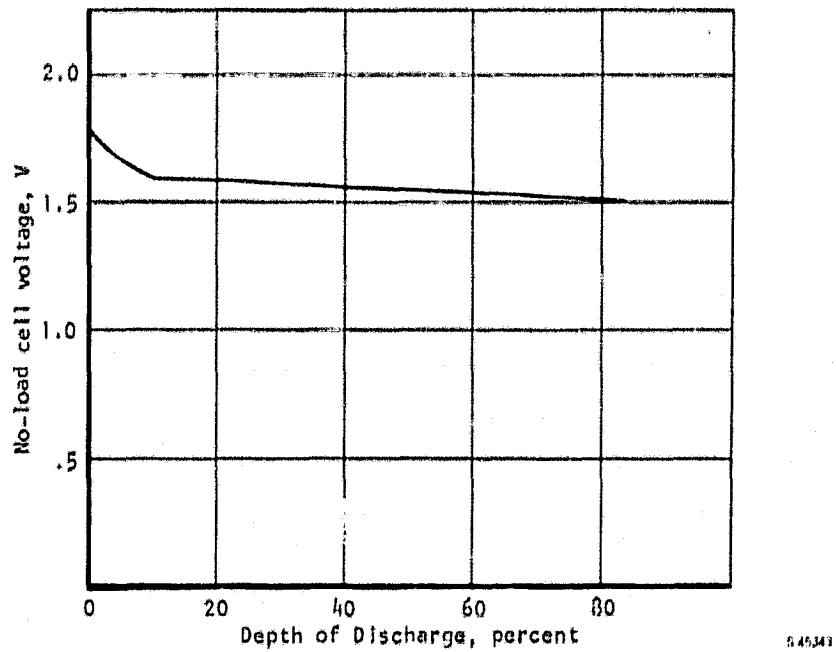


Figure 26.--No-load cell voltage for nickel-zinc battery.

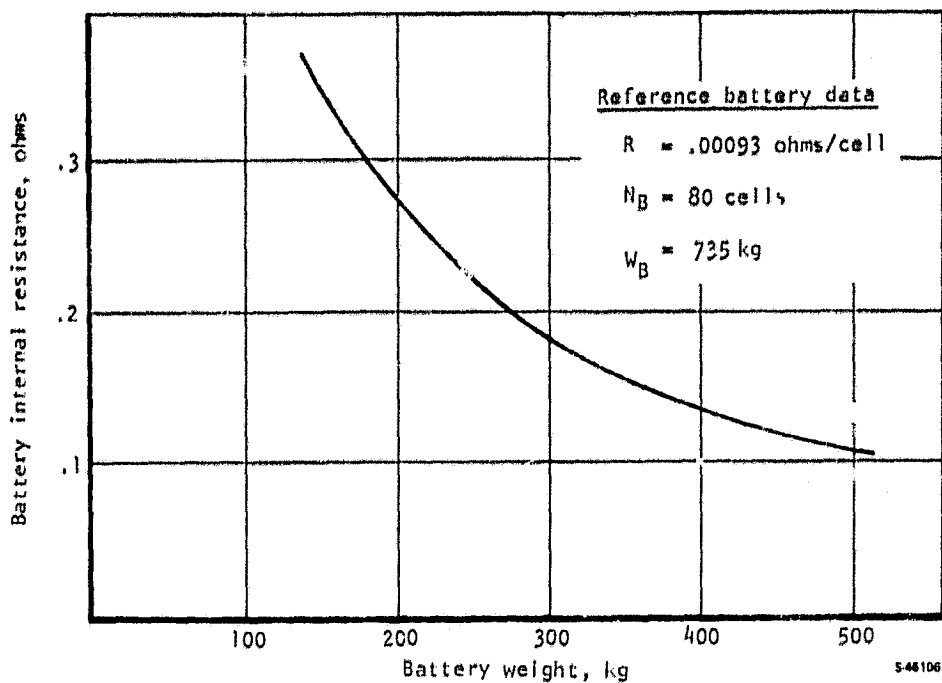


Figure 27.--Internal resistance characteristics of lead-acid battery.

The battery cycle life vs depth of discharge is shown in fig. 29. This relationship and baseline cycle life for each battery type was supplied by NASA as part of the contract. The information was used to calculate the battery life-cycle cost by determining the number of battery pack replacements in a 10-year period as a function of how the battery is used.

TABLE 9.--BASELINE BATTERY PACK DEFINITIONS

Battery type	Battery pack voltage	Weight based on SOA pack-aging techniques	SOA power density	Internal resistance, ohms		Variation with battery pack weight
				Total	Per cell	
Lead-acid	168 V	735 kg based on SOA Eagle-Picher EP200AH	100 w/kg	0.074 for 80 cells	0.00093	$R_{\alpha} \frac{1}{\text{Battery weight}}$
Nickel-zinc	160 V	386 kg based on Yardney design, report 2033-76, dated 10-76	150 w/kg	0.104 for 100 cells	0.00104	$R_{\alpha} \frac{1}{\text{Battery weight}}$

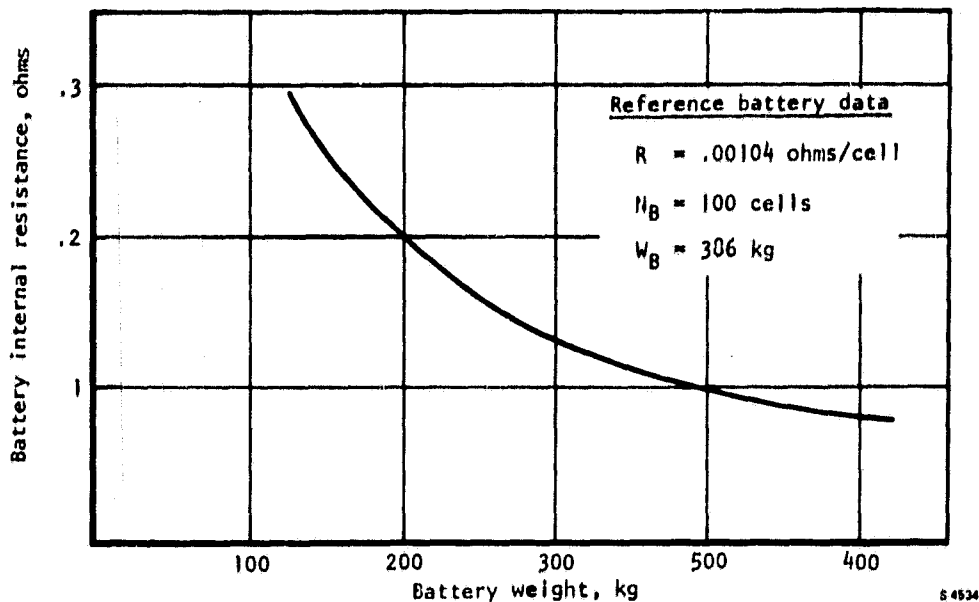


Figure 28.--Internal resistance characteristic of nickel-zinc battery.

Battery computer methodology: The calculation procedure used to predict the performance of both the nickel-zinc and the lead-acid batteries is summarized in fig. 30. Shown in the figure are the computer flow chart and the equations that were used to predict the bottom-line-performance, i.e., electrical range of vehicle. The calculation procedure begins with the power required at the battery terminals (P_{in}). Using the relationship shown as equation 2, the battery current is calculated. The nickel-zinc battery no-load voltage is set at 155 V and is not varied as a function of depth-of-discharge (DOD). This procedure is valid because the no-load voltage remains relatively constant up to 80 percent DOD (see fig. 26). For the lead-acid battery, the drop in no-load voltage with DOD (see fig. 26) is approximated by using two values, i.e., 160 V for the DOD region defined by 0 percent < DOD < 60 percent and 148 V for the region 60 percent < DOD < 80 percent.

The specific power is calculated and used to determine the battery specific energy during the sample interval. If the battery is being discharged, specific energy is read from the discharge curve in figs. 23 or 24. If the battery is being charged, however, such as occurs during regeneration, specific energy is read from the charge curve in figs. 23 or 24.

The incremented DOD, for the sample interval, is calculated by dividing the specific power by the specific energy and multiplying by the sample time interval. An accumulated DOD value is calculated for the total driving cycle, which is the sample interval discharge incremental DOD minus the sum of each sample interval charge incremental DOD. The 80 percent DOD range is then predicted.

In the case of the lead-acid battery, an accumulated DOD is calculated using a terminal voltage of 160 V, and a second accumulated DOD is calculated using a voltage of 148 V. The vehicle range is predicted as shown in fig. 30.

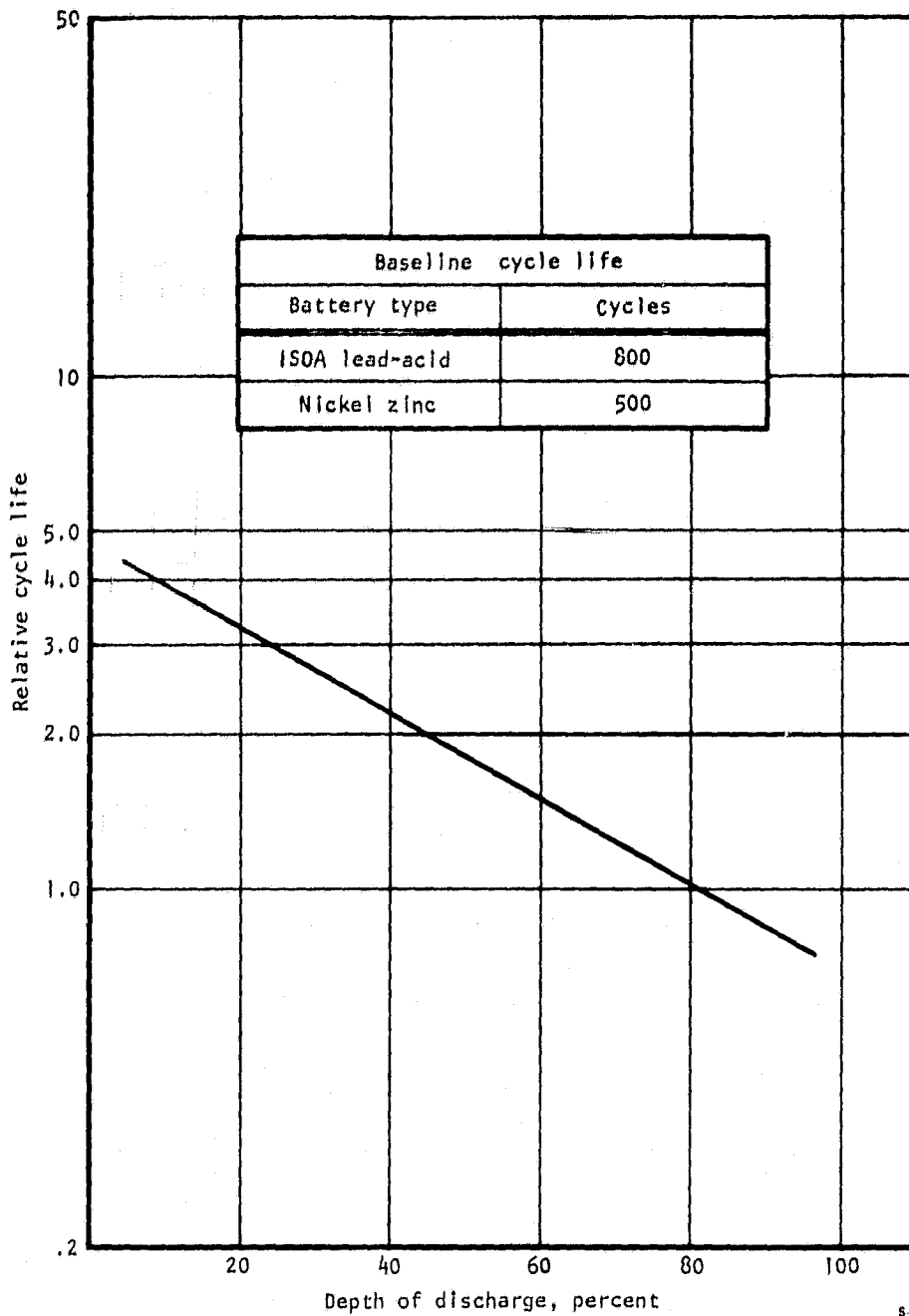


Figure 29.--Battery cycle life vs depth of discharge.

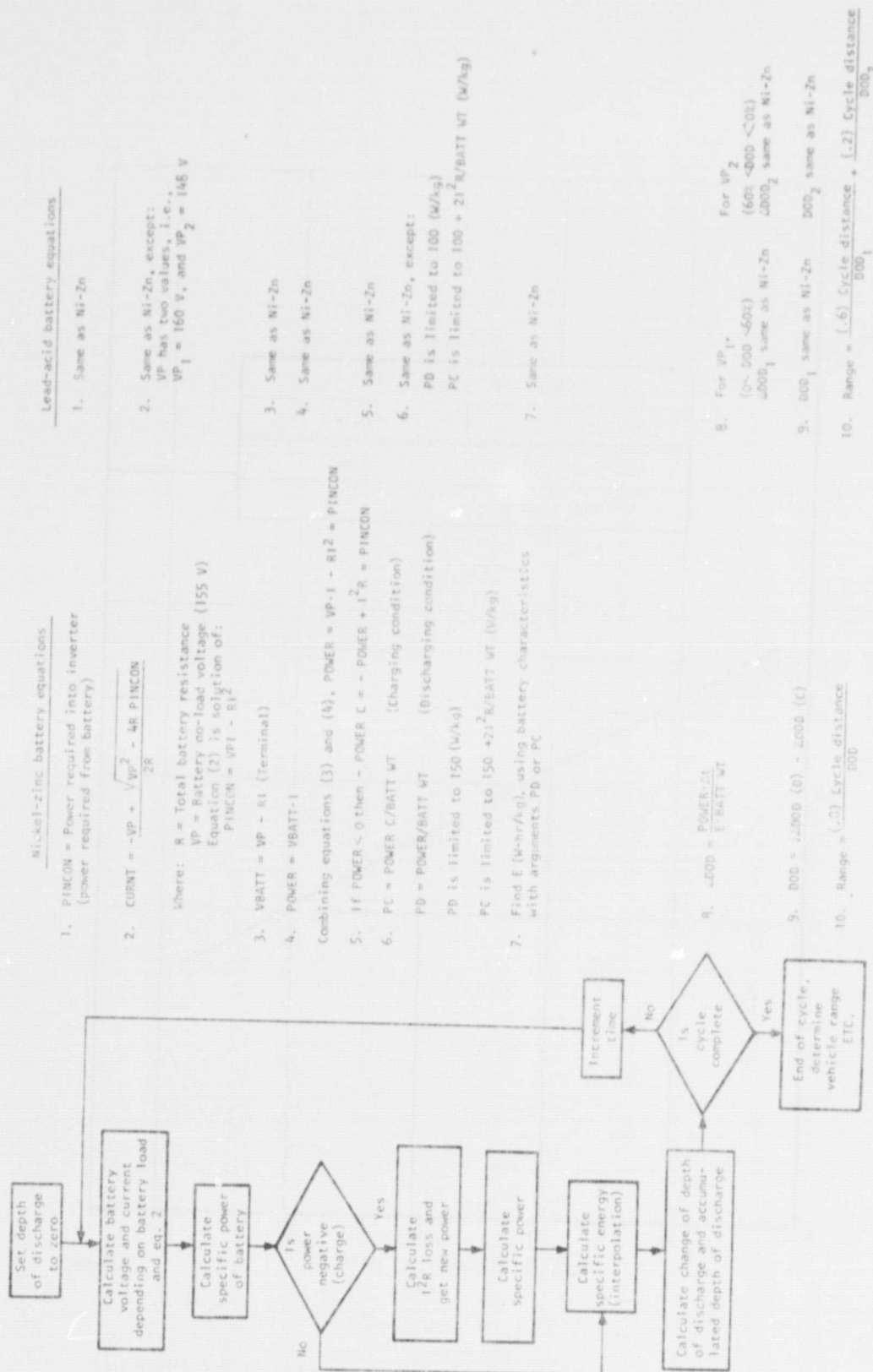


Figure 30.--Battery computer methodology.

Battery performance calculation procedure comparison: There are many methods used for calculating how a battery responds to the varying load demands that are encountered in a vehicle application. The method used in this advanced hybrid propulsion system study is based on the fractional utilization concept (ref. 5). The calculation procedure used in this study was compared with an averaging procedure being developed by NASA to determine how sensitive the prime electrical range of the propulsion system was to the battery performance prediction method used. The results of this comparison are shown in fig. 31 for concept 1.1 for both a nickel-zinc and lead-acid battery pack of 273 kg that is used on a vehicle with a test weight of 2157 kg.

The propulsion system used power sharing between the battery and the heat engine during acceleration, used the battery only for cruise, and regenerated into the battery during braking. The special test cycle (STC), shown in fig. 6, was used to predict prime electrical ranges.

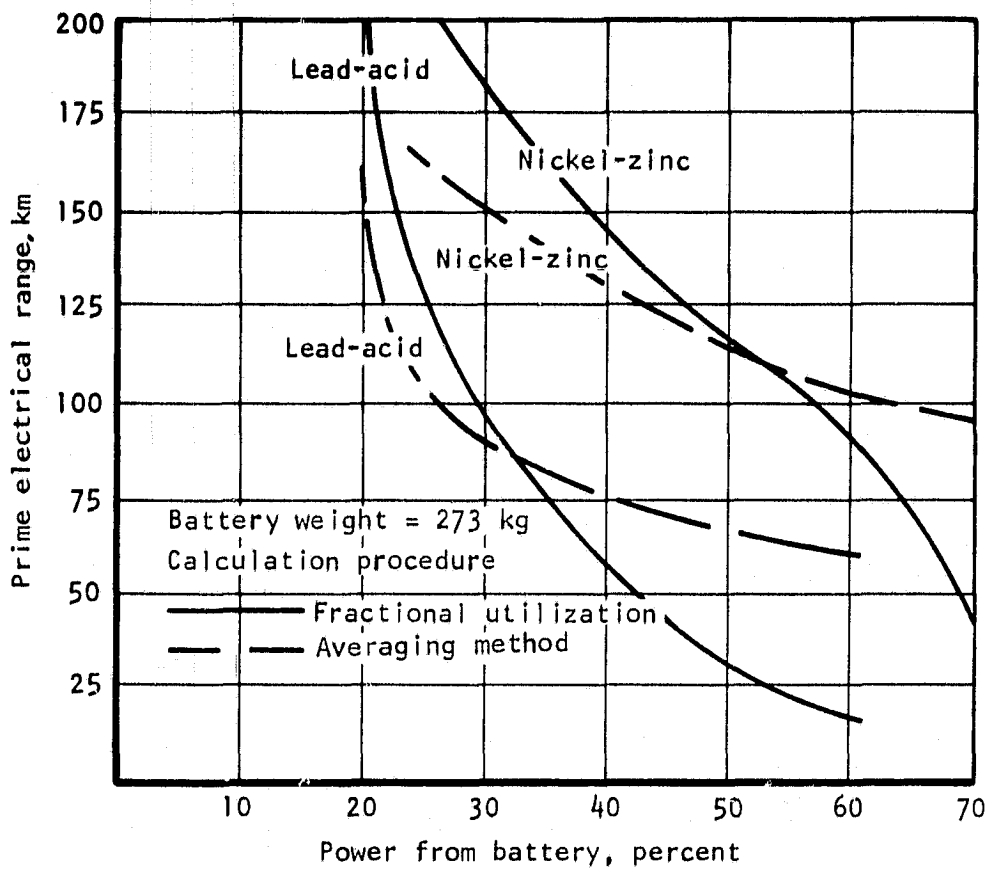
Prime electrical range (ordinate axis, fig. 31) is defined as the distance the vehicle can travel prior to the battery reaching 80 percent depth of discharge. The percent of power from the battery (abscissa axis) represents the degree of power sharing between the battery and heat engine during the STC acceleration leg. Thus, as the percent of power from the battery decreases, the engine power contribution increases, which implies increased use of petroleum energy over the driving cycle. The reason that battery power contribution values greater than 72 percent are not shown in the figure is that neither of the 273-kg battery packs provide enough power to transverse the STC without being aided by the heat engine.

The following conclusions may be drawn from the data presented in fig. 31:

- (1) The lead-acid battery is more sensitive than the nickel-zinc battery to the two calculation methods discussed.
- (2) The averaging calculation method predicts longer prime electrical ranges than does the method used in this study, as the percent of power from the battery increases, i.e., as the total power approaches pure electric power.
- (3) The more heavily the battery is buffered by the heat engine (decreasing percent of power from the battery), the closer the two prediction methods agree.
- (4) For a hybrid propulsion system, the two performance estimation methods (fractional utilization and averaging) converge in the range of power splits of interest (convergence zone identified in fig. 31).

It is concluded, that for a hybrid propulsion system, the two methods discussed will predict essentially the same battery performance.

The hybrid study battery estimation procedure was placed into the performance model that was used in the NASA/AiResearch advanced electric propulsion system study (ref. 16). An unbuffered propulsion system configuration from the referenced study was evaluated using the battery model from the hybrid study,



S-46170

Figure 31.--Battery performance calculation method comparison for a hybrid propulsion system.

as previously described. The SAE J227a schedule D driving cycle was used. The vehicle power was provided by a 679-kg lead-acid battery pack, and the vehicle test weight was 1668 kg. Regeneration during braking was into the battery pack.

A comparison was made between the hybrid study battery model used in this study and the "Driving Cycle Dynamic Program" used in the previously referenced advanced electric propulsion system study (ref. 16). The advanced electric study reported an electric range of 164 km for an unbuffered electric vehicle. The hybrid study battery model was then used in the advanced electric computer program to predict the range of the same unbuffered electric vehicle. The hybrid battery model predicted a range of 188 km. Therefore, the two calculation procedures correlate within 15 percent.

The advanced electric propulsion system performance model, with its own battery model intact, was used to show how power demand on the battery affects the range of an unbuffered electric propulsion system. This was accomplished by modifying the J227a(D) driving cycle to use a higher acceleration from 0 to 72 km/hr. Several rates were selected, of which the highest rate is acceleration of 0 to 72 km/hr in 12.3 s. This highest rate is representative of rates used in the Federal Urban Driving Cycle. The results, presented in fig. 32, show that the basic system has a considerable sensitivity to acceleration, with a range decrease of over 50 percent at the highest acceleration rate. It also predicts that the nickel-zinc battery has less sensitivity to increasing power demands than the lead-acid battery.

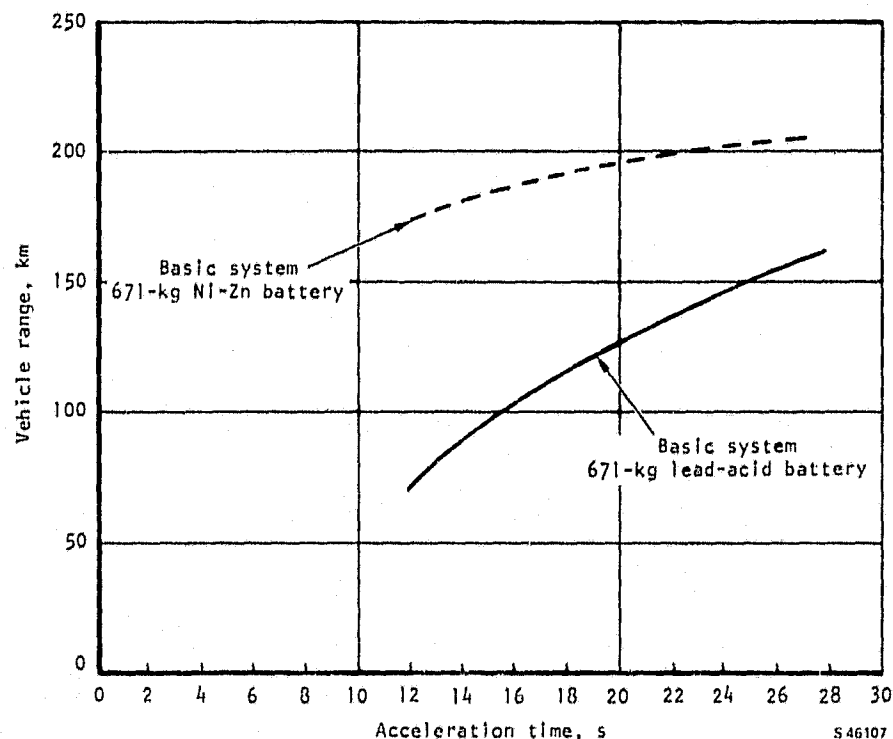


Figure 32.--Range comparisons with driving cycle using varying acceleration rates

In conclusion the battery performance prediction technique that is used in the hybrid study correlates well with

- The proposed NASA averaging method when used in a hybrid propulsion system performance model as long as the battery is buffered
- The AIResearch driving cycle dynamic program used in the advanced electric propulsion system study

In addition, the hybrid battery model predicts that lead-acid and nickel-zinc batteries are sensitive to high power demand driving cycles. This conclusion agrees with the trends that are obtained when the advanced electric propulsion system battery model is used.

Hardware Performance Maps

Hardware component performance maps were prepared for insertion into the digital computer programs that were developed for each propulsion system concept. These maps were based on available information for existing components or for components proposed for near term (1983) development. In most cases some extrapolation of existing data was required to meet the desired power and speed characteristics.

Heat engines.--Three types of heat engines were characterized and used in the study. The baseline engine was a conventional spark-ignition type. The other two types were a modern high-speed diesel and a single-shaft advanced gas turbine that used ceramic technology.

Spark-ignition engine performance: Three engine sizes were characterized. The basic data were for a 56-kW internal combustion engine that was obtained from ref. 6. The basic engine map was scaled using the following factors to obtain the other maps:

- (1) 37-kW size, using 4.3 percent brake specific fuel consumption (BSFC) penalty
- (2) 75-kW size, using 5.0 percent BSFC improvement
- (3) 112-kW size or greater, using 10.0 percent BSFC improvement

The resulting engine maps are shown in figs. 33 through 35.

Diesel engine performance: Three diesel engine sizes were characterized. The basic data were for a 40-kW modern high-speed engine that is currently used in passenger automobiles. The data were obtained from ref. 7. The basic engine map was scaled using the following factors to obtain the other maps:

- (1) 56-kW size, using 2.5 percent BSFC improvement

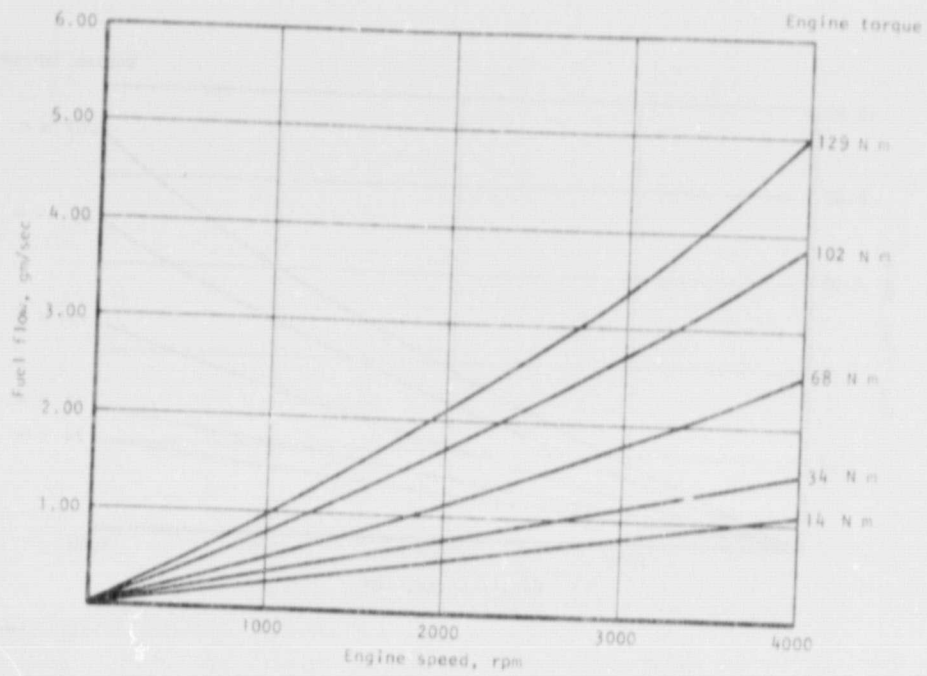


Figure 33.--Map of 56-kW engine.

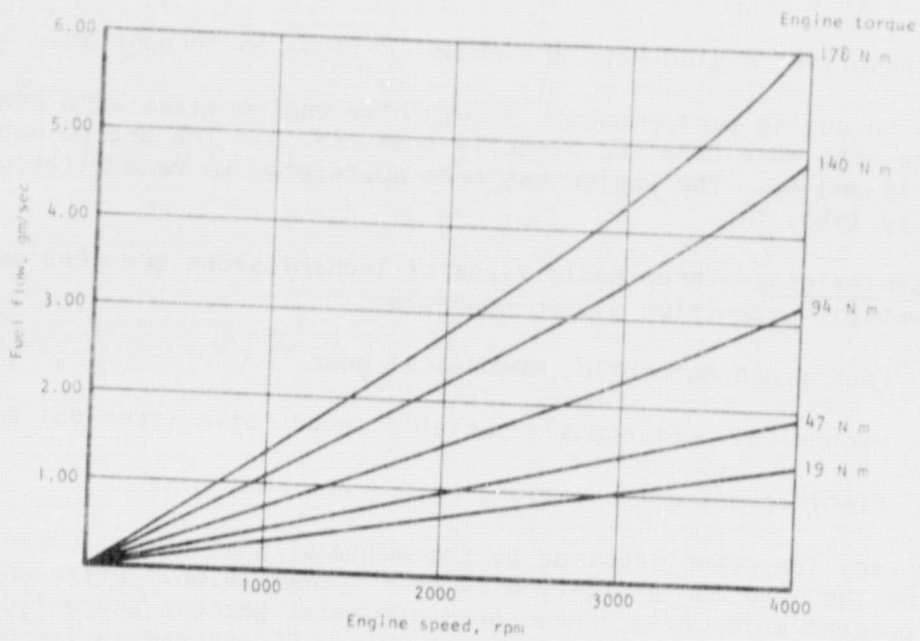
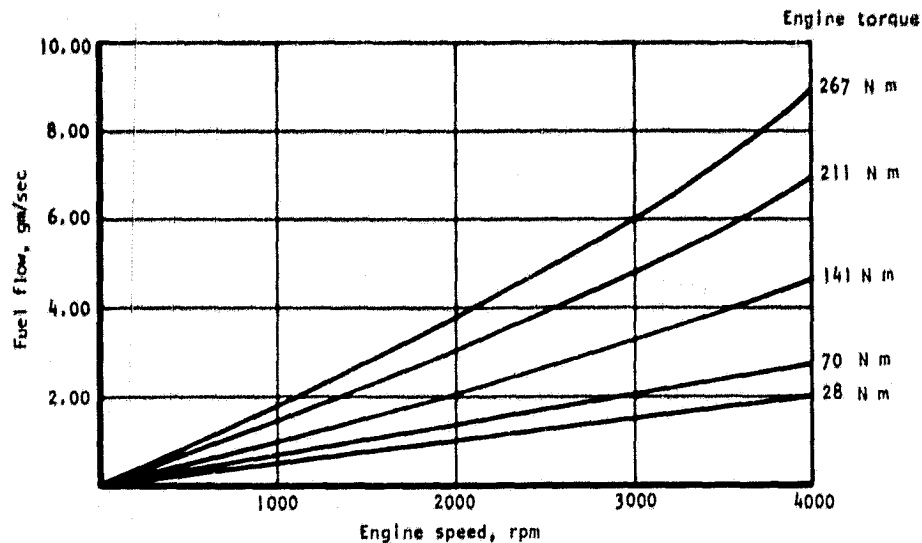


Figure 34.--Map of 75-kW engine.

ORIGINAL PAGE IS
OF POOR QUALITY



S 44173

Figure 35.--Map of 112 kW engine.

- (2) 75-kW size, using 5.0 percent BSFC improvement
- (3) 112-kW or greater using 10.0 percent BSFC improvement

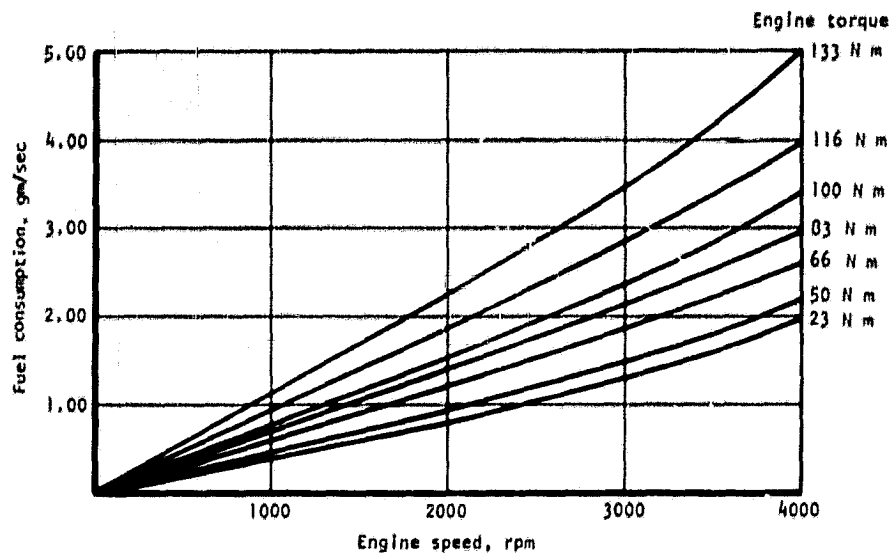
The resulting engine maps are shown in figs. 36 through 38.

Turbine engine performance: Two turbine engine sizes were characterized. The engine data were obtained directly from ref. 8. The engine maps are shown in figs. 39 and 40. The engine has been postulated to be available for demonstration by 1983.

Transmissions.--Three basic types of transmissions are considered in the various vehicle/propulsion system concepts:

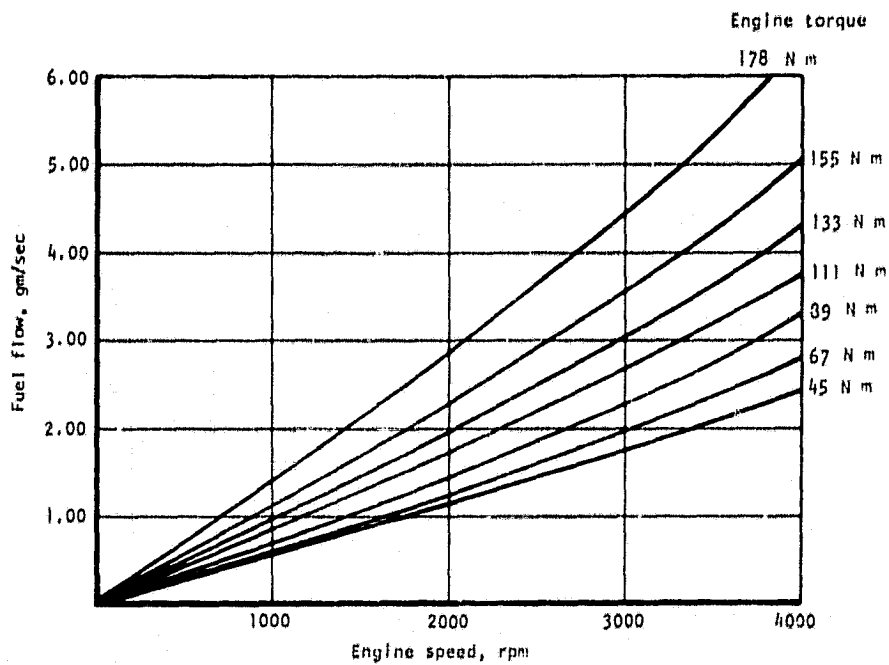
- (1) Four-speed automatic, mechanical gear
- (2) Mechanical continuously variable speed ratio (toroidal drive)
- (3) Electric drive (generator, motor, and controls)

The very low power required by the automobile at normal urban cruise speeds emphasizes the need for a highly efficient transmission. Efficiencies of a typical current automobile three-speed automatic gearbox and a typical forward and reverse gearbox are usually between 80 and 90 percent in the normal urban speed range (ref. 2). Such efficiencies can be improved by careful sizing of capacity and design of components.



S 46176

Figure 36.--Map of 56-kW engine (diesel).



S 46166

Figure 37.--Map of 75-kW engine (diesel).

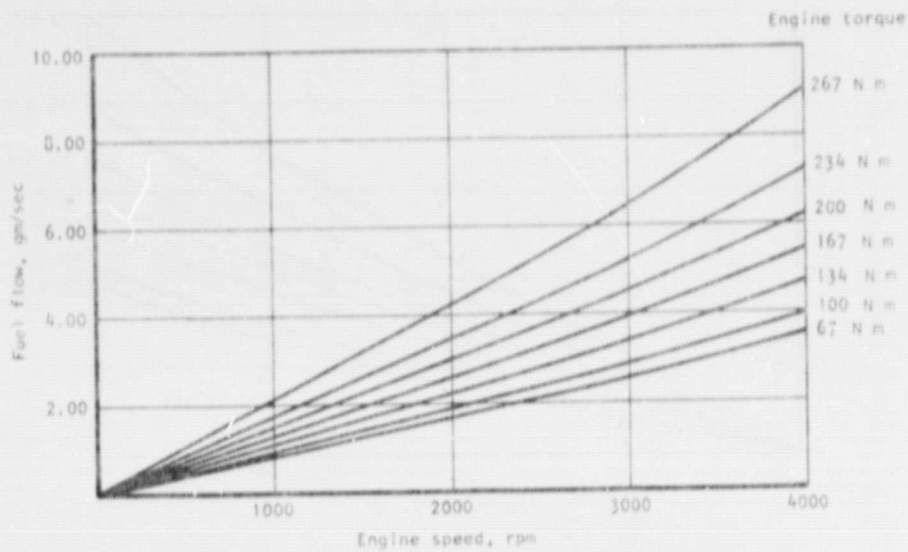


Figure 38.--Map of 112-kW engine (diesel). 648117

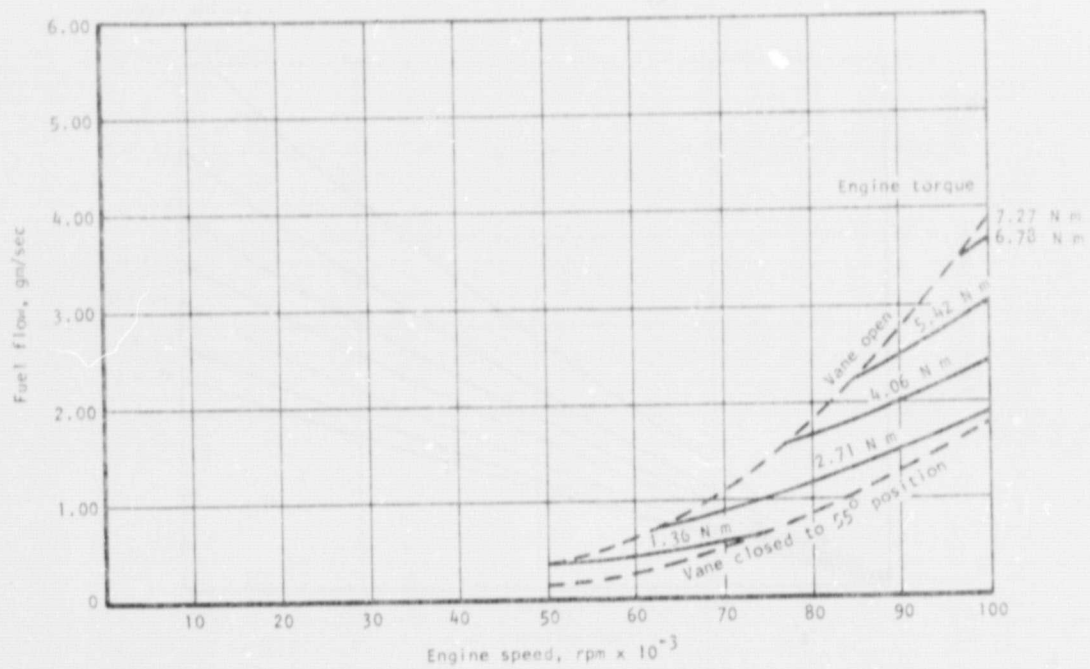


Figure 39.--Map of B of 75-kW turbine. 648117

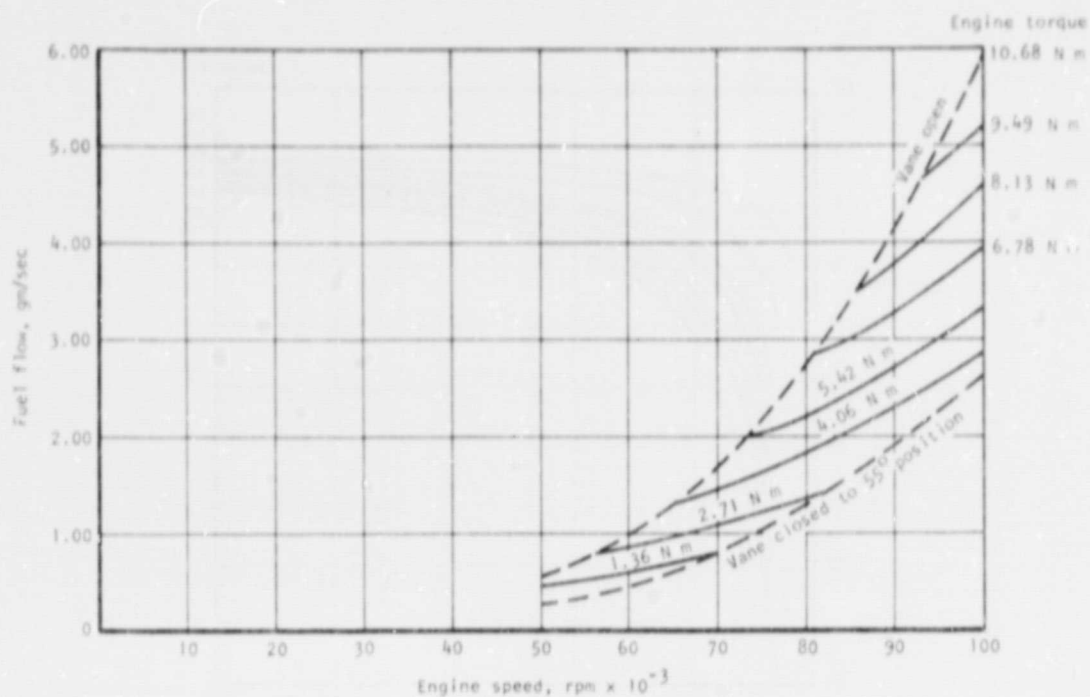


Figure 40.--Map B Of 112-kW turbine.

Four-speed automatic: Two of the Task I propulsion system concepts used a four-speed automatic transmission of contemporary design. The performance of the transmission was described in terms of gear ratios, shift schedule, and efficiency. The shifting schedule shown below was devised to favor the heat engine and electrical machinery so as to maximize the vehicle/propulsion system efficiency when operated over the study driving cycle.

Shift Schedule

Gear selected	Vehicle velocity, km/h
First	0 to 24
Second	24 to 48
Third	48 to 52
Fourth	72 to 105

An actual transmission design would have to allow for some speed overlap in shifting up and shifting down, but these details do not significantly affect the digital simulation. The performance map used is shown in fig. 41. It is representative of current passenger vehicle technology and was obtained from ref. 6.

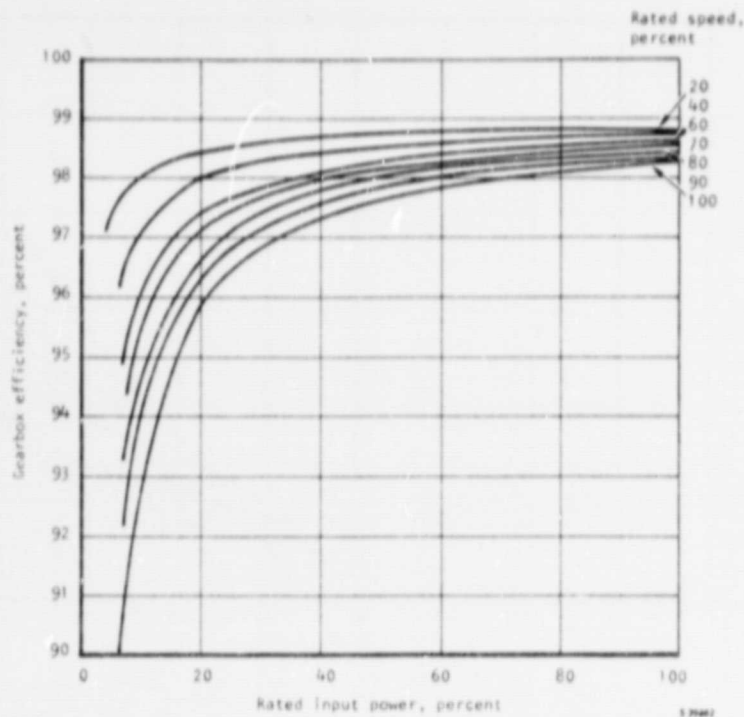


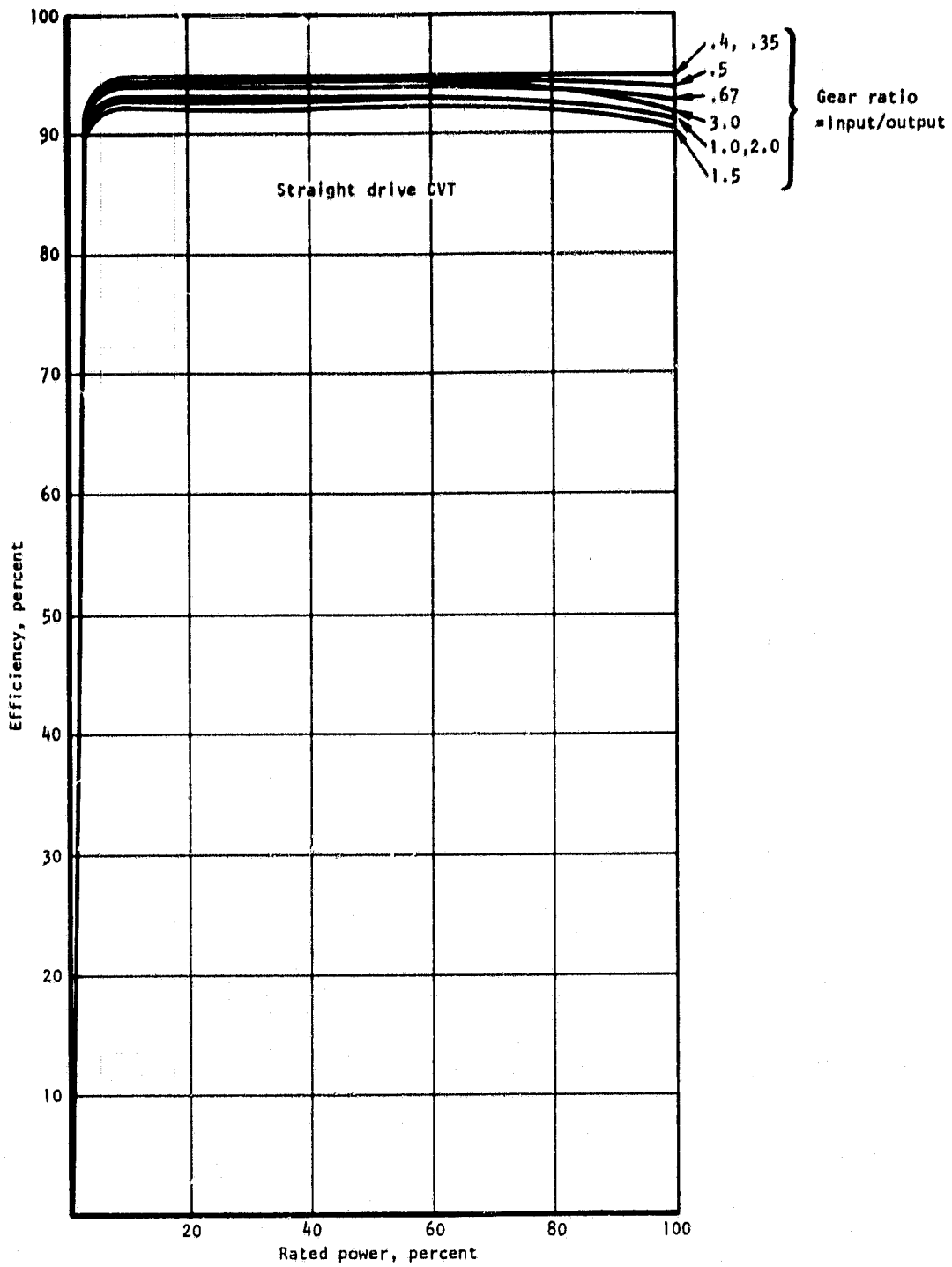
Figure 41.--Gearbox efficiency.

Traction transmission: A traction transmission employs some type of traction element in which power is transmitted through smooth rolling elements loaded against each other. By varying the position of the rolling elements, the speed ratio of the input and output can be smoothly and continuously varied from the minimum to the maximum value.

The transmission of power between smooth rolling surfaces requires a substantial normal force, but contact loads must be low enough to ensure an adequate fatigue life. Power transmission also is limited by the possibility of slip between the rollers, since slip leads to rapid wear failure. The method used to increase these limits involves the use of modern traction lubricants, which provide high resistance to slip and high viscosity to reduce wear. These new lubricants have considerably extended the power range of traction transmissions.

The information on proven traction transmissions is rather modest in power rating due to previous limitations in traction capacity. Now that higher powers are available, it appears entirely reasonable that automotive traction transmissions can be available by 1983. The performance map shown in fig. 42 was estimated for this study using the computer model that was developed by AiResearch as part of the NASA advanced traction transmission program.

Differentials and gearboxes.--All the propulsion system configurations employ a differential to permit relative motion of the wheels during change in vehicle direction, and to permit a reduction in drive train shaft speed. In addition, there is a need for a fixed-ratio gearbox in all of the configurations to supplement the basic speed reduction in the differential and transmission.



S-46167

Figure 42.--Straight drive CVT efficiency.

ORIGINAL DRAWING IS
OF POOR QUALITY

In practice, such a gearbox could be incorporated in the design of the differential or transmission, but to simplify the analysis procedure, it has been considered as a separate element.

Differential: The design of differentials is well advanced due to the many years of automobile applications; however, as recent studies have emphasized, the design criteria for typical automotive components are not completely suitable for electric and hybrid vehicle use (refs. 1 and 2). The use of hypoid gears in differentials is popular because it permits not only a 90-deg change in shaft direction, but an offset in the axis as well, so that the drive shaft can be lowered below the axle level. This arrangement is very desirable for a front engine drive to the rear wheels; however, for a close-coupled drive train mounted either in the front or the rear of a vehicle, a differential can be constructed using skew bevel gears or chain drives, which are more efficient than the typical hypoid gearing. This improved efficiency is particularly important for vehicles that use power regeneration, since hypoid gearing is very inefficient with reverse power flow (ref. 22). Also, improvements in lubrication techniques can eliminate the oil churning losses associated with the usual splash-type lubrication.

The overall differential and axle efficiency used in this study is shown in fig. 43. This performance map is based on work done on gas turbine transmissions (ref. 22) and illustrates the effect of both power and speed on efficiency. Rated power and speed for the transmission are the maximum vehicle conditions, and it is apparent they should not be overstated if maximum operating efficiency is to be obtained. The values are considered representative of current good design practice, and can probably be improved with careful design for a specific application.

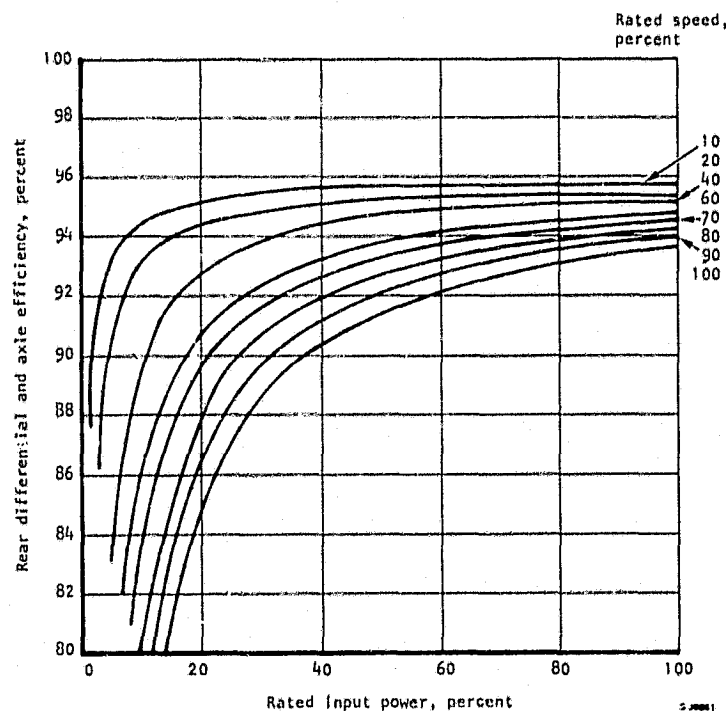


Figure 43.--Combined rear differential and axle overall efficiency.

Gearbox: Fixed-ratio gearboxes using straight spur or helical gear sets can be extremely efficient if proper care is taken to minimize bearing and lubrication losses. Maximum efficiency also depends on the reduction ration, with 1 to 1 being the best possible. The performance map (ref. 9) presented in fig. 41 has been used as representative of all the required gearboxes, through actual operating efficiency depends on the individual power and speed ratings used in each case.

Electric motors and controllers.--The traction motor must be considered in conjunction with a controller to achieve a particular performance characteristic. The motor also must be capable of functioning as a generator to achieve regenerative braking. In general, the approach is to use motors operating at a speed as high as possible to achieve the required power with minimum motor size and weight.

In this study two types of motors were considered:

- (1) Permanent-magnet, axial-gap motor, which is designated the baseline design
- (2) Dc, mechanically commutated shunt motor.

The permanent-magnet motor was designated by NASA as the baseline machine for the study. It was used exclusively for the Task I and II study efforts. The dc shunt motor was introduced into the study for comparison with the baseline motor. A discussion of the results of this comparison, including a description of the motor, is included in the sensitivity study writeup that is part of the Task II section of this report.

Permanent-magnet motor.--The permanent-magnet (PM) electronically-commutated, dc motor is a lightweight, high efficiency motor of the required power with the following features: The following particular features of the design contribute to this performance:

- (1) Field losses are eliminated.
- (2) Field cooling, which can be a problem in relatively small high-speed machines, is not required.
- (3) Slip rings are not required.
- (4) A variable-voltage field power supply is not required.
- (5) The performance equivalent of field weakening can be achieved in the electronic commutator by varying the switching angle with respect to motor back emf.

The disadvantage of the PM machine is the fixed field, which tends to cause undesirable losses at high speed. The losses can be minimized by using an axial-gap, ironless design.

This PM dc motor produces a speed-torque curve that is linear as the speed is increased from stall to rated speed. The voltage applied must also vary linearly with velocity. For a traction motor application, it is desirable to

have a suitable transmission so that the motor speed can be maintained within the optimum range for all driving conditions. In addition, a variable-frequency, inverter-type controller is needed to tailor motor operation to the imposed load.

The estimated PM dc motor performance characteristics shown in fig. 44 were derived based on the NASA advanced dc motor currently being developed by AIResearch. The machine scales in such a manner as to require only one performance characteristic to cover the power spectrum that was encountered in the Task I parametric study.

Power control unit: The controller for the PM dc motor must have a variable-voltage, variable-frequency capability.

The controller can consist of six silicon-controlled rectifiers (SCR's) plus one series transistor operated in pulse-width modulation (PWM) mode or six transistors operated in both PWM and commutation mode. The PWM is necessary to condition the input voltage down to the required volts per Hertz that constitutes adequate torque at the lowest current that is drawn. These controllers are now practical because of recent technological advances in:

- (1) Development of fast, high-surge current thyristors that can be made immune to high rates of di/dt and dv/dt .
- (2) Development of rapid signal processing and compact logic that provides gates, time delays, counters, thresholds, memory, and combinations at rates sufficient to drive ac motors. The logic and input/output (I/O) signal capacity in one compact microprocessor or one large-scale-integrated (LSI) circuit can handle the ac motor/generator plus energy management logic.

The controller losses for the performance simulation were modeled as follows:

$$\text{Controller loss} = (\text{Battery current}) \times (3 \text{ volts}) + 0.035 (\text{motor power})$$

Flywheel energy storage device.--The energy storage device used on several of the configurations is a flywheel. Recent studies (ref. 10) indicate the advantages of flywheels over alternative devices, such as hydraulic or pneumatic systems, and flywheels are currently being used in various automotive applications. Since the energy storage device is required only for maximum acceleration conditions and not for long grade situations, the required energy storage is not large. Based on work from previous studies (refs. 6 and 10), the baseline energy storage capacity of the flywheel (100 percent speed) was selected as 333 W-hr.

A useful index of the energy that can be stored in a flywheel is the specific energy, defined as:

$$\text{Specific energy} = \frac{\text{Kinetic energy}}{\text{Weight}}$$

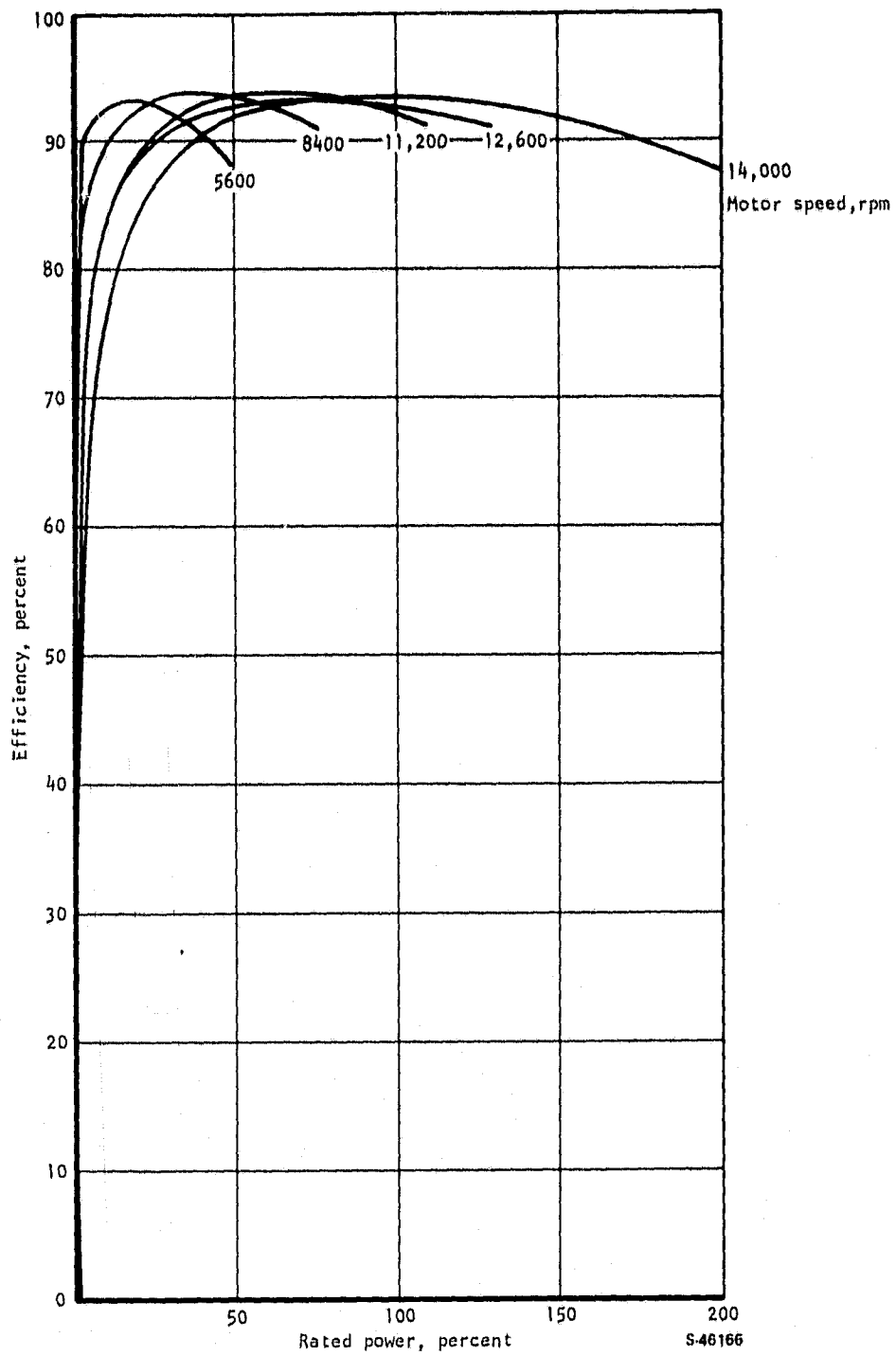


Figure 44.--PM dc motor performance.

There is a relationship between these terms and the flywheel geometry and material, expressed as follows:

$$\frac{\text{Kinetic energy} - K_S (\sigma/\delta)}{\text{Weight}}$$

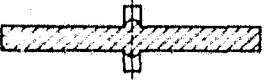
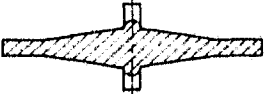
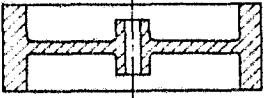
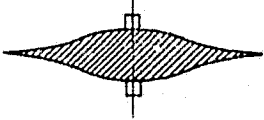
Where:

- K_S = nondimensional shape factor
- σ = allowable working stress
- δ = weight density

For flywheels fabricated from isotropic materials such as steel, a variety of shapes is possible; some common forms are shown in fig. 45. To take the best advantage of filament composite materials having directional stress properties, specialized flywheel designs are required (ref. 11). Some promising design configurations are shown in fig. 46. The composite flywheels have a relatively low shape factor (K_S); however, the high strength-to-weight ratio of composite materials more than compensates for their shape factor and provides a much higher specific energy and lower cost, as shown in fig. 47. Therefore, the selected flywheel configuration is a composite type.

The characteristics presented in fig. 47 do not represent specific designs, but are considered typical based on a number of units that have been built and operated (refs. 12 and 13). The relatively high containment weight for the steel flywheel is necessary because of the worst-case failure mode where relatively large pieces of material having appreciable energy must be contained. In contrast, the failure of a composite flywheel results in a mass of material in the form of fluff, which dissipates energy in internal friction. The cost numbers are based on material costs projected for 100,000 units. Costs include estimates of fabrication and assembly costs.

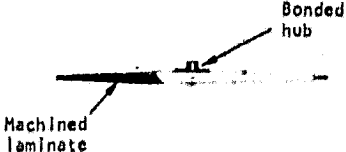
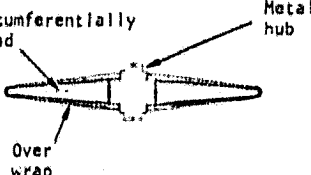
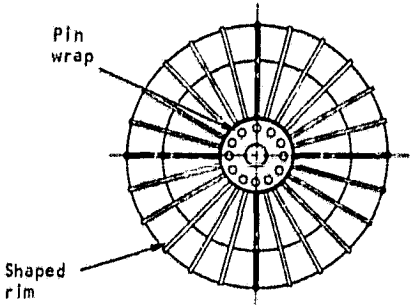
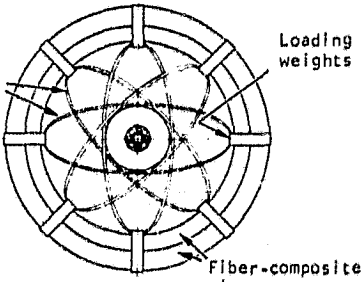
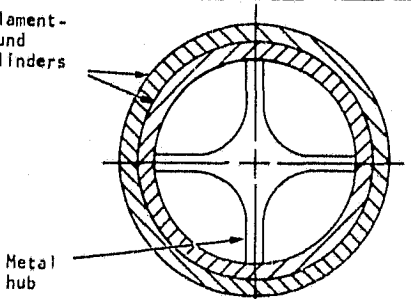
The loss characteristic for a vehicular size flywheel is shown in fig. 48 (ref. 6). This characteristic is a composite of the four major losses associated with flywheels: windage losses, bearing losses, dynamic seal losses, and lubrication and vacuum pumping losses. This loss characteristic used in the computer program was based on maximum full speed losses of 300 W for the 333 W-hr flywheel.

Flywheel configuration	Typical relative shape factor, K_s
1. Flat disc (with hole) 	0.30
2. Flat disc (no hole) 	0.61
3. Modified constant stress disc (with hole) 	0.45
4. Modified constant stress disc (no hole) 	0.90
5. Rimmed disc 	0.40
6. Constant stress disc (no hole) 	1.0 (OD \rightarrow ∞)

S-40158-A

Figure 45.--Flywheel geometry comparison.

ORIGINAL PAGE IS
OF POOR QUALITY

Flywheel configuration	Typical relative shape factor, K_s
<p>1. Laminated disc with bonded hub (General Electric)</p>  <p>Machined laminate</p> <p>Bonded hub</p>	0.30
<p>2. Circumferential core with tape overwrap (Rockwell)</p>  <p>Circumferentially wound</p> <p>Over wrap</p> <p>Metal hub</p>	0.30
<p>3. Filament wound rim with radial bands (Sandia)</p>  <p>Pin wrap</p> <p>Shaped rim</p>	0.35
<p>4. Concentric cylinders with composite catenary spokes (Brobeck)</p>  <p>Tension balanced spokes</p> <p>Loading weights</p> <p>Fiber-composite rings</p>	0.35
<p>5. Concentric cylinders with solid hub (AIResearch)</p>  <p>Filament-wound cylinders</p> <p>Metal hub</p>	0.35

S-40188-A

Figure 46.--Composite flywheel configurations.

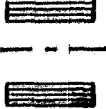
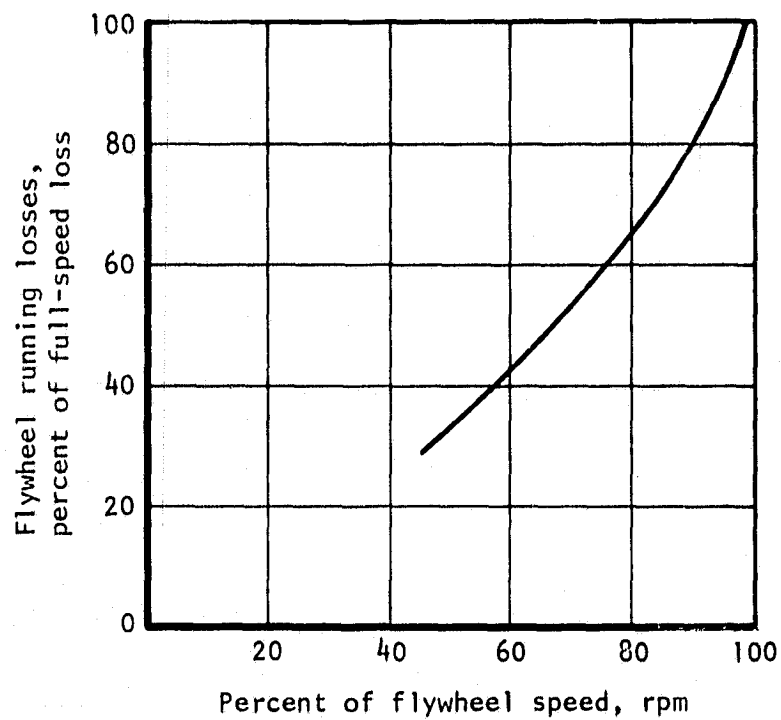
	Laminated rotor 	Multi-drum 	Multi-drum 
Material	Steel	E-glass epoxy	Kevlar epoxy
Rotor specific energy (W-hr/kg)	12.3	26.0	44.1
Rotor weight (relative)	1.0	0.47	0.28
Approx. housing and containment weight (relative to laminated rotor)	0.5	0.3	0.3
Flywheel assembly energy per assembly volume (W-hr/cm ³)	0.027	0.016	0.016
Flywheel assembly specific energy (W-hr/kg)	8.1	16.1	21.3
Flywheel assembly cost (\$/W-hr)	0.5	0.3	0.4

Figure 47.--Flywheel weight and cost comparisons.

S40120 A



S-46168

Figure 48.--Flywheel module loss characteristics.

Cost And Weight Analysis Procedures

This section documents the weight and cost analysis performed to evaluate the initial 15 vehicle/propulsion system concepts as well as the final selected system. During the Task I parametric studies, the 15 vehicle/propulsion system concepts were parametrically examined by varying battery pack weight, battery type (nickel-zinc and lead acid), and heat engine type. Two propulsion systems (concept 1.1 and 2.1) and one vehicle type (family sedan) were selected for a more in detailed evaluation (Task II, Design Tradeoff Studies) based on cost and potential for petroleum savings. During the Task II effort, a reference propulsion system was developed to provide baseline weight and cost information that could be used to help rank and select the final hybrid system. This reference or conventional system is comprised of a spark-ignition heat engine, automatic transmission, and differential, all sized to provide the family sedan with the performance necessary to meet the study requirements.

Weight analysis.--To evaluate and rank the five types of hybrid propulsion systems shown in figs. 1 to 5, it was necessary to associate the systems with specific vehicles to make performance estimations. NASA provided the weight estimation procedure to predict each vehicle test weight for the five mission/vehicle designations as a function of propulsion system weight. These weight relationships are displayed in tables 5 and 6 in the study ground rules section of the report.

Each propulsion system weight was estimated using the information contained in table 10. The source of the information along with the parametric weight relationships is also shown in the table.

A weight growth factor of 1.30 was used to adjust each vehicle test weight as a function of the propulsion system variations examined. Vehicle performance (i.e., acceleration, passing, and hill-climbing) was always maintained.

Cost analysis.--A life-cycle cost analysis was performed to aid in selecting the recommended hybrid propulsion system. The analysis consists of breaking down the lifetime vehicle costs into three cost categories: (1) research, development, testing, and engineering; (2) acquisition; and (3) ownership or operating costs. Each category is then further defined by its respective elements.

A digital computer program was developed so that answers could be generated quickly and results could be interpreted easily. The output of this program is used to display cost categories for each propulsion system considered.

In cost analysis performance the following premises were used:

- (1) All costs are based on 1976 figures.
- (2) Propulsion system lifetime is 10 years.
- (3) Propulsion system lifetime mileage is 160 000 km.
- (4) Cost estimates assume a production rate of 100,000 vehicle/propulsion systems per year.

TABLE 10.--PROPULSION SYSTEM COMPONENT WEIGHTS

Component	Type	Rating, kw	Weight, kg	Weight relationship (WR), kg/kw
Heat engine	(1) Spark- ignition (ref. 14)	(a) 56	171	3.06
		(b) 75	213	2.84
		(c) 112	293	2.62
	(2) Diesel, N.A. (refs. 7 and 15)	(a) 56	222	3.97
		(b) 75	283	3.77
		(c) 112	358	3.20
(3) Turbine (ref. 8)	(a) 56	102	1.83	
	(b) 75	137	1.83	
Transmission	(1) 4-speed automatic (ref. 14)	≥ 37	≥ 37	1.00
	(2) Mechanical CVT (ref. 14)	≥ 37	≥ 39.6	1.07
Electric motor	Electronically commutated, dc (ref. 16)	≥ 20	≥ 12	0.60
Power control unit	Solid-state inverter (ref. 16)	20 to 60 >60	18 to 55 >46	0.91 0.76
Flywheel, housing, and lube and vacuum system	Composite (ref. 12)	0.333 kW-hr	22.7	68 kg/kW-hr
Drive system	Front wheel drive (ref. 14)	>40	>26	0.66
Gearbox	Fixed ratio (ref. 6)	>20	>6	0.30

- (5) Recurring costs are averaged over the propulsion system lifetime.
- (6) Acquisition costs are suggested retail selling prices, which do not include transportation, dealer preparation, or sales tax.
- (7) Propulsion system acquisition cost (purchase price) is assumed to be the installed price to the consumer.

Research, development, testing, and engineering costs (RDT&E): This cost category represents the manufacturer in-house development effort prior to committing large capital investments required for mass production. In total RDT&E cost estimation, the following elements have been defined:

- (1) Initial engineering
- (2) Development tooling
- (3) Development support
- (4) Manufacture of the R&D vehicles
- (5) Test facilities
- (6) Test operations
- (7) Contractor profit

The general calculational algorithm for RDT&E costs is:

$$\text{Total cost} = (\text{element hours}) (\text{composite rate}) + (\text{man-hour related costs}) \\ + (\text{profit}), (\$)$$

RDT&E costs used in the present study are based on initial AIRsearch estimates. The impact on vehicle life-cycle costs is minimal for the assumed 5-year amortization period and the 100 000-vehicle/year production rate. The RDT&E costs were estimated to be about \$20.00 per propulsion system. This cost element is included for completeness.

Acquisition cost: The propulsion system acquisition cost comprises all cost associated with the manufacturing, distribution, and marketing of the system, as reflected in the sticker price. In estimating the manufacturing costs--namely labor, raw materials, and capitalization--each propulsion system was reduced to its components and subsystems.

The costs of the propulsion system components were obtained for existing components from ref. 14. The costs of new components were developed by AIRsearch. Cost estimating relationships (CER's) were based on these data. Table 11 shows the CER used, its dimensional units, where it was obtained, and the total manufacturing cost definition.

TABLE 11.--COST ESTIMATING RELATIONSHIPS (CER's)

Component	Type	CER reference	CER	Units
Heat engine	(1) Spark-ignition	Reference 14	1.05	\$/kg
	(2) Diesel, N.A.	Reference 14	1.16	\$/kg
	(3) Turbine	Reference 8	4.00	\$/kg
Transmissions	(1) Four-speed automatic	Reference 14	1.30	\$/kg
	(2) Mechanical CVT	Reference 14	1.42	\$/kg
Electrical motor	Electronically commutated, dc	Reference 16	15.95	\$/kg
Power control unit	Solid-state inverter	Reference 6	12.81	\$/kg
Flywheel, housing, and lube and vacuum system	Composite	Reference 16	13.2	\$/kg
Drive system	Front wheel drive	Reference 14	1.70	\$/kg
Gearbox	Fixed ratio	Reference 6	2.42	\$/kg
Battery	(1) Lead-acid	Contract	2.00	\$/kg
	(2) Nickel-zinc	Contract	6.00	\$/kg
Total manufacturing cost (includes variable and fixed material and labor costs, engineering tooling costs, and quality control costs)	----	Reference 6	Summation of CER values (see note, below)	\$

Note: $\sum_{i=1}^n (\text{CER})_i \times (\text{WR})_i \times (\text{RATING})_i$

The markup factors, as defined in table 12, account for all costs attributed to the distribution and marketing of the propulsion system. Sample calculations that show what the markup factors include are shown in table 12. The cost item definitions in the table result in an overall manufacturing cost markup factor for the propulsion system of 1.962. The battery is assumed to be a purchased item that is marked up by 1.30 for both the initial and replacement costs.

In Tasks I and II a curb weight and test weight for each baseline vehicle/propulsion system concept under investigation was estimated, as well as the cost of each baseline propulsion system. As the variables of interest of the study were parametrically changed, the weight and cost of each baseline propulsion system and the weight of vehicle were redefined. The new vehicle weights were calculated using a structural growth factor of 1.30. It required an iterative process to arrive at each new vehicle/propulsion system weight and cost definition.

Ownership (operating) costs: This cost category was used to develop the operating and maintenance costs for the candidate propulsion systems. The operating cost model that was used was defined in terms of 10-year life-cycle cost.

Cost definitions for each propulsion system component have been based on data from refs. 6, 16, 17, and 19, and the contract; on a history for similar components; and on duty-cycle environments. Table 13 lists the definitions used in this cost category.

Total propulsion system life-cycle cost: The sum of RDT&E, acquisition, and ownership costs presented above is the total system lifetime cost, or life-cycle cost of the propulsion system. This total cost was calculated on a system lifetime basis and a per-kilometer basis. The life-cycle costs for all the propulsion systems are presented in subsequent sections of this report.

TABLE 12.--PURCHASE PRICE OF PROPULSION SYSTEMS
WITH BATTERY PACK (SAMPLE CALCULATION)

Cost Item	Propulsion system concept X	
	With lead-acid battery	With nickle-zinc battery
Manufacturing cost of propulsion system	755	755
Manufacturing overhead (22%)	166	166
Cost of sales	921	921
General and administrative (25%)	230	230
Cost of propulsion system	1151	1151
Return on investment (10%)	115	115
Wholesale price	1266	1266
Dealer markup (17%)	215	215
Purchase price of propulsion system	1481	1481
Battery cost	1334	2238
Battery markup (30%)	400	672
Battery purchase price	1734	2910
Total purchase price	3215	4391

TABLE 13.--OWNERSHIP COST DEFINITIONS (10 YEAR PERIOD)

Component	Type	Determination method	Units	Reference
Heat engine	(1) Spark-ignition (2) Diesel, N.A. (3) Turbine	$732.20 + 10.83(\text{kW})$ where kW = power rating	\$	17
Transmission	(1) Four-speed automatic (2) Mechanical CVT	$37.66 \sqrt{\text{kg}}$ where kg = unit weight	\$	17,19
Electric motor	Electronically commutated, dc	No maintenance required over the life of the vehicle	\$	6
Power control unit	Solid-state inverter	$36.83 \sqrt{\text{kg}}$ where kg = unit weight	\$	6
Flywheel assembly	Composite	300	\$/kW-hr	18
Drive system	Front wheel drive	No maintenance required over the life of the vehicle	\$	17
Gearbox	Fixed ratio	$14.40 \sqrt{\text{kg}}$ where kg = unit weight	\$	17
Battery maintenance	(1) Lead-acid (2) Nickel-zinc	320	\$	16
Battery replacement	(1) Lead-acid (2) Nickel-zinc	2 6	\$/kg \$/kg	Contract Contract
Battery salvage	(1) Lead-acid (2) Nickel-zinc	10 percent of purchase price	\$	Contract
Petroleum*	(1) Gasoline (2) Diesel	0.40 0.36	\$/liter \$/liter	Contract Contract
Electricity*	Wall-plug	0.06	\$/kW-hr	Contract

*1985 estimate

TASK I ANALYTICAL RESULTS

A summary of the initial or baseline data that defines each vehicle propulsion system concept investigated in Task I is shown in fig. 49. Parametric investigations around the baseline definition of each concept were performed by varying battery weight and observing the effects on the following parameters:

- Prime electrical range
- Heat engine fuel usage
- Annual fuel usage
- Acquisition cost (1976 \$)
- Life-cycle cost (1979 \$)

In addition, the importance of buffering the battery with another power source, identified as a 50/50 power split (fig. 49), was examined and the results are presented below. The parametric propulsion systems were sized to conform to both the performance requirements of the study and the Task I ground rules.

The spectrum of baseline vehicle/propulsion system concepts had vehicle test weights that varied between 1222 kg (concept 1.1A) and 6088 kg (concept 2.2D). The baseline vehicle test weights varied between 3084 and 14 061 kg. The acquisition costs of the baseline propulsion systems varied between \$2897 (concept 1.1A, lead-acid battery) to \$14 927 (concept 2.1D, lead-acid battery).

Task I Hybrid Propulsion System Parametric Results

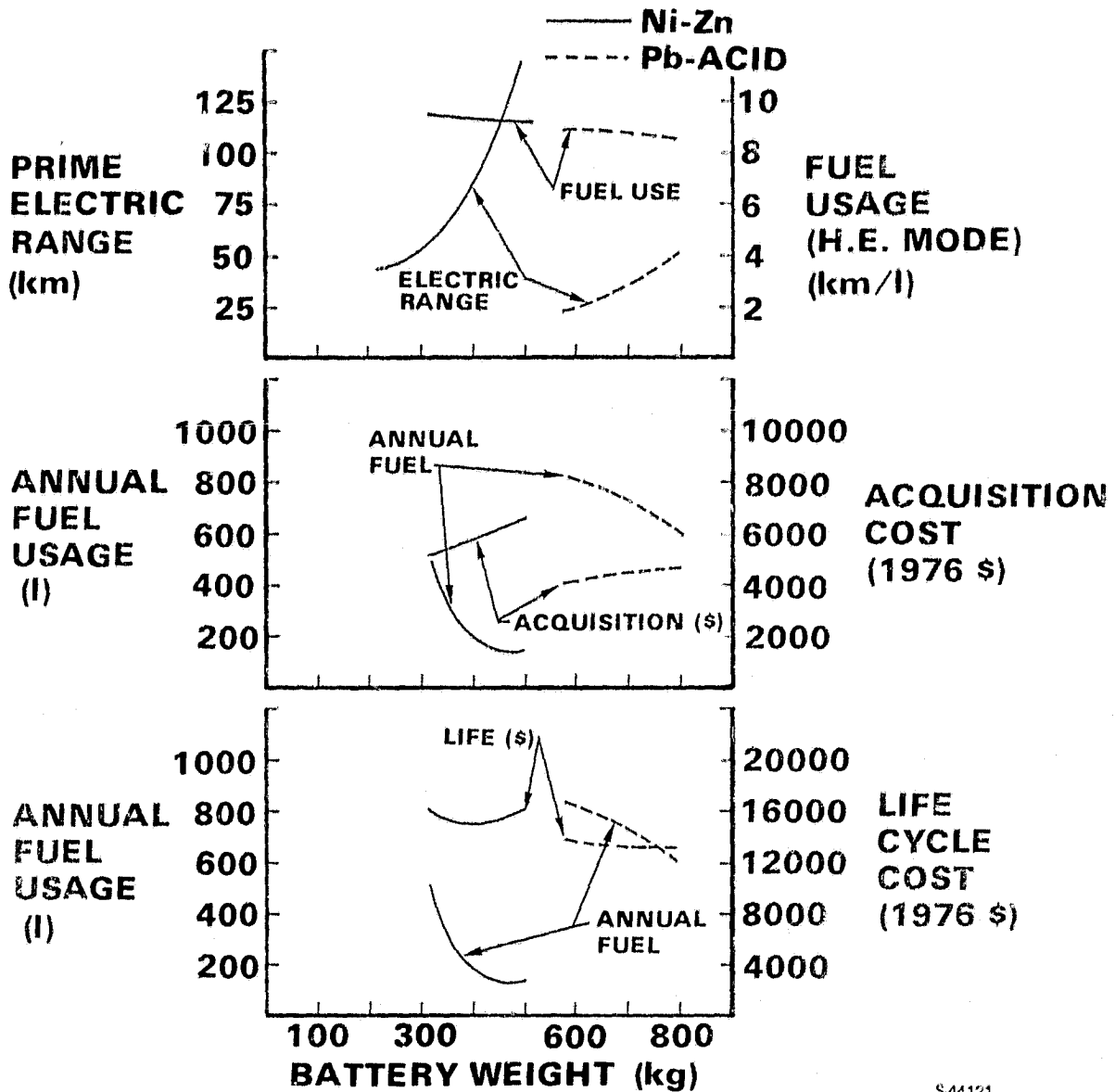
Typical results of the Task I parametric studies are shown in figs. 50 and 51 (a complete set of the results is presented in Appendix A). The results in fig. 50 are for vehicle/propulsion concept 1.1B for both nickel-zinc and lead-acid batteries. The results are presented in terms of the five most important parameters as a function of battery type and weight. In the upper plot of fig. 50, the prime electric range (km) and heat engine mode fuel usage (km/liter) are displayed for both nickel-zinc and lead-acid batteries. In Task I, the battery and the heat engine were sized in such a way that they were not required to be operated simultaneously for the special test cycle. Therefore, the prime electric range is defined as the distance the vehicle can travel solely on the battery prior to the battery reaching 80 percent depth of discharge (DOD). During the heat engine mode, the vehicle is propelled solely by the engine using petroleum energy. The electric range and fuel usage values were computed using the designated special test cycle.

Type of use Mission/vehicle designation	Battery type	Propulsion system concepts															
		Concept 1.1			Concept 1.2			Concept 2.1			Concept 2.2			Concept 2.3			
		No power split	50/50 power split	No power split	50/50 power split	No power split	50/50 power split	No power split	50/50 power split	No power split	50/50 power split	No power split	50/50 power split	No power split	50/50 power split		
 A. Commuter car	Nickel-zinc	a.* 181	240	—	—	—	—	—	—	—	—	—	—	—	—	—	
		b.* 507	617	—	—	—	—	—	—	—	—	—	—	—	—	—	—
		c.* 1222	1367	—	—	—	—	—	—	—	—	—	—	—	—	—	—
		d.* 3406	5082	—	—	—	—	—	—	—	—	—	—	—	—	—	—
A. Commuter car	Lead-acid	a.* 349	408	—	—	—	—	—	—	—	—	—	—	—	—	—	
		b.* 674	735	—	—	—	—	—	—	—	—	—	—	—	—	—	
		c.* 1440	1583	—	—	—	—	—	—	—	—	—	—	—	—	—	
		d.* 2897	4266	—	—	—	—	—	—	—	—	—	—	—	—	—	—
 B. Family sedan (local)	Nickel-zinc	a.* 318	386	340	170	340	170	340	170	340	170	340	170	340	170	340	
		b.* 779	1019	872	702	872	702	872	702	872	702	872	702	872	702	872	
		c.* 2031	2337	2152	1931	2152	1931	2152	1931	2152	1931	2152	1931	2152	1931	2152	
		d.* 5136	9219	8184	6853	8184	6853	8184	6853	8184	6853	8184	6853	8184	6853	8184	
B. Family sedan (local)	Lead-acid	a.* 561	680	590	295	590	295	590	295	590	295	590	295	590	295	590	
		b.* 1042	1309	1121	826	1121	826	1121	826	1121	826	1121	826	1121	826	1121	
		c.* 2373	2720	2476	2093	2476	2093	2476	2093	2476	2093	2476	2093	2476	2093	2476	
		d.* 4165	7977	7060	6291	7060	6291	7060	6291	7060	6291	7060	6291	7060	6291	7060	
 C. Family sedan (intercity)	Nickel-zinc	a.* 463	—	499	245	499	245	499	245	499	245	499	245	499	245	499	
		b.* 1078	—	1223	973	1223	973	1223	973	1223	973	1223	973	1223	973	1223	
		c.* 3109	—	3497	2973	3497	2973	3497	2973	3497	2973	3497	2973	3497	2973	3497	
		d.* 6378	—	11513	9661	11513	9661	11513	9661	11513	9661	11513	9661	11513	9661	11513	
C. Family sedan (intercity)	Lead-acid	a.* 803	—	950	426	950	426	950	426	950	426	950	426	950	426	950	
		b.* 1418	—	1574	1150	1574	1150	1574	1150	1574	1150	1574	1150	1574	1150	1574	
		c.* 3552	—	3754	3203	3754	3203	3754	3203	3754	3203	3754	3203	3754	3203	3754	
		d.* 5252	—	9727	8621	9727	8621	9727	8621	9727	8621	9727	8621	9727	8621	9727	
 D. Van (variable route)	Nickel-zinc	a.* 830	—	782	392	782	392	782	392	782	392	782	392	782	392	782	
		b.* 1897	—	1690	1300	1690	1300	1690	1300	1690	1300	1690	1300	1690	1300	1690	
		c.* 4880	—	5130	4623	5130	4623	5130	4623	5130	4623	5130	4623	5130	4623	5130	
		d.* 11249	—	17382	14330	17382	14330	17382	14330	17382	14330	17382	14330	17382	14330	17382	
D. Van (variable route)	Lead-acid	a.* 1406	—	1406	703	1406	703	1406	703	1406	703	1406	703	1406	703	1406	
		b.* 2313	—	2313	1610	2313	1610	2313	1610	2313	1610	2313	1610	2313	1610	2313	
		c.* 5914	—	5914	4686	5914	4686	5914	4686	5914	4686	5914	4686	5914	4686	5914	
		d.* 14527	—	14527	11094	14527	11094	14527	11094	14527	11094	14527	11094	14527	11094	14527	
 E. Bus (variable route)	—	a.* —	—	—	—	—	—	—	—	—	—	—	—	—	—	—	
		b.* —	—	—	—	—	—	—	—	—	—	—	—	—	—	—	—
		c.* —	—	—	—	—	—	—	—	—	—	—	—	—	—	—	—
		d.* —	—	—	—	—	—	—	—	—	—	—	—	—	—	—	—
E. Bus (variable route)	—	a.* —	—	—	—	—	—	—	—	—	—	—	—	—	—	—	
		b.* —	—	—	—	—	—	—	—	—	—	—	—	—	—	—	—
		c.* —	—	—	—	—	—	—	—	—	—	—	—	—	—	—	—
		d.* —	—	—	—	—	—	—	—	—	—	—	—	—	—	—	—

* Legend: a. M_B = Battery weight, kg. b. M_p = Propulsion system weight, kg. c. M_v = Vehicle test weight, kg. d. C_A = Propulsion system acquisition cost, \$/kWh

Figure 49. --Task 1 initial (baseline) vehicle/propulsion system data.

(VEHICLE / PROPULSION CONCEPT 1.1B)

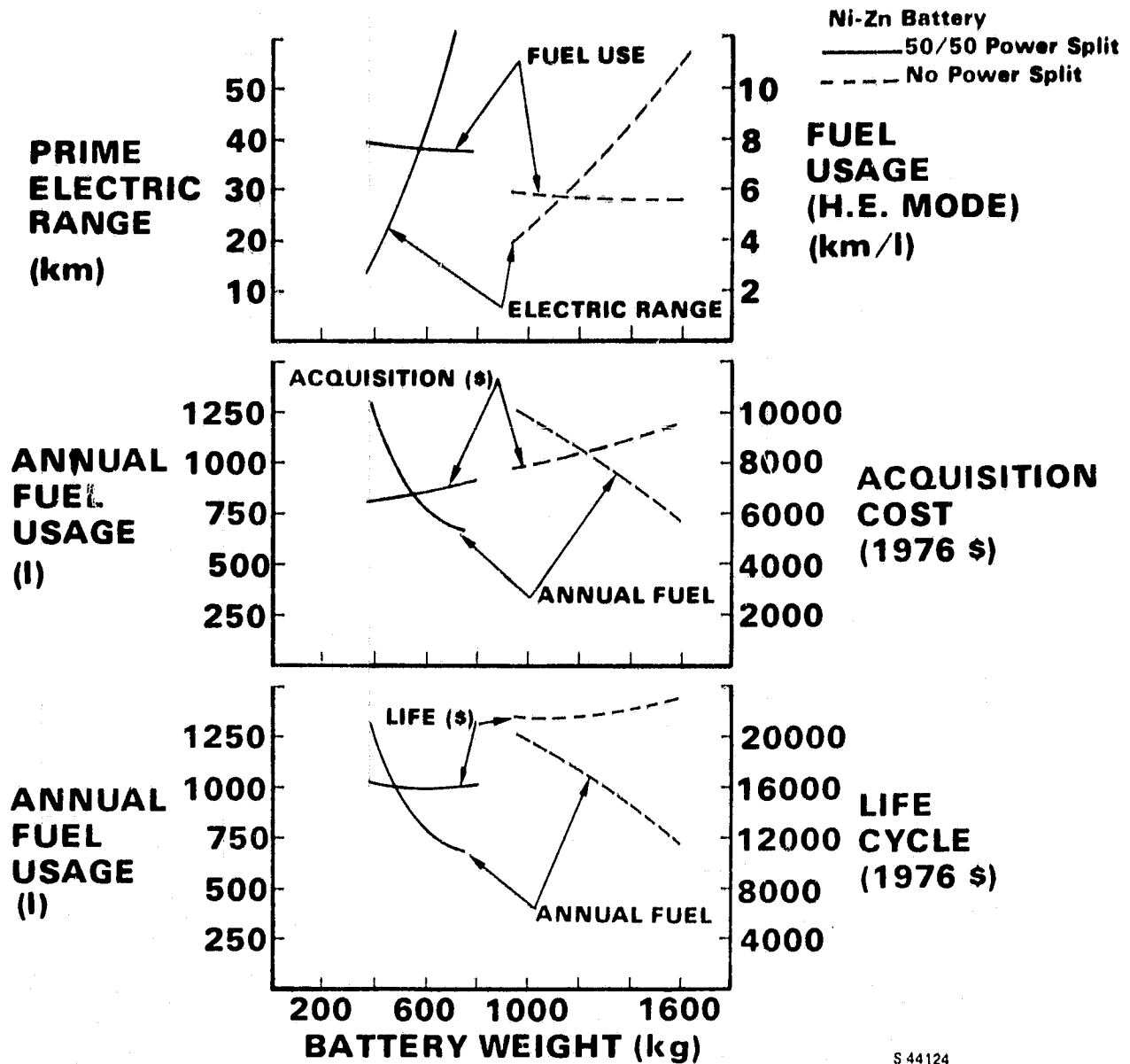


S44121

Figure 50.--Typical Task 1 parametric results.

ORIGINAL PAGE IS
OF POOR QUALITY

(VEHICLE / PROPULSION CONCEPT 2.2C)



S 44124

Figure 51.--Typical Task 1 parametric results.

The upper plot of fig. 50 illustrates the following:

- (1) For a given battery weight, the nickel-zinc battery provides more range than the lead-acid battery.
- (2) The energy availability of the lead-acid battery is more sensitive to the high power requirements of the special test cycle (acceleration from 0 to 72 km/hr in 14 s) than the nickel-zinc battery.
- (3) The difference between the fuel usage values for the two battery types shows the impact of propulsion system weight on the fuel economy of the vehicles.
- (4) A family sedan (for local use) has an electric range of 50 km with 275 kg of nickel-zinc batteries or 775 kg of ISOA lead-acid batteries when it is configured with a parallel propulsion system (concept 1.1).

In the middle plot of fig. 50 the annual fuel usage (liters) and propulsion system acquisition cost (1976 \$) vs battery weight are displayed for both types of batteries. The annual fuel usage (petroleum) was computed using the annual daily range frequency table (see table 14). The 16 000-km annual mileage is traversed by driving on the battery until it is 80 percent discharged and then turning the heat engine on and using petroleum fuel to complete the remainder of the daily range requirement.

TABLE 14.--DAILY RANGE FREQUENCY FOR ONE YEAR

Daily range, km (mi)	No. of days of the year	Total range, km (mi)
0 (0.0)	16	0 (0)
10 (6.2)	130	1300 (808)
30 (18.6)	85	2550 (1585)
50 (31.1)	57	2850 (1771)
80 (49.7)	54	4320 (2685)
130 (80.8)	12	1560 (970)
160 (99.4)	7	1120 (696)
500 (311.0)	3	1500 (932)
800 (497.0)	1	800 (497)
Totals	365	16000 (9944)

The middle plot of fig. 50 illustrates the following:

- (1) With nickel-zinc batteries the annual fuel usage reaches a minimum of 150 liters at a weight of 475 kg; however, the propulsion system acquisition cost is \$6300. The fuel usage begins to increase for higher battery weights mainly because of the increased power required by a heavier vehicle, especially for the 90 km/hr cruise condition.

- (2) It costs the consumer \$1400 in increased acquisition cost to save 370 liters of petroleum per year by increasing battery weight from 315 to 500 kg.
- (3) With lead-acid batteries the minimum annual fuel usage of 600 liters occurs at a battery weight of 800 kg. The propulsion system acquisition cost is \$4800.
- (4) It costs the consumer \$800 to save 225 liters of petroleum per year using ISOA lead-acid batteries.

Examination of the lower plot of fig. 50 reveals the following:

- (1) The propulsion system configured with nickel-zinc batteries uses a minimum of 1500 liters of petroleum per 10-yr period and costs \$15 500 to own and operate. The use of lead-acid batteries increases the fuel consumption to 6000 liters over a 10-yr period and decreases the cost of ownership to 13 500.
- (2) Use of nickel-zinc batteries saves fuel in comparison with the use of lead-acid batteries, but the petroleum savings occur at an increase in acquisition and life-cycle cost to the consumer.

Fig. 51 displays the effects of power sharing between a battery and a second energy source for a parallel-power-path propulsion system that uses mechanical energy storage (MES), concept 2.2, and is sized for the intercity family sedan (vehicle C). In the example shown the second energy source is a flywheel MES device. The 50/50 power split means that during the STC acceleration period 50 percent of the power is supplied by the battery and 50 percent by the flywheel. The results presented are for the ISOA lead-acid battery and are shown for no power split (no flywheel) and a fixed 50/50 power split.

The following trends are illustrated by the upper plot of fig. 51:

- (1) A 50-km electric range is provided by 650 kg of batteries when power sharing (50/50 split) is used, while it takes 1500 kg to attain the same range without power sharing.
- (2) As the battery weight increases, the heat engine mode fuel usage (economy) decreases. This trend shows the effect of vehicle weight on fuel economy.
- (3) The magnitude of the difference between the 50/50-power-split and no-power-split heat engine fuel economy is an indication of improvements in fuel economy that are obtainable by load-leveling a spark-ignition heat engine with a flywheel.
- (4) The large difference in electric range between the 50/50-power-split and no-power-split cases is due to the following effects:
 - (a) Sensitivity of the energy available from the lead-acid battery to the power loading. Nickel-zinc batteries are not as sensitive to this effect as lead-acid batteries.

- (b) The reduction in the relative power contribution by the battery (specific power) as the battery weight was increased because of the constant 50/50-power-split ground rule.

Examination of the second graph of fig. 51 indicates both a reduction in petroleum usage and a lower acquisition cost for a power sharing system in comparison with its no-power-split equivalent. The lower graph of fig. 51 reveals the same trends exist between the power sharing and no-power-split systems when their life-cycle costs are evaluated.

All the parametric vehicle/propulsion systems were examined to determine the battery weight that results in the minimum life-cycle cost for each vehicle/propulsion concept. The performance and cost data for each of these minimum cost configurations are presented in figs. 52 to 54.

In all cases the nickel-zinc battery (in comparison with the ISOA lead-acid battery) provides the best performance (electric range and engine mode fuel economy) and requires the smallest battery weight. The concepts that use lead-acid batteries, however, are less costly to purchase and operate for 10 yr. This longer operating life is due to the relatively poor cycle life and high acquisition cost of the nickel-zinc battery.

Task I Flywheel MES/Heat Engine Parametric Results

In addition to the pure hybrid propulsion systems that use a storage battery and heat engine, a flywheel MES/heat engine propulsion system was evaluated in mission vehicles C, D, and E. The results of this parametric investigation are shown in fig. 55.

The design limit line in the figure represents a boundary of feasibility. For example, a flywheel with an energy storage capability larger than 3 kW-hr becomes impractical for an intercity sedan (vehicle C); i.e., the volume required for a larger flywheel would infringe on the existing passenger and/or luggage compartments of the vehicle; and therefore it could no longer be considered the same class of vehicle. The practical limit for vehicle D is estimated to be 5 kW-hr and vehicle E, 15 kW-hr. To make maximum use of wall-plug energy (electricity), this type of system is restricted to use on a fixed route that has charging stations located at intervals that are within the flywheel range of the vehicle.

Task I Heat Engine Comparison

An alternate engine comparison was made by the substitution of a modern, high-speed, naturally aspirated diesel engine and an advanced, single-shaft, ceramic gas turbine engine into the vehicle/propulsion system concepts shown in fig. 56. The propulsion systems are configured with nickel-zinc batteries, and the battery pack weight was selected to minimize the life-cycle cost.

TASK I PERFORMANCE RESULTS (NO POWER SPLIT)

CONCEPT	BATTERY TYPE	MISSION/VEHICLE DESIGNATION		TYPE OF USE FAMILY SEDAN (LOCAL)
		A. COMMUTER CAR	B. FAMILY SEDAN (LOCAL)	
1.1	Ni-Zn	a. 12.5	9.3	
		b. 107	115	
		c. 272	408	
1.2	Pb-Acid	11.9	8.8	
		31	33	
		440	671	
1.2	Ni-Zn	11.0	7.6	
		126	114	
		354	499	
2.1	Pb-Acid	9.9	6.6	
		39	34	
		567	862	
2.1	Ni-Zn		9.0	
			109	
			431	
2.2	Pb-Acid		8.5	
			55	
			907	
2.2	Ni-Zn		7.4	
			113	
			499	
2.2	Pb-Acid		6.9	
			30	
			816	

LEGEND: (TYP)
 a. STC FUEL ECONOMY (km/l)
 b. ELECTRIC RANGE (km)
 c. BATTERY WEIGHT (kg)

S-4114

TASK I COST RESULTS (NO POWER SPLIT)

CONCEPT	BATTERY TYPE	MISSION/VEHICLE DESIGNATION		TYPE OF USE FAMILY SEDAN (LOCAL)
		A. COMMUTER CAR	B. FAMILY SEDAN (LOCAL)	
1.1	Ni-Zn	a. 118	127	
		b. 4115	5846	
		c. 10 893	14969	
1.2	Pb-Acid	621	787	
		3134	4403	
		9799	13264	
1.2	Ni-Zn	125	161	
		5969	10106	
		13783	20630	
2.1	Pb-Acid	678	1018	
		4680	8450	
		12229	19207	
2.1	Ni-Zn		133	
			8894	
			18358	
2.2	Pb-Acid		564	
			7888	
			16729	
2.2	Ni-Zn		131	
			8050	
			18408	
2.2	Pb-Acid		742	
			6275	
			16127	

LEGEND: (TYP)
 a. ANNUAL PETROLEUM USAGE (l)
 b. ACQUISITION COST (1976 \$)
 c. LIFE CYCLE COST (1976 \$)

S-4111

Figure 52.--Task I performance and cost for minimum life-cycle cost systems.

ORIGINAL PAGE IS
OF POOR QUALITY

TASK I PERFORMANCE RESULTS (50/50 POWER SPLIT)

CONCEPT	BATTERY TYPE	TYPE OF USE	
		MISSION/VEHICLE DESIGNATION	MISSION/VEHICLE DESIGNATION
1.1	Ni-Zn	C FAMILY SEDAN (INTERCITY)	D VAN (VARIABLE ROUTE)
		a. 6.8	4.5
		b. 105	87
2.1	Pb-Acid	c. 553	830
		6.2	
		34	
2.2	Ni-Zn	984	
		6.5	4.3
		118	108
2.1	Pb-Acid	635	975
		6.2	4.0
		34	38
2.2	Ni-Zn	1043	1758
		5.5	4.4
		103	106
2.2	Pb-Acid	680	1134
		5.9	4.4
		19	28
2.2	Pb-Acid	953	1814
		8.2	5.6
		86	63
2.1	Ni-Zn	386	488
		8.0	5.4
		33	36
2.2	Pb-Acid	522	880
		7.9	5.5
		75	63
2.2	Ni-Zn	331	522
		7.7	5.3
		44	26
2.2	Pb-Acid	635	816

LEGEND: (TYP)

- a. STC FUEL ECONOMY (km/l)
- b. ELECTRIC RANGE (km)
- c. BATTERY WEIGHT (kg)

S-44062

TASK I PERFORMANCE RESULTS (NO POWER SPLIT)

CONCEPT	BATTERY TYPE	TYPE OF USE	
		MISSION/VEHICLE DESIGNATION	MISSION/VEHICLE DESIGNATION
1.1	Ni-Zn	C FAMILY SEDAN (INTERCITY)	D VAN (VARIABLE ROUTE)
		a. 6.8	4.5
		b. 105	87
2.1	Pb-Acid	c. 553	830
		6.2	
		34	
2.2	Ni-Zn	984	
		6.5	4.3
		118	108
2.1	Pb-Acid	635	975
		6.2	4.0
		34	38
2.2	Ni-Zn	1043	1758
		5.5	4.4
		103	106
2.2	Pb-Acid	680	1134
		5.9	4.4
		19	28
2.2	Pb-Acid	953	1814

LEGEND: (TYP)

- a. STC FUEL ECONOMY (km/l)
- b. ELECTRIC RANGE (km)
- c. BATTERY WEIGHT (kg)

S-44113

Figure 53.---Task I performance for minimum life-cycle cost systems.

TASK I COST RESULTS (NO POWER SPLIT)

CONCEPT	BATTERY TYPE	TYPE OF USE	
		MISSION/VEHICLE DESIGNATION 	MISSION/VEHICLE DESIGNATION 
		C FAMILY SEDAN (INTERCITY)	D VAN (VARIABLE ROUTE)
1.1	Ni-Zn	a. 150	275
		b. 7488	12,668
		c. 19,712	32,300
1.1	Pb-Acid	1018	—
		5725	
		17,498	
2.1	Ni-Zn	158	269
		12,478	18,890
		25,308	38,664
2.1	Pb-Acid	1041	1571
		10,230	15,844
		22,256	34,258
2.2	Ni-Zn	151	305
		10,637	14,439
		24,744	37,314
2.2	Pb-Acid	1124	1514
		8389	10,298
		21,640	

LEGEND: (TYP)

- a. ANNUAL PETROLEUM USAGE (l)
- b. ACQUISITION COST (1976 \$)
- c. LIFE CYCLE COST (1976\$)

S-44117

TASK I COST RESULTS (50/50 POWER SPLIT)

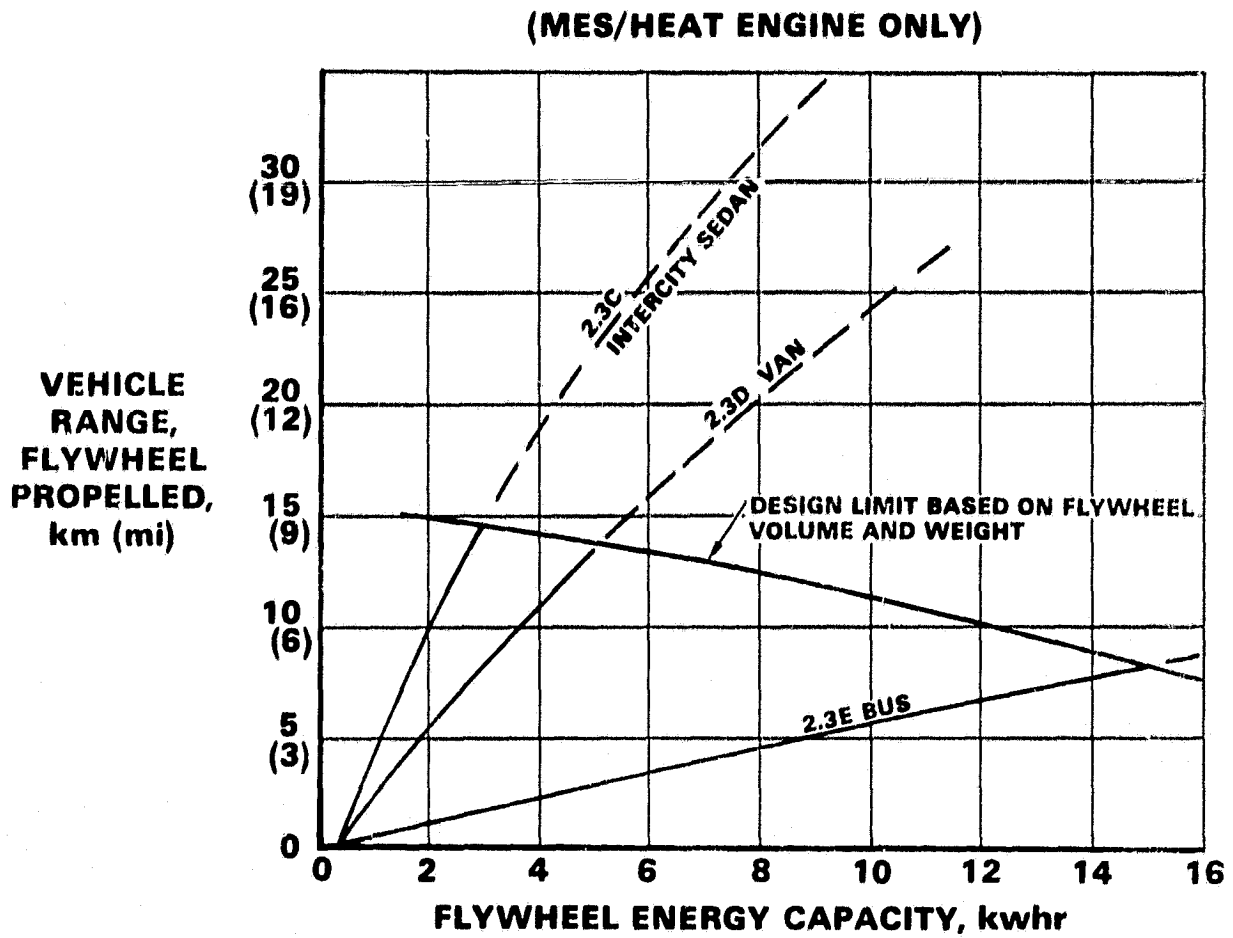
CONCEPT	BATTERY TYPE	TYPE OF USE	
		MISSION/VEHICLE DESIGNATION 	MISSION/VEHICLE DESIGNATION 
		C FAMILY SEDAN (INTERCITY)	D VAN (VARIABLE ROUTE)
1.1	Ni-Zn		
2.1	Ni-Zn	a. 188	678
		b. 10,526	15,075
		c. 21,268	32,814
2.1	Pb-Acid	886	1378
		8869	13,555
		18,188	27,706
2.2	Ni-Zn	462	937
		7904	9647
		19,527	28,810
2.2	Pb-Acid	731	1643
		6969	7695
		16,123	23,407

LEGEND: (TYP)

- a. ANNUAL PETROLEUM USAGE (l)
- b. ACQUISITION COST (1976\$)
- c. LIFE CYCLE COST (1976\$)

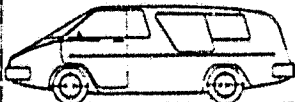
S-44117

Figure 54.--Task I cost for minimum life-cycle cost systems.



S44092

Figure 55.--Task I performance results (MES/heat engine only).

MISSION/VEHICLE DESIGNATION	PROPULSION CONCEPTS/ENGINE TYPES					
	1.1		1.2		2.2	
	S.I.	DIESEL	S.I.	TURBINE	S.I.	DIESEL
 A COMMUTER CAR	a. 12.5	14.2	11.0	11.8		
	b. 118	116	125	85		
	c. 4115	4313	5969	6369		
	d. 10 893	11 255	13 783	14 342		
 B FAMILY SEDAN (LOCAL)	9.3	9.7	7.6	7.9	7.4	7.8
	127	119	161	126	131	114
	5846	6064	10 106	10 666	8050	8268
	14 969	15 083	20 830	21 884	18 488	18 796
 C FAMILY SEDAN (INTERCITY)	6.8	6.9			5.5	5.5
	150	127			151	127
	7488	7814			10 637	10 963
	19 712	20 206			24 744	25 095
 D VAN (VARIABLE ROUTE)	4.5	4.5			4.4	4.5
	276	232			305	257
	12 668	12 994			14 439	14 787
	32 242	32 481			37 314	37 836

LEGEND: (TYP.)

- a. STC FUEL ECONOMY (km/l)
- b. ANNUAL PETROLEUM USAGE (l)
- c. ACQUISITION COST (1976 \$)
- d. LIFE CYCLE COST (1976 \$)

5 44086

Figure 56.--Task I alternate engine comparison.

The comparisons are summarized in terms of heat engine mode fuel economy, annual petroleum usage, and propulsion system acquisition and life-cycle costs.

The spark-ignition engine was operated in an on-off (on-demand) mode; the diesel and turbine were allowed to idle continuously. There is no noticeable difference in the fuel economy and annual fuel usage for the three engines, because the idle losses of the spark-ignition engine were eliminated, and the turbine engine was used only in a configuration in which it could operate at nearly constant speed. Both the acquisition cost and life-cycle costs are comparable for each vehicle/propulsion system concept, independent of engine type. The diesel system would be easier to develop because no new technology is needed.

C-2

TASK I RECOMMENDATIONS

In Task I, 15 vehicle/propulsion system concepts were investigated. The main purpose of the investigation was to determine which combination of vehicle and propulsion system had the best chance of meeting the overall cost and fuel usage objectives of the study.

It was recommended that propulsion system concepts 1.1 and 2.2 be carried into Task II for a more detailed evaluation. The Task I data indicated that these two systems had the greatest potential of meeting the cost objectives of the study. It was recognized that cost has a stronger influence in the hybrid propulsion system selection process than petroleum usage.

A second recommendation was made that the simultaneous mixing of heat engine and battery power be investigated in Task II. The Task I results of the comparison made between the 50/50 power split and no power split indicated a large cost and fuel savings benefit for power sharing between the battery and a second energy source.

A third recommendation was that the mission vehicle to be used in the remainder of the study be designated a five-passenger family sedan, since it has the greatest potential for petroleum savings. This class of vehicle lies between the local family sedan (vehicle B) and the intercity family sedan (vehicle C) of the study in terms of its size, weight, and payload, and is in line with the scaling down trends that are currently occurring in the automotive industry. Historically, a family sedan vehicle has been the largest consumer of liquid petroleum (primarily, gasoline). Fig. 57 shows the recent petroleum usage by vehicle type for the five mission vehicle designations of the study. These data were obtained from ref. 28 and show that currently the full size family sedan is the largest petroleum user, followed closely by the intermediate/compact sedan.

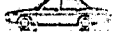
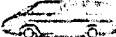
VEHICLE TYPE	APPROXIMATE CURRENT PETROLEUM USAGE (BILLIONS OF GALLONS)	POTENTIAL PETROLEUM SAVINGS (BILLIONS OF GALLONS)
 A. COMMUTER CAR	UNDEFINED - NEW APPLICATION	UNKNOWN - DEPENDS ON FLEET INTRODUCTION RATE
 B. FAMILY SEDAN (LOCAL)	12.73	12.09
 C. FAMILY SEDAN (INTERCITY)	20.25	19.24
 D. VAN (VARIABLE ROUTE)	5.89	5.80
 E. BUS (VARIABLE ROUTE)	0.86	0.63

Figure 57.--Potential petroleum savings vs vehicle type.

PART B
TASK II, DESIGN TRADEOFF STUDIES

TASK II DESIGN TRADEOFF STUDY METHODOLOGY

This section describes the Task II tradeoffs and the modifications to the propulsion system concepts and to the analytical procedures. Computer simulation results of performance and cost for the two propulsion system concepts recommended in Task I are presented in the following section, Cost and Performance Tradeoffs. Final propulsion system performance is presented in the subsequent section, Cost Optimization Tradeoffs. Following that the section, Performance Sensitivity Studies, presents results of analytical work that shows how certain study procedures and goals affected the design and performance of the recommended final propulsion system.

Revised Vehicle Characteristics

A review of current automotive markets and size trends in Task I showed that a five-passenger vehicle has the greatest potential for petroleum savings. Tradeoff studies in Task II were specifically directed toward a propulsion system for this five-passenger vehicle. The basic design constraints provided by NASA are reiterated in table 15 for the selected configuration, and the performance goals that apply to this vehicle are presented in table 16.

TABLE 15.--BASIC DESIGN CONSTRAINTS

Mission/vehicle designation	BC
Payload:	
Number of passengers	5
Cargo, kg (lb)	75 (165)
Total, kg (lb)	415 (915)
Carriage characteristics:	
Test payload, kg (lb)	207 (456)
Fixed weight, kg (lb)	510 (1124)
Aerodynamic coefficient, $C_D A$, M^2 (ft ²)	0.60 (6.5)
Tire rolling resistance ($V = \text{km/hr}$)	$0.008 + 1 \times 10^{-5}v + 8 \times 10^{-2} v^2$
Tire rolling radius, m (ft)	0.30 (1.0)
Accessory load (maximum), W	600

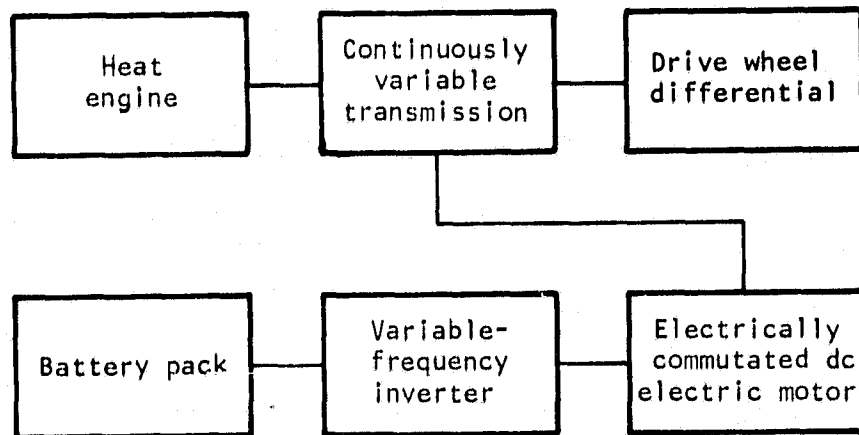
TABLE 16.--VEHICLE BC PERFORMANCE GOALS

Min. top speed on level road, km/hr (mph)	105 (65)
Max. accel. time:	
0 to 50 km/hr (0 to 31 mph), s	5
0 to 90 km/hr (0 to 56 mph), s	12
40 to 90 km/hr (25 to 56 mph), s	10
Gradeability at speed for specified distance:	
3% grade, 90 km/hr (56 mph), km (mi)	1.5 (0.93)
8% grade, 50 km/hr (31 mph), km (mi)	0.5 (0.31)
15% grade, 25 km/hr (16 mph), km (mi)	0.3 (0.19)
Min. ramp speed attainable from a stop on uphill 6% grade in 300 m (984 ft), km/hr (mph)	90 (56)
Min. sustained speed up 4% grade, km/hr (mph)	90 (56)

Revised System Concept Definition

Propulsion system concepts 1.1 and 2.2 were chosen as the systems with the greatest potential for improvement in Task II tradeoff studies. Modifications were made to both concepts based on the experience gained from the Task I parametric studies.

Modified concept 1.1.--Concept 1.1 was chosen for simplicity, low weight, and good overall efficiency. It was modified for the Task II tradeoff studies by replacing the discrete four-speed transmission with a continuously variable mechanical transmission. The modified concept 1.1 is shown in fig. 58.



S-46492

Figure 58.--Modified concept 1.1.

The continuously variable mechanical transmission (CVT) provides a more flexible propulsion system. Heat engine speed and motor speed are not locked to the differential speed by discrete ratios, but can be set to the most efficient operating speed for the required power output. Differences in cost and weight between the CVT and the four-speed automatic transmission are minimal. The CVT is slightly less efficient at all operating points than the four-speed transmission, but the increase in efficiency of the heat engine and motor, due to the better speed range, more than makes up for this decrease in transmission efficiency. The transmission is capable of a range of ratios from 0.3:1 to 3:1. A schematic diagram and efficiency curves for the CVT are shown in figs. 59 and 60.

The variable action of the CVT is achieved in the double-cavity toroidal drive. The main shaft of the transmission has a drive disc attached to each end; the discs have a section of toroidal shape. Two similar discs are located inboard of the outer discs, and form the two cavities. The inboard discs are mounted on separate bearings and are capable of a limited amount of axial motion. Rollers, mounted on swivel shafts, contact each set of inboard and outboard discs. The drive ratio is changed by swiveling the contact rollers from contacts close to center on the drive discs and far from center on the driven discs to the other extreme of far from center on the drive discs to close to center on the driven discs. The rollers are not forced into ratio position but are steered as the wheels of a car by low-pressure hydraulic pistons that balance internal tangential forces that are generated at the roller contacts.

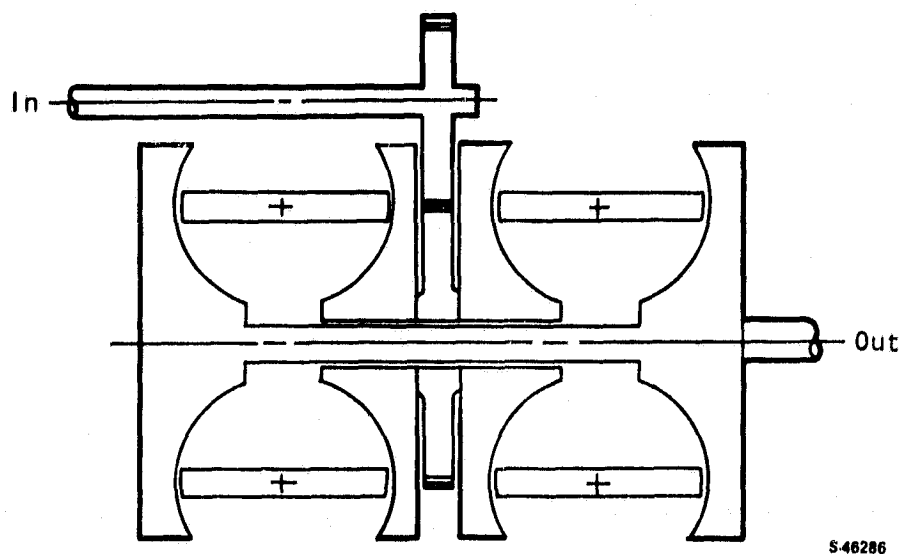
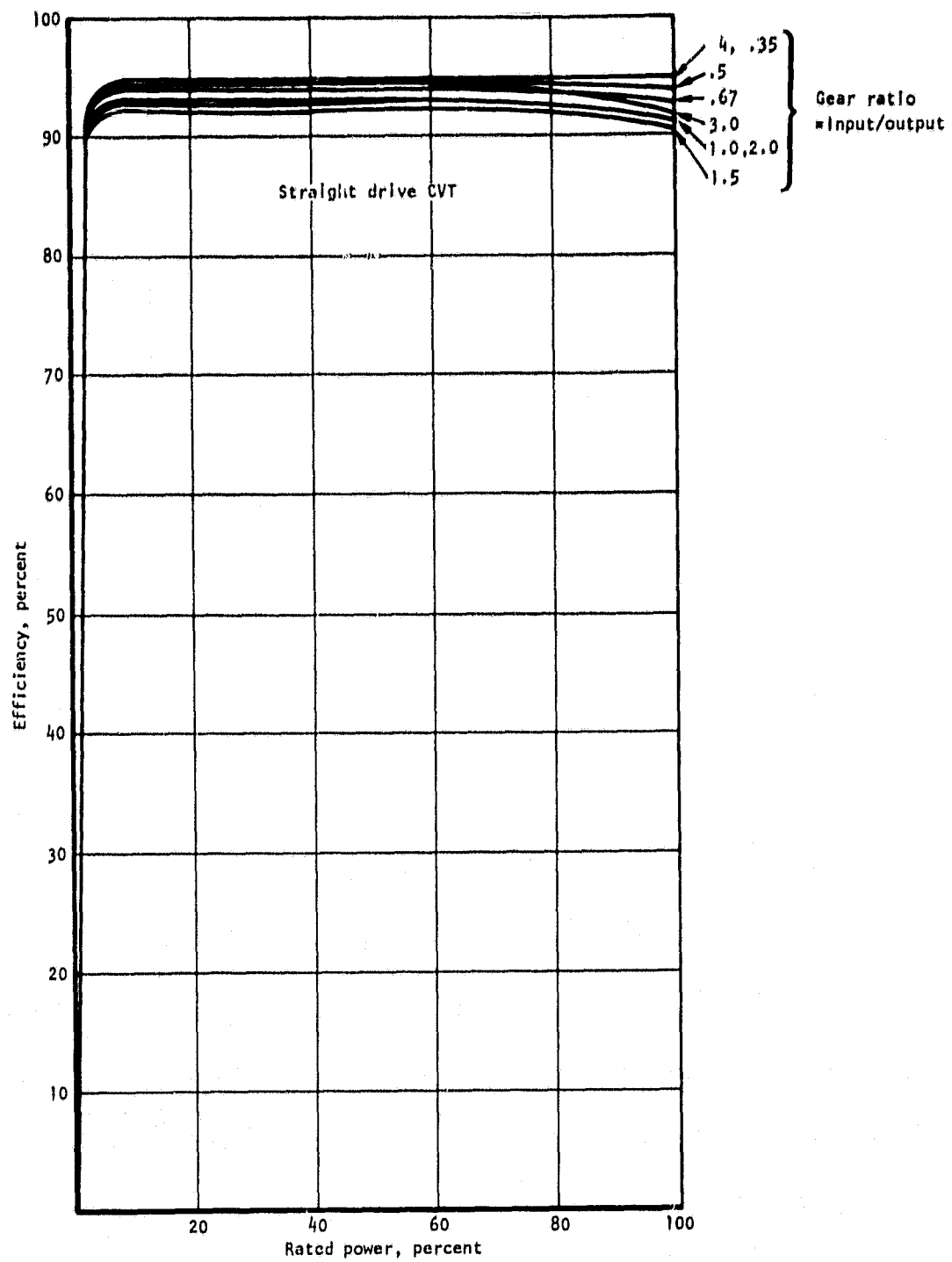


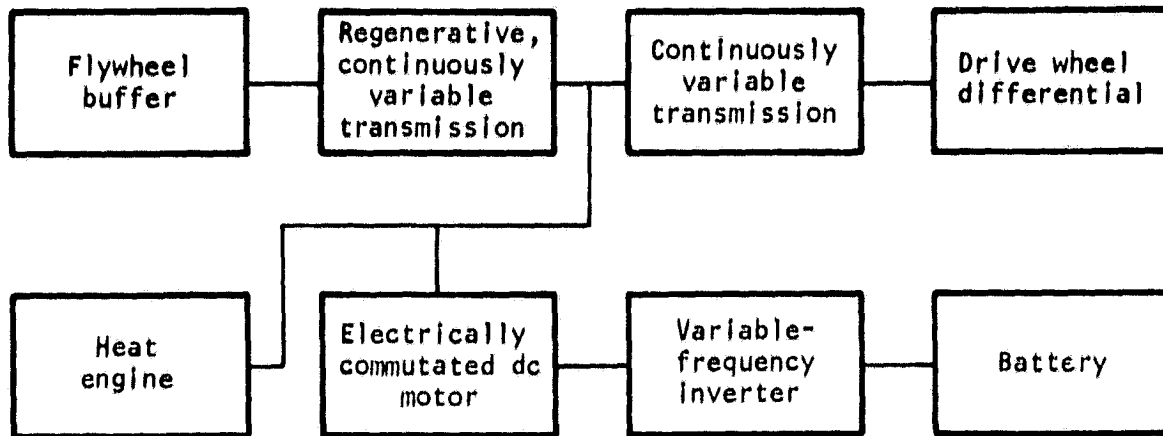
Figure 59.--Continuously variable transmission (CVT).

Modified concept 2.2.--Concept 2.2 was chosen for its high efficiency and potential for improvement. A regenerative continuously variable transmission (CVT) was added to decouple the flywheel from the heat engine and electric motor. The modified concept 2.2 is shown in fig. 61.



S-46167

Figure 60.--CVT efficiency.



546272

Figure 61.--Modified concept 2.2.

The original concept required the flywheel, heat engine, and electric motor to be mechanically geared together. The major limitation of this previous system is that the flywheel sets the speed of the heat engine and electric motor near their maximum speed points, and therefore precludes efficient operation of the two power sources.

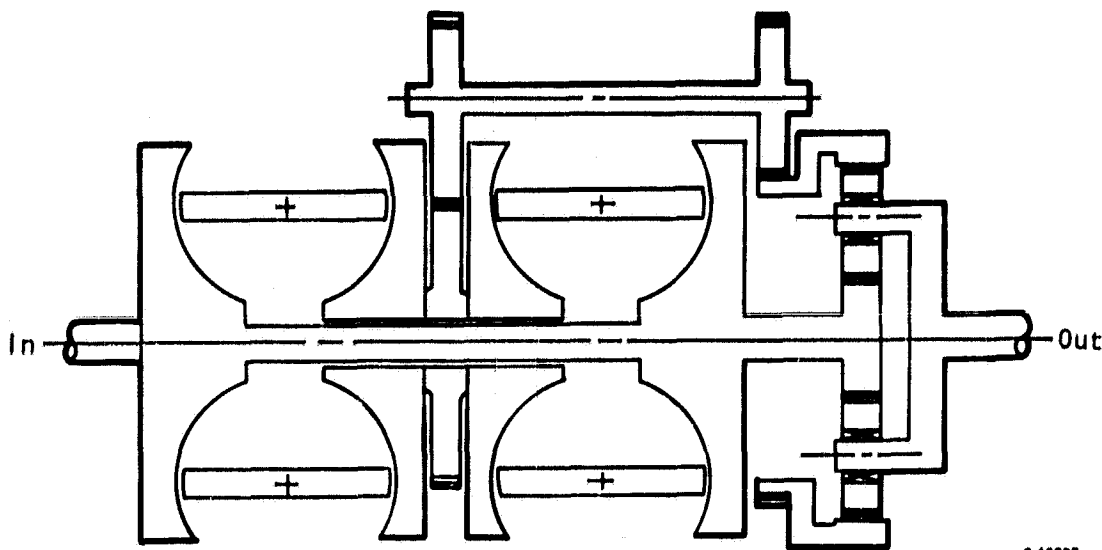
The addition of the regenerative CVT in the modified concept 2.2 allows the flywheel speed to be independent of heat engine speed and motor speed. The heat engine or motor can be operated at the best operating speed using the primary drive CVT. The flywheel is always available at the driveline through the regenerative CVT.

The variable action of the regenerative CVT is achieved in the double-cavity toroidal drive as was described for the primary drive CVT. The main shaft of the transmission has a drive disc attached to each end, and two similar discs are located inboard of the outer discs, forming the two cavities. Rollers, mounted on swivel shafts, contact each set of inboard and outboard discs, and the drive ratio is changed by swiveling the contact rollers. The contact force is adjusted by a loading cam located between the two central discs that provides a separating force, thereby generating equal forces for the two cavities. The contact forces are balanced within the end discs, and no heavy thrust bearings are required for the rotating assembly.

The output from the inboard discs is taken through a gear train to a final planetary gear set with the sun on the main shaft and the output taken from the planet carrier. This final CVT output then goes to the output drive and differential.

A schematic diagram of the regenerative CVT is shown in fig. 62. The addition of power regeneration, using an epicyclic gear set, expands the ratio range of the transmission to infinity. The high reduction required to match flywheel speed to driveline speed is possible with this regenerative CVT. The efficiency, shown in fig. 63, is lower than the primary drive CVT because of internal losses in the regeneration path.

The regenerative and primary CVT would be built using a common housing and controls. The addition of the regenerative unit would add about 14 kg to the transmission weight and \$50 to the cost.



5-46285

Figure 62.--Regenerative continuously variable transmission.

Power and Energy Management Tradeoffs

The power and energy management scheme for computer simulation of concepts 1.1 and 2.2 is presented in tables 17 and 18. The systems are in the electric mode until the battery depth of discharge reaches 80 percent. The battery pack is the main energy source in this mode, supplying 100 percent of all energy requirements in all vehicle states except acceleration. The acceleration state is the most critical as the large power drain required can quickly discharge the battery. The power taken from the battery during acceleration can be limited to any value from zero to the maximum battery capacity. Any power requirement over the battery power limit is supplied by the heat engine in concept 1.1 or the flywheel in concept 2.2. Thus, the power required at the transmission can be split between the battery pack and the heat engine or flywheel. This power split is an important analytical tool that allows the battery to be used efficiently and leads to smaller battery packs and lower costs. The distance that the vehicle can travel in the electric mode on the test cycle to 80 percent depth of discharge is defined as the prime electric range.

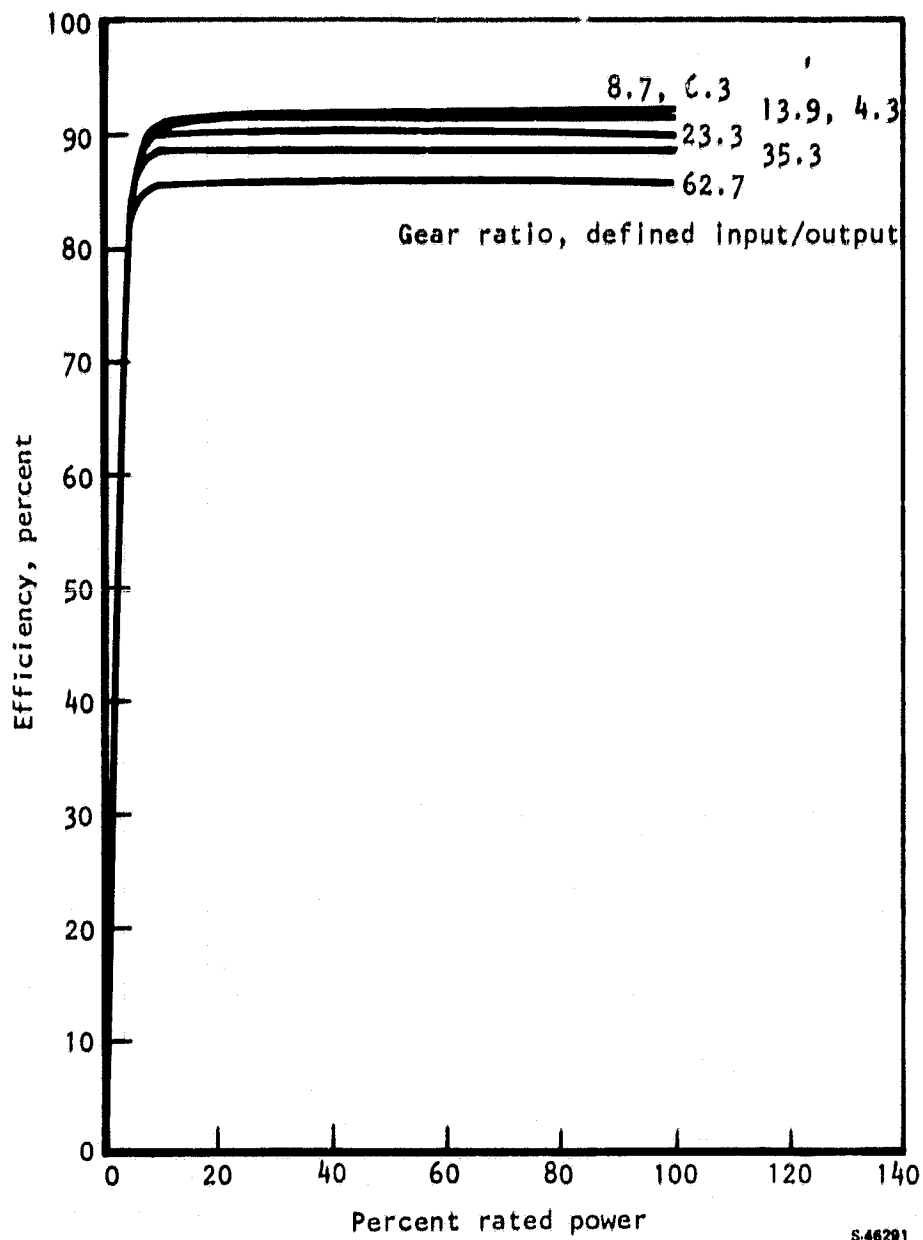


Figure 63.--Regenerative continuously variable transmission performance.

TABLE 17.--POWER AND ENERGY MANAGEMENT FOR CONCEPT 1.1

Mode	Vehicle state	Power and energy flow
Electric	Acceleration	Battery supplies all power up to a preset limit. Heat engine supplies any excess power requirement.
	Cruise	Battery supplies all power.
	Brake	Braking energy regenerated into battery.
Engine	Acceleration	Heat engine supplies all power up to a preset limit. Battery supplies any excess power requirement.
	Cruise	Heat engine supplies all power.
	Brake	Braking energy regenerated into battery.
	Stop	Heat engine used to charge battery to 80 percent xxx .

TABLE 18.--POWER AND ENERGY MANAGEMENT FOR CONCEPT 2.2

Mode	Vehicle state	Power and energy flow
Electric	Acceleration	Battery supplies all power up to a preset limit. Flywheel supplies any excess power requirement.
	Cruise	Battery supplies all power.
	Brake	Braking energy regenerated into flywheel. When flywheel is at full speed, braking energy regenerated into battery.
	Stop	Heat engine used to charge flywheel to full speed.
Engine	Acceleration	Heat engine supplies all power up to a preset limit. Flywheel supplies any excess power requirement.
	Cruise	Heat engine supplies all power.
	Brake	Braking energy regenerated into flywheel. When flywheel is at full speed, braking energy regenerated into battery.
	Stop	Heat engine used to charge flywheel to full speed.

The propulsion system is in the engine mode after the battery has reached 80 percent depth of discharge. The same type of power split can be made between the heat engine and the battery pack in concept 1.1 or the flywheel in concept 2.2. The power split allows the heat engine to be operated in a low BSFC region and thus reduce the expended fuel. The heat engine supplies 100 percent of all power requirements for all vehicle states except acceleration in the engine mode.

Scope of Task II Analysis

The Task II analysis was completed in two phases. Cost and performance tradeoffs were done to choose between concept 1.1 and concept 2.2. Optimization tradeoffs were performed once the best concept was chosen.

Acquisition cost, life-cycle cost, and annual fuel usage were viewed as the most important characteristics of each propulsion system. These characteristics were heavily dependent upon three input parameters: engine size, battery pack size, and power split. The effects of two of these parameters, battery pack size and power split, were investigated in the initial cost and performance tradeoffs of Task II. A heat engine size of 56 kW was chosen and kept constant throughout the initial comparison. A minimum battery pack size to meet the design performance goals was found for concepts 1.1 and 2.2, using both nickel-zinc and lead-acid batteries. Thus, four different propulsion systems were defined.

Battery pack size was increased so a total of nine propulsion systems were investigated in the initial comparison as shown in table 19. The power split was varied for each of the nine propulsion systems to find the optimum operating conditions. Comparisons of the analytical results show concept 1.1 with lead-acid batteries to be the most cost effective, as shown in the Cost and Performance Tradeoffs section.

The cost optimization tradeoffs were performed to investigate the following major input parameters: engine size, battery size, and power split. Three engine sizes were chosen. A minimum battery pack size was found for each engine size, thus defining three propulsion systems. Additional systems were defined with increased battery packs, as shown in table 20. Optimum operating conditions were found by varying the power split in each propulsion system. A system with a 65-kW engine and 386 kg of lead-acid batteries was chosen in the optimization subtask, as shown in the Cost Optimization Tradeoffs section.

The optimization continued, once the heat engine and battery pack size were chosen, by accurately sizing all system components, based on maximum power loads and hardware efficiency characteristics. A study was made of the sensitivity of the propulsion system to electric motor type, heat engine type, acceleration rate on special test cycle, and vehicle performance goals.

TABLE 19.--SCOPE OF COST AND PERFORMANCE TRADEOFFS

Concept	Engine rating, kW	Battery pack weight, kg	Battery type
1.1	56	204*	Nickel-zinc
		272	Nickel-zinc
		363	Nickel-zinc
		499*	Lead-acid
2.2	56	204*	Nickel-zinc
		272	Nickel-zinc
		363	Nickel-zinc
		363*	Lead-acid
		499	Lead-acid

*Minimum battery pack size to meet performance goals

TABLE 20.--SCOPE OF COST OPTIMIZATION TRADEOFFS

Concept	Engine rating, kW	Battery pack weight, kg	Battery type
1.1	56	499*	Lead-acid
		612	
		725	
	65	272*	
		386	
		499	
	75	136*	
		249	
		363	

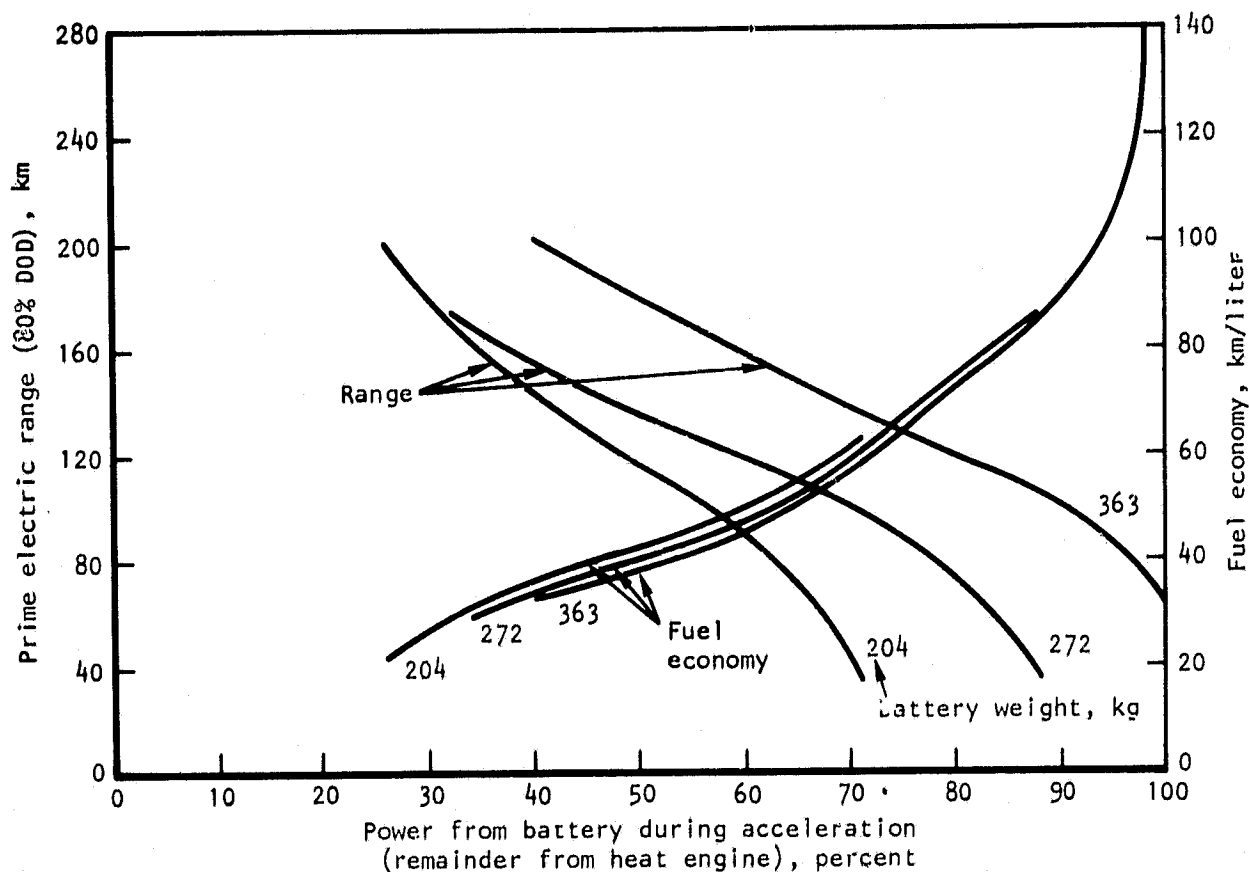
*Minimum battery pack weight to meet performance goals

COST AND PERFORMANCE TRADEOFFS

This section contains results of the initial tradeoffs. These tradeoffs were performed to show the effect of varying power split on vehicle cost and performance, and to choose between concept 1.1 and concept 2.2 as the final concept.

Prime Electric Range and Fuel Economy

Prime electric range and fuel economy are plotted against power split in figs. 64 to 67. Each curve represents one propulsion system operated on the special test cycle varying the power limit on the battery pack during acceleration. The effect of reducing the battery power is to increase electric range and reduce fuel economy. The 100 percent battery power line represents an all electric mode of operation. Not all propulsion systems studied are capable of running the STC on battery alone, so the 100 percent battery power line cannot be achieved in all cases.



546281

Figure 64.--Concept 1.1 electric mode performance (nickel-zinc battery).

ORIGINAL PAGE IS
OF POOR QUALITY

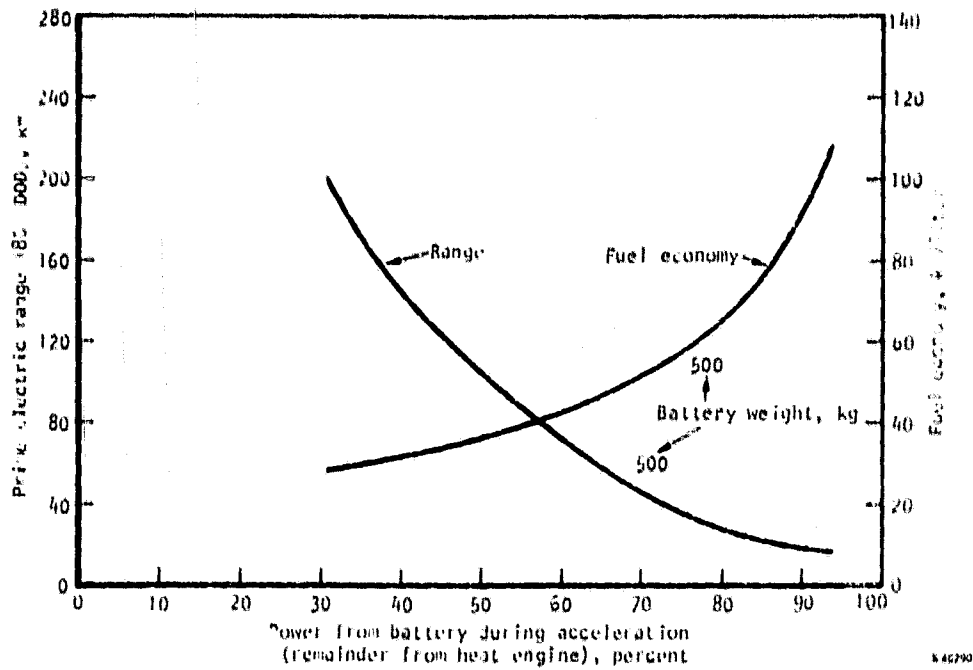


Figure 65.--Concept 1.1 electric mode performance (lead-acid battery)

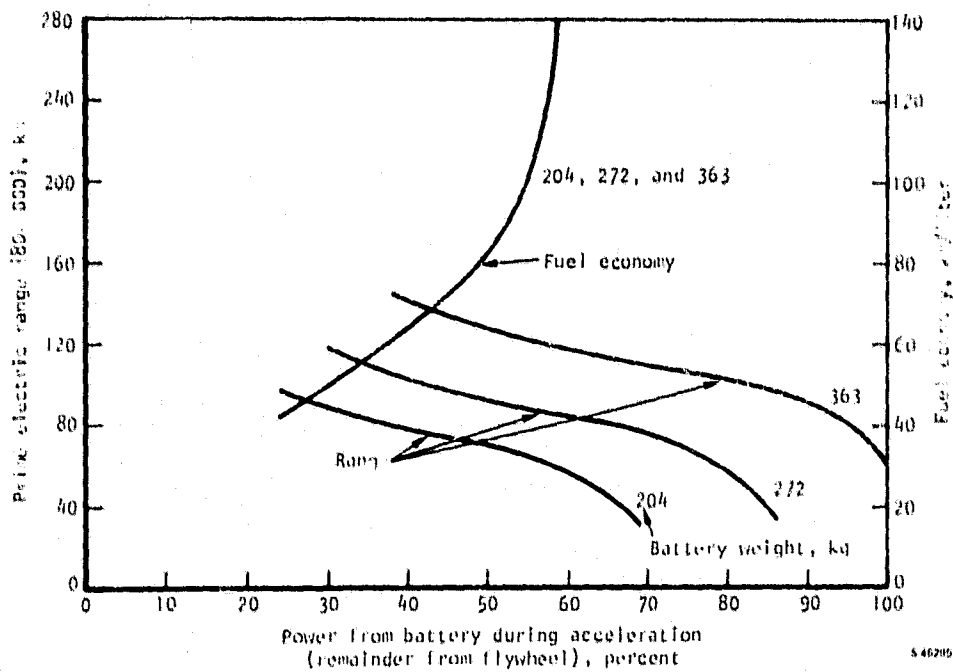
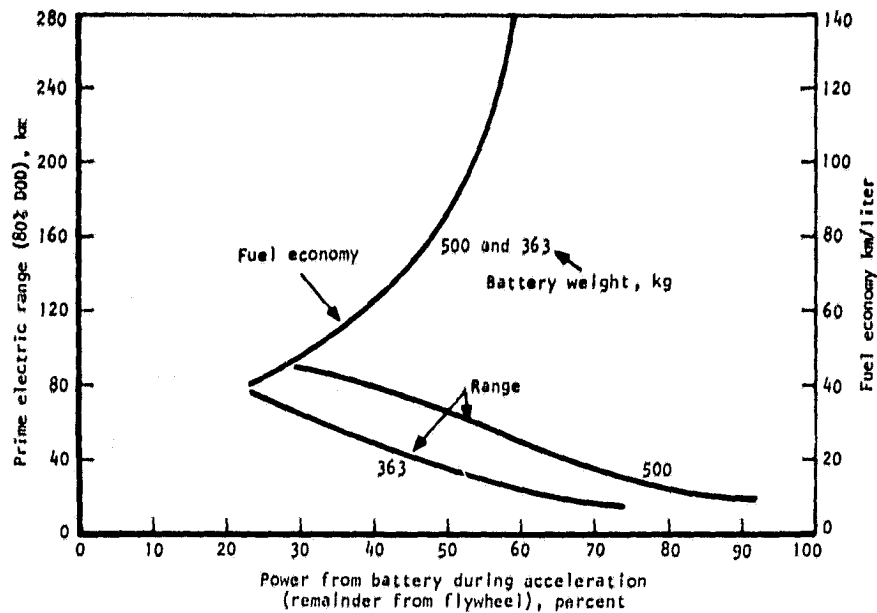


Figure 66.--Concept 2.2 electric mode performance (nickel-zinc battery).



840771

Figure 67.--Concept 2.2 electric mode performance (lead-acid battery).

Concept 1.1 shows more extreme changes in both electric range and fuel economy than concept 2.2 as the battery power is reduced.

The heat engine is heavily used to meet acceleration power requirements in concept 1.1 when the battery power is reduced. The battery receives all the regenerative braking energy. Thus the lightly loaded battery receives the full benefit of regenerative braking energy to increase electric range at the expense of using more fuel during acceleration.

The flywheel is used to meet power requirements as battery power is reduced during acceleration in concept 2.2. The regenerative braking energy is used to restore flywheel speed. The heat engine is only used in concept 2.2 to bring the flywheel up to full speed if the regenerative braking energy is inadequate. Thus the lightly loaded battery does not receive the benefit of regenerative braking energy to boost the range, but less fuel is used.

Annual Fuel Usage

Annual fuel usage for various power splits is shown in figs. 68 and 69. There are many factors that affect the annual fuel calculation. The specific fuel consumption in the electric mode, engine mode, and cruise at 90 km/hr, as well as the prime electric range, cruise range, and daily range frequency are all considered to obtain the annual fuel usage. The minimum point on the annual fuel usage curves occurs at a different power split for each propulsion system.

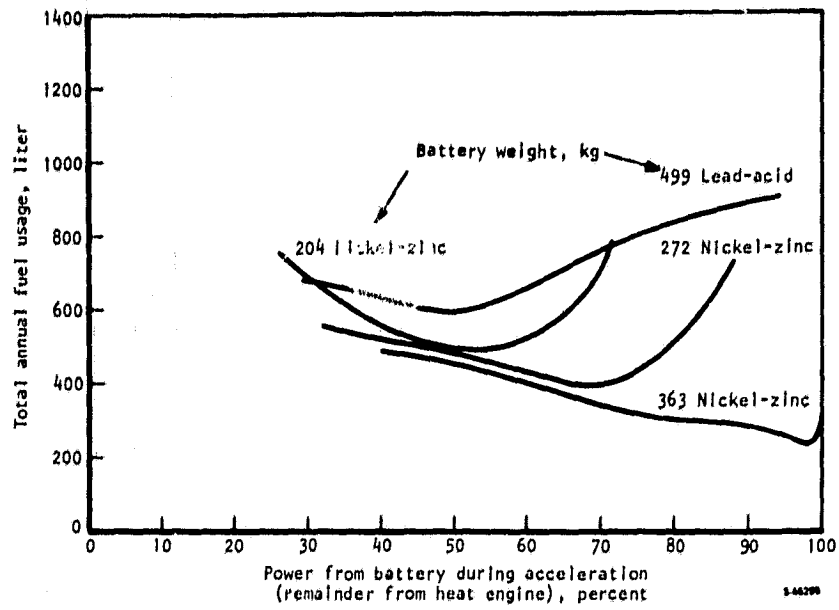


Figure 68.--Concept 1.1 annual fuel usage vs power split.

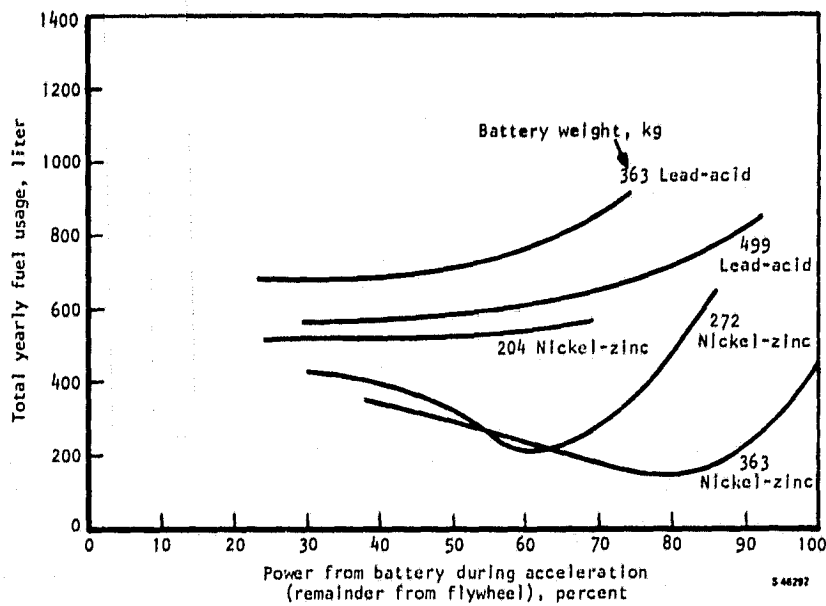


Figure 69.--Concept 2.2 annual fuel usage vs power split.

Life-Cycle Cost

Life-cycle cost vs power split curves are shown in figs. 70 and 71. These curves show that the most economical operation of a particular propulsion system occurs at low battery power. Systems with lead-acid batteries have lower life-cycle costs than those systems with nickel-zinc batteries.

Fuel Usage and Cost Comparison

Minimum annual fuel usage, acquisition cost, and life-cycle cost for the nine propulsion systems studied in the initial comparison are shown in figs. 72 to 74. The power split chosen for minimum annual fuel usage and life-cycle cost is that power split that gives the least annual fuel usage. The acquisition cost is not dependent upon power split for a fixed battery weight and engine size. These charts illustrate the inverse relationship between cost and fuel usage. Lower cost systems use more fuel.

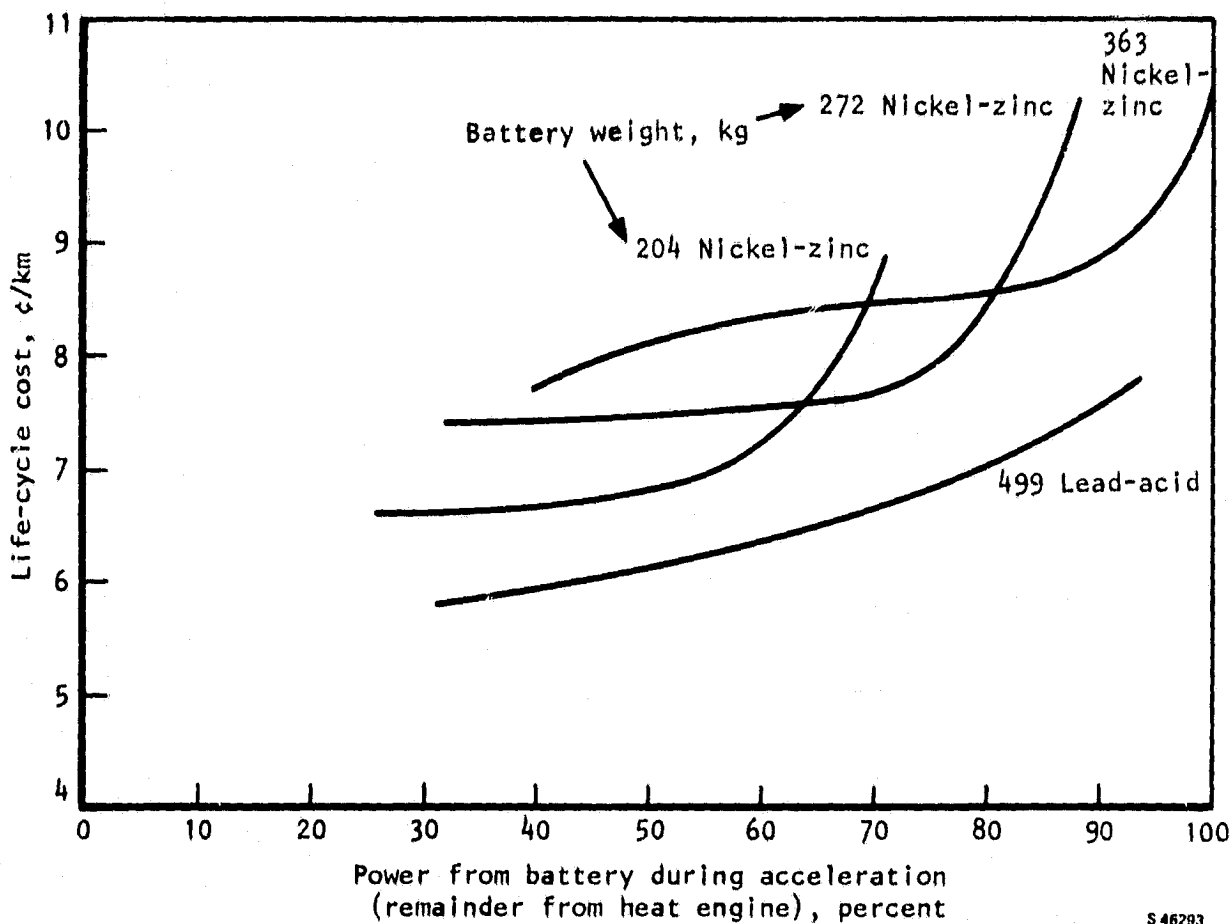
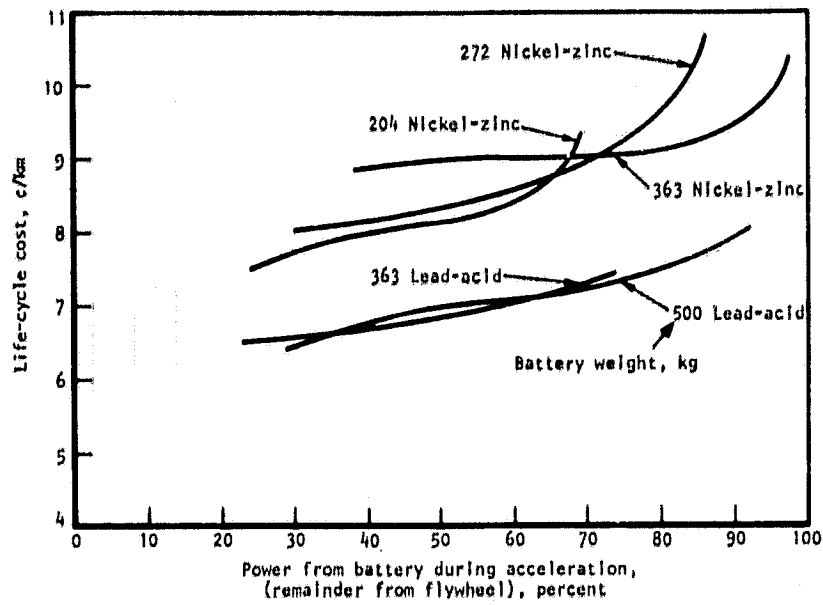
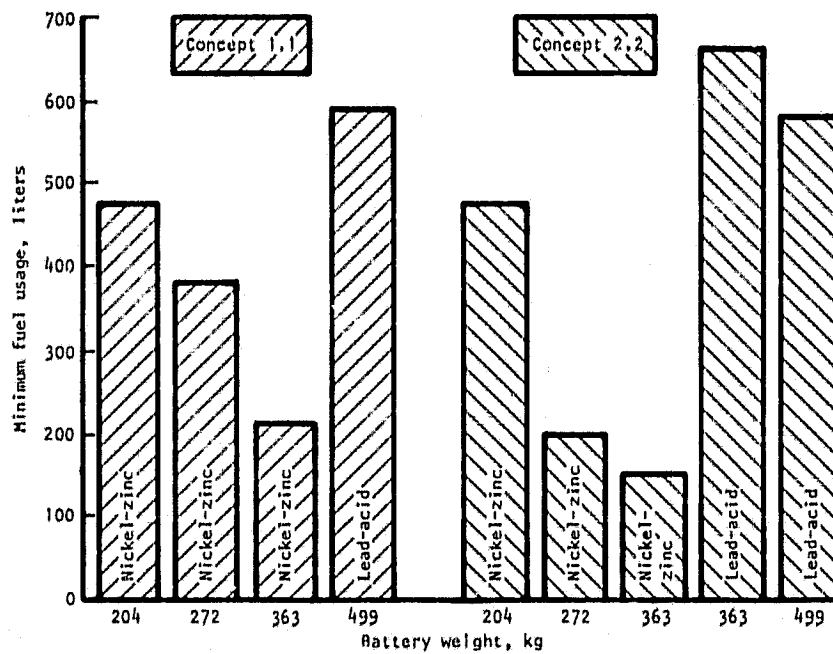


Figure 70.--Concept 1.1 life-cycle cost.



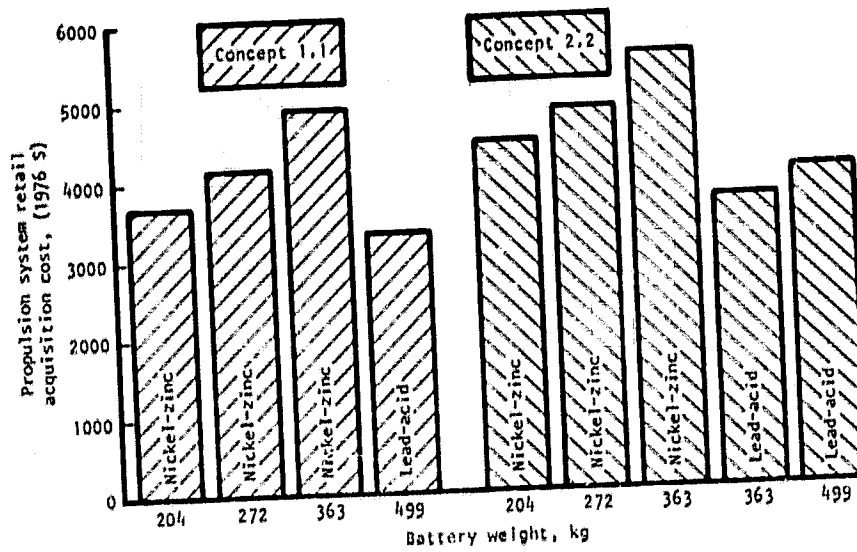
846707

Figure 71.--Concept 2.2 life-cycle cost.



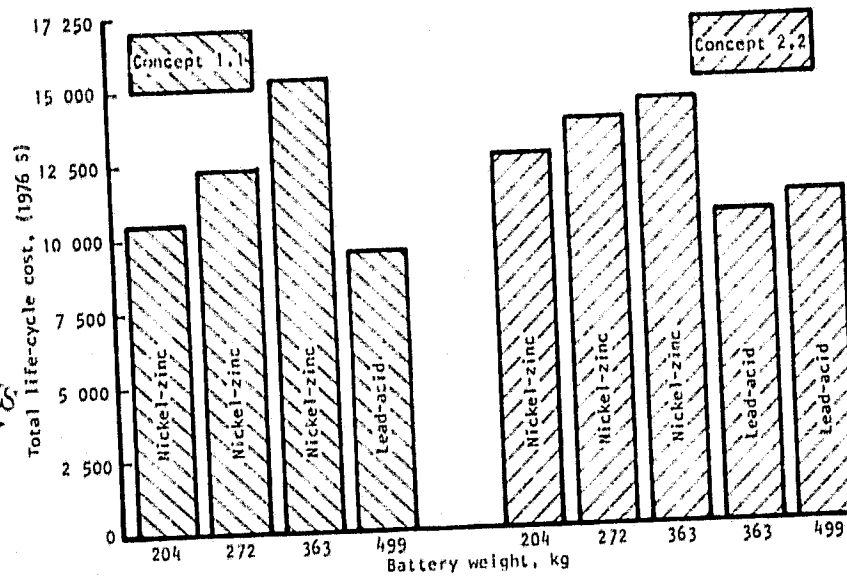
846702

Figure 72.--Minimum annual fuel usage vs battery weight and type.



54827A

Figure 73.--Acquisition cost vs battery weight and type.



54827B

Figure 74.--Life-cycle cost vs battery weight and type.

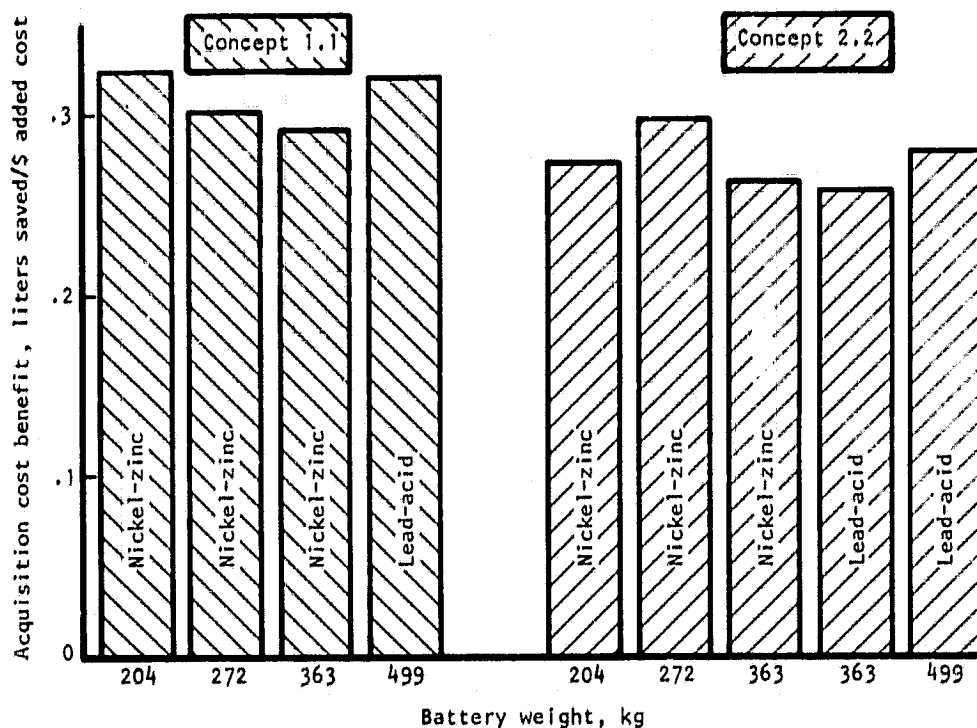
ORIGINAL PAGE IS
OF POOR QUALITY

Cost Benefit Comparisons

Acquisition cost benefits and life-cycle cost benefits are presented in figs. 75 and 76. Cost benefits compare fuel savings as a function of added cost to the owner for the different propulsion systems. The performance of a conventional, all-gasoline propulsion system was estimated using the analytical methods used throughout the study. The conventional propulsion system weighs 322 kg, which leads to a vehicle test weight of 1411 kg. The conventional system uses 1416 liters (374 gal) of fuel annually, costs \$767, and has life-cycle costs of \$7600. Fuel savings and added costs are computed for each hybrid propulsion system by comparing it to the conventional all-gasoline propulsion system. Acquisition cost benefits are the ratio of fuel saved to added acquisition cost. Life-cycle cost benefits are the ratio of fuel saved to added life-cycle cost.

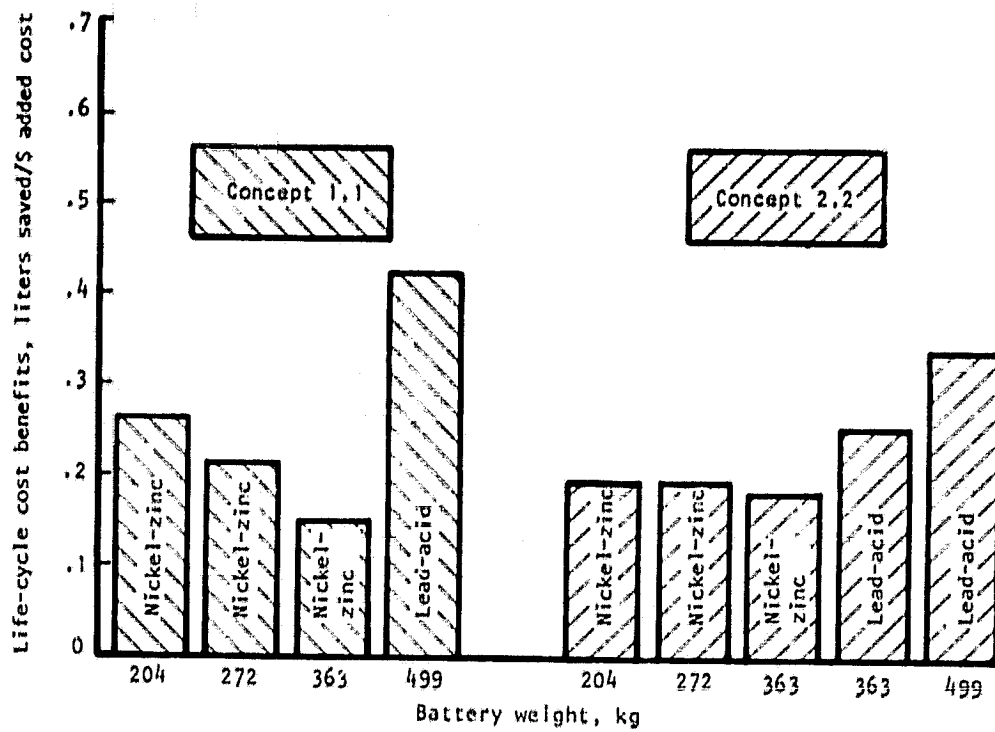
The acquisition cost benefits generally show concept 1.1 to be more cost effective than concept 2.2. The life-cycle cost benefits show concept 1.1 with lead-acid batteries to be far superior.

Concept 1.1 was selected, with NASA concurrence, as the selected propulsion system for optimization in this study.



5-46284

Figure 75.--Acquisition cost benefits vs battery weight and type.



546273

Figure 76.--Life-cycle cost benefit vs battery weight and type.

ORIGINAL PAGE IS
OF POOR QUALITY

COST OPTIMIZATION TRADEOFFS

The initial comparison subtask showed concept 1.1 with lead-acid batteries to be the most cost effective. The purpose of the optimization subtask was to size the final propulsion system components. The engine size and battery pack size were the most important variables. Nine different propulsion systems were investigated, as shown in table 20. Analysis was made on the nine systems in the same manner used in the initial comparison. The cost benefit charts for the nine propulsion systems showed the 65-kW heat engine and 386 kg of batteries to be the best system. All other components could then be sized based on the maximum power loads that occur in each component.

Cost Benefit Comparison

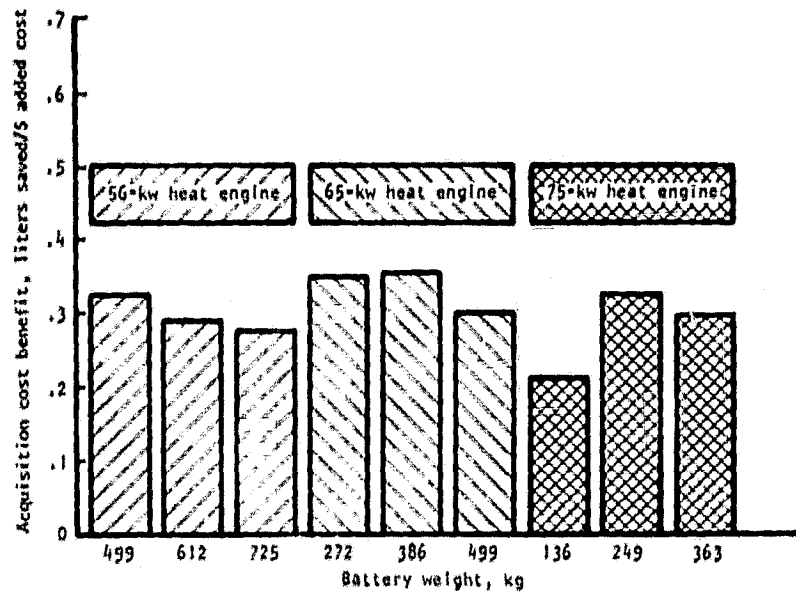
Acquisition cost benefits and life-cycle cost benefits are shown in figs. 77 and 78. The 65-kW (87-hp) heat engine with 386 kg (850 lb) of lead-acid batteries is clearly the most cost effective system. This system yields the most petroleum saved for each dollar spent.

Final System Performance

The remaining propulsion system components were sized to permit maximum power loads during the acceleration goal of 0 to 90 km/hr in 12 s. The final propulsion system design summary is shown in table 21, along with the weight and cost statement of each component in the final propulsion system. The guidelines used in calculation of component costs and weight can be found in tables 10 and 11.

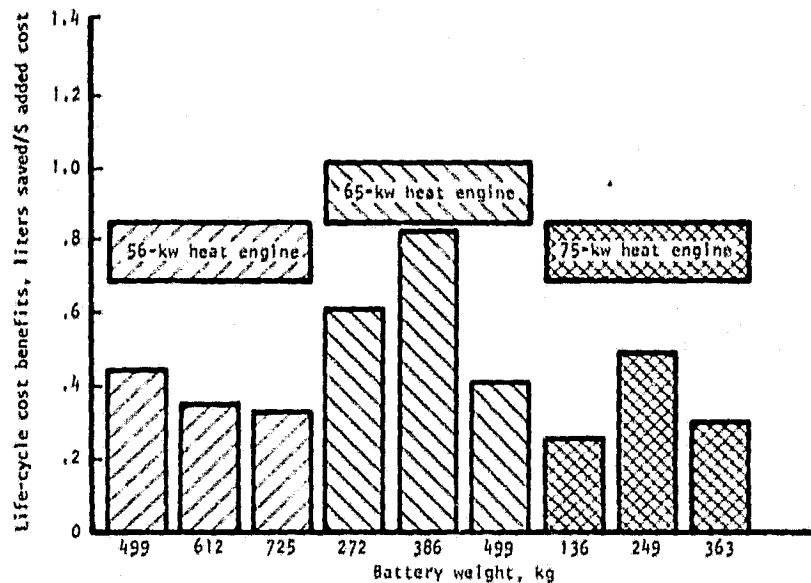
The final propulsion system performance summary is shown in table 22. The special test cycle (STC), shown in fig. 6, represents the urban driving cycle, and the constant vehicle speed of 90 km/hr represents the highway driving cycle. Performance was also calculated using the federal urban driving cycle and the federal highway driving cycle. Battery life, annual fuel and electricity consumption, and life-cycle cost were calculated using the daily range frequency specified in table 4. For days with an 80-km range or more, the highway driving cycle is used exclusively. For days with more than an 80-km range, the highway driving cycle is used 90 percent of the distance, and the urban driving cycle is used 10 percent of the distance. There is electric recovery in the engine mode, because more energy is put into the battery during braking than is removed during acceleration. The annual fuel average is the annual mileage divided by total annual fuel usage.

Additional results and cost worksheets are presented in figs. 79 through 83 and table 23.



544700

Figure 77.--Acquisition cost benefit vs battery weight and engine size for concept 1.1 with lead-acid batteries.



544711

Figure 78.--Life-cycle cost benefit vs battery weight and engine size for concept 1.1 with lead-acid batteries.

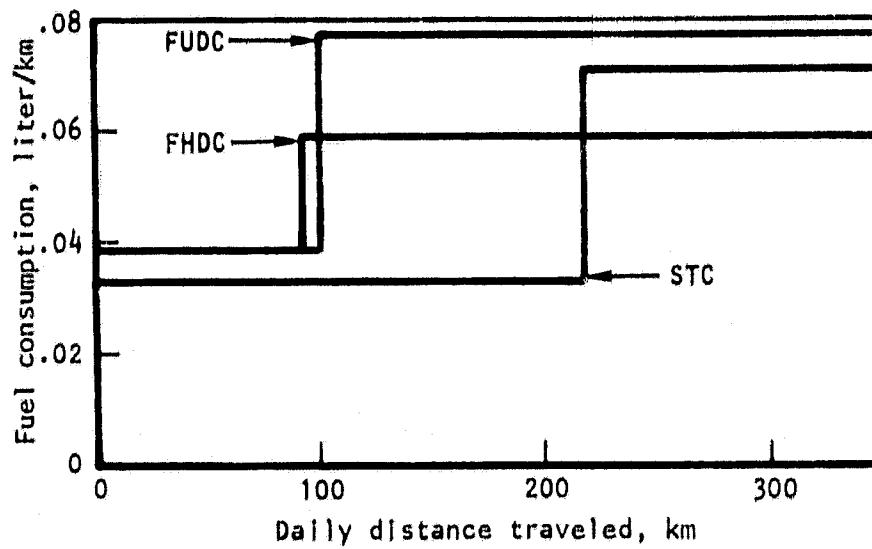
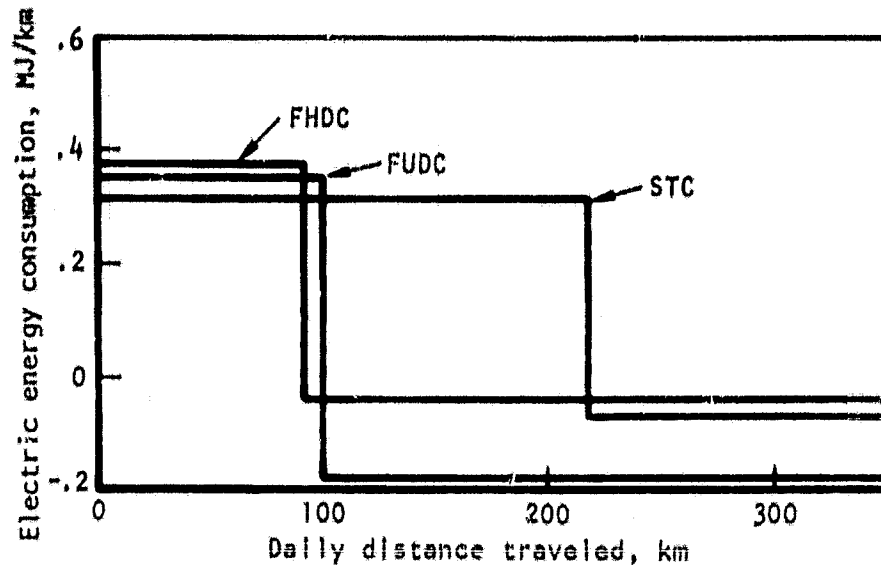
ORIGINAL PAGE IS
OF POOR QUALITY

TABLE 21.--FINAL PROPULSION SYSTEM COMPONENT COST AND WEIGHT SUMMARY

Component	Rating	Weight, kg	Acquisition cost, \$
Heat engine, spark-ignition	65 kW at 4000 rpm	199	410
Electrical machine	20 kW 14,000 rpm	12	375
Inverter and controls	40 kW	36	905
Mechanical CVT	90 kW 3:1 to 0.3:1 ratio	96	267
Gearbox	40 kW 3.5:1 ratio	12	57
Differential (fwd)	90 kW 4:1 ratio	59	196
ISOA Lead-acid	100 W/kg 40 W-hr/kg at 3-hr rate	386	1004
Total propulsion system		800	3214
Vehicle test weight		2032	-

TABLE 22.--FINAL PROPULSION SYSTEM PERFORMANCE SUMMARY

Test cycle	STC	FUDC/FHDC
Heat engine/battery power split during acceleration	30/70	30/70
Urban driving cycle electric mode:		
Prime electric range, km	218	101
Electricity usage, W-hr/km	88	98
Fuel usage, km/liter	30	26
Urban driving cycle engine mode:		
Fuel usage, km/liter	14	13
Electricity recovery, W-hr/km	20	51
Highway driving cycle electric mode:		
Highway electric range, km	39	93
Electric usage, W-hr/km	183	105
Fuel usage, km/liter	0	26
Highway driving cycle engine mode:		
Fuel usage, km/liter	18	17
Electricity recovery, W-hr/km	0	12
Battery pack life, yr	7.9	5.5
Annual electricity usage, kW-hr	1475	1659
Annual fuel usage, liters	590	666
Annual fuel average, km/liter	27	24
Acquisition cost, \$	3214	3214
Life-cycle cost, ¢/km	5.4	5.8



S46283

Figure 79.--Final propulsion system specific energy consumption.

LIFE CYCLE COST WORKSHEET

YEAR	"0"	1	2	3	4	5	6	7	8	9	10
1 PURCHASE PRICE	\$3214										
2 FUEL		235	235	235	235	235	235	235	235	235	235
3 ELECTRICITY		88	88	88	88	88	88	88	88	88	88
4 REPAIR + MAINTENANCE		240	240	240	240	240	240	240	240	240	240
5 BATTERY REPLACEMENT			0	0	0	0	0	0	1004	0	0
6 SYSTEM SALVAGE (MINUS)											
7 BATTERY SALVAGE (MINUS)			0	0	0	0	0	0	-100	0	-365
8 TOTAL	3214	563	563	563	563	563	563	563	1467	563	154
9 DISCOUNT FACTOR	1.00	.980	.961	.942	.924	.906	.888	.871	.854	.837	.820
10 PRESENT VALUE (8 x 9)	3214	552	541	530	520	510	500	490	1252	471	126

11 PRESENT VALUE OF LIFE CYCLE COST (SUM OF 10) = \$8706

12 PRESENT VALUE OF LIFE CYCLE COST PER KILOMETER DRIVEN (11/TOTAL KM) = \$-.0544

S-45678

Figure 80.--Life-cycle-cost worksheet for the final propulsion system operated on the special test cycle.

ORIGINAL PAGE IS
OF POOR QUALITY

OPERATING COST WORKSHEET

COSTS IN CENTS PER KILOMETER	YEAR									
	1	2	3	4	5	6	7	8	9	10
Distance Dependent Costs										
Maintenance										
Engine System	\$.50	.50	.50	.50	.50	.50	.50	.50	.50	.50
Electric	0	0	0	0	0	0	0	0	0	0
Battery	.20	.20	.20	.20	.20	.20	.20	.20	.20	.20
Energy Buffer	0	0	0	0	0	0	0	0	0	0
A TOTAL	.70	.70	.70	.70	.70	.70	.70	.70	.70	.70
Repair										
Engine System	.40	.40	.40	.40	.40	.40	.40	.40	.40	.40
Electric	0	0	0	0	0	0	0	0	0	0
Auxiliaries	.17	.17	.17	.17	.17	.17	.17	.17	.17	.17
Transmission	.23	.23	.23	.23	.23	.23	.23	.23	.23	.23
D TOTAL	.80	.80	.80	.80	.80	.80	.80	.80	.80	.80
Electricity	.55	.55	.55	.55	.55	.55	.55	.55	.55	.55
Fuel	1.47	1.47	1.47	1.47	1.47	1.47	1.47	1.47	1.47	1.47
E TOTAL	2.02	2.02	2.02	2.02	2.02	2.02	2.02	2.02	2.02	2.02
F TOTALS A+D+E	3.52	3.52	3.52	3.52	3.52	3.52	3.52	3.52	3.52	3.52
G DISTANCE EACH YEAR (KM)	16 000	16 000	16 000	16 000	16 000	16 000	16 000	16 000	16 000	16 000
H TOTAL DOLLARS (F/100) x G	563	563	563	563	563	563	563	563	563	563
Battery Replacement	0	0	0	0	0	0	0	908	0	0
YEAR TOTALS	563	563	563	563	563	563	563	1467	563	563

TOTAL OPERATING COST = \$6534 OPERATING COST PER KILOMETER = \$.0408 S-46677

Figure 81.-- Operating-cost worksheet for the final propulsion system operated on the special test cycle.

LIFE CYCLE COST WORKSHEET

YEAR	"0"	1	2	3	4	5	6	7	8	9	10
1 PURCHASE PRICE	\$3214										
2 FUEL											
3 ELECTRICITY		263	263	263	263	263	263	263	263	263	263
4 REPAIR + MAINTENANCE		100	100	100	100	100	100	100	100	100	100
5 BATTERY REPLACEMENT		240	240	240	240	240	240	240	240	240	240
6 SYSTEM SALVAGE (MINUS)			0	0	0	0	1004	0	0	0	0
7 BATTERY SALVAGE (MINUS)											
8 TOTAL	3214	603	603	603	603	603	1507	603	603	603	-100
9 DISCOUNT FACTOR	1.00	.980	.951	.924	.894	.866	.837	.811	.784	.757	.731
10 PRESENT VALUE (8 x 9)	3214	591	579	568	557	546	1338	524	515	504	376
11 PRESENT VALUE OF LIFE CYCLE COST (SUM OF 10)											59312
12 PRESENT VALUE OF LIFE CYCLE COST PER KILOMETER DRIVEN (11 TOTAL KM) =											\$-.0582

S-45678

Figure 82.-- Life-cycle-cost worksheet for the final propulsion system operated on the F100 and F111.

OPERATING COST WORKSHEET

YEAR	1	2	3	4	5	6	7	8	9	10
COSTS IN CENTS PER KILOMETER										
Distance Dependent Costs										
Maintenance										
Engine System										
Electric	.50	.50	.50	.50	.50	.50	.50	.50	.50	.50
Battery	0	0	0	0	0	0	0	0	0	0
Energy Buffer	.20	.20	.20	.20	.20	.20	.20	.20	.20	.20
A TOTAL	.70									
COSTS IN CENTS PER KILOMETER										
Repair										
Engine System										
Electric	.40	.40	.40	.40	.40	.40	.40	.40	.40	.40
Auxiliaries	0	0	0	0	0	0	0	0	0	0
Transmission	.17	.17	.17	.17	.17	.17	.17	.17	.17	.17
D TOTAL	.23									
COSTS IN CENTS PER KILOMETER										
Electricity	.63	.63	.63	.63	.63	.63	.63	.63	.63	.63
Fuel	1.64	1.64	1.64	1.64	1.64	1.64	1.64	1.64	1.64	1.64
E TOTAL	2.27									
F TOTALS A+D+E	3.77									
G DISTANCE EACH YEAR (KM)	16 000									
H TOTAL DOLLARS (F/100) x G	603									
Battery Replacement	0	0	0	0	0	904	0	0	0	0
YEAR TOTALS	603	603	603	603	603	1507	603	603	603	603

TOTAL OPERATING COST = \$6934 OPERATING COST PER KILOMETER = \$.0433 S-45677

Figure 83.--Operating-cost worksheet for the final propulsion system operated on the FUDC and FHDC.

TABLE 23.-- ENERGY FLOW DISTRIBUTION FOR FINAL PROPULSION SYSTEM OPERATED THROUGH ONE CYCLE OF SPECIAL TEST CYCLE

Summary of energy losses in electric mode, W-hr.

	Acceleration	Cruise	Coast	Brake	Dwell	Total
Road drag	13.236	94.194	17.472	5.585	0.000	130.487
Differential	8.137	17.476	0.000	5.109	0.000	30.722
Transmission	11.978	8.157	0.000	7.551	0.000	27.687
Motor	3.626	9.410	0.153	5.961	0.383	19.533
Controller	2.672	8.985	0.012	4.611	0.301	16.691
Brake	0.000	0.000	0.000	0.000	0.000	0.000
Gearbox	1.005	3.197	0.069	1.374	0.174	5.819
Accessory	2.333	8.333	1.667	1.500	4.167	18.000
Total	42.987	149.753	19.482	31.692	5.024	248.939
Battery	44.535	149.753	2.010	-72.243	5.024	129.079
Engine	119.863	0.000	0.000	0.000	0.000	119.863

Summary of energy losses in engine mode, W-hr.

	Acceleration	Cruise	Coast	Brake	Dwell	Total
Road drag	13.236	94.194	17.472	5.585	0.000	130.487
Differential	8.137	17.476	0.000	5.109	0.000	30.722
Transmission	11.675	6.167	0.000	7.551	0.000	25.393
Motor	3.009	0.000	0.000	5.961	0.000	8.970
Controller	2.566	0.000	0.000	4.611	0.000	7.177
Brake	0.000	0.000	0.000	0.000	0.000	0.000
Gearbox	0.882	0.000	0.000	1.374	0.000	2.256
Accessory	2.333	8.333	1.667	1.500	4.167	18.000
Total	41.838	126.170	19.139	31.692	4.167	223.006
Battery	42.766	0.000	0.000	-72.243	0.000	-29.477
Engine	120.484	126.170	1.667	0.000	4.167	252.487

PERFORMANCE SENSITIVITY STUDIES

A study was performed to measure the sensitivity that some of the ground rules had upon final vehicle design, performance, and cost. This sensitivity study was by no means exhaustive and further work in this area might be productive.

Electric Motor Sensitivity

Both Task I and Task II studies used a permanent magnet dc electric motor. The effect on the final propulsion system of substituting a mechanically commutated dc shunt motor was investigated.

Shunt-wound dc motors are particularly well-suited as traction motors where close speed control is desired. Using a separately excited field, with the field winding shunting the armature winding, the speed control is achieved by varying the relatively low power in the shunt circuit.

The dc motor with a separately excited field can provide constant horsepower from base speed to rated speed. This feature shapes the torque-speed relationship so that the torque at base speed is approximately 250 percent of the torque at rated speed. Base speed is defined as the lowest equilibrium speed reached by the motor when full armature voltage is applied and the field is fully excited. Below base speed, the torque can be held constant by decreasing the armature voltage in proportion to the speed reduction. The motor develops full power at base speed, with maximum efficiency. Above base speed, the power that can be developed remains nearly constant, using field weakening to control velocity, subject to the power constraints of commutation limit, saturation limit, and thermal limit. The motor performance map used for the dc shunt motor is shown in fig. 84, and it includes the losses associated with field control. This map represents the estimated performance for a motor with 100 percent rated power of 20 kW. The map is accurate for motors that are rated within ± 10 percent of the basic machine.

Direct current machinery is limited by the requirement for a commutator and brush network to supply armature power. The brushes wear and require periodic maintenance, and the limitation on peripheral speed of the commutator in turn limits the amount of size reduction, with speed increase, which can be accomplished to improve power density. The estimated motor size to achieve the performance in fig. 84 is 55 kg. This size and performance is based on current high-performance motor designs. There is no overall weight penalty compared to the permanent magnet dc electric motor because no electronic inverter is required for the dc shunt motor.

It is apparent that the optimum dc shunt motor performance is achieved at base speed. When the motor is used in a system with a variable transmission, the transmission is employed to allow the motor to reach base speed as soon as possible, and to operate close to base speed over as much of the driving cycle as possible. In this case the motor starting operation can be accomplished by the simple expedient of reduced voltage applied to the armature in steps to limit current, and this regime of operation is so short, up to a vehicle speed of approximately 6 km/hr, that the efficiency of operation is not a significant concern.

ORIGINAL PAGE IS
OF POOR QUALITY

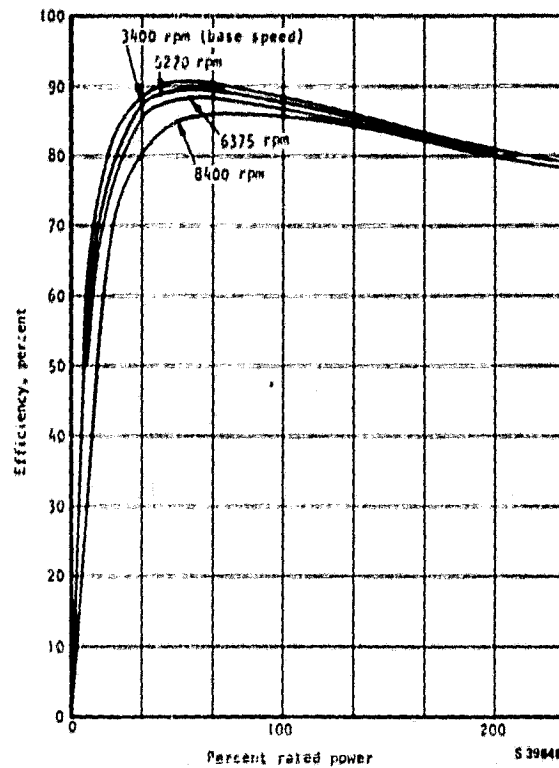


Figure 84.--Dc shunt motor performance.

The results of this investigation are shown in table 24 and figs. 85 and 86. The lower efficiency of the dc shunt motor results in a shorter electric range and more electric energy usage compared to the final propulsion system. The fuel consumption is slightly lower with the dc shunt motor because in the electric mode the best operating speed is lower for the dc shunt motor than for the permanent magnet motor that is used in the final system. When the heat engine is required to buffer the electric motor, the lower speed of the dc shunt motor allows the heat engine to operate at a better efficiency. The greatest effect of substituting the dc shunt motor into the final propulsion system is in the reduction of the acquisition cost by \$717.

Heat Engine Sensitivity

The final system was evaluated with four different engine/operating mode combinations: (1) gasoline, on-off, (2) gasoline, idle, (3) diesel, on-off, and (4) diesel, idle. The final propulsion system uses a gasoline engine operated in an on-off mode. In this mode the engine does not idle. No fuel is consumed if no power is required from the engine. This on-off operation leads to reduced fuel usage, but some technical risks are involved in developing such a system.

The results for the four propulsion systems operated on the special test cycle are shown in table 25. The diesel engine vehicle weighs 83 kg and costs \$190 more than the gasoline engine vehicle. The diesel engine is capable of a much lower idle fuel flow than the gasoline engine; thus annual fuel usage does not increase with the diesel as much as with the gasoline engine when the engine is allowed to idle.

TABLE 24.--PERFORMANCE SUMMARY FOR PROPULSION SYSTEM WITH DC SHUNT MOTOR

Test Cycle	STC	FUDC/FHDC
Heat engine/battery power split during acceleration	30/70	30/70
Urban driving cycle electrical mode:		
Prime electric range, km	195	87
Electricity usage, W-hr/km	95	116
Fuel usage, km/liter	29	30
Urban driving cycle engine mode:		
Fuel usage, km/liter	13	13
Electricity recovery, W-hr/km	18	46
Highway driving cycle electric mode:		
Highway electric range, km	42	91
Electricity usage, W-hr/km	179	107
Fuel usage, km/liter	0	33
Highway driving cycle engine mode:		
Fuel usage, km/liter	18	17
Electricity recovery, W-hr/km	0	11
Battery pack life, yr	7.5	5.0
Annual electricity usage, kW-hr	1579	1913
Annual fuel usage, liters	602	590
Annual fuel average, km/liter	27	27
Acquisition cost, \$	2411	2411
Life-cycle cost, ¢/km	5.0	5.3

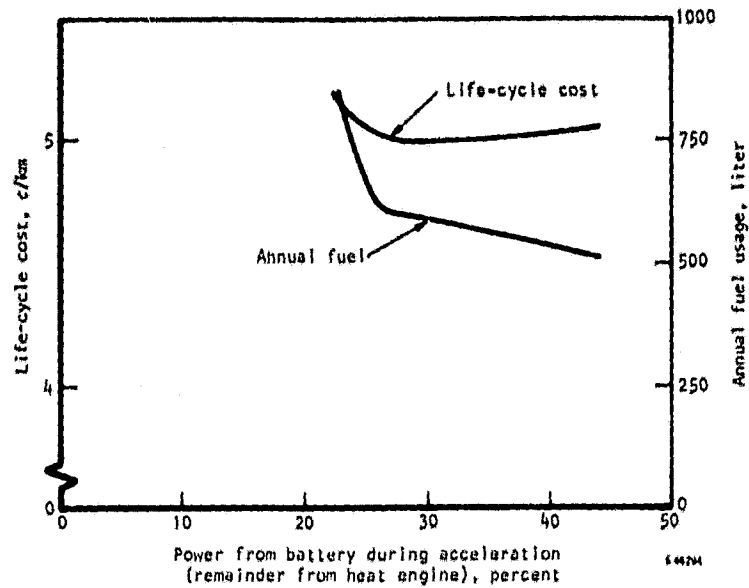


Figure 85.--Life-cycle cost and annual fuel usage vs power split for propulsion system with dc shunt motor.

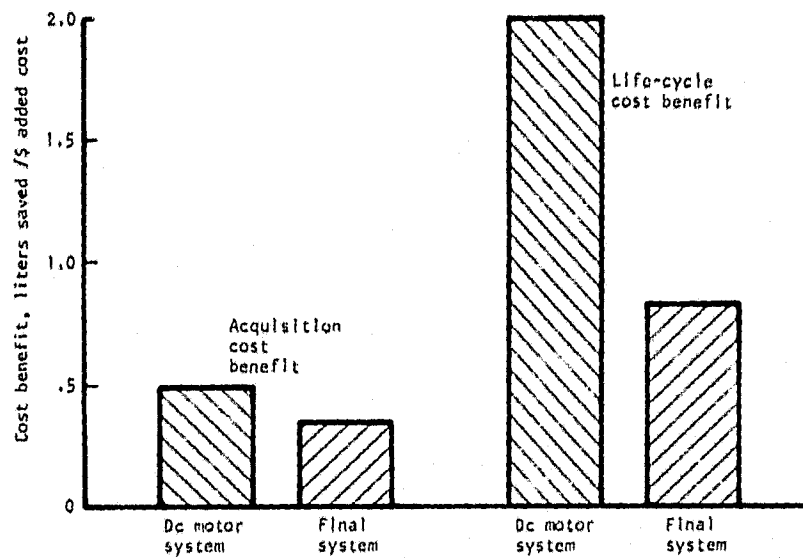


Figure 86.--Cost benefit comparison between the final propulsion system and propulsion system with dc shunt motor.

TABLE 25.--SENSITIVITY OF VEHICLE PERFORMANCE TO HEAT ENGINE TYPE AND MODE OF OPERATION

Heat engine type	Gasoline		Diesel	
	On-Off	Idle	On-Off	Idle
Operation of heat engine				
Heat engine/battery power split during acceleration	30/70	30/70	30/70	30/70
Urban driving cycle electrical mode:				
Prime electric range, km	218	218	236	236
Electricity usage, W-hr/km	88	88	89	89
Fuel usage, km/liter	30	19	31	23
Urban driving cycle engine mode:				
Fuel usage, km/liter	14	14	15	15
Electricity recovery, W-hr/km	20	20	20	20
Highway driving cycle electric mode:				
Highway electric range, km	39	39	37	37
Electricity usage, W-hr/km	183	183	185	185
Fuel usage, km/liter	0	0	0	0
Highway driving cycle engine mode:				
Fuel usage, km/liter	18	18	17	17
Electricity recovery, W-hr/km	0	0	0	0
Battery pack life, yr	7.9	7.9	8.1	8.1
Annual electricity usage, kW-hr	1475	1475	1480	1480
Annual fuel usage, liters	590	804	507	628
Annual fuel average, km/liter	27	20	32	25
Acquisition cost, \$	3128	3128	3318	3318
Life-cycle cost, ¢/km	5.4	5.8	5.2	5.4

ORIGINAL PAGE .
OF POOR QUALITY

Fuel and Electricity Cost Sensitivity

Three fuel and electric cost scenarios were postulated by NASA for the future. The mid values of projected costs were used to calculate life-cycle costs and operating costs throughout Task I and Task II. The life-cycle cost for the final propulsion system was computed using all three sets of projected energy costs. These results, along with the cost upon which the results are based, are presented in fig. 87. The four propulsion system/operating mode combinations presented in the heat engine sensitivity were operated on the special test cycle. A conventional, all-heat-engine propulsion system was also evaluated for comparison.

The sensitivity to energy costs is quite apparent. The three cost scenarios indicate a 100-percent increase in fuel cost but only a 40-percent increase in electric cost. Under these circumstances propulsion systems using more fuel rise in cost more rapidly than systems using less fuel. The proposed final propulsion system will become less costly than a present-day conventional system when the energy costs of the third scenario are realized.

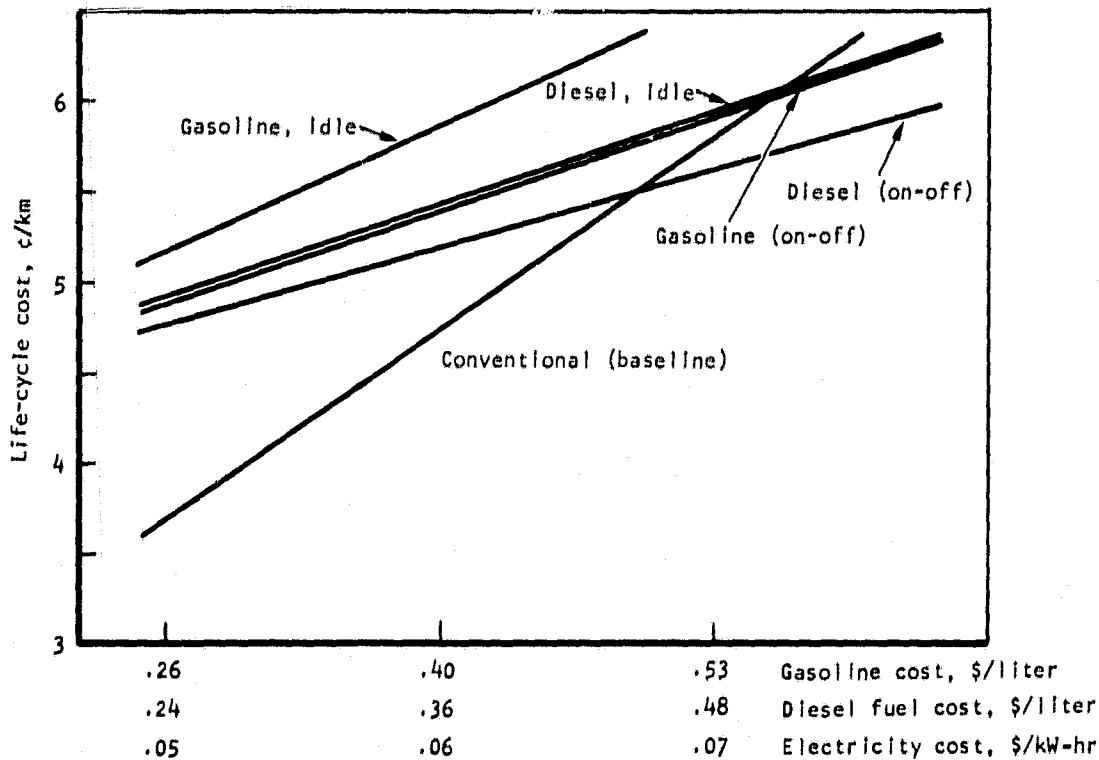


Figure 87.--Life-cycle cost sensitivity to petroleum and electricity costs.

546274

Test Cycle Sensitivity

The special test cycle, fig. 6, requires an acceleration from 0 to 72 km/hr in 14 s. The time to accelerate was extended successively to 20 s and 28 s to measure the effect of acceleration time upon vehicle performance. Cruise, coast, brake, and dwell time and vehicle, battery, and propulsion system were kept constant. The performance of the final propulsion system was calculated using the three different acceleration times. The results are shown in table 26.

These results do not show great variations as a function of acceleration time. The prime electric range varies only slightly. This can be explained by plotting battery depth of discharge (DOD) against time (fig. 88). The depth of discharge profile is the same after the acceleration phase for each test cycle. The only difference occurs during the acceleration phase. Each acceleration ends at approximately 0.4 percent DOD. The lower acceleration rate requires less power from the battery, but the time is longer. The energy to accelerate a car at any rate is essentially constant. The battery is buffered by the engine in all three cases to keep battery power low. The specific energy is nearly constant at low specific power (see figure 7).

The fuel consumption is reduced by 10 percent as acceleration is increased to 28 s. The lower power required in the slower accelerations allows the engine to be used at a speed and torque point that is more fuel efficient.

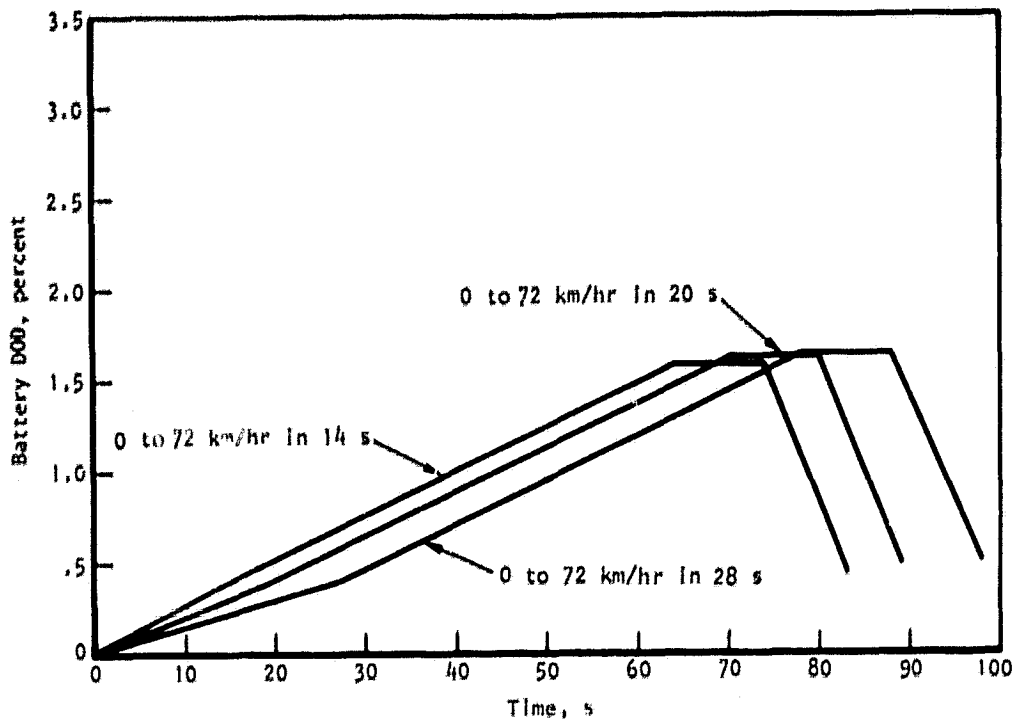
Performance Goal Sensitivity

The basic performance goals for the new mission vehicle designated BC are presented in table 16. The maximum acceleration goal of 0 to 90 km/hr in 12 s was used to size the propulsion system components. The sensitivity to this acceleration goal was investigated by designing two new propulsion systems, one capable of 0 to 90 km/hr acceleration in 16 s and the second in 20 s. It was assumed that, as the 0 to 90 km/hr acceleration goal was reduced, all the other performance goals were lowered so that the 0 to 90 km/hr acceleration goal still sizes the components. Two more systems were designed with small engines (22 kW) and larger battery packs that could accelerate to 90 km/hr in 15 s and 18 s. All five propulsion systems studied are presented in table 27. Each of the new propulsion systems was evaluated on the three test cycles used in the test cycle sensitivity. The performance results are shown in tables 28 and 29.

The propulsion system that allowed 0 to 90 km/hr in 16 s had a 37-kW heat engine, 272 kg of lead-acid batteries, and a test weight of 1824 kg. The purchase cost of \$2705 included \$707 for batteries. This price represents a decrease from the final propulsion system cost of \$423. The annual fuel usage does not change a great deal (5 percent) when compared to the final propulsion system.

TABLE 26.--FINAL PROPULSION SYSTEM PERFORMANCE SENSITIVITY TO TEST CYCLE,
CAPABLE OF ACCELERATING 0 TO 90 KM/HR IN 12 S

Acceleration time to 72 km/hr In test cycle, s	14	20	28
Heat engine/battery power split during acceleration	30/70	30/70	30/70
Urban driving cycle electric mode:			
Prime electric range, km	218	219	227
Electricity usage, W-hr/km	88	90	87
Fuel usage, km/liter	30	33	35
Urban driving cycle engine mode:			
Fuel usage, km/liter	14	14	15
Electricity recovery, W-hr/km	20	10	4
Highway driving cycle electric mode:			
Highway electric range, km	39	39	39
Electricity usage, W-hr/km	183	183	183
Fuel usage, km/liter	0	0	0
Highway driving cycle engine mode			
Fuel usage, km/liter	18	18	18
Electricity recovery, W-hr/km	0	0	0
Battery pack life, yr	7.9	7.9	8.0
Annual electricity usage, kW-hr	1475	1491	1462
Annual fuel usage, liters	590	553	538
Annual fuel average, km/liter	27	29	30
Acquisition cost, \$	3128	3128	3128
Life-cycle cost, ¢/km	5.4	5.3	5.2



846279

Figure 88.--Battery depth of discharge vs time for final propulsion system on three different test cycles.

TABLE 27.--SCOPE OF PERFORMANCE GOAL SENSITIVITY

Maximum acceleration to 90 km/hr, s	12*	16	20	18	15
Heat engine rating, kW	65*	37	22	22	22
Battery pack size, kg	386*	272	181	363	544
Test weight, kg	2078*	1824	1324	1560	1785

*Final propulsion system

TABLE 28.--PERFORMANCE SUMMARY FOR A PROPULSION SYSTEM WITH 37-KW HEAT ENGINE AND 272 KG OF LEAD-ACID BATTERIES, CAPABLE OF ZERO TO 90 KW/HR ACCELERATION IN 16 S

Acceleration time to 72 km/hr on test cycle, s	14	20	28
Heat engine/battery power split during acceleration	35/65	30/70	30/70
Urban driving cycle electric mode:			
Prime electric range, km	91	141	146
Electricity usage, W-hr/km:	93	84	83
Fuel usage, km/liter	34	32	32
Urban driving cycle engine mode:			
Fuel usage, km/liter	14	15	15
Electricity recovery, W-hr/km	8	3	4
Highway driving cycle electric mode:			
Highway electric range, km	21	21	21
Electricity usage, W-hr/km	174	174	174
Fuel usage, km/liter	0	0	0
Highway driving cycle engine mode:			
Fuel usage, km/liter	18	18	18
Electricity recovery, W-hr/km	0	0	0
Battery pack life, yr	5.1	6.5	6.6
Annual electricity usage, kW-hr	1446	1312	1297
Annual fuel usage, liters	560	579	583
Annual fuel average, km/liter	29	28	27
Acquisition cost, \$	2705	2705	2705
Life-cycle cost, ¢/km	5.0	4.9	4.9

TABLE 29.--PERFORMANCE SUMMARY FOR PROPULSION SYSTEM WITH 22-KW HEAT ENGINE AND 181 KG OF LEAD-ACID BATTERIES CAPABLE OF ZERO TO 90 KM/HR ACCELERATION IN 20 S

Acceleration time to 72 km/hr on test cycle, s	14	20	28
Heat engine/battery power split during acceleration	50/50	40/60	30/70
Urban driving cycle electric mode:			
Prime electric range, km	13	42	57
Electricity usage, W-hr/km	106	88	79
Fuel usage, km/liter	54	38	35
Urban driving cycle engine mode:			
Fuel usage, km/liter	15	15	14
Electricity recovery, W-hr/km	0	6	0
Highway driving cycle electric mode:			
Highway electric range, km	9	9	9
Electricity usage, W-hr/km	157	157	157
Fuel usage, km/liter	0	0	0
Highway driving cycle engine mode:			
Fuel usage, km/liter	19	19	19
Electricity recovery, W-hr/km	0	0	0
Battery pack life, yr	2.6	3.5	4.0
Annual electricity usage, kW-hr	671	964	1012
Annual fuel usage, liters	791	651	621
Annual fuel average, km/liter	20	25	26
Acquisition cost, \$	2385	2385	2385
Life-cycle cost, ¢/km	5.3	4.9	4.8

The prime electric range was shorter in the new propulsion system than in the final propulsion system. This is caused primarily by the fact that there are fewer batteries in the new system. There is another factor that further reduces the range in the test cycle with 0 to 72 in 14 s. The battery pack must operate at a higher specific power (50 W/kg) to accelerate to 72 km/hr in 14 s, compared to the 20- and 28-s acceleration cycles (30 W/kg). The higher specific power leads to lower specific energy. The battery used at 50 W/kg is discharged much quicker than the battery used at 30 W/kg. The battery depth of discharge vs time curve is shown in fig. 89.

The propulsion system that could accelerate to 90 km/hr in 20 s had a 22-kW heat engine, 181 kg of lead-acid batteries, and a vehicle test weight of 1324 kg. The propulsion system is underpowered and, for all but the slowest acceleration (0 to 72 km/hr in 28 s), both engine and battery operated near their maximum. This resulted in short electric range and a relatively large fuel usage. The test cycle with the slowest acceleration did allow both heat engine and battery to be partly loaded, but the electric range is still quite short, and large amounts of fuel are required. The short electric range leads to more miles in the engine mode. A small underpowered engine operated near full power is not very efficient.

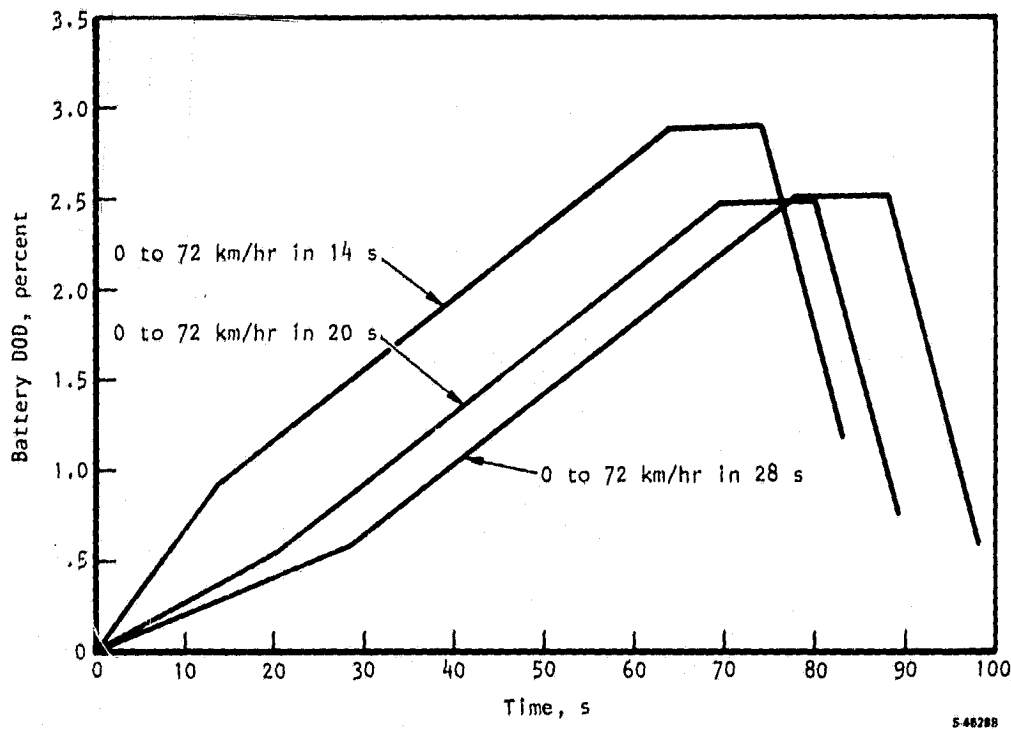


Figure 89.--Battery depth of discharge vs time for propulsion system with 37-kW heat engine and 272 kg of lead-acid batteries capable of zero to 72 km/hr acceleration in 16 s.

There has been interest in propulsion systems sized similar to the last system with very small gasoline engines. Two additional propulsion systems were drawn up with the same 22-kW heat engine and increased battery weight. The propulsion system shown in table 30 has a 22-kw heat engine, 363 kg of lead-acid batteries, test weight of 1560 kg, and an acquisition cost of \$2858. The propulsion system shown in table 31 has the 22-kW heat engine, 544 kg of lead-acid batteries, test weight of 1785 kg, and acquisition cost of \$3332. These two systems were included for completeness, and rigorous optimization of the systems was not attempted.

TABLE 30.--PERFORMANCE SUMMARY FOR A PROPULSION SYSTEM WITH A 22-KW HEAT ENGINE AND 363 KG OF LEAD-ACID BATTERIES CAPABLE OF ZERO TO 90 KM/HR ACCELERATION IN 18 S

Acceleration time to 72 km/hr on test cycle, s	14	20	28
Heat engine/battery power split during acceleration	60/40	50/50	30/70
Urban driving cycle electric mode:			
Prime electric range, km	62	109	182
Electricity usage, W-hr/km	114	100	77
Fuel usage, km/liter	52	38	28
Urban driving cycle engine mode:			
Fuel usage, km/liter	13	13	13
Electricity recovery, W-hr/km	0	0	0
Highway driving cycle electric mode:			
Highway electric range, km	42	42	42
Electricity usage, W-hr/km	165	165	165
Fuel usage, km/liter	0	0	0
Highway driving cycle engine mode:			
Fuel usage, km/liter	19	19	19
Electricity recovery, W-hr/km	0	0	0
Battery pack life, yr	4.2	5.7	7.3
Annual electricity usage, kW-hr	1521	1643	1307
Annual fuel usage, liters	526	496	602
Annual fuel average, km/liter	30	32	27
Acquisition cost, \$	2858	2858	2858
Life-cycle cost, ¢/km	5.4	5.0	5.0

TABLE 31.--PERFORMANCE SUMMARY FOR A PROPULSION SYSTEM WITH A 22-KW HEAT ENGINE AND 544 KG OF LEAD-ACID BATTERIES CAPABLE OF ZERO TO 90 KM/HR ACCELERATION IN 15 S

Acceleration time to 72 km/hr on test cycle, s	14	20	28
Heat engine/battery power split during acceleration	70/30	55/45	35/65
Urban driving cycle electric mode:			
Prime electric range, km	98	156	244
Electricity usage, W-hr/km	128	113	89
Fuel usage, km/liter	53	39	28
Urban driving cycle engine mode:			
Fuel usage, km/liter	12	13	13
Electricity recovery, W-hr/km	0	5	5
Highway driving cycle electric mode:			
Highway electric range, km	79	79	79
Electricity usage, W-hr/km	173	173	173
Fuel usage, km/liter	0	0	0
Highway driving cycle engine mode:			
Fuel usage, km/liter	18	18	18
Electricity recovery, W-hr/km	0	0	0
Battery pack life, yr	5.4	6.8	8.2
Annual electricity usage, kW-hr	2229	2013	1676
Annual fuel usage, liters	371	450	560
Annual fuel average, km/liter	43	36	29
Acquisition cost, \$	3332	3332	3332
Life-cycle cost, ¢/km	5.5	5.4	5.4

PART C

TASK III, CONCEPTUAL DESIGN

TASK III CONCEPTUAL DESIGN ACTIVITY

The studies conducted in Task I and II led to the selection of a vehicle and propulsion system configuration to achieve maximum petroleum savings at reasonable cost. The vehicle type is a five-passenger sedan with a total test weight of 2032 kg. A hybrid propulsion system was designed in Task III to power the selected vehicle and meet the performance standards summarized in table 32.

TABLE 32.--FIVE-PASSENGER VEHICLE PERFORMANCE SUMMARY

Vehicle test weight, kg	2032
Battery pack weight (lead-acid), kg	386
Power train weight, kg	414
Maximum acceleration 0 to 90 km/hr, s	12
Maximum speed, km/hr	105
Prime electric range, special test cycle, km	218
Battery usage	80 percent DOD
Fuel usage, km/liter	30
Extended range (engine mode)	Limited by fuel capacity
Fuel usage with special test cycle, km/liter	14
Fuel usage at constant 90 km/hr, km/liter	18
Life-cycle cost, special test cycle	\$0.054/km
Acquisition cost	\$3128

DESCRIPTION OF CONCEPTUAL DESIGN

The hybrid propulsion system is configured as a front-wheel drive unit, and a conceptual arrangement is shown in fig. 90. The equipment is compact enough to fit easily within the engine compartment of a typical five-passenger automobile. The power train components, including the heat engine, the traction motor, and all the mechanical power transmission devices, are integrated into a single compact unit. The electronic control unit, packaged as a separate item, is shown to the side and rear of the drive train package. A radiator, not considered a part of the power train, is required for engine cooling. The battery pack is shown at the rear of the vehicle to provide good weight distribution.

A side view of the drive train unit is shown in fig. 91. The unit is 759.09 cm long, and the central drive section is 53.3 cm high. The heat engine is indicated by the maximum envelope, which is within the available clearance of 48.3 cm from axle to firewall as measured on an actual five-passenger vehicle (1979 Fairmont). The indicated hood line clearance is also typical for a five-passenger vehicle. The drive train unit has an estimated weight of 414 kg.

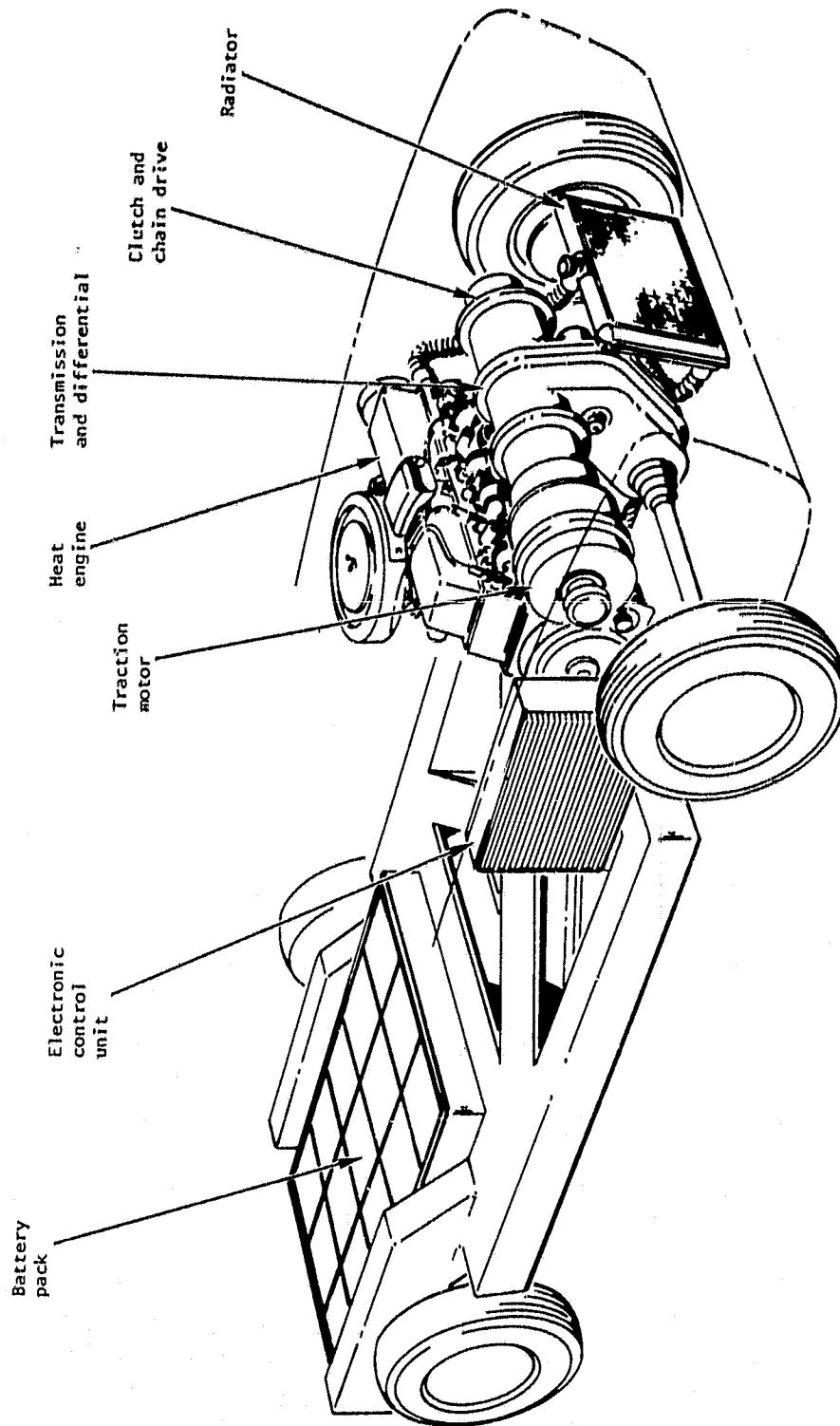
A cross-sectional view of the drive train package is shown in fig. 92, and the major components are identified. The dc traction motor, on the left, connects through a fixed-ratio speed reducer to the main shaft of the continuously variable traction transmission. The heat engine connects through a chain drive to the opposite end of the transmission main shaft. The output of the CVT is through a single gear set and then a chain drive to the differential.

Component Descriptions

The individual components of the hybrid propulsion system have been parametrically defined in the tradeoff studies. The following descriptions provide the details of the construction and operation of units designed to meet the performance definitions.

Traction motor.--The traction motor is a brushless dc permanent-magnet (PM) motor, rated at 20 kW, and operates off the battery voltage of 168 V. This motor is of the same design as a motor currently being built under a NASA contract*, though rated power is 20 percent less.

*NASA Contract DEN 3-77 for an Advanced Electric Motor was awarded to AiResearch Manufacturing Company of California on October 18, 1978.



S-45071

Figure 90.—Conceptual arrangement of propulsion system.

ORIGINAL PAGE IS
OF POOR QUALITY

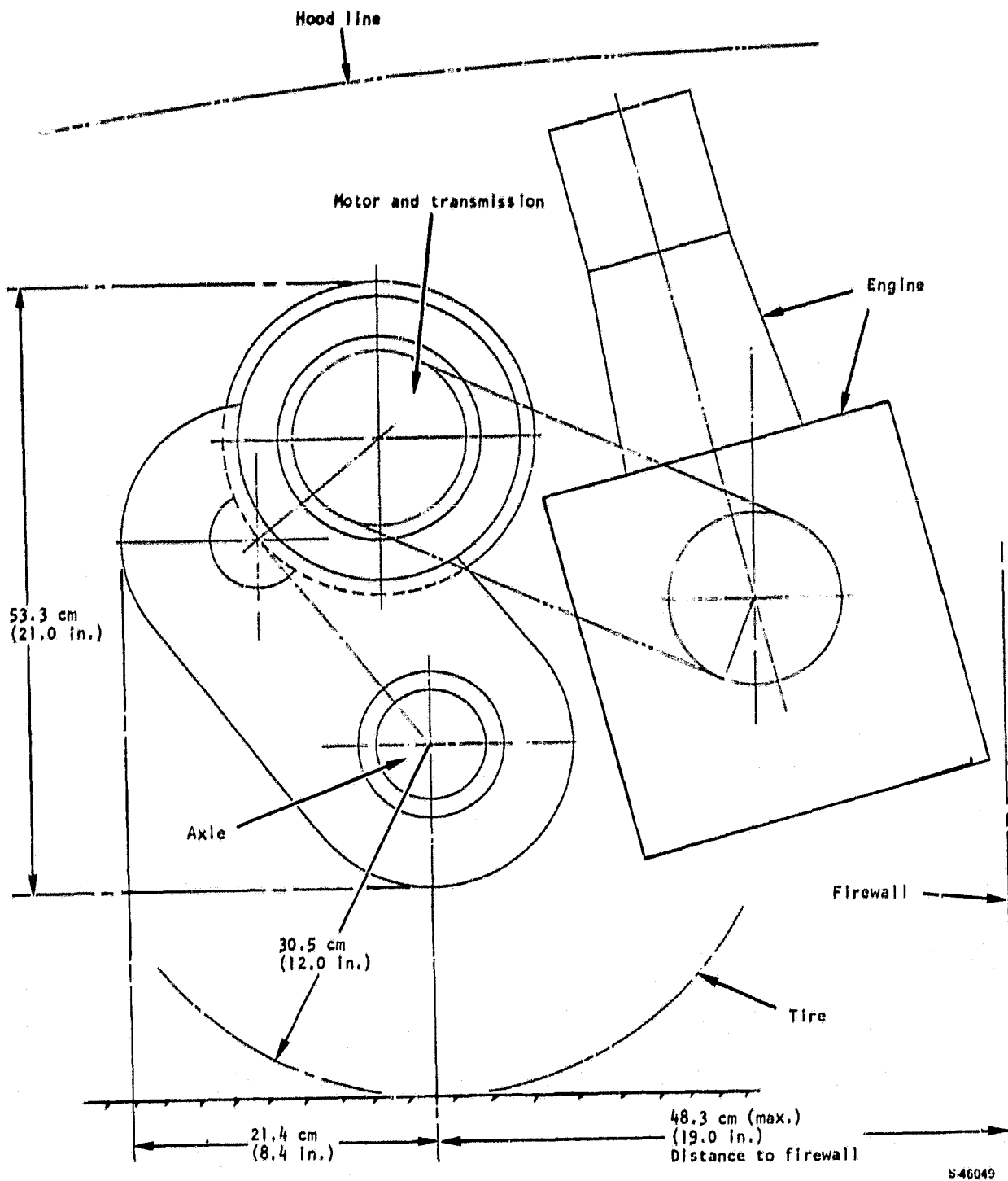


Figure 91. --Side view of drive train package.

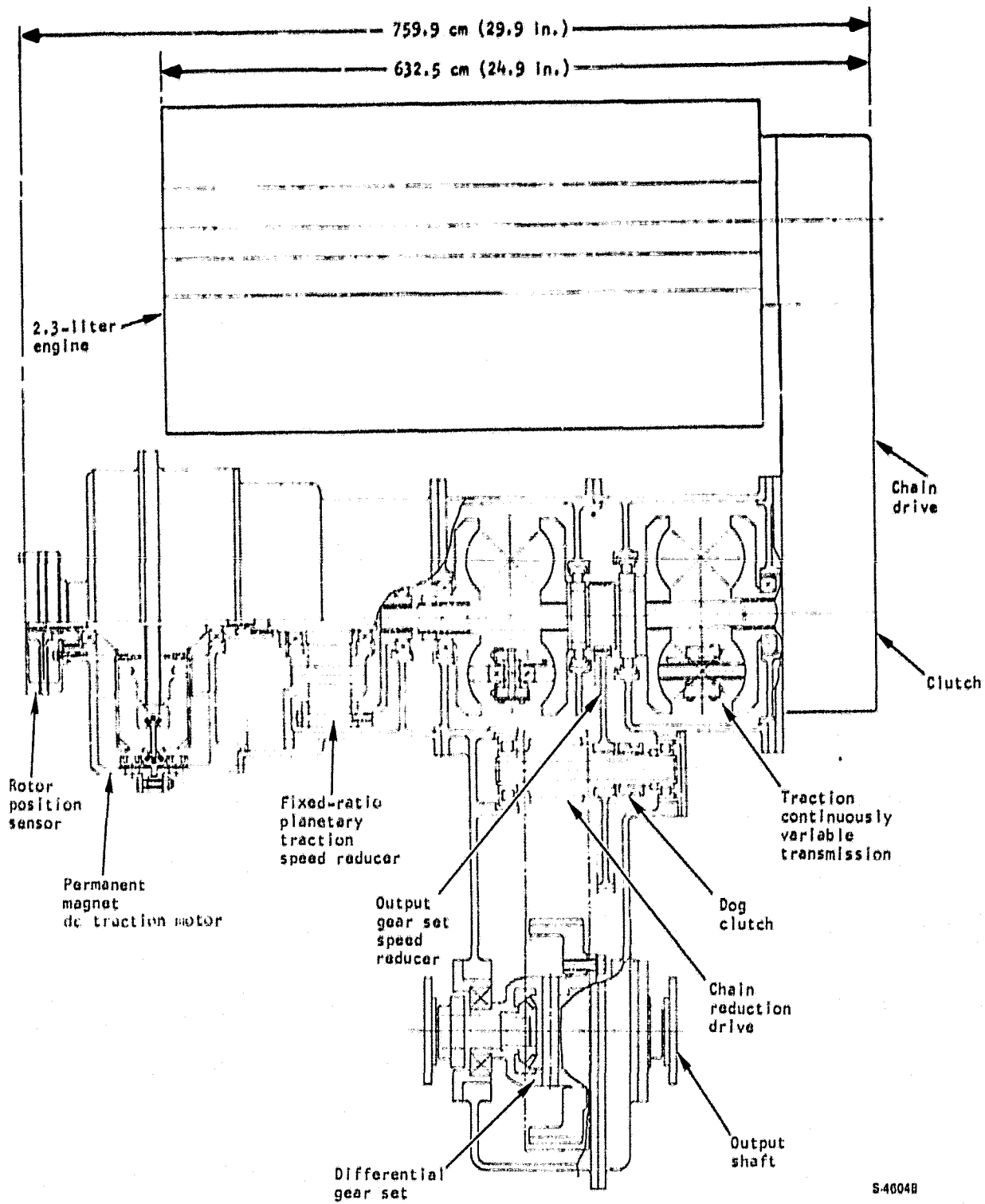


Figure 92.--Section view of propulsion system drive train.

The motor is an axial-gap inductor machine with an ironless stator. Excitation is provided by a 15 MG-Oe misch metal magnet. To permit self-synchronous starting and running, the rotor position of the motor will be sensed by a six-element, solid-state, infrared source and sensor, reading slots in a cylinder attached to the motor shaft. This is a proven device used in various self-synchronous PM motors to control inverter firing angle, and is contained within the housing on the left end.

During starting and running the rotor poles and the stator magnetomotive force are maintained in a synchronous relationship by inverter logic circuits so that no slip occurs. The logic circuits respond to rotor position signals up to approximately five percent of rated motor speed. Above this speed the logic circuits respond to the voltage induced in the stator winding by the rotor field. This method of operation takes into account the field distortion caused by armature current and improves the power factor of the motor as compared to what is possible by only sensing rotor position. At all times the motor is functioning as a synchronous machine. This type of operation is called self synchronous because the system is continually self adjusting, always maintaining synchronous operation, and pull-out cannot occur regardless of applied load.

A primary factor favoring the axipolar concept is its simplicity and suitability for low-cost production. The rotor is comprised of two identical, five-fingered sections separated by a magnet. The two rotor sections could be either forged or cast. An aluminum shroud covers each rotor section to direct the rotor-induced airflow over the stationary stator coils. The shroud also reduces rotor windage loss.

The stator is comprised of simple, machine-wound coils, and ribbon conductors are used to minimize eddy loss in the conductors. The ribbon conductors provide desired rigidity to the coils, which are bonded together and supported at the stator OD. Ribbon conductors provide superior heat transfer as compared to round wire, mush-wound coils or substrate-mounted, printed-circuit conductors. Ribbon conductors also provide the most efficient utilization of the space between the poles. The stator does not contain iron so the typical iron losses are eliminated.

The rotor inherently provides centrifugal fan action. Pumping loss is regulated automatically to stator heating requirements by using a butterfly valve actuated by a bimetal coil actuator in the stator exit air duct. This is similar to the choke actuator on automobile engines. Thus, at higher-speed cruise conditions with low power demand, the motor efficiency is improved by reducing airflow pumped by the motor rotor.

Rated motor power is 20 kW, and top speed is 14 000 rpm. The 10-pole machine has a frequency at maximum speed of 1166 Hz. The calculated motor performance characteristics are shown in fig. 93.

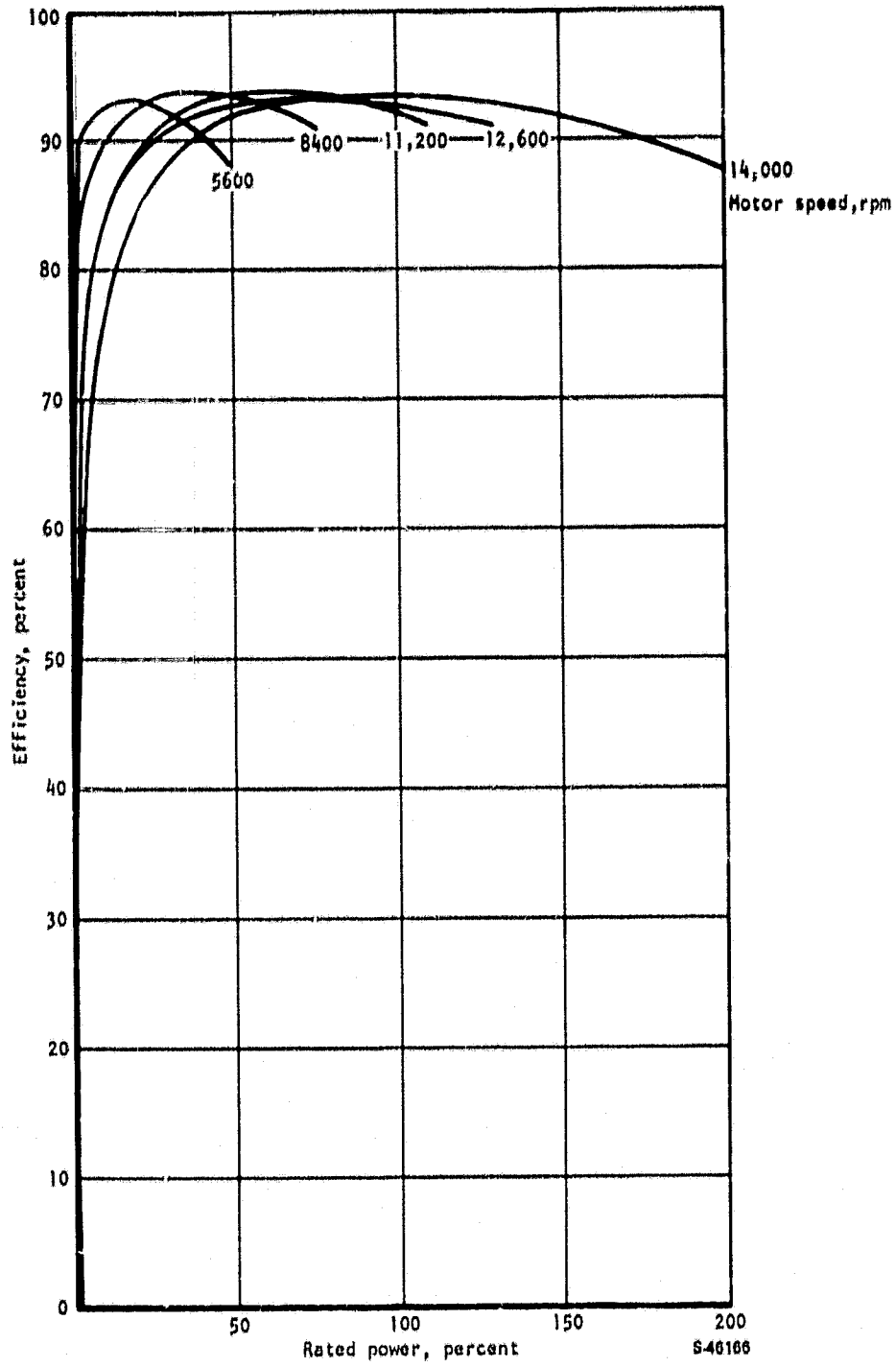


Figure 93.--Permanent magnet motor performance.

Transmission.--The initial transmission stage is a fixed ratio 3.5:1 speed reducer. This device is a traction unit configured in a planetary design with the planet rollers fixed to the housing. All elements operate in pure rolling contact. This design was chosen because it provides smooth, quiet power transmission at efficiencies in excess of 97 percent. The design is similar to other units that have been built and tested (refs. 20 and 21).

The variable action of the CVT is achieved in the double-cavity toroidal drive. The main shaft of the transmission has a drive disc attached to each end; the discs have a section of toroidal shape. Two similar discs are located inboard of the outer discs, and form the two cavities. The inboard discs are mounted on separate bearings and are capable of a limited amount of axial motion. Rollers, mounted on swivel shafts, contact each set of inboard and outboard discs. The drive ratio is changed by swiveling the contact rollers from contacts close to center on the drive discs and far from center on the driven discs to the other extreme of far from center on the drive discs to close to center on the driven discs. The rollers are not forced into ratio position but are steered as the wheels of a car by low-pressure hydraulic pistons that balance internal tangential forces that are generated at the roller contacts.

The transmission of power between smooth rolling surfaces requires a substantial normal force, but the contact loads must be low enough to ensure an adequate fatigue life. Power transmission also is limited by the possibility of slip between the rollers, since slip leads to rapid wear failure. These limits have been increased by the use of modern traction lubricants that provide high resistance to slip and high viscosity to reduce wear. These new lubricants have considerably extended the power range of traction transmissions, permitted the use of higher forces, and extended transmission life. The contact forces required are heaviest when the traction contact is close to the centerline of the drive disc, and lower as the contact running radius becomes greater on the drive disc. This contact force is adjusted by a loading cam located between the two central discs that provides a separating force and thereby generates equal forces for the two cavities. The contact forces are balanced within the end disc, and no heavy thrust bearings are required for the rotating assembly.

An oil pump is located within the housing to provide pressure for the hydraulic control pistons and circulation of lubrication. Control of the pistons, which position the traction rollers, is accomplished by an electrohydraulic valve, which establishes the CVT ratio in response to an electrical control signal. The power output of the CVT is through the central gear, with a reduction ratio of 4:1. The CVT ratio ranges from a reduction of 3.0:1 to an overdrive of 0.3:1. The fixed-ratio planetary traction speed reducer at the CVT input reduces the maximum motor shaft speed of 14 000 rpm to a CVT input of 4000 rpm. The speed of the electric motor and heat engine are varied as a function of vehicle velocity and load using the CVT. The CVT ratio is adjusted to favor the electrical motor by placing it in its ideal efficiency region. The calculated CVT performance is shown in fig. 94.

ORIGINAL PAGE IS
POOR QUALITY

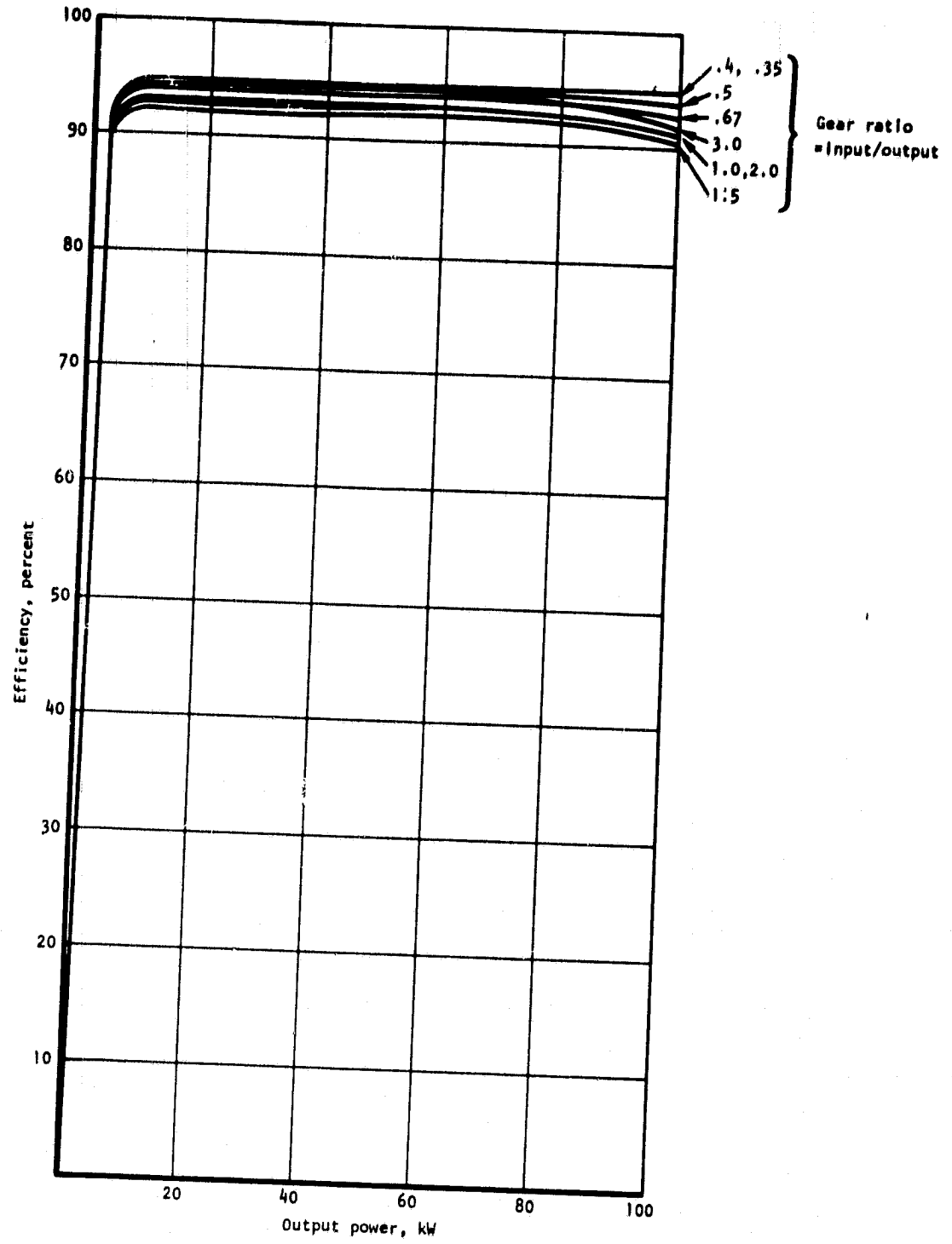


Figure 94.--Traction continuously variable transmission.

S-46167

Output drive and differential.--The output of the CVT is first through a gear reduction, and then through a chain reduction of 3:1 to the differential. This output speed reduction can be accomplished at high efficiency by careful attention to gear design, bearing selection, and lubrication control.

The losses in a speed reducer are attributed to several principal effects:

- (1) Meshing Losses--Sliding losses of the tooth surfaces, proportional to load, speed, tooth accuracy, and surface finish
- (2) Bearing Losses--Proportional to torque, bearing size, and the square of the speed
- (3) Lubricant Churning and Pumping Losses--Proportional to the square of the speed

The design presented minimizes meshing losses by use of spur gears where the predominant motion is rolling rather than sliding. Bearing losses are minimized by the use of ball bearings carefully sized for the load. Lubricant churning and pumping losses are minimized by use of mist lubrication and avoidance of moving elements in the oil sump. Lubrication is common with the CVT, using the same lubricant and with circulation by the CVT oil pump. By proper attention to all these points, it is possible to achieve a gear mesh efficiency as high as 99 percent.

Chain drives have been shown to achieve very high efficiencies over a broad range of operation. Comparative data on gear and chain drives is shown in table 33 (ref. 22).

TABLE 33.--GEAR AND CHAIN DRIVE EFFICIENCY

Torque, N m	Hypoid gear efficiency, percent	*Hy Vo Chain	Spiral bevel gear efficiency, percent
250	96.5	98.5	98
150	93	98.5	97.5
25	89	98	94.5

*Chain manufactured by Morse Chain Company

Heat engine.--The heat engine selected for the power train is a standard Ford 2300-cm³-displacement engine. The four-cylinder overhead cam engine is of cast iron construction, with a total weight of 199 kg. The crankshaft is supported by five main bearings, and the camshaft by three bearings. The camshaft is belt driven by the crankshaft.

The engine is equipped with all the required smog controls. Ventilation of the crankcase is effected by the vacuum created in the intake manifold when the engine is running and varies with the changes in vacuum. A portion of the fresh air entering the air cleaner bypasses the carburetor to be drawn into the intake manifold via primary vent hose, cylinder head cover, crankcase, oil separator (on left side of engine), ventilation control valve, and secondary vent hose.

O/
OE

The engine lubrication system is the force-feed type incorporating a full-flow oil filter. The oil pump draws oil from the pan through a screen and forces it via a short passage into the full flow oil filter. From the center passage of the oil filter, the oil enters the main oil gallery. The five crankshaft main bearings and the three camshaft bearings are in direct connection with the main oil gallery. The connecting rod bearings are supplied with oil from the front and rear main bearings via inclined passages. A squirt hole in each connecting rod crankpin end supplies oil to the piston thrust side. The auxiliary shaft is in direct connection with the main oil gallery. The distributor shaft is intermittently supplied with oil from a passage drilled in the auxiliary shaft at right angles to the shaft axis. The cams and cam follower arms are supplied with oil from the center camshaft bearing (which is provided with a groove 180 deg around its periphery) via an oil line.

As long as the engine is cold, the coolant passes only from water pump through engine and intake manifold, automatic choke, and heater core back to the pump. This ensures a quick warming up of the engine to operating temperature. As soon as the engine has attained operating temperature at a thermostat setting of 90°C opening temperature, the coolant flows via the outlet housing to the radiator (where it is cooled), back to the pump, and into the engine. The engine coolant drain plug is located on the right side near the clutch housing. The thermostat is located in the water outlet housing.

The heat engine is connected by a chain drive, without speed change, to a clutch. The clutch is mounted on the transmission shaft, so that the transmission input is at engine speed.

Electronic control unit.--The electronic control unit is located in a separate package with an estimated weight of 36 kg. This weight includes electronic components, heat sinks, and cooling fan. The electronic control unit consists of two main systems: the power control unit for control of motor power; and the system controller, a microprocessor, that controls system operation in response to drive commands.

The basic control scheme for the power control unit includes the following: a chopper that controls the motor current; a silicon-controlled rectifier (SCR) inverter with an auxiliary commutator for commutating the inverter switches during the motor start sequence; and a regenerative switching scheme that returns energy to the battery during braking. A block diagram of the electronic control unit is shown in fig. 95.

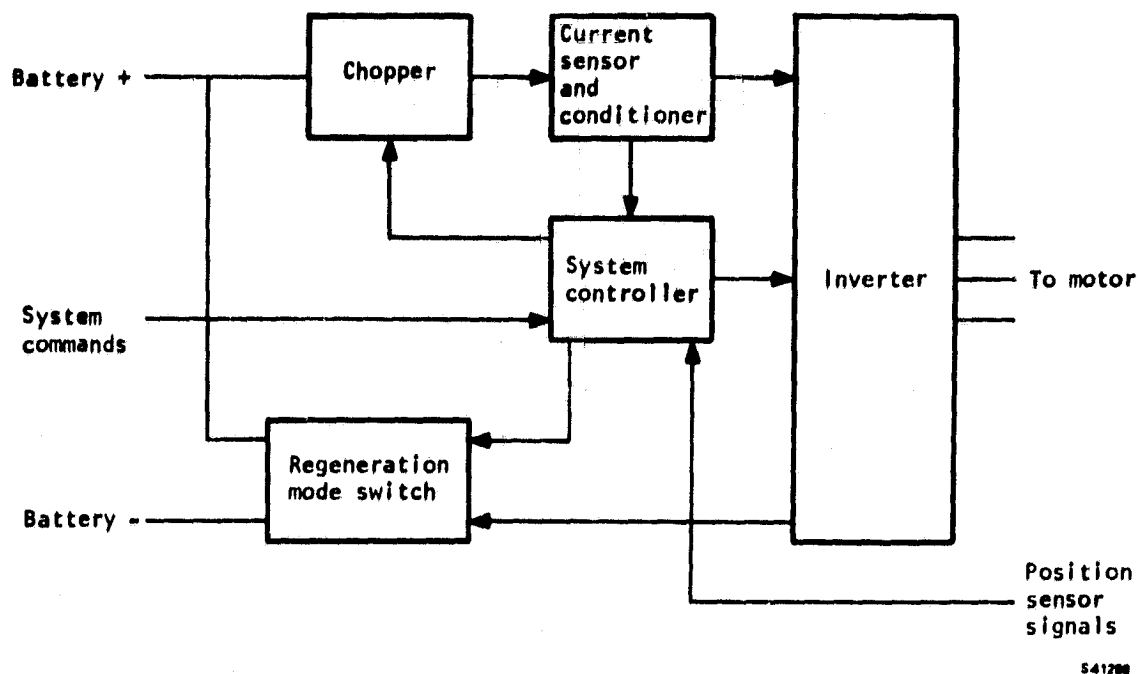
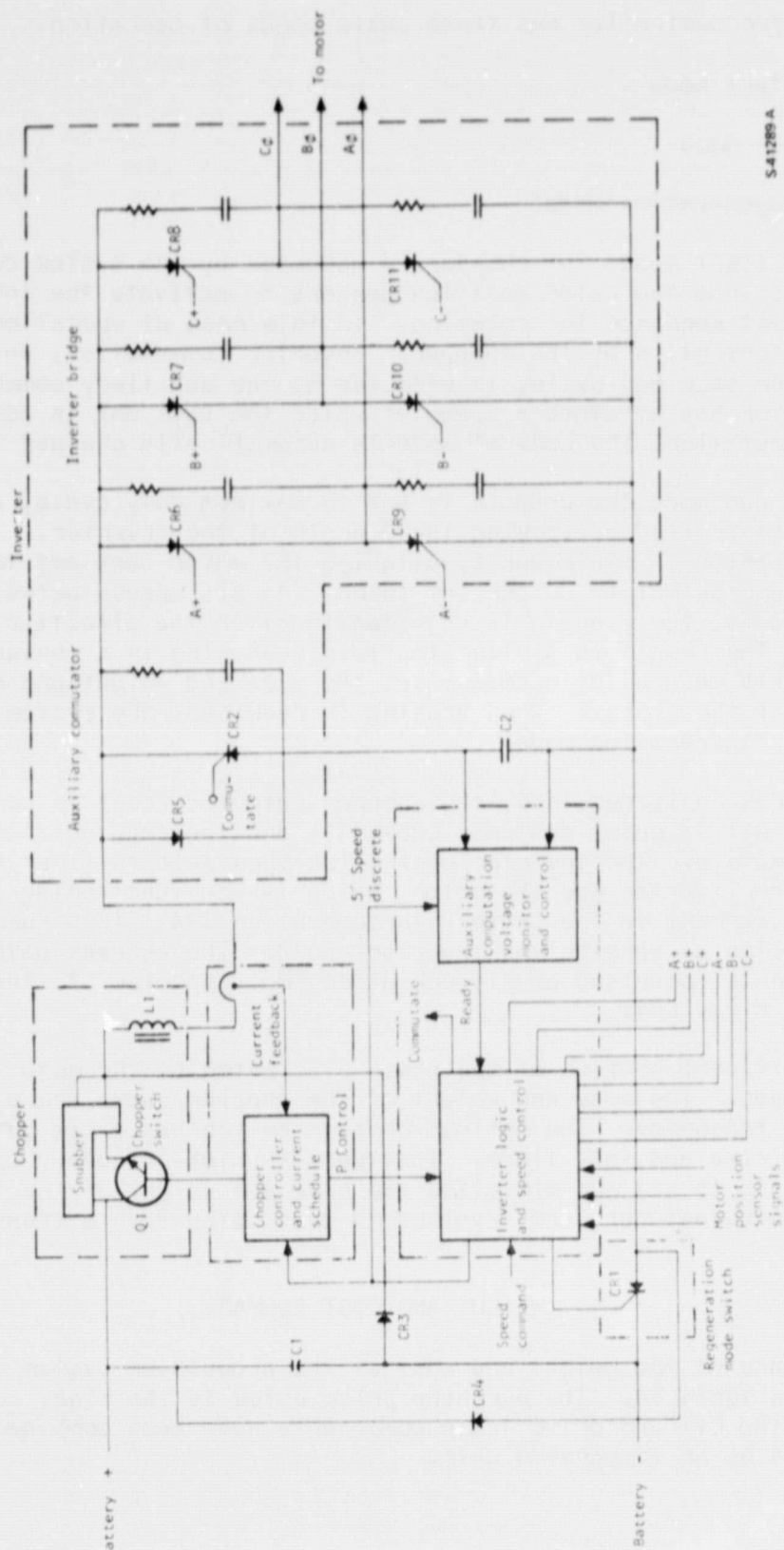


Figure 95.--Electronic control unit block diagram.

The electronic control unit is completely solid state. There are no relays or mechanical switches, and the basic control scheme has been structured so that state-of-the-art components (e.g., pulse width modulation integrated circuit, CMOS switches, microprocessor) can be utilized to improve flexibility and minimize cost, size, and weight. The risk involved in mechanization of the proposed controller is minimal since all of the major concepts involved have been used in previously built state-of-the-art hardware.

The inverter power section is functionally identical to those used for a pump motor controller. These inverter bridges are of conventional design and require minimal development effort. A schematic of the unit is shown in fig. 96.

The auxiliary commutator is also identical to that recently developed for a pump motor controller. As shown on the diagram, this commutator utilizes three significant components: a diode (CR5), an SCR (CR2), and a capacitor (C2). The inverter devices are inhibited from functioning until capacitor (C2) is charged by the chopper. When the voltage across C2 has reached a predetermined value, the inverter devices are allowed to operate under control of the inverter logic circuit. When commutation is required, SCR CR2 is turned on allowing the motor inductance to resonate with capacitor C2. During the first negative half-cycle of resonance, the inverter devices that had previously been on are commutated together with SCR CR2, and the logic drive to the inverter is inhibited, which prevents any further activity in the inverter until the capacitor C2 is recharged. This sequence is repeated six times per cycle until the inverter commutation mode is changed from forced commutation to line commutation.



S-41289 A

Figure 96.--Power control unit schematic.

ORIGINAL PAGE IS
OF POOR QUALITY

The motor controller has three basic modes of operation:

- (1) Start mode
- (2) Run mode
- (3) Regeneration mode

In the start mode, the chopper is actuated by the system controller, which uses signals from the rotor position sensors to activate the inverter switches in the correct sequence for rotation. In this mode of operation, the motor current is controlled by the chopper. Inverter commutation, which is required six times per back emf cycle, is effected by the auxiliary commutation circuit. When the motor has attained a speed at which the back emf is adequate for natural commutation, the control mode is automatically changed to the run mode.

In the run mode the chopper is set to maximum duty cycle, and the motor current is controlled by varying the β angle of the inverter. Thus the system power dissipation is minimized by allowing the motor back emf to be at maximum voltage at approximately 50 percent speed. At all speeds between 50 percent and 100 percent, the β angle is adjusted to alter the effective back emf of the motor. The result is similar to field weakening in a conventional dc machine. This mechanization minimizes the size and weight and maximizes the efficiency of the system. When braking is required, the system controller selects the regeneration mode.

When braking is required, the chopper output current is commanded to zero. This allows all inverter devices, CR6-CR11, and the regeneration mode switch, CR1, to commutate. The inverter controller then selects first quadrant operation for the inverter and the motor, which is now functioning as a generator, and returns current to the battery through diode CR4. This current level is also controlled by varying the inverter angle. The current path in this mode of operation is comprised of flyback diode CR3, inductor L1, the inverter bridge, and diode CR4.

A significant portion of the power dissipated by the motor controller is in the chopper. The size and weight of the chopper/choke are also affected by the chopper frequency. The optimum chopper switch has a low saturation voltage and minimal rise and fall times. This permits high-frequency operation of the chopper (10 to 15 kc) and minimizes the size and weight of the choke. Several transistor manufacturers are involved in developing such a transistor.

WEIGHT AND COST SUMMARY

A summary of the weight and cost of the propulsion system components is presented in table 34. The purchase price noted is the final cost to the consumer. The CVT and drive train components have been combined, since they are designed as an integrated unit.

TABLE 34.--PROPULSION SYSTEM COST AND WEIGHT SUMMARY

Component	Rating	Weight, kg	Purchase price, \$
Heat engine, spark ignition	65 kW at 4000 rpm	199	410.00
Electrical traction motor	20 kW at 14 000 rpm	12	375.00
Electronic control unit	40 kW	36	905.00
Transmission and drive train	90 kW	167	520.00
ISOA lead-acid batteries	100 W/kg, 40 W-hr/kg	386	1004.00
Total		800	3214.00

SYSTEM OPERATION AND CONTROL

The following description of the propulsion system operation is presented to illustrate the manner in which the various components operate when the vehicle negotiates driving maneuvers. In general, operator commands from the control devices, such as the accelerator pedal and brake pedal, are transmitted to the system controller. The system controller, a microprocessor, responds to operator commands in accordance with the preestablished control logic, and controls the active components to produce the required system performance.

Starting Sequence

The system is activated by turning on the ignition key; however, the starting sequence varies depending on whether the heat engine temperature is above or below a preset operating level.

Cold start.--When the heat engine temperature is below the preset limit, the heat engine will automatically start and run at idle speed as soon as the operator turns on the ignition. The engine starter is a fast-start device activated by the system controller, and does not require operator action.

Hot start.--When the heat engine temperature is above the preset limit, the heat engine will not start until some power output is required. Turning the ignition key will activate the system but not initiate any activity in the power train.

Acceleration

To put the vehicle in motion, the operator depresses the accelerator pedal. This action causes the controller to supply electrical energy to the traction motor immediately. The CVT is spring biased to be in the maximum reduction ratio when the vehicle is stopped. Therefore, the traction motor can rapidly accelerate to an operating speed within the range of good motor efficiency while the vehicle speed is still very low, below 3 km/hr. During the regime of initial acceleration the heat engine is not connected to the CVT since the engine clutch is not engaged.

At a vehicle speed of approximately 3 km/hr, with the CVT still in maximum ratio, the input shaft of the CVT, driven by the traction motor, will reach the nominal idle speed of the heat engine, at which point the heat engine is started and clutched into the power train. Following this action, power is supplied by both the traction motor and the heat engine in accordance with the power split conditions programmed into the system controller.

Power command.--The operator commands system power by use of the accelerator pedal, with the power supplied proportionate to the accelerator pedal excursion. The operator command goes to the system controller, and the system

controller achieves the programmed balance of power by the coordinated adjustment of three parameters:

- (1) Electrical power flow from the power control unit to the traction motor
- (2) Input/output ratio of the CVT
- (3) Throttle setting of the heat engine

Power split.--The primary controller objective is to achieve the commanded power by a 70/30 power split, where the heat engine supplies 70 percent of the power and the traction motor supplies 30 percent. An adjustment is first made, however, to ensure that the traction motor is operating at optimum efficiency; then the heat engine is regulated to supply the balance of the required power.

An examination of table 35 shows that for any given output power from the traction motor, maximum efficiency is achieved at a particular speed. Conversely, if the motor is operated at one of four different speed levels throughout the power range, it will always be at, or near, maximum efficiency. Therefore, if the power control unit supplies a given power to the traction motor, the CVT can then be adjusted to provide the ratio of motor shaft speed to vehicle axle speed such that the motor is operating at top efficiency.

Selecting the traction motor speed by adjustment of the CVT automatically sets the heat engine speed. Adjustment of the throttle will then achieve the necessary output power of the heat engine.

Power limit.--The 70/30 power split condition is applied up to the point where the traction motor is supplying maximum output. Beyond this point the heat engine power is increased, in response to increased commands, until maximum heat engine power is achieved. This condition represents maximum system output.

Steady-state Operation

After a period of acceleration, the operator can adjust the acceleration pedal position until the power level is just sufficient to maintain a constant speed. When the vehicle is no longer accelerating, the power source is further regulated by reference to the battery depth of discharge, and the system operates either in electric mode or heat engine mode, as shown in table 35.

Electric mode.--When the battery has not been discharged below 80 percent, the system operates in the steady-state condition as an electric propulsion system. All propulsion power is supplied by the batteries. Therefore, if the system were used only for short trips with periodic wall-plug recharging, the only petroleum usage would be during acceleration. The heat engine simply serves as an energy buffer for acceleration.

Heat engine mode.--When the battery has been discharged to a depth of 80 percent, the heat engine is used as the steady-state energy source. The heat engine supplies energy to power the system, but no power is used to charge the

TABLE 35.--SYSTEM CONTROL STRATEGY

Mode	Vehicle state	Percent of power demand (P_D) supplied or accepted	
		Battery	Heat Engine
Electric (DOD < 80%)	$\frac{\Delta V^*}{\Delta t} = 0$	100%	0
	$\frac{\Delta V}{\Delta t} > 0$	Normal: ($P_D < 0.8$ H.E. rating) 30%	70%
		High: ($P_D < 0.8$ H.E. rating) 30% < Batt. < 38 kW	100% of rating
	$\frac{\Delta V}{\Delta t} < 0$	100%	0
Heat engine (DOD = 80%)	$\frac{\Delta V}{\Delta t} = 0$	0	100%
	$\frac{\Delta V}{\Delta t} > 0$	Normal: ($P_D < 0.8$ H.E. rating) 30%	70%
		High: ($P_D > 0.8$ H.E. rating) 30% < Batt. < 38 kW	100% of rating
	$\frac{\Delta V}{\Delta t} < 0$	100%	0

* If $\frac{\Delta V}{\Delta t} = 0$ and $P_D \geq 20$ kW, then power split goes to 30% batt. and

70% H.E. (hill climb)

battery. The battery may recover some energy in regeneration, and it will still be used to provide power during acceleration. In the heat engine mode the battery serves as a buffer to the heat engine for acceleration.

Coasting

If the accelerator pedal is allowed to return to its undepressed or null position, the power output of the traction motor and the heat engine will cease. The heat engine will be declutched, but the CVT and the traction motor will continue to rotate. To provide some positive deceleration force, similar to compression braking in a conventional automobile, the traction motor is used to provide a low level of electrical regeneration to the battery. The regenerated power would occur at the expense of vehicle kinetic energy, hence the vehicle would slow down more than if there were only frictional losses.

Deceleration and Braking

When the brake is applied, electrical regeneration to the battery takes place at a progressively greater rate, proportionate to the pressure on the brake pedal. When the maximum capacity of the traction motor, acting as a generator, is reached, further braking is obtained by use of friction brakes.

EFFECTS OF HEAT ENGINE OPERATING MODES

The selected propulsion system design uses the heat engine to supply power to the system when needed, and to be inoperative when not needed. This type of on-off operation can have a significant effect on engine life, depending on the environmental temperature and the frequency and duration of the intermittent operation. The principal problem is cold operation during which the engine crankcase and water jacket are operated below their optimum temperature level.

Cold Operation

Present-day engines and cooling systems are designed to prevent the crankcase oil from reaching excessive temperatures and to keep coolant well below the boiling point with engine operation at maximum rated speed and load in the hottest summer temperatures of the desert. As a result most engines are overcooled when run under less severe conditions, and particularly in intermittent, moderate, or light duty operation.

This overcooling means that operating a heat engine in an on-off mode may result in undesirably low water-jacket and crankcase temperatures. Engine jacket and crankcase temperatures are of vital importance in controlling blow-by of combustion products past the pistons and subsequent oil contamination with soots, moisture, lead salts, and fuel residues. Oil contamination, in turn, leads to both erosive and corrosive wear in the engine (ref. 23).

Engine warmup.--After the engine has been started, the length of the warmup period is influenced by the ambient temperature, the design of the engine, and the fuel volatility. Generally, the less volatile the fuel, the longer the warmup time at a given atmospheric temperature. As the temperature decreases, warmup time increases. Tests with various cars (ref. 24) showed that a drop in atmospheric temperature from 10°C to -20°C more than doubled the warmup time, and some cars require more than 12 min to warmup at the coldest temperature.

Engine cooling.--Tests of engines cooling after a run indicate that the cooldown time is much longer than the warmup time (ref. 25). Cooldown time may take several hours, depending on engine design and environmental temperature. Therefore, engine design for optimum warmup appears to be more critical than protection against cooldown.

Engine Wear

Although motor oil is commonly regarded as the chief preventive (or cause) of engine wear, oil can effect relatively little change or improvement in engines where high rates of wear prevail. Following are three basic causes

of engine wear; the first two, erosion and corrosion, are accelerated to even a greater degree by cold engine starting:

- (1) Erosion: Wear caused by metal-to-metal contact from inadequate lubrication.
- (2) Corrosion: Chemical attack of metal surfaces by corrosive constituents and moisture originating from the combustion process.
- (3) Abrasion: Wear caused by dust, dirt, and solid particles in the intake air to the engine induction and ventilation systems.

Erosive wear.--Engine wear by erosion has been defined as that caused by lack of or inadequate lubrication. Obviously, one of the chief functions of motor oil is to prevent erosive wear by interposing fluid oil films between rubbing surfaces to preclude metal-to-metal contact and consequent wear, scoring, or seizure. In certain phases of engine operation, however, maintenance of adequate lubricating oil films is not possible, and erosive wear results not from inadequate qualities of the oil but from an insufficient quantity to provide the required lubrication. Such conditions of oil starvation pertain in the piston and ring zones during starting of cold engines. During the starting interval and the first few minutes of running after starting, engine speeds and temperatures are too low to allow circulation of oil to the cylinder walls, and the only lubrication available is thus from oil remaining on the walls and rings from previous operation. Additionally, these films of residual oil are subject to dilution and washing by raw gasoline from the rich mixtures during starting. In cold weather, during which the carburetor choke is used for appreciable intervals, high rates of gasoline dilution and washing of the oil prevail for appreciable time intervals, and the rings and cylinders then receive little if any viscous lubrication. Erosive wear is thus a major factor during starting, and engines subject to frequent stops and starts are accordingly subject to high wear (ref. 23).

Corrosive wear.--The low engine temperatures that prevail until an engine is adequately warmed up foster corrosive attack by condensation of combustion products. For every gallon of fuel burned in an engine, approximately one gallon of water is formed within the combustion chambers. The combustion of fuels also results in formation of carbon dioxide, small amounts of sulfur oxides from organic sulfur compounds in the fuels, traces of nitrogen oxides from fixation of nitrogen by the high combustion temperatures, and small amounts of bromine or chlorine compounds during the use of tetraethyl lead treated gasolines. All of these combustion by-products, on condensation or reaction with water, form acidic and potentially corrosive materials, comprising carbonic acid, sulfurous and sulfuric acids, nitrous and nitric acids, and hydrobromic or hydrochloric acids.

In engines that operate at adequately high temperature levels, these combustion products are largely blown out the exhaust and thus have limited opportunity to cause engine damage. In engines operated under conditions fostering low cylinder-wall temperatures, however, the moisture and acidic products may readily condense and collect to promote corrosive attack of the wall and piston ring surfaces, and to accumulate within the engine and in the crankcase oil (ref. 26).

Cold-Engine Sludge

If an engine is operated with low cylinder-wall temperatures, condensation and washing of combustion chamber products past the pistons causes oil contamination. If the crankcase temperatures are also undesirably low, and if the engine also suffers from poor ventilation, moisture and volatile fuel contamination cannot be purged from the oil. The blow-by contaminants in the oil then accumulate and increase in quantity until a critical point is reached at which they begin to coagulate and separate out as cold-engine sludges. In this first phase of formation, the sludge is usually of the soft pasty type and can readily be carried by the oil to those parts of an engine where oil flow is slow or restricted and where the sludges can then settle out and deposit. This action results in the accumulation of deposits in such places as valve galleries, overhead rocker-arm compartments, timing gear cases, crankcase sumps, oil filter housings, and oil pump screens.

Sludge composition.--The composition of cold-engine sludge has been analyzed (ref. 23), and the results are presented in table 36.

TABLE 36.--COMPOSITION OF COLD-ENGINE SLUDGE

Substance	Content in gasoline engine, percent	Content in diesel engine, percent
Oil	50	42
Water	8	3
Soot and carbon	21	34
Lead salts	10	0
Oxidized hydrocarbons	10	19
Trace elements	1	2

Note that the composition of these sludges for the two types of engines is very similar. The only significant difference is the absence of lead salts and the presence of high amounts of oxidized hydrocarbons in diesel sludge. Since diesel fuels are considerably less volatile than gasoline, it is entirely possible that unburned and partially oxidized diesel fuel will be even more susceptible to oxidized hydrocarbons than is the case with gasoline. Operating a combustion engine at higher temperatures will reduce the percentage of water and increase the percentage of lead salts.

Since diesel fuels are relatively heavy and nonvolatile, they require near perfect conditions to assure good combustion. Any engine factor that interferes with good combustion of the heavy fuel immediately results in poor burning and formation of large volumes of soot. When a diesel is operated in such a fashion, the amount of oil contamination with blow-by soot can reach massive proportions.

Crankcase ventilation.--Adequate crankcase ventilation is a vital factor in sludge formation. Most engine ventilating systems function efficiently only at high road speeds, and are ineffective at low speeds or idling. A combination of low water-jacket and crankcase temperatures plus poor ventilation means that blow-by contaminants that enter the crankcase stay there and accumulate. The low-temperature type of engine sludge deposit thus originates from excessive oil contamination with combustion products; it is a condition that cannot be corrected by oil or fuel alone, regardless of their qualities, and depends essentially upon details of engine design.

Operating Tests

Tests have been run to determine some of the effects on a gasoline spark-ignition engine during prolonged cold engine operation (ref. 27). The tests were in the form of 48-hr idling tests conducted to study the effect of providing an oil filter, forced crankcase ventilation, and modification of the carburetor air-fuel ratio. The results are summarized in table 37.

TABLE 37.--EFFECT OF ENGINE MODIFICATIONS ON OIL CONTAMINATION AS FOUND IN 48-HR ENGINE IDLING TESTS

Jacket inlet temperature, 49°C Jacket outlet temperature, 54°C		Crankcase oil temperature, 52°C Engine speed, no load, 600 rpm		
	Test 1 Stock engine setup	Test 2 Oil filter installed	Test 3 2400 cm ² /s Forced ventilation	Test 4 14:1 Air- fuel ratio
Oil drain analysis:				
Fuel dilution, percent	19.0	21.0	3.0	3.6
Total insolubles, percent	3.0	0.2	1.0	0.8
Lead salts, soot, percent	2.3	0.1	0.8	0.6
Resins, percent	0.7	0.1	0.2	0.2
Engine condition:				
Sludge deposits	Heavy	Slight	Slight	Slight
Moisture condensation	Heavy	Heavy	None	None

Oil filtration.--Results of an idling test with a stock engine run with a jacket inlet temperature of 49°C and a crankcase temperature of 52°C are shown in Test 1. Oil contamination was severe, and sludge formation and water condensation within the engine were heavy. Results of a repeat test under identical conditions but with an oil filter installed are shown in Test 2. Oil contamination with insolubles was almost eliminated although fuel dilution was of the same high order. Engine deposits were minor, as would be expected from the low insoluble content of the oil, although moisture condensation within the engine was still heavy. The oil filter did an efficient job of removing insoluble contaminants from the oil during the test period, but had no effect on soluble contaminants. Of even greater interest was the fact the oil filter required two cartridge changes (three cartridges in 48 hr) to keep the oil continuously clean. Under these idling conditions, the rate of oil contamination with blow-by insolubles was so high that the cartridges plugged up and lost filtering efficiency in very short periods of time. Although the oil filter was of definite benefit in controlling the insoluble content of the crankcase oil, its limitations are equally obvious.

Forced ventilation.--Test 3 shows results of an idling test in which the engine modification consisted of forced ventilation at the rate of 2400 cm²/s. In spite of the very low engine operating temperatures in this test, the positive ventilation reduced fuel dilution very markedly, and eliminated moisture condensation within the engine. Oil contamination with insolubles was also reduced very materially, although the reason for this finding is not known. Repeat tests gave the same results. In line with the reduced oil contamination brought about by positive ventilation, the sludge deposits within the engine were very slight.

Carburetion.--Test 4 shows results of a 48-hr test, with the engine fitted with a special carburetor installation to produce a 14:1 air-fuel ratio at idling (no load). Results in oil contamination and engine deposits were almost identical to the run with forced ventilation. With the standard carburetor, air-fuel ratios at idling cannot be determined accurately but are probably richer than 10:1. Control of air-fuel mixtures in a more efficient range produced a most noteworthy improvement in the oil contamination-sludge deposit characteristics.

Water condensation.--During the engine idling tests, some 300 oil samples were withdrawn from the engines at various intervals for analysis. While these samples showed heavy contamination with fuel and blow-by solids, in no case did the amount of water contamination ever exceed 0.3 percent. On the other hand, examination of the engines at the end of 48-hr test intervals frequently revealed large amounts of water condensation in the push-rod compartment, rocker arm compartment, and crankcase sump. In some cases the water existed as droplets condensed on the metal surfaces, and in other cases as puddles or pasty emulsion sludges.

The amount of water condensation found in the various idling tests correlated quite closely with the engine jacket and crankcase temperatures. With crankcase oil temperatures of 50°C and lower, free water or emulsion sludge was found in the crankcase sump. These quantities diminished with increase in crankcase temperatures, and were substantially absent with oil temperatures of 60°C

and higher. Similarly, water condensation in the overhead rocker arm compartment was extremely low when thermostats maintained coolant outlet temperatures above 60°C, but condensation was very heavy in tests with the thermostat removed and with coolant outlet temperatures of approximately 50°C and lower.

Water condensation in the push-rod compartment was found to correlate closely with jacket inlet temperatures. Heavy condensation was noted with jacket temperatures of about 50°C and lower, and became negligible with inlet coolant temperatures of 60°C and higher. At any section of an engine in which prevailing temperatures were below about 55°C, moisture condensation was found, and with temperatures of 40°C and less, condensation was frequently very heavy.

Operating limit.--Since water is known to be an essential factor in contamination sludge formation, as well as rusting and corrosion of engine surfaces, these tests present the following important indications:

- (1) Water condensation tends to occur in any section of an engine where prevailing temperatures are below 55°C. Elimination of moisture condensation requires minimum temperatures of 55°C throughout the engine, including cylinder and head jackets, crankcase, and valve compartments.
- (2) Large amounts of moisture condensation can develop within an engine, with little or no indication in the crankcase oil itself. Water tends to accumulate on convenient engine surfaces or pockets and does not readily circulate in the oil stream. Analysis of oil samples alone may not indicate potential or existing emulsion sludge deposits.

In summary, the means of preventing excessive cold engine wear is to reduce cold-engine sludge, reduce blow-by contamination with improved carburetion, provide adequate crankcase ventilation, and increase cooling system and crankcase oil temperatures through the use of temperature control devices, such as radiator shutters and automatic, thermally controlled fans. Engine insulation on crank pans and valve covers will also be beneficial.

PART D
DISCUSSION OF RESULTS
AND RECOMMENDATIONS

PRECEDING PAGE BLANK NOT FILMED

DISCUSSION OF RESULTS

This report has presented a study of various mission vehicle/hybrid propulsion system concepts. Each vehicle/propulsion system combination was required to meet the performance goals that were established as part of the contract.

The general results of the study are as follows:

- (1) Significant fuel savings are available with hybrid propulsion systems.
- (2) At current (1985 projected) fuel and electricity prices, the hybrid propulsion system will cost the consumer more to own in both acquisition and life-cycle costs than would be required for an equivalent conventional heat engine system.
- (3) Power sharing between the two energy sources (heat engine and battery) is required to maximize the electric range of the hybrid propulsion system and minimize the cost of ownership.
- (4) Addition of a third energy source such as a flywheel to an integrated hybrid propulsion system is not cost effective.
- (5) A conventional spark-ignition heat engine is a cost effective power plant for a hybrid propulsion system.
- (6) The nickel-zinc battery is not currently cost effective for a hybrid propulsion system.
- (7) A hybrid system is less sensitive to battery performance characteristics than a purely electric propulsion system; however, the hybrid system is still sensitive to battery purchase price and cycle life.
- (8) A hybrid propulsion system is sensitive to the power control method employed as well as the method used to manage the power sharing between the two sources.
- (9) A hybrid system requires a more sophisticated driver control and power management system than is currently used by the automotive industry.
- (10) A hybrid propulsion system that uses a mechanically commutated dc shunt motor is competitive with the advanced motor system of this study in terms of fuel usage and cost to the consumer.
- (11) Reduction in the performance goals may offer a means for reducing the hybrid propulsion system costs to the consumer.

CONCLUSIONS AND RECOMMENDATIONS

Based on the results of the study, an advanced hybrid propulsion system for a five-passenger family sedan can be developed by the mid-80's. Such a system would have both the performance comparable to current conventional automobiles and sufficient range in the predominantly electric mode to satisfy the majority of consumer trips.

To maximize the success of a hybrid propulsion system requires:

- (1) Development of a continuously variable transmission (CVT)
- (2) Development of a control and power management system
- (3) Characterization of heat engine on-off operation with regard to its effects on engine efficiency, durability, and emissions and the possible specialization of engine designs for on-off operation
- (4) Initiation of battery research and testing to accumulate knowledge on the performance of a battery when it is operated in a hybrid system that uses power sharing

In general, a hybrid propulsion system is more costly to own than its conventional (heat engine) counterpart. The above recommendations have been identified as items that, if successfully accomplished, will minimize the costs of owning a hybrid propulsion system. In addition, the recommended items will have an impact on electric range and fuel efficiency.

PRECEDING PAGE BLANK NOT FILMED

REFERENCES

1. Mighdol, P., W. F. Hahn: Preliminary Power Train Design for a State-of-the-Art Electric Vehicle. Booz, Allen & Hamilton, Report No. DOE/NASA/0595-78/1, September 1978.
2. Ross, J. A., G. A. Wooldridge: Preliminary Power Train Design for a State-of-the-Art Electric Vehicle. Rohr Industries, Report No. DOE/NASA/0592-78/1, September 1978.
3. U. S. Department of Energy: Near-Term Electric Vehicle Program. Report No. SAN/1213-02, SAN/1294-02, August 1978.
4. Yardney Electric Corp: Design and Cost Study Zinc/Nickel Oxide Battery for Electric Vehicle Propulsion. Report No. ANL-K-76-3543-1, October 1976.
5. Rowlette, J., C. Leising: Electric Vehicle Battery Test Report. Jet Propulsion Laboratory Report No. 5030-286, December 1978.
6. AiResearch Manufacturing Company of California: Study of Heat Engine/Flywheel Hybrid Propulsion Configuration with Electrical Transmission System. ALG-41/1, April 1978.
7. Hofbauer, P., K. Sator: A Diesel for a Subcompact Car. Society of Automotive Engineers, Paper 770113, 1978.
8. AiResearch Manufacturing Company of Arizona: Advanced Gas Turbine Powertrain. Report No. 31-3192-1, April 13, 1979.
9. AiResearch Manufacturing Company: Automobile Gas Turbine Optimization Study for the Environmental Protection Agency. Report AT-610-R7, July 10, 1972.
10. Behrin, E. et al.: Energy Storage Systems for Automobile Propulsion. Volumes 1 and 2, Lawrence Livermore Laboratories, Report UCRL-52303, December 15, 1978.
11. U. S. Department of Energy: Proceedings of the 1978 Mechanical and Magnetic Energy Storage Contractors' Review Meeting. CONF-781046, October 24, 1978.
12. Towgood, D. A.: An Advanced Vehicular Flywheel System for the ERDA Electric Powered Passenger Vehicle: DOE Flywheel Technology Symposium Abstracts, October 5-7, 1977.
13. Satchwell, D. L.: An Advanced Energy Storage Unit for a U.S. Postal Service Delivery Vehicle: DOE Flywheel Technology Symposium Abstracts. October 5-7, 1977.

14. Rath and Strong, Inc.: Estimated Weights and Manufacturing Costs of Automobiles: Fuel Economy Goals Beyond 1980. Report to U. S. Department of Transportation, Transportation Systems Center.
15. Chiltons Automotive Industries, 1979 Specification Tables on Gasoline and Diesel Engines. Chilton Book Company, New York, N. Y., 1979.
16. Raynard, A. E., F. E. Forbes: Advanced Electric Propulsion System Concept for Electric Vehicles. AIResearch Manufacturing Company, Report No. DOE/NASA/0081-79-1, August 1979.
17. Liston, L. L., R. W. Sherrer: Cost of Operating an Automobile. U. S. Department of Transportation, Federal Highway Administration, April 1974.
18. AIResearch Manufacturing Company of California: Electric-Powered Passenger Vehicle Design Study Program. Report No. 76-13465, December 1976.
19. Kirkwood, T. F., A. D. Lee: A Generalized Model for Comparing Automobile Design Approaches to Improve Fuel Economy. Rand Corporation, Report No. R-1562-NSF, January 1975.
20. Hewko, L. O.: Roller Traction Drive for Extremely Quiet Power Transmission: Journal of Hydronautics. Vol. 2. No. 3, July 1968.
21. Loewenthal, S. H. et al.: Performance of a Nasvytis Multiroller Traction Drive. NASA Technical Paper 1378, AVRADCOM Technical Report 78-36, November 1978.
22. Dudley, D. W.: Gear Handbook. McGraw-Hill Book Co., 1962.
23. Georgi, C. W.: Motor Oils and Engine Lubrication. Reinhold Publishing Corp., 1950.
24. Moxey, J. G.: Engine Warm-up--A Study of Today's Fuels and Engines: SAE Journal. Society of Automotive Engineers, June 1947.
25. Gohn, E. P.: Cold Starting and Fleet Operation: SAE Journal. Society of Automotive Engineers, June 1945.
26. Kendall, N., R. Greenshields: Deposition and Wear in Light Duty Automotive Service. SAE paper, Society of Automotive Engineers, January 1948.
27. Georgi, C. W., N. Kendall, R. Greenshields: Better Engine Design Can End Sludge: SAE Journal. Society of Automotive Engineers, May 1948.
28. Loebel, A. S., et al.: Transportation Energy Conservation Data Book. Oak Ridge National Laboratory, Report No. ORNL-5198, October 1976.

BIBLIOGRAPHY

AIResearch Manufacturing Company of California: Flywheel Energy Storage Unit Technology Development Program: 1st Quarterly Technical Report. Report No. 78-15345, August 14, 1978.

Bode, H.: Lead-Acid Batteries. John Wiley and Sons, Inc., New York, N.Y.

Brennand, J., R. Curtis, H. Fox, W. Hamilton: Electric and Hybrid Vehicle Performance and Design Goal Determination Study. General Research Corporation Report No. SAN/1215-1, August 1977.

Carson, R. W.: New and Better Traction Drives are Here: Machine Design. Vol. 46, No. 10, April 18, 1974.

Cataldo, R. L.: Response of Lead-Acid Batteries to Chopper-Controlled Discharge: Preliminary Results. NASA Lewis Research Center, NASA TM-73834, February 1978.

Chang, M. C.: Computer Simulation of an Advanced Hybrid Electric-Powered Vehicle. Society of Automotive Engineers, Paper No. 780217, February 27, 1978.

Frank, H. A., A. M. Phillips: Evaluation of Battery Models for Prediction of Electric Vehicle Range. Jet Propulsion Laboratory, Publication 77-29, August 1, 1977.

Hoxie, E. A.: Some Discharge Characteristics of Lead-Acid Batteries: AIEE Transactions. Vol. 73, Part 2, March 1954.

Huntley, P.: Design Factors of Hydro-Mechanical Transmissions of Passenger Cars. Proceedings of the Fourth International Symposium on Automotive Propulsion Systems, NATO/CCMS N. 61, Vol. 11, April 18, 1977.

Kleckner, K. R.: Modeling and Testing of Storage Batteries. Society of Automotive Engineers, Paper No. 730251, January 8, 1973.

Klein, E. A., G. A. Norris: Hydrostatics Tackle Tough New Jobs: Machine Design. Vol. 49, No. 19, August 25, 1977.

Krouse, J. K.: Belt Drives That Shift Themselves: Machine Design. Vol. 49, No. 19, August 25, 1977.

Druse, R. E., T. A. Huls: Development of the Federal Urban Driving Schedule. Society of Automotive Engineers, Paper 730553, 1973.

Lawson, L. J., A. K. Smith, G. D. Davis: Study of Flywheel Energy Storage, Final Report. Report No. UMTA-CA-06-0106-77-1, September 1, 1977.

Marello, L.: Optimizing the Engine-Transmission system by Means of an Electronically Controlled Gearbox. Proceedings of the Fourth International Symposium on Automotive Propulsion Systems, NATO/CCMS n. 61, Vol. 11, page 610, April 18, 1977.

Morris, R.: Variable-Speed Belt Drives, Automatic Transmission of the Future: Machine Design. Vol. 48, No. 19, August 12, 1976.

Shepherd, C. M.: Design of Primary and Secondary Cells, II An Equation Describing Battery Discharge: Journal of the Electromechanical Society. July 1965.

Simanaitis, D. J.: Emission Test Cycles Around the World: Automotive Engineering. Vol. 85, No. 8, August 1977.

Society of Automotive Engineers, Inc.: Electric Vehicle Test Procedure J227a. February 1976.

Soltis, R. F., E. McBrien, J. M. Bozek, F. Gourash: Baseline Tests of the Volkswagen Transporter Electric Delivery Van. NASA Lewis Research Center, NASA TM-73766, January 1978.

Taylor, D. F., E. G. Siwek: The Dynamic Characterization of Lead-Acid Batteries for Vehicle Applications. Society of Automotive Engineers, Paper No. 730252, January 8, 1973.

The Aerospace Corporation: Hybrid Heat Engine/Electric Systems Study. Report No. TOR-059 (6769-01) -2, June 1, 1971.

U. S. Department of Energy: Electric and Hybrid Vehicle Program. 3rd EHV Program Contractors' Meeting, Presentation Aids, June 25, 1979.

Vinal, G. W.: Storage Batteries. 4th Edition, Chapter 5, John Wiley and Sons, Inc., New York, N.Y.

Wallin, A. W.: Efficiency of Synchronous Belts and V-Belts. Uniroyal Inc.

APPENDIX A

TASK 1 PARAMETRIC RESULTS

Task 1 parametric results are presented in Appendix A. Curves of prime electric range, fuel economy, annual fuel usage, life-cycle cost, and acquisition cost are plotted as a function of battery weight. The vehicle/propulsion system designation for each figure in Appendix A was presented in figs. 1 to 5. The parameters are briefly defined as follows: prime electric range is the distance the vehicle can travel in the electric mode beginning with a fully charged battery pack until the battery is 80 percent discharged; fuel economy is the fuel consumed divided by distance travelled in the heat engine mode; annual fuel usage is the total fuel consumed over a specified one-year, 16 000-km driving schedule; life-cycle cost is the total operating cost of the propulsion system over a 10-year, 160 000-km life; acquisition cost is the retail cost of the propulsion system alone to the consumer.

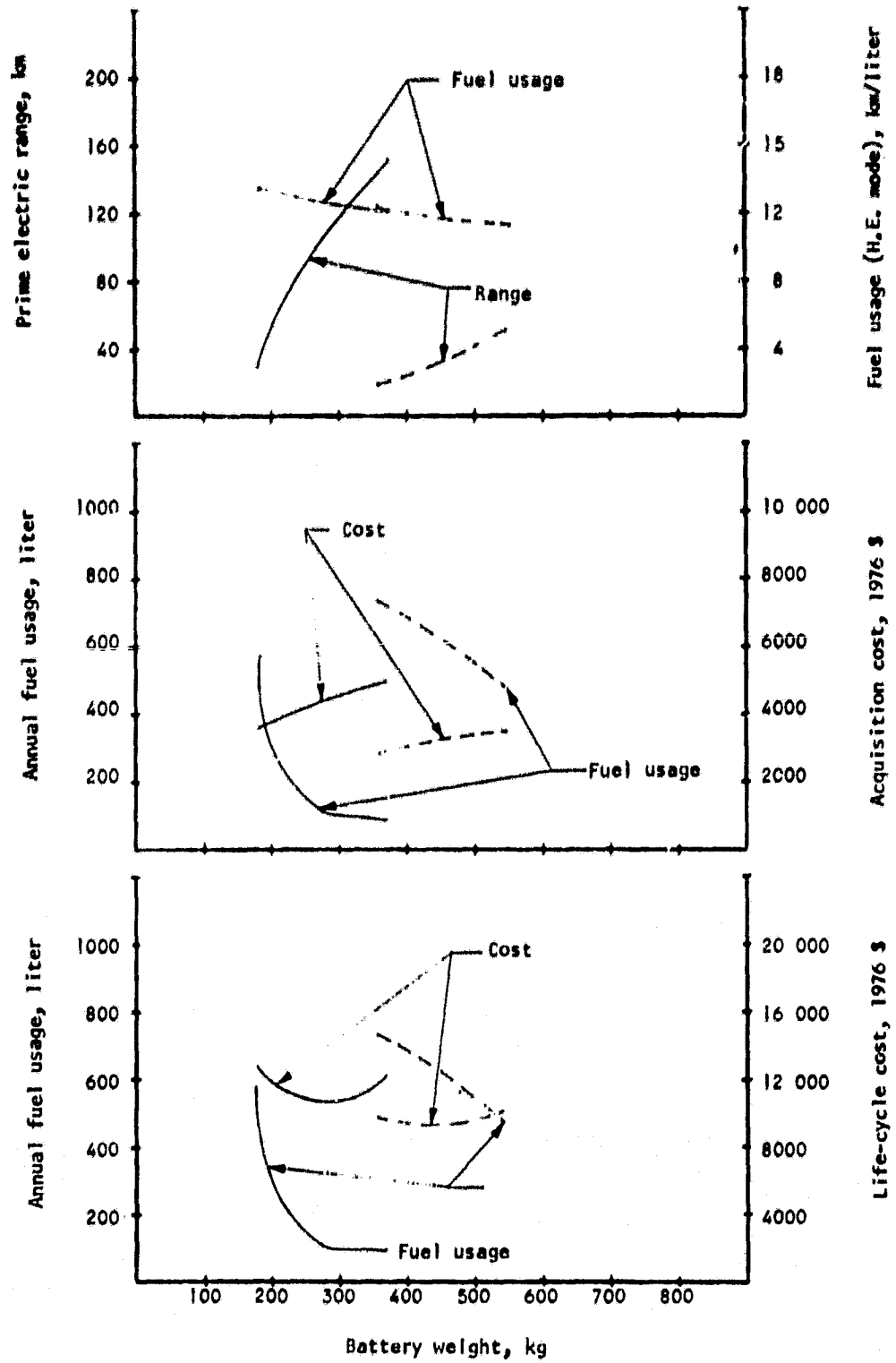


Figure A-1.--Task I parametric results for configuration 1.1A (no M.E.S.).

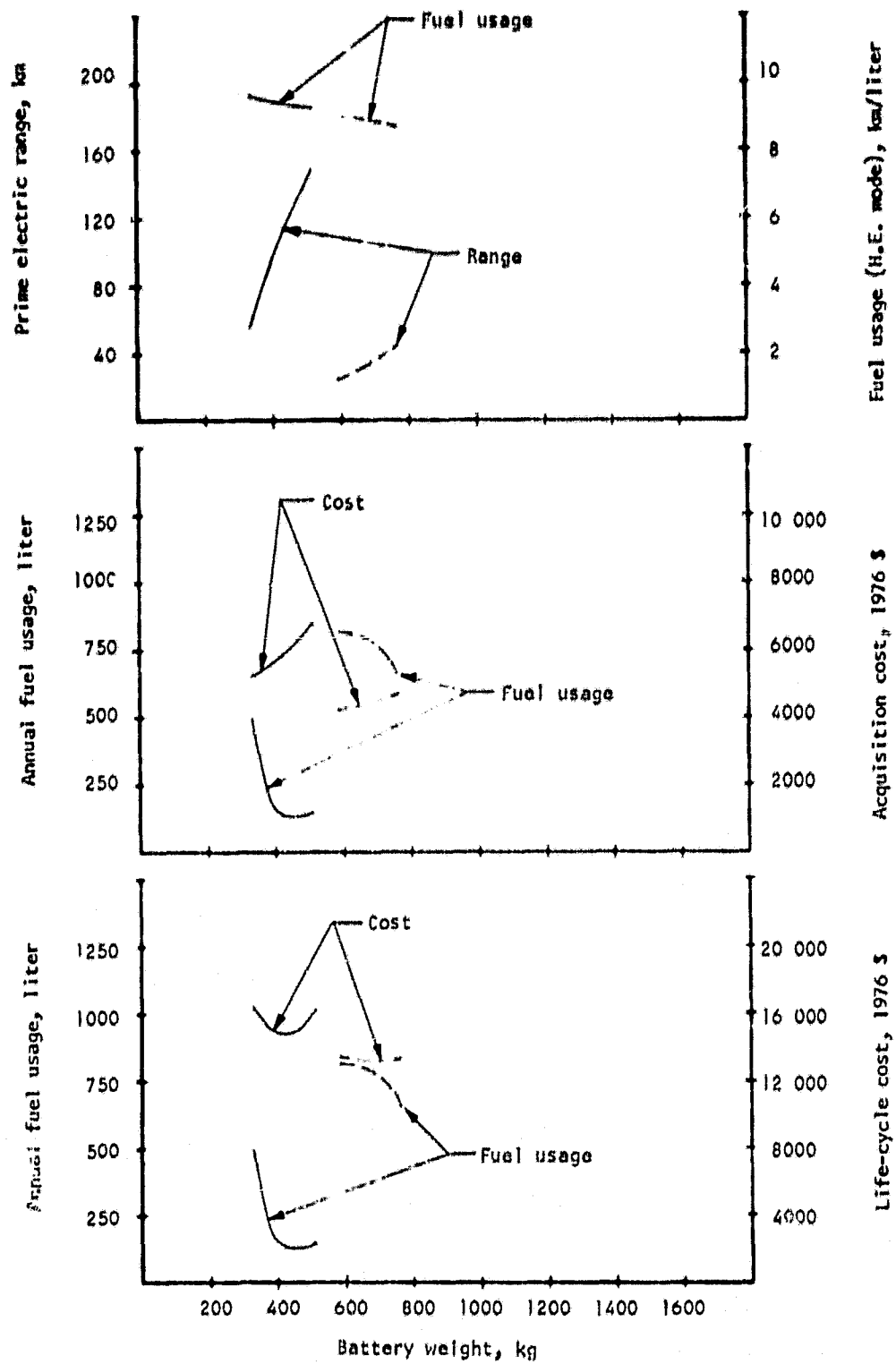


Figure A-2.--Task I parametric results for configuration 1.1B (no M.E.S.).

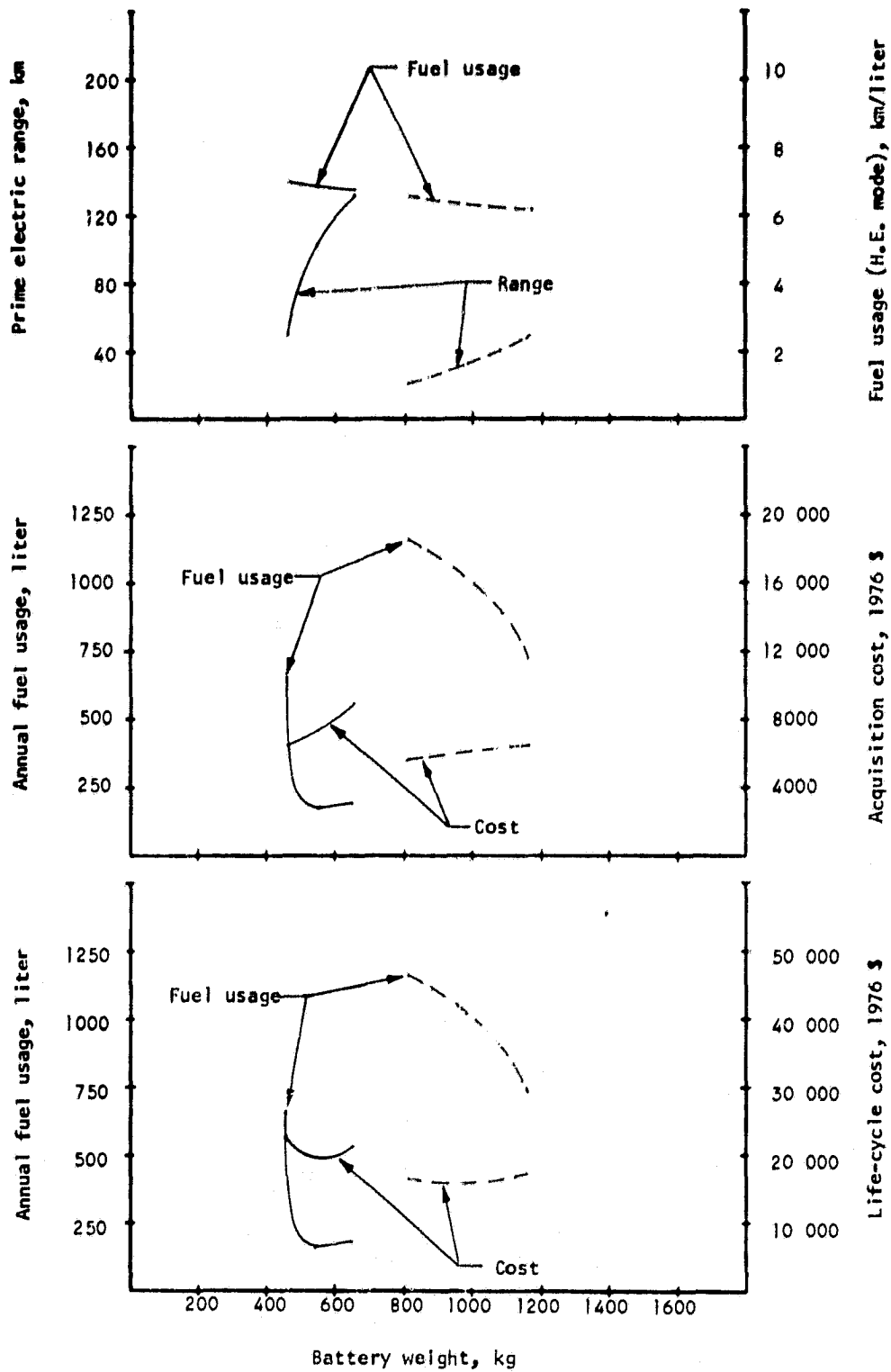


Figure A-3.--Task I parametric results for configuration 1.1C (no M.E.S.).

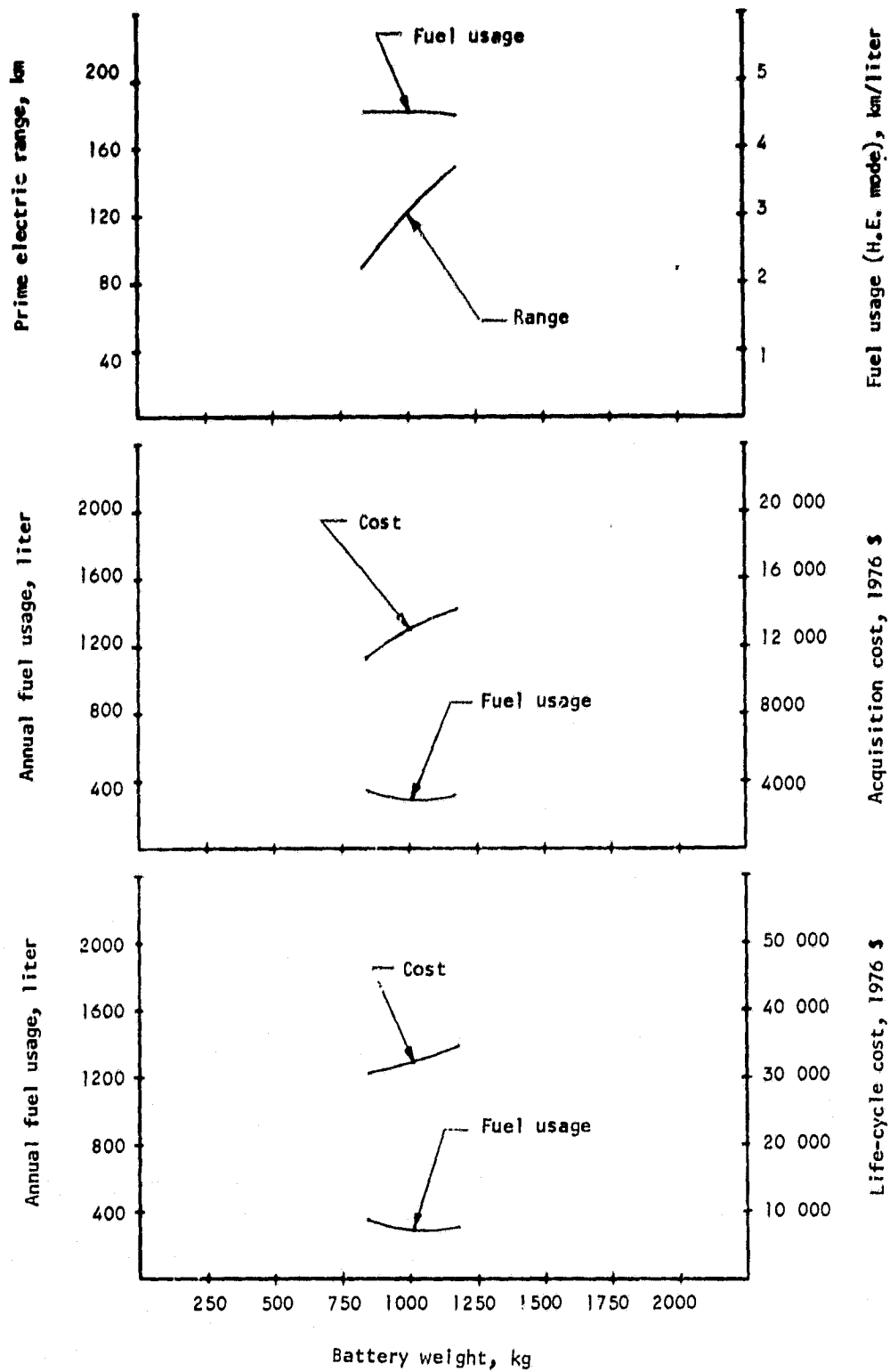


Figure A-4.--Task I parametric results for configuration 1.1D (no M.E.S.).

ORIGINAL PAGE
OF POOR QUALITY

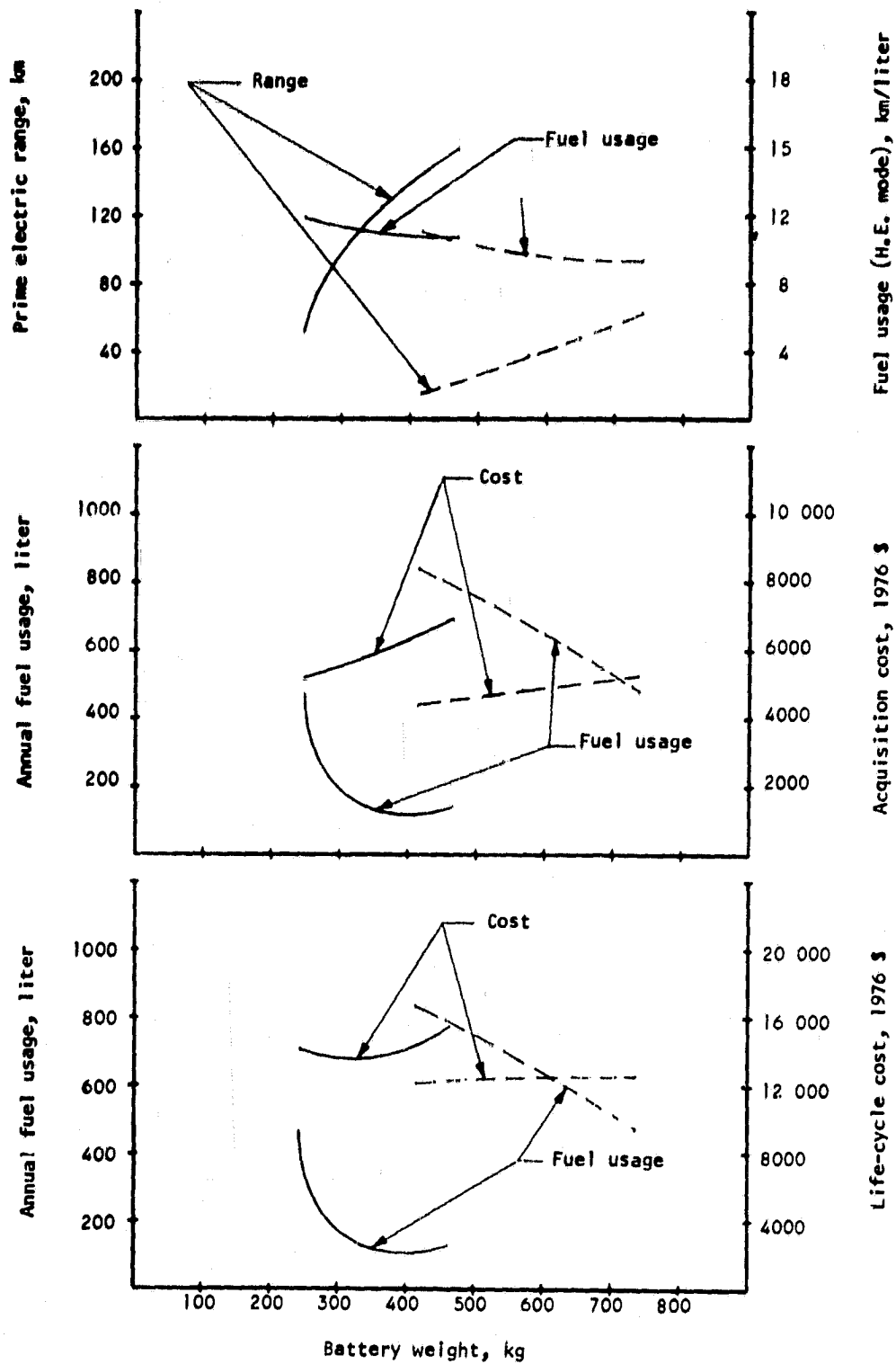


Figure A-5.--Task I parametric results for configuration 1.2A (no M.E.S.).

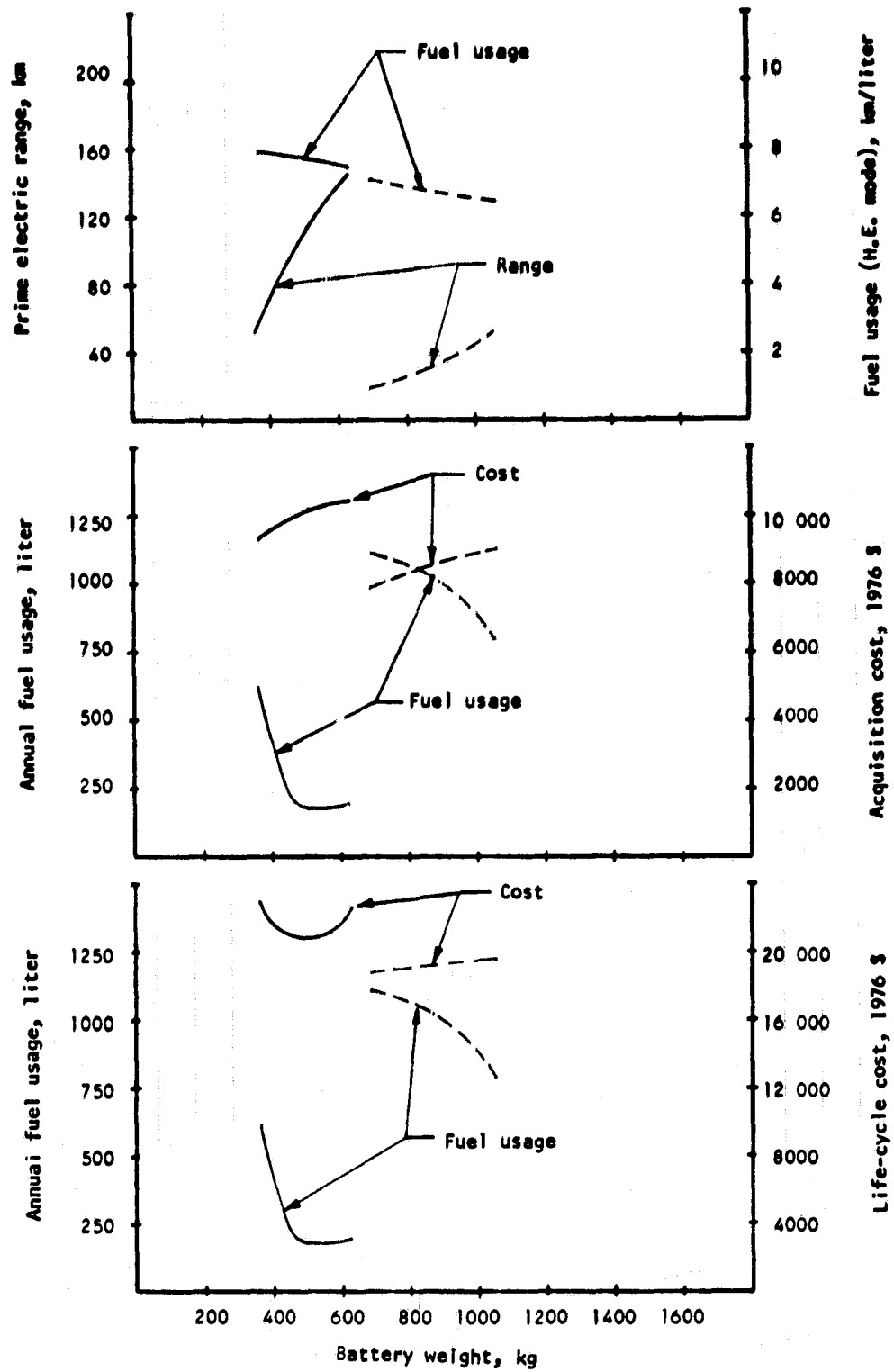


Figure A-6.--Task I parametric results for configuration 1.2B (no M.E.S.).

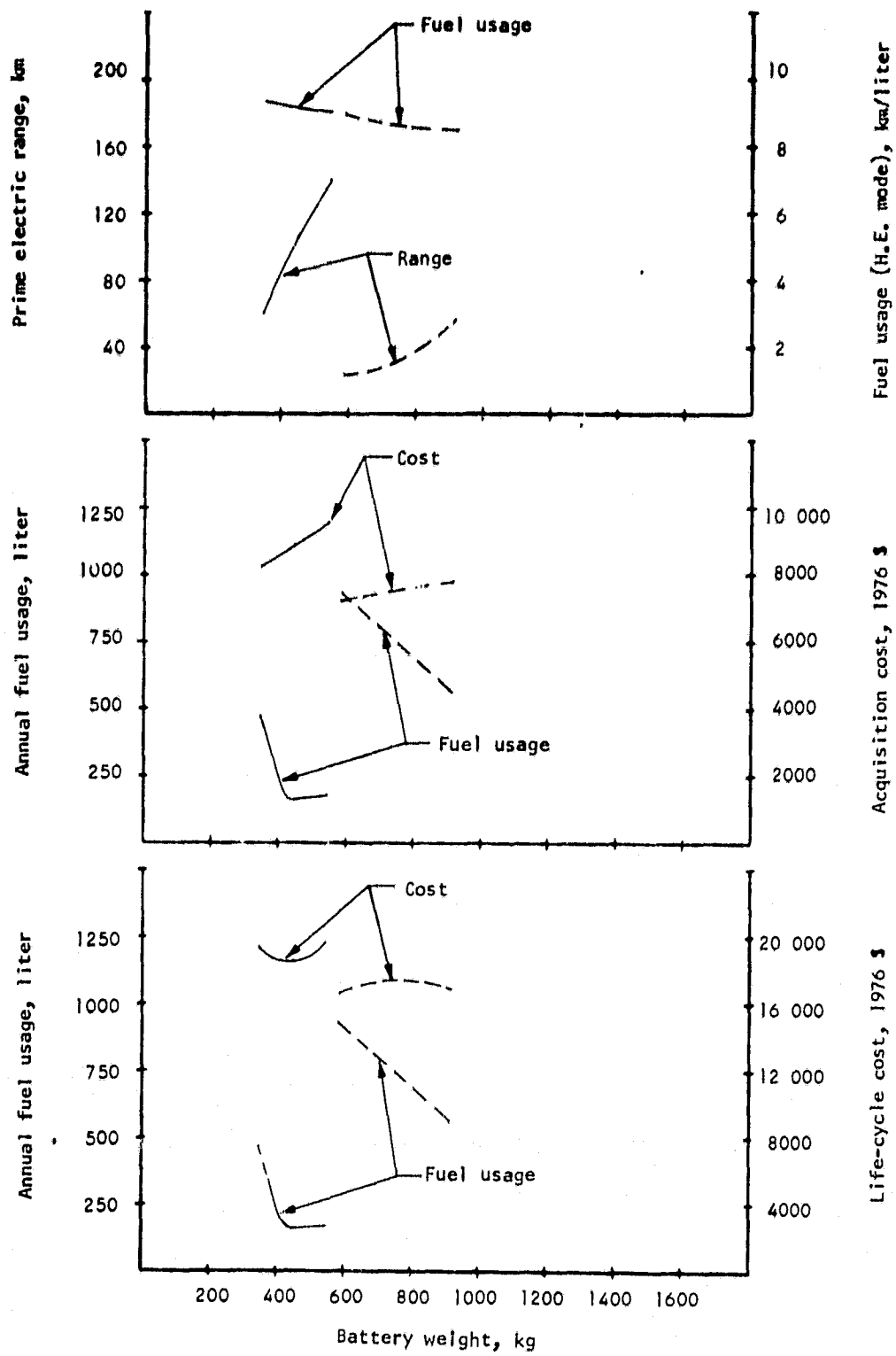


Figure A-7.--Task I parametric results for configuration 2.1B (M.E.S., no power split).

ORIGINAL PAGE IS
OF POOR QUALITY

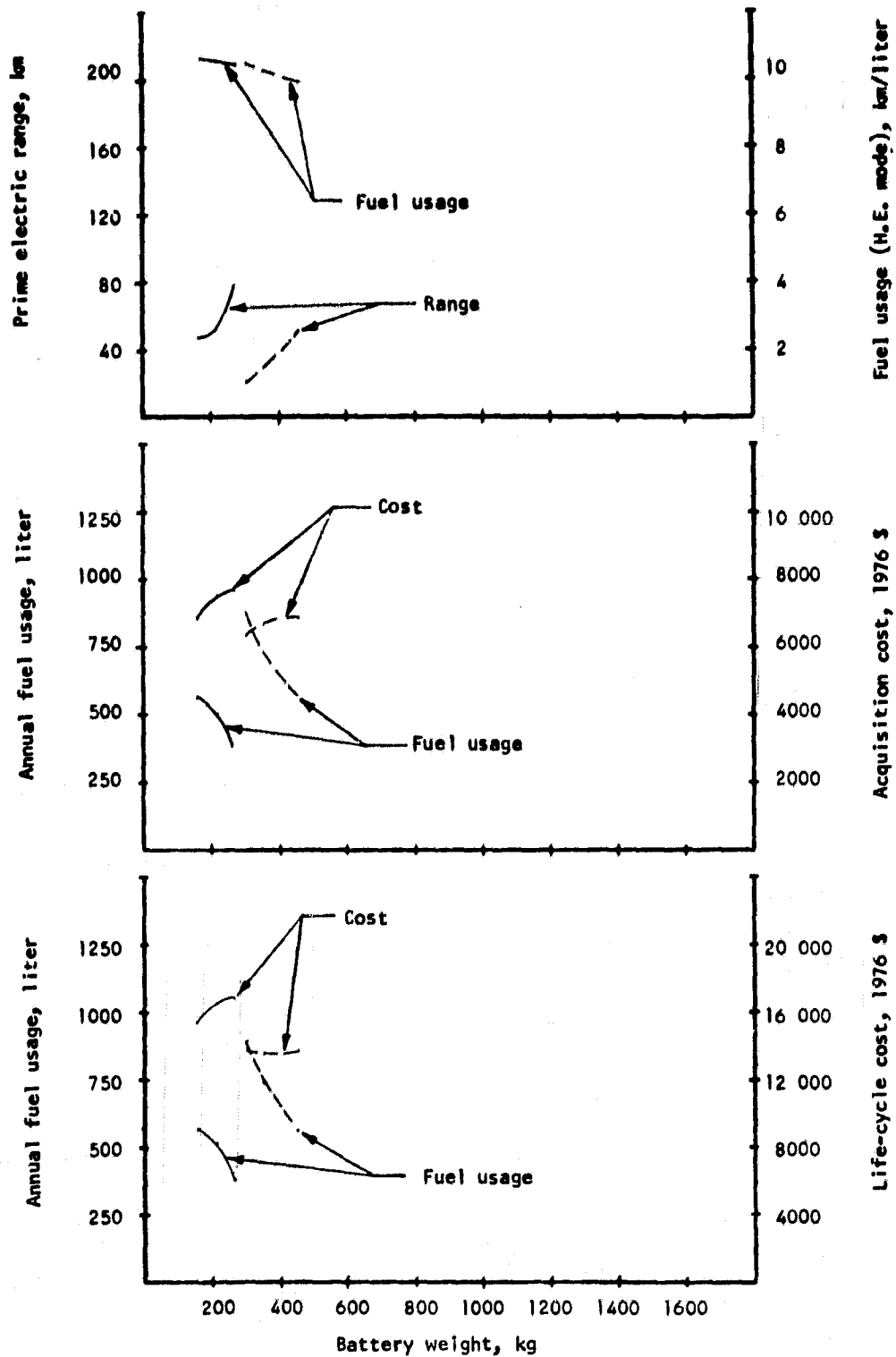


Figure A-8.--Task I parametric results for configuration 2.1B (M.E.S., with power split).

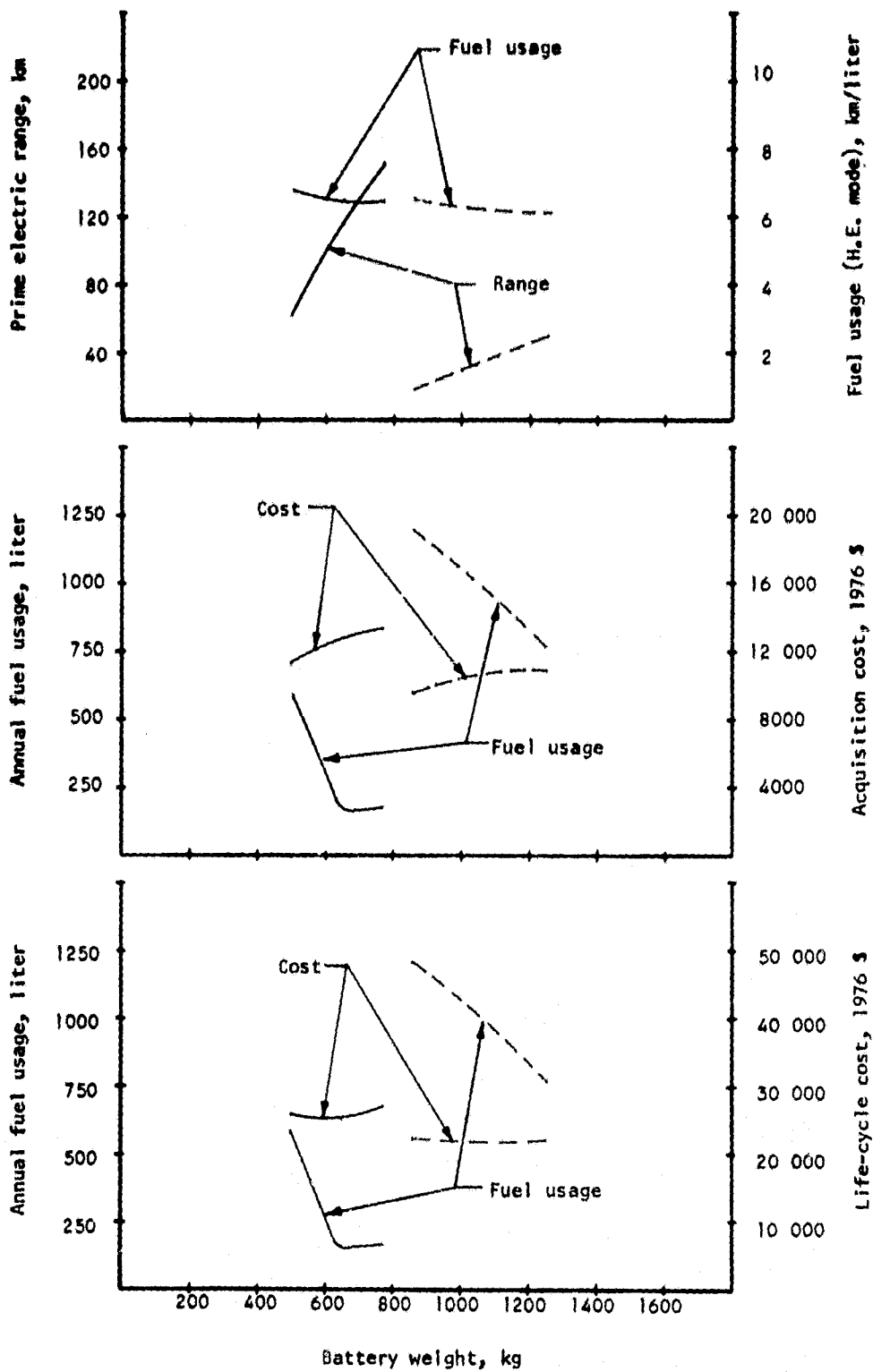


Figure A-9.--Task I parametric results for configuration 2.1C (M.E.S., no power split).

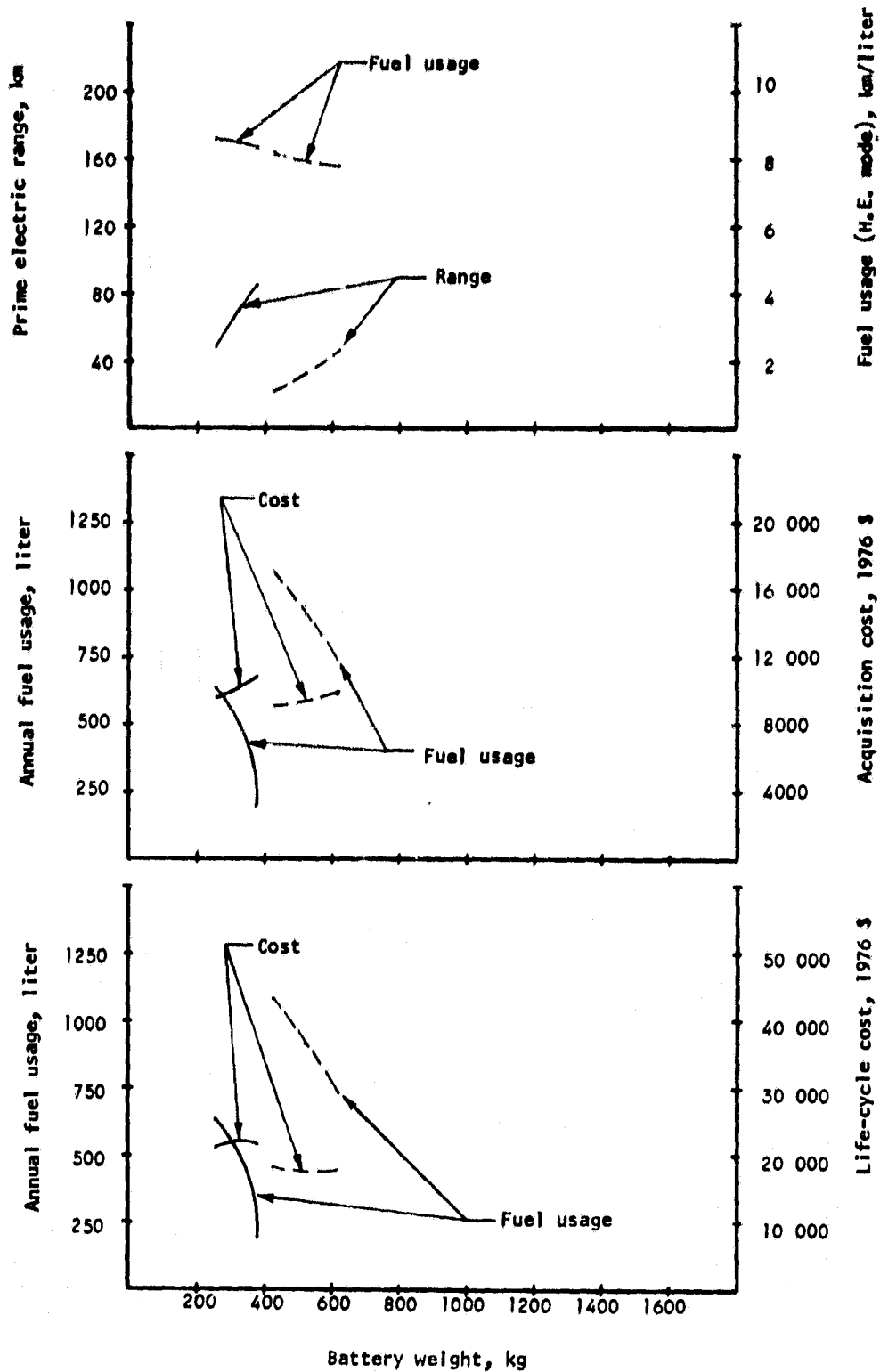


Figure A-10.--Task I parametric results for configuration 2.1C (M.E.S., with power split).

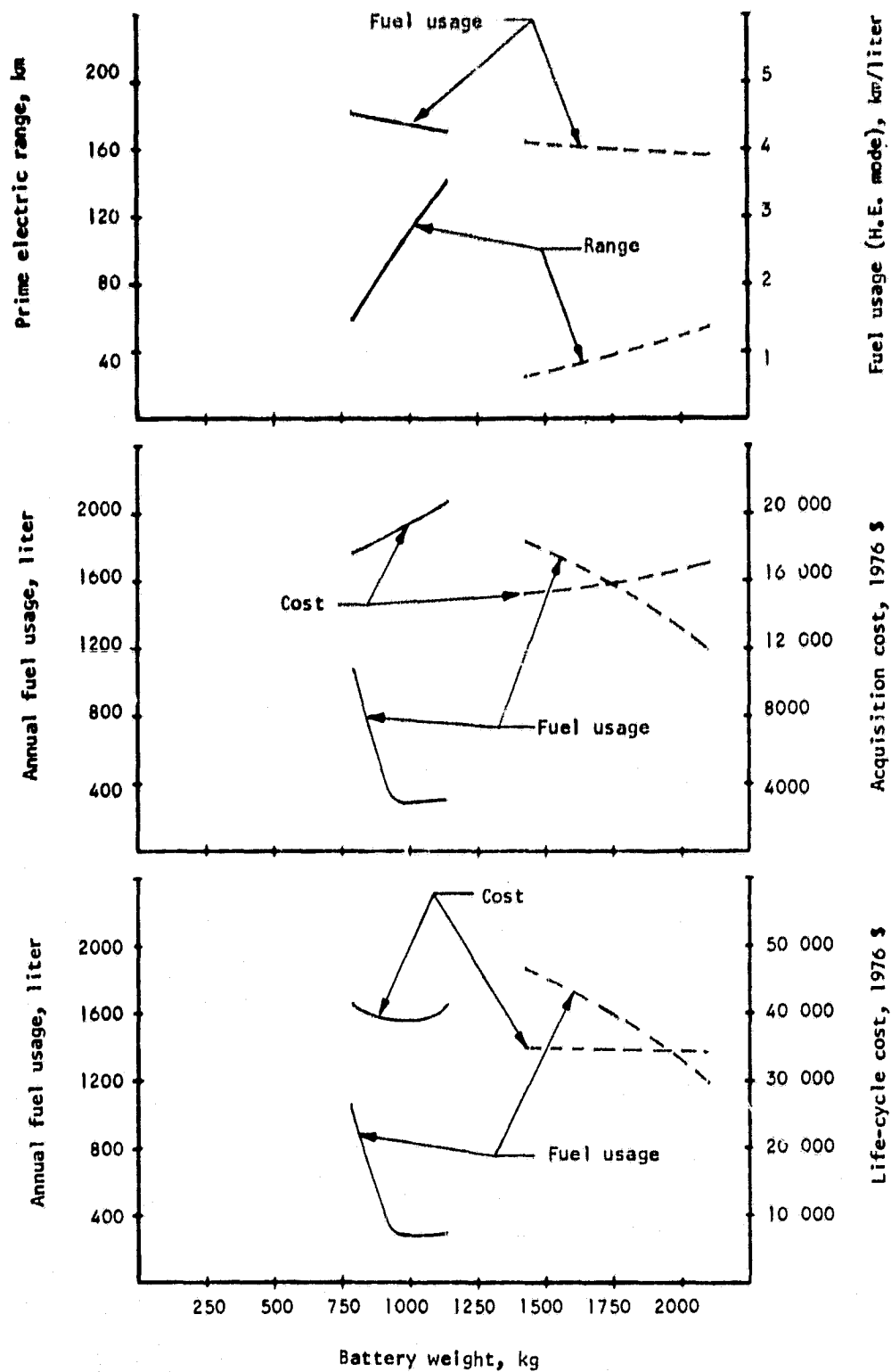


Figure A-11.--Task I parametric results for configuration 2.1D (M.E.S., no power split).

ORIGINAL PAGE IS
OF POOR QUALITY

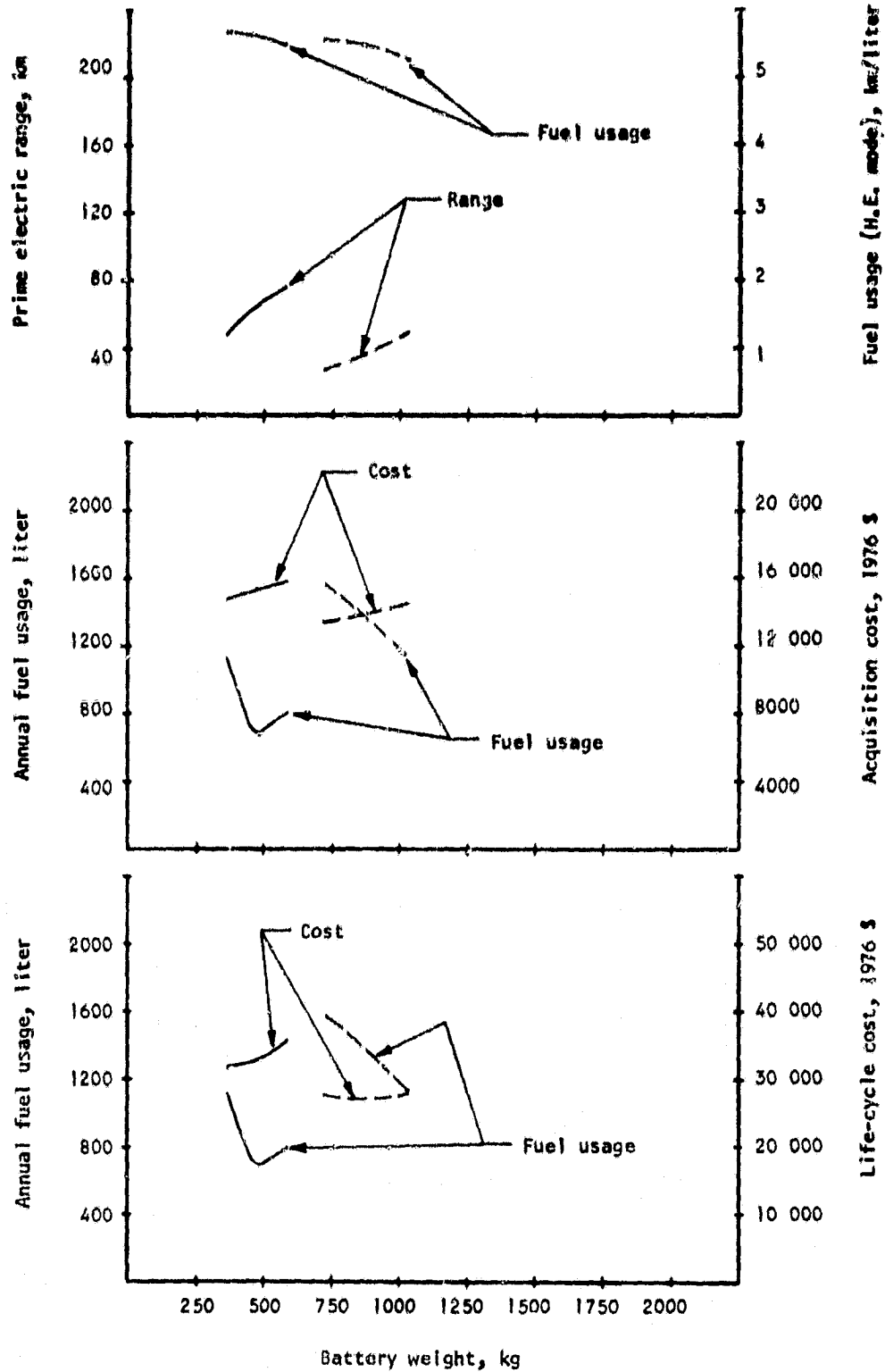


Figure A-12.--Task I parametric results for configuration 2.1D (M.E.S., with power split).

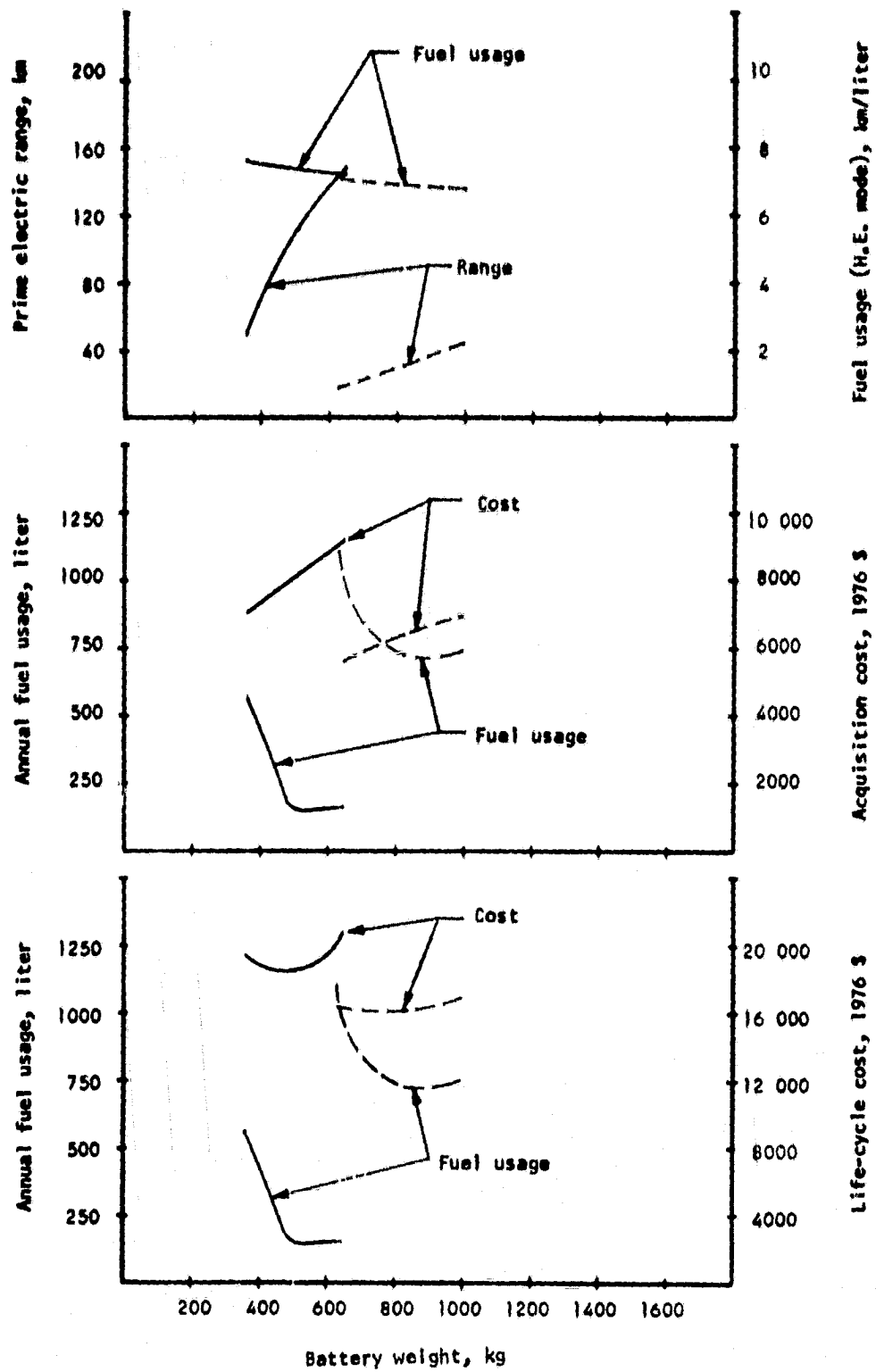


Figure A-13.--Task I parametric results for configuration 2.2B (M.E.S., no power split).

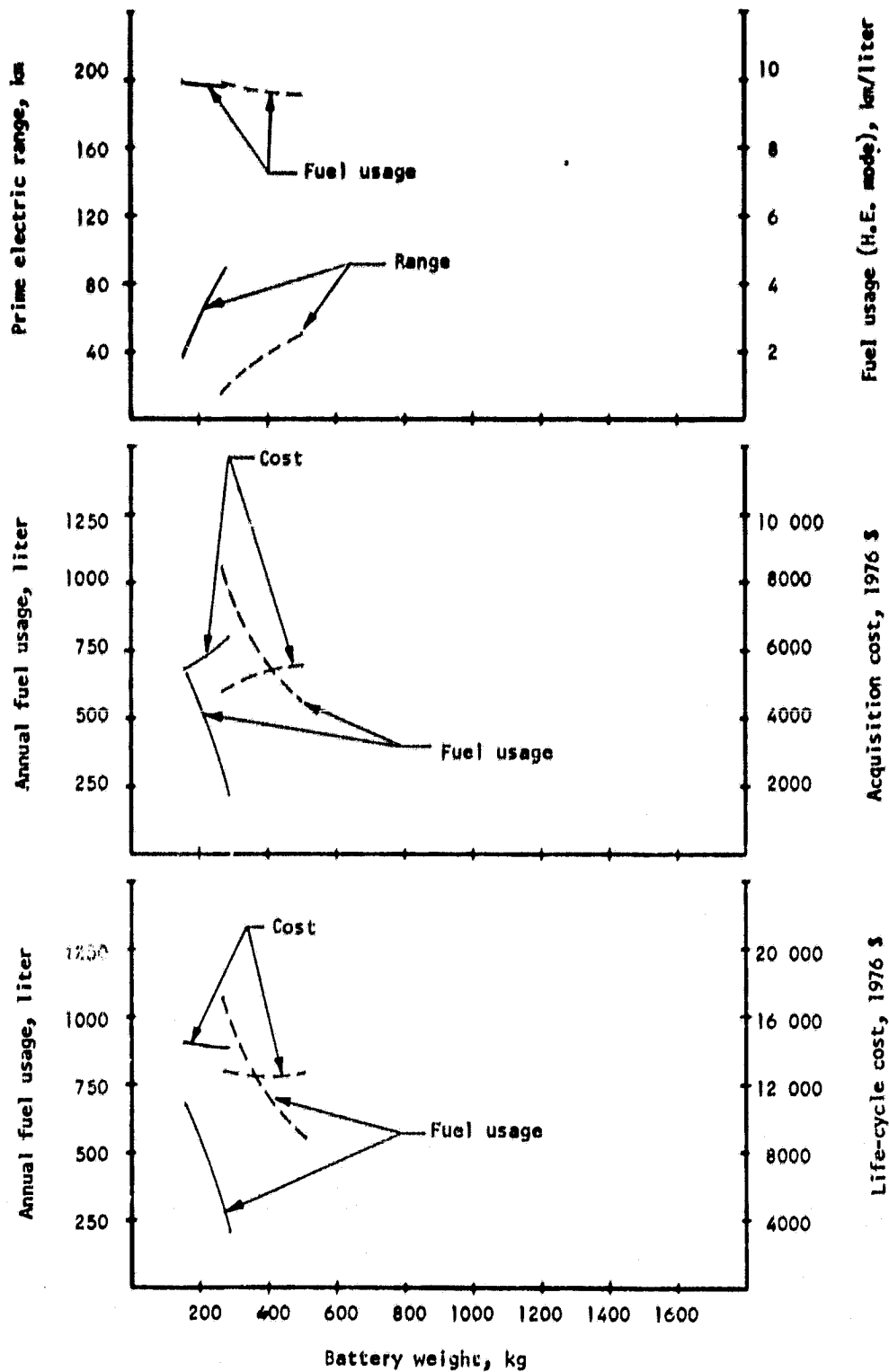


Figure A-14.--Task I parametric results for configuration 2.2B (M.E.S., with power split).

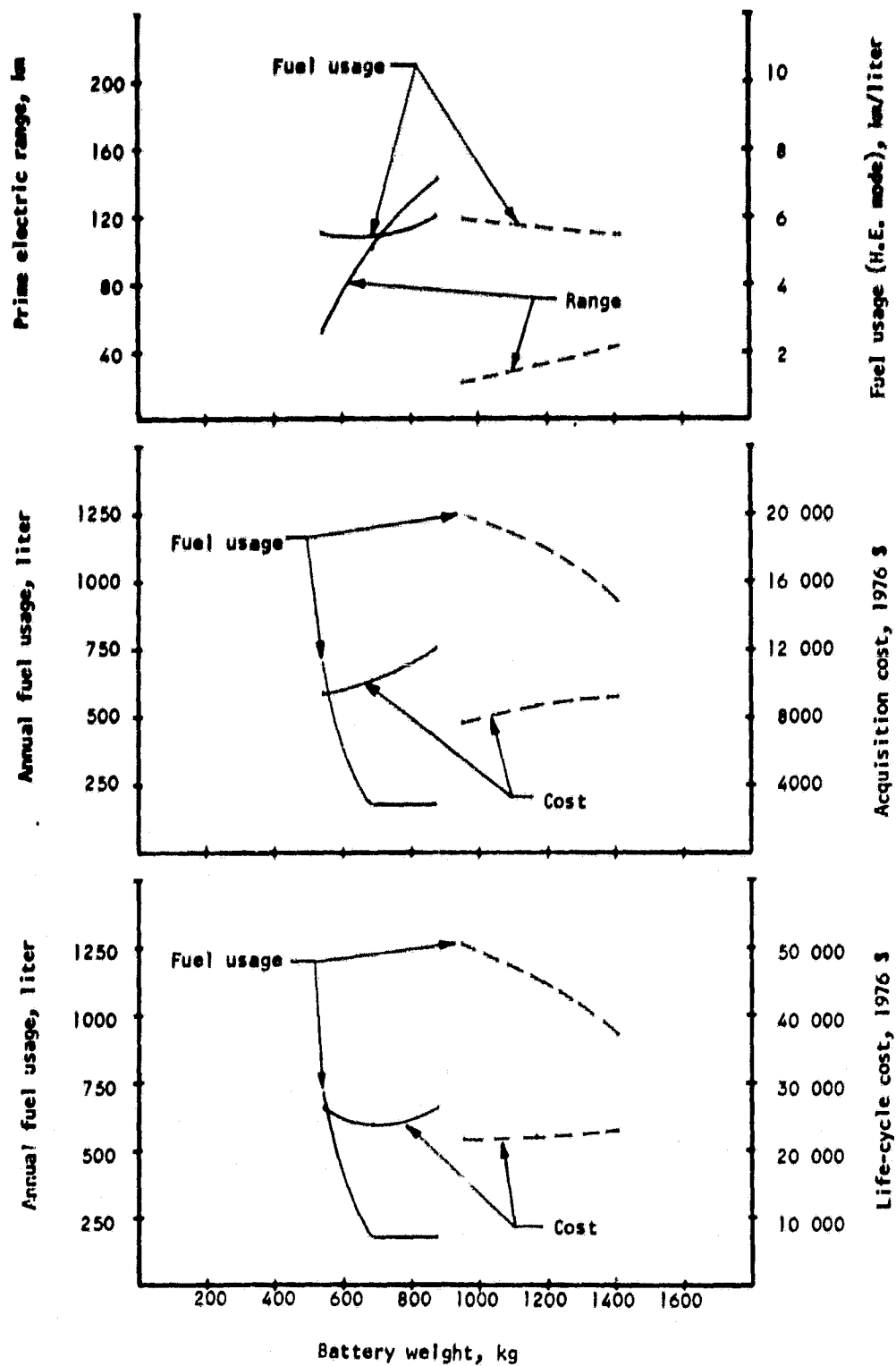


Figure A-15.--Task I parametric results for configuration 2.2C (M.E.S., no power split).

ORIGINAL PAGE IS
OF POOR QUALITY

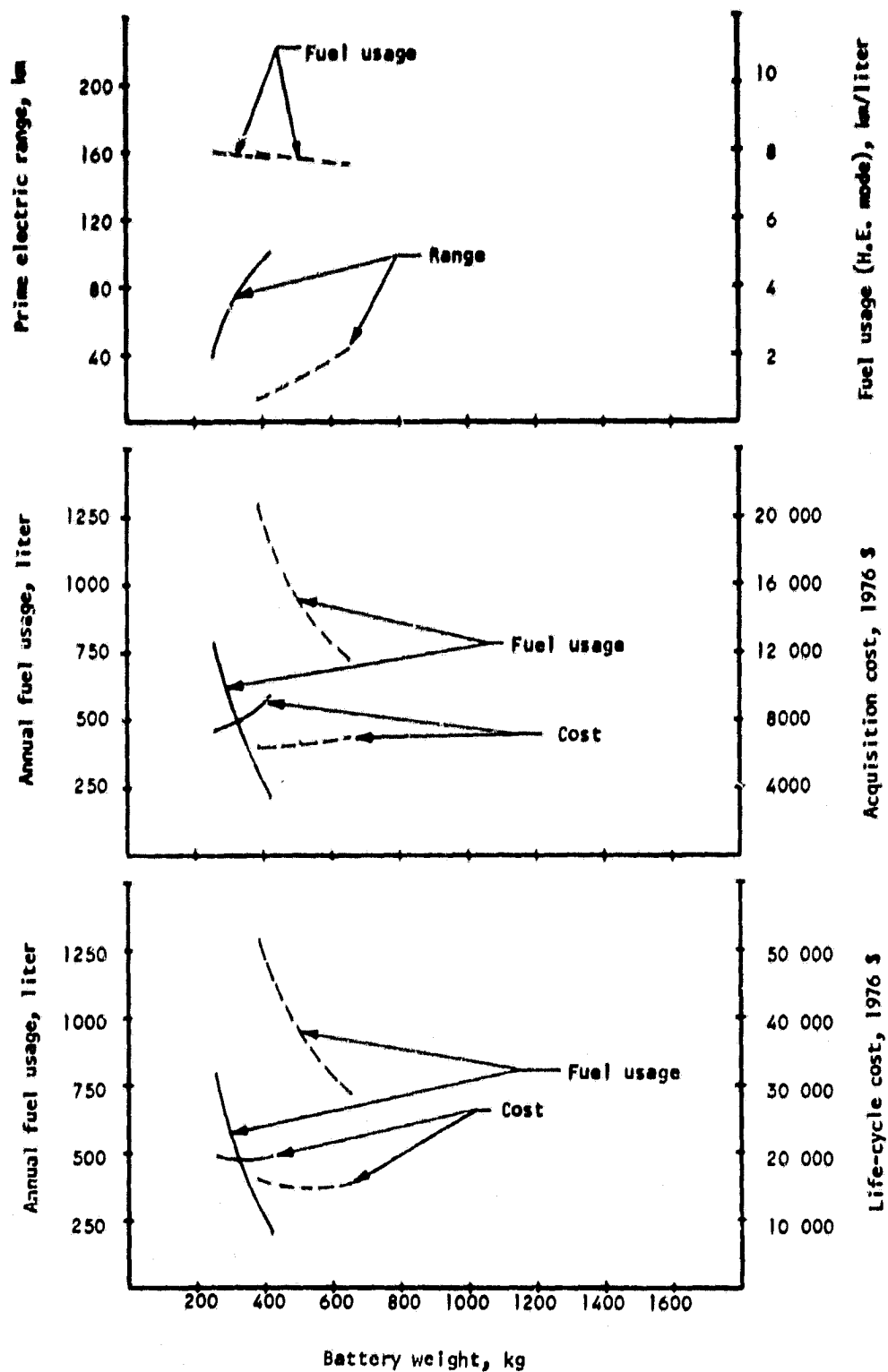


Figure A-16.--Task I parametric results for configuration 2.2C (M.E.S., with power split).

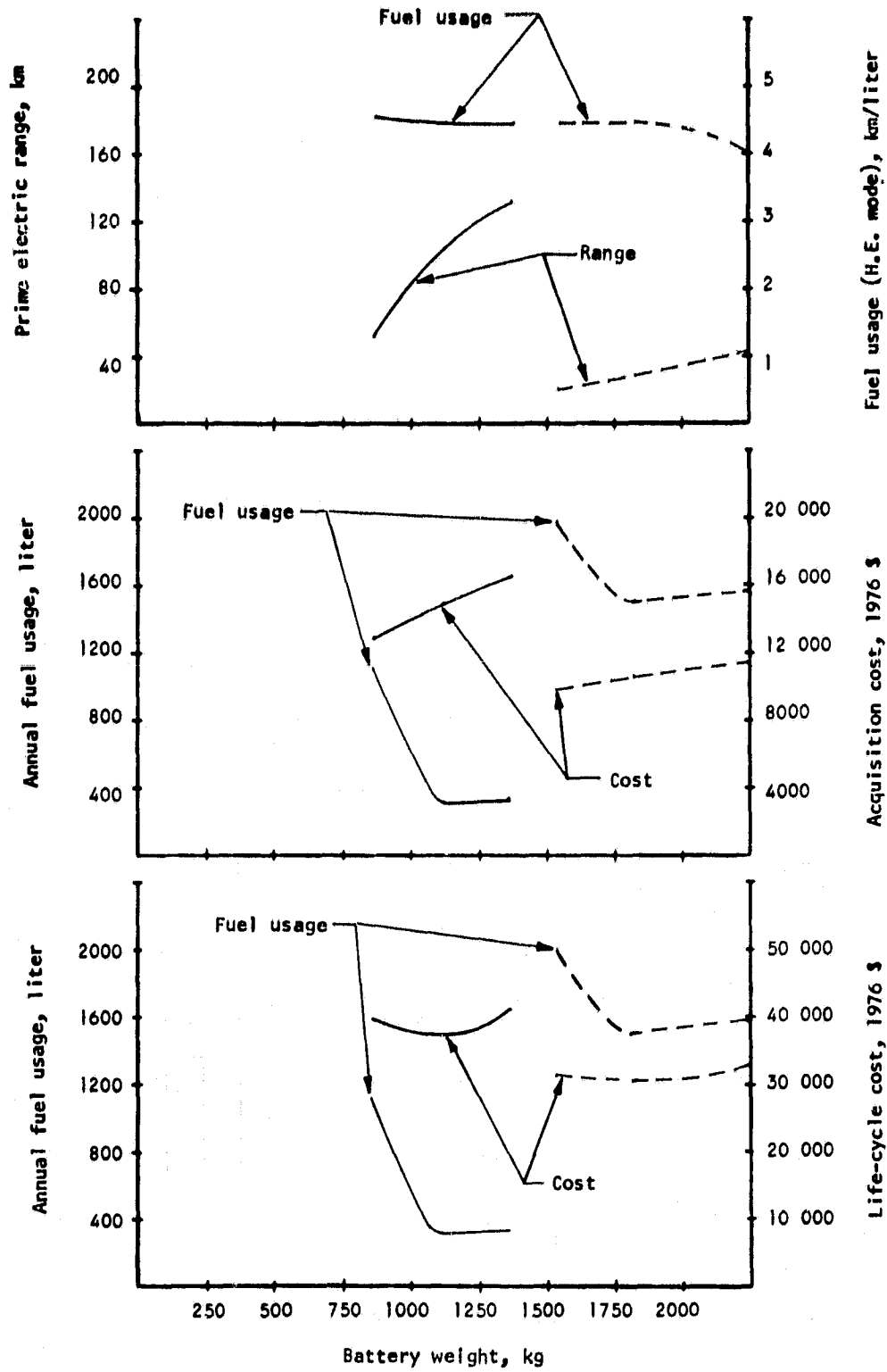


Figure A-17.--Task I parametric results for configuration 2.2D (M.E.S., no power split).

ORIGINAL PAGE IS
OF POOR QUALITY

23

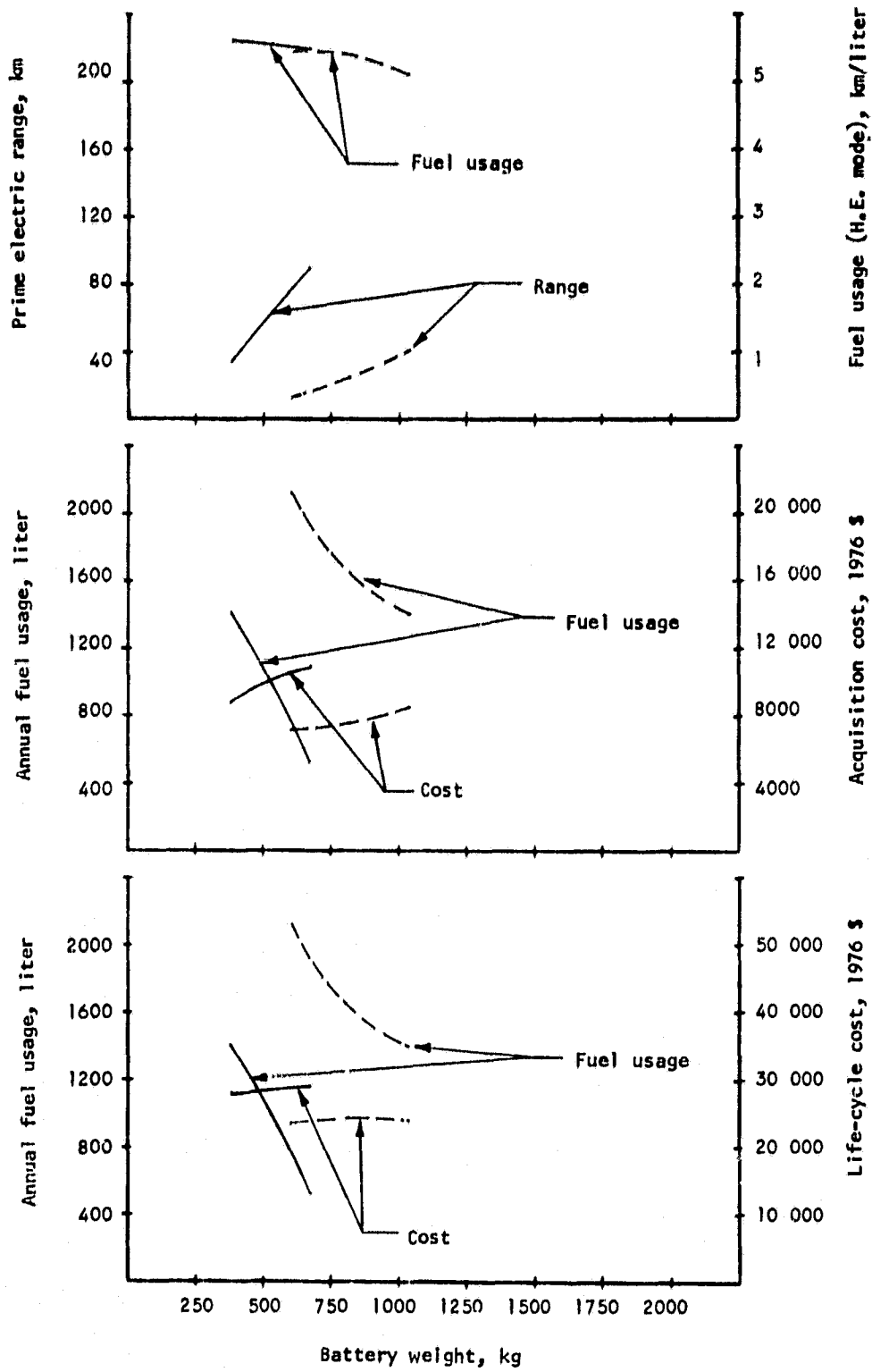


Figure A-18.--Task I parametric results for configuration 2.2D (M.E.S., with power split).

APPENDIX B
WORK PLAN

PROGRAM SCOPE AND WORK PLAN

The work presented in this section describes the program established to fulfill the requirements of NASA Contract DEN 3-91. The program for the analysis, design evaluation, and ultimate selection of an advanced hybrid propulsion system concept for on-road vehicles was performed in six tasks accomplished in a 10-month period. The work plan was prepared during the first 2 weeks of the program to refine and clarify the contract commitments. Two iterations between AIResearch and NASA took place to arrive at the plan as described here.

PROGRAM TASKS

The program tasks and the expected completion periods are described in the contract statement of work. The following flow diagrams and descriptions show in greater detail the work effort to be covered under each of the six tasks. The flow diagram of the total contract, shown in fig. B-1, includes the time span for task and the major objectives.

Task I, Parametric Studies

The five vehicles considered and the five propulsion concepts that are to be parametrically traded off to determine the vehicle/propulsion system concept selected for further refining and analysis in Task II are shown in figs. B-2 through B-6 (identical to figs. 1 through 5).

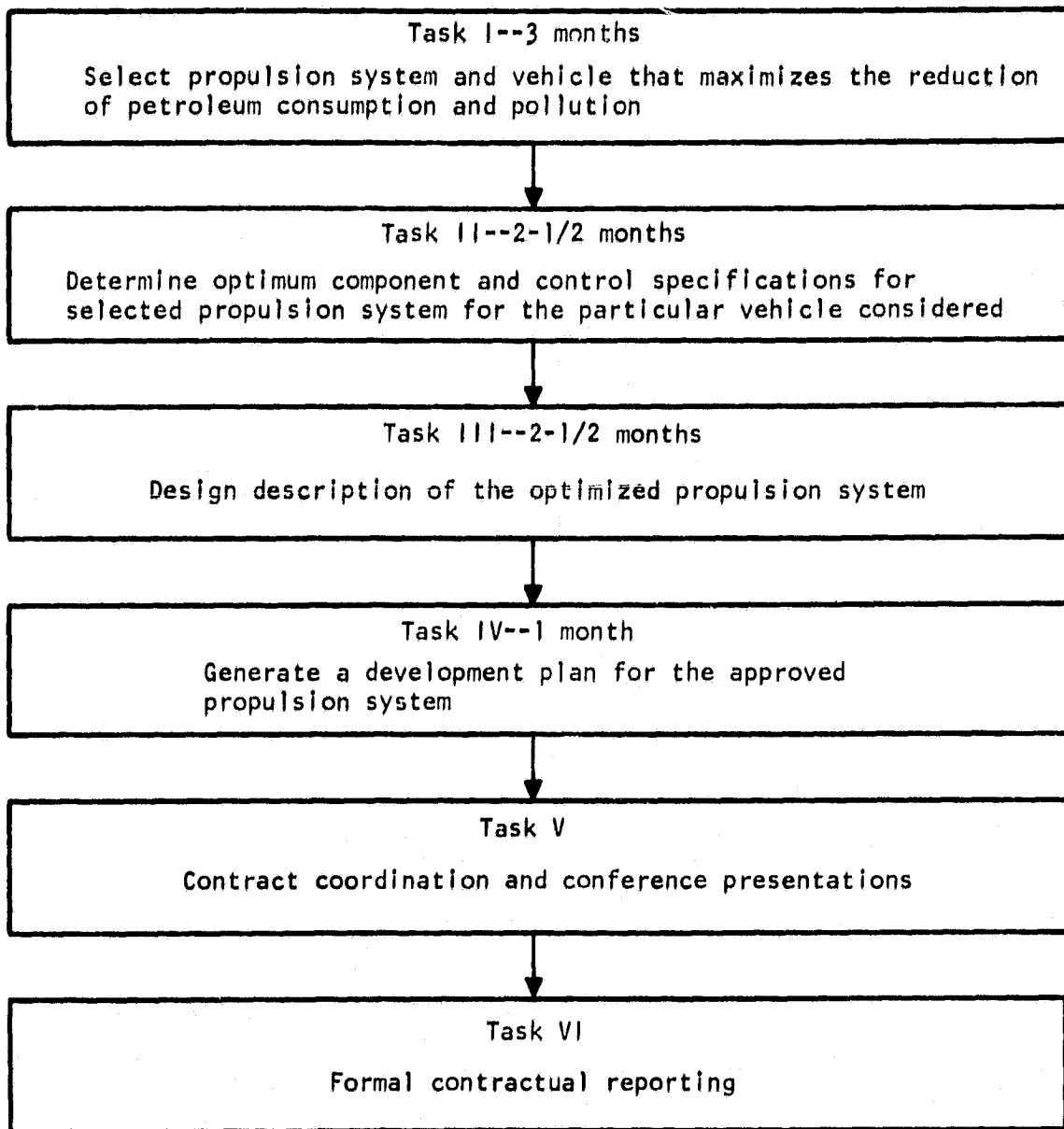
A flow diagram of the subtasks to be accomplished in Task I is presented in fig. B-7. The interrelationship is shown between the subtasks, data needed to perform the work, and the source and status of this data.

The computer parameter format for all the major components is presented in fig. B-8. These formats are compatible with the simulation methodology program called SIMHYB developed by AIResearch. Within each group of hardware alternatives, the components are characterized using the same format. This standardization facilitates the programming of the digital computer for each of the fifteen vehicle/propulsion system concepts.

Task II, Design Tradeoff Studies

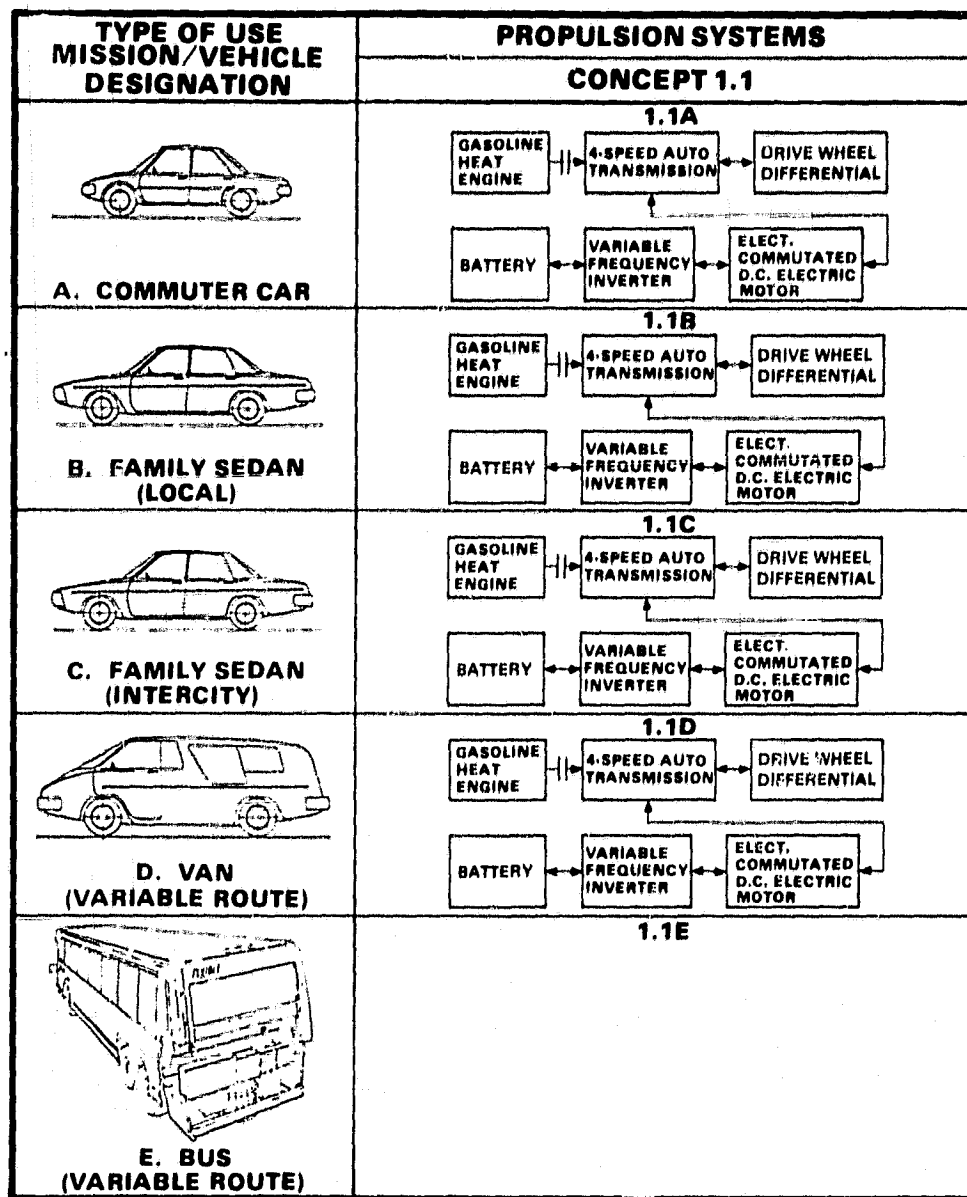
A work subtask flow chart for Task II is presented in fig. B-9. The interrelationship between each subtask, the data needed to perform the work, and the source and status of this data is depicted. The overall objective of Task II is to optimize the propulsion system concept selected in Task I.

Task flow diagram



S-46305

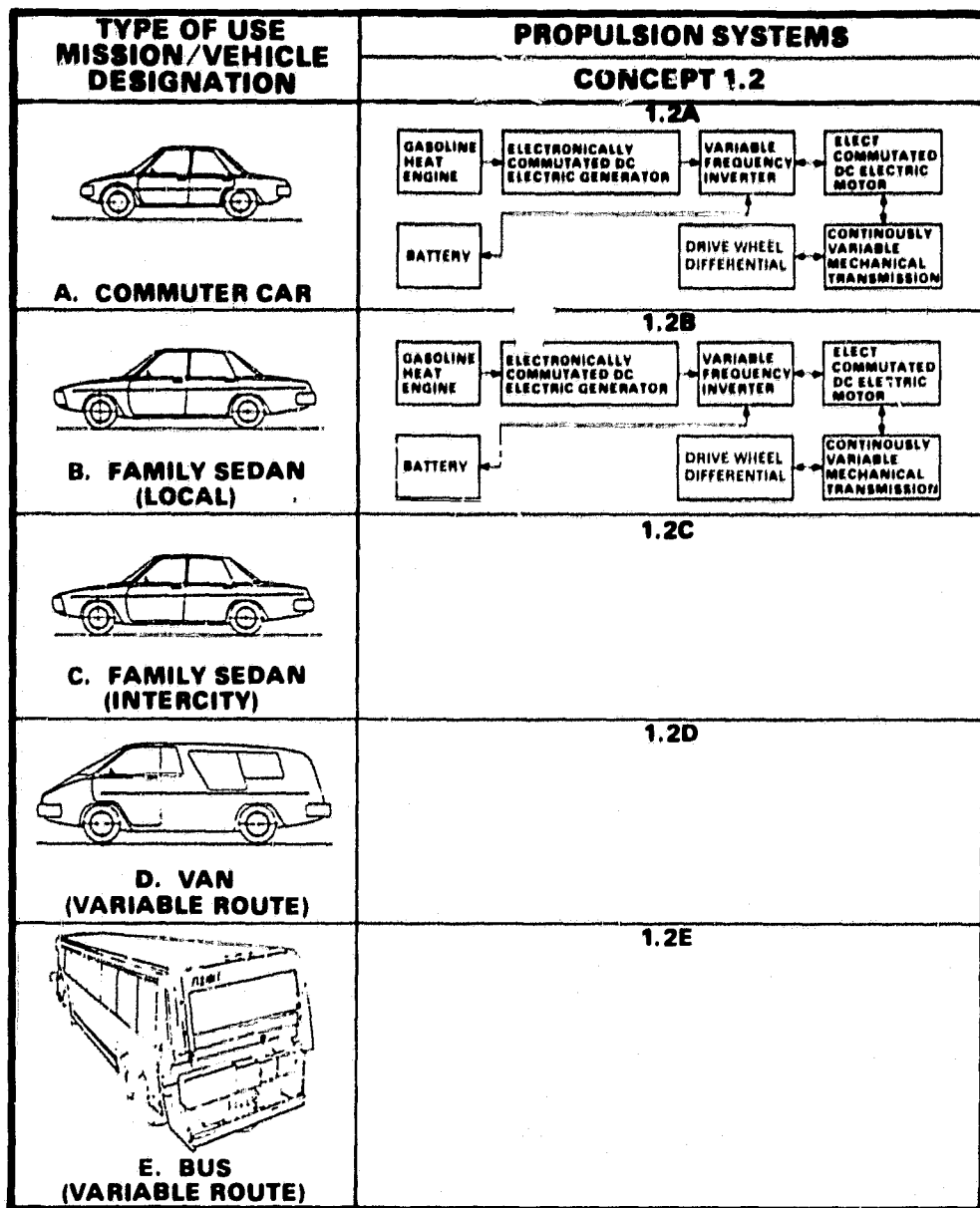
Figure B-1.--Advanced hybrid propulsion system work plan.



S-45305

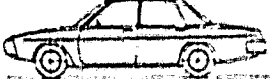
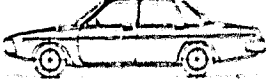
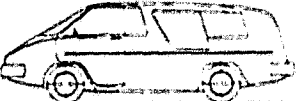
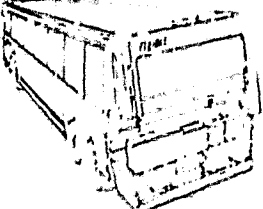
Figure B-2.--Hybrid propulsion system concept 1.1.

ORIGINAL PAGE IS
OF POOR QUALITY



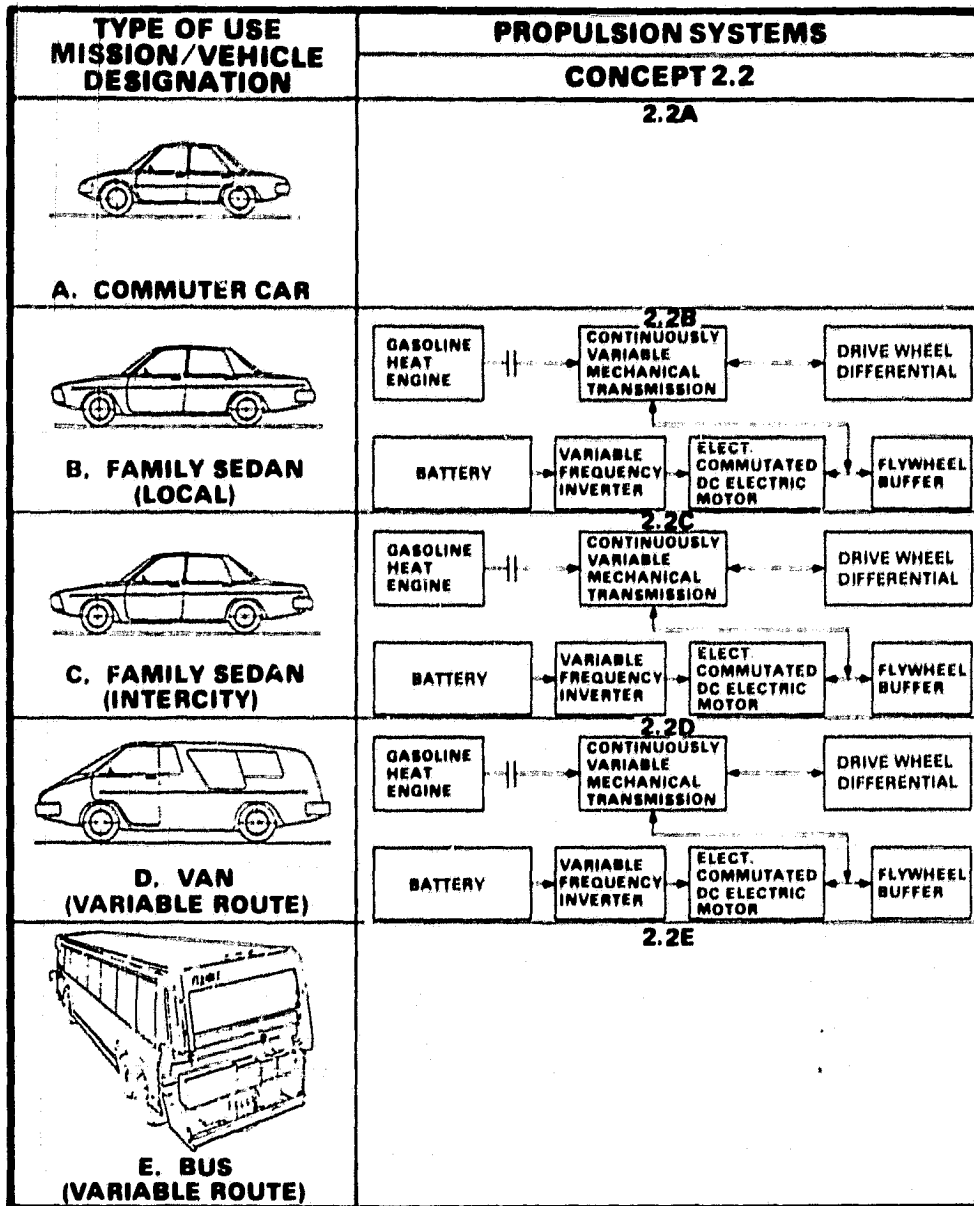
S 45306 A

Figure B-3.--Hybrid propulsion system concept 1.2.

TYPE OF USE MISSION/VEHICLE DESIGNATION	PROPULSION SYSTEMS
	CONCEPT 2.1
 A. COMMUTER CAR	<p style="text-align: center;">2.1A</p>
 B. FAMILY SEDAN (LOCAL)	<p style="text-align: center;">2.1B</p> <pre> graph LR G[Gasoline Heat Engine] --> T[4 Speed Auto Transmission] T --> DD[Drive Wheel Differential] B[Battery] --> VI[Variable Frequency Inverter] VI --> EDCM[Elect Commutated DC Electric Motor] EDCM --> FWS[Flywheel Buffer] FWS --> DD EDCM --> EDCM2[Elect Comm DC Motor] EDCM2 --> FWS </pre>
 C. FAMILY SEDAN (INTERCITY)	<p style="text-align: center;">2.1C</p> <pre> graph LR G[Gasoline Heat Engine] --> T[4 Speed Auto Transmission] T --> DD[Drive Wheel Differential] B[Battery] --> VI[Variable Frequency Inverter] VI --> EDCM[Elect Commutated DC Electric Motor] EDCM --> FWS[Flywheel Buffer] EDCM --> EDCM2[Elect Comm DC Motor] EDCM2 --> FWS </pre>
 D. VAN (VARIABLE ROUTE)	<p style="text-align: center;">2.1D</p> <pre> graph LR G[Gasoline Heat Engine] --> T[4 Speed Auto Transmission] T --> DD[Drive Wheel Differential] B[Battery] --> VI[Variable Frequency Inverter] VI --> EDCM[Elect Commutated DC Electric Motor] EDCM --> FWS[Flywheel Buffer] EDCM --> EDCM2[Elect Comm DC Motor] EDCM2 --> FWS </pre>
 E. BUS (VARIABLE ROUTE)	<p style="text-align: center;">2.1E</p>

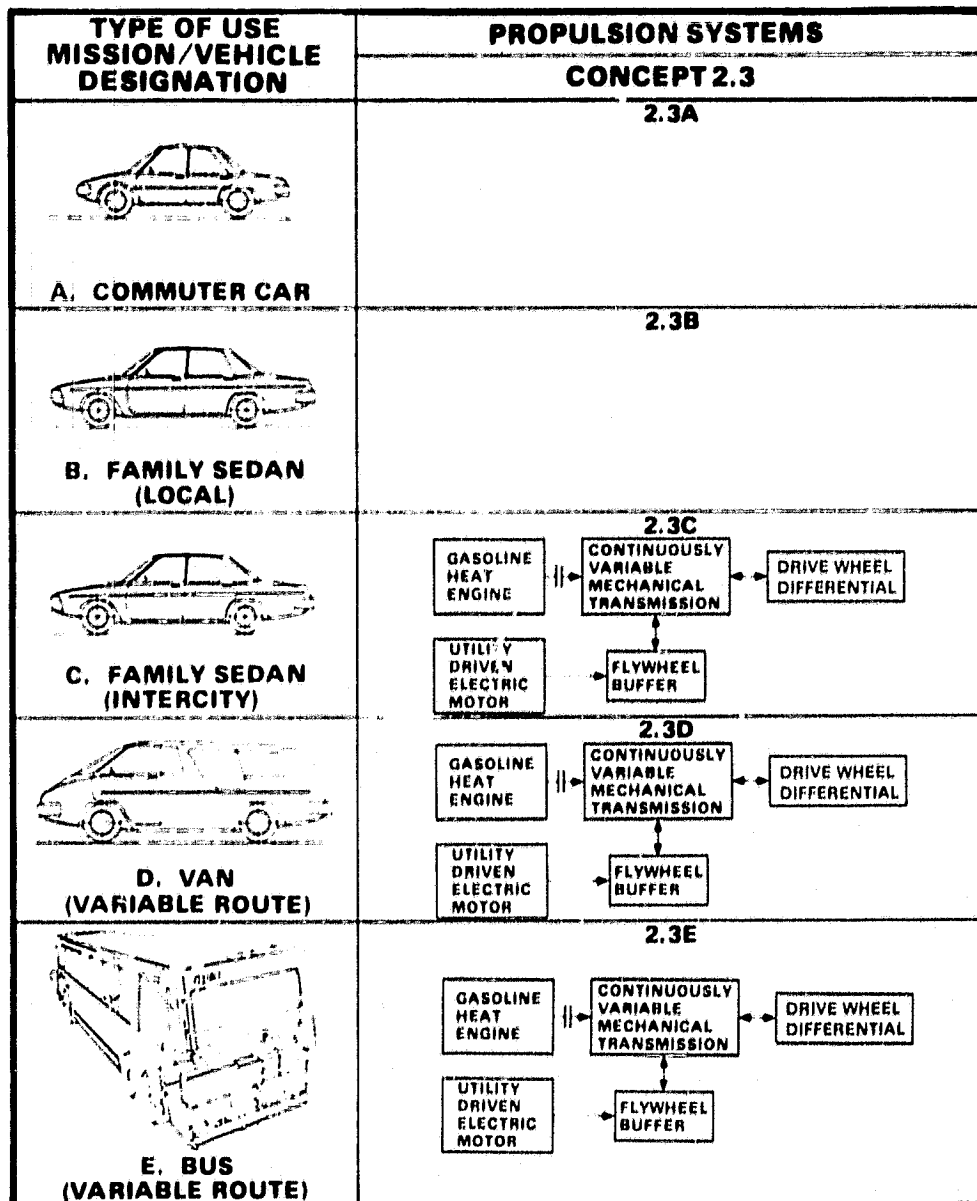
S 45307 .A

Figure B-4.--Hybrid propulsion system concept 2.1
(with mechanical energy storage).



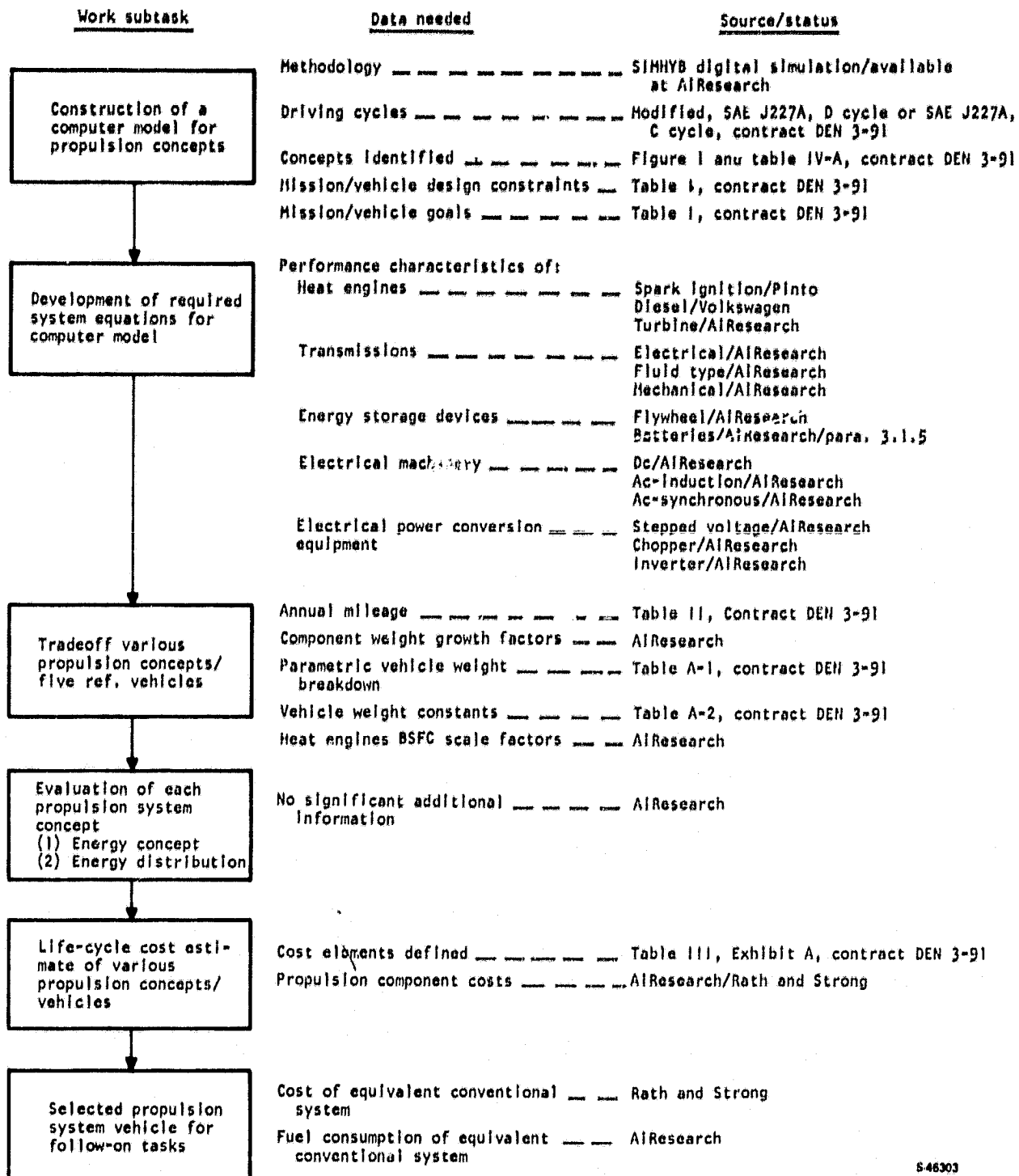
5 45308 A

Figure B-5.--Hybrid propulsion system concept 2.2
(with mechanical energy storage).



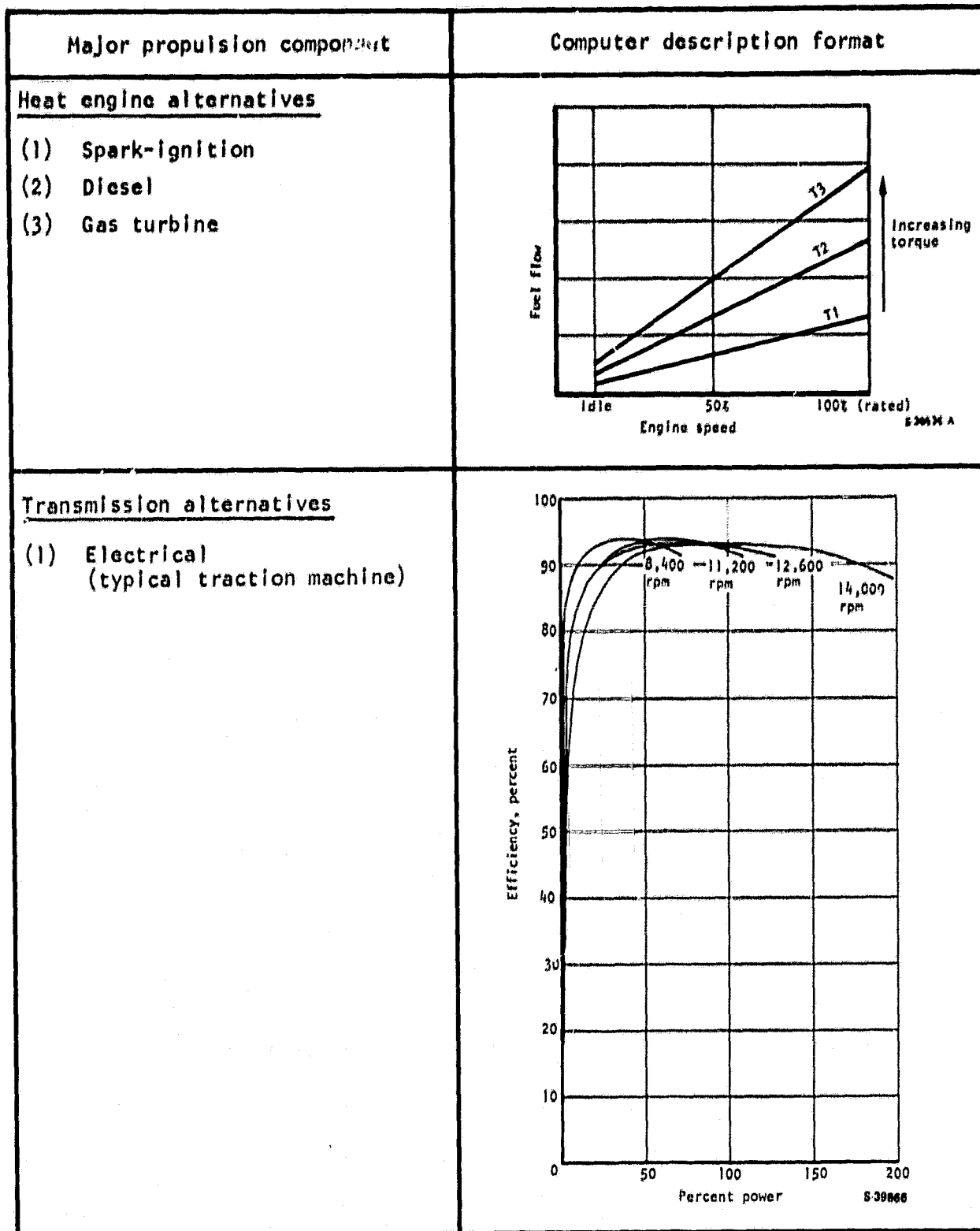
S 46309 A

Figure B-6.--Propulsion system concept 2.3 (with mechanical energy storage and heat engine power).



S-46303

Figure B-7.--Task I flow diagram.



S-46253

Figure B-8.--Computer parameter format for major components.

ORIGINAL PAGE IS
OF POOR QUALITY

Major propulsion component	Computer description format
<p><u>Transmission alternatives</u> (cont'd)</p> <p>(2) Mechanical (CVT)</p>	<p>Efficiency, percent</p> <p>Speed ratio, output/input</p> <p>Percent of rated power</p> <p>5 20840</p>
<p><u>Energy storage alternatives</u></p> <p>(1) Flywheel</p> <p>(2) Battery (lead-acid)</p>	<p>Flywheel module losses</p> <p>Flywheel speed</p> <p>5 20854</p> <p>No-load cell voltage, V</p> <p>Depth of discharge, percent</p> <p>5 20855</p>

Figure B-8.-- (Continued)

546230

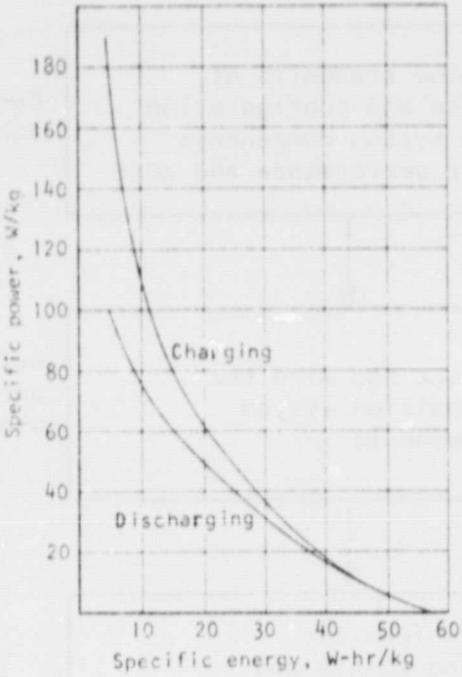
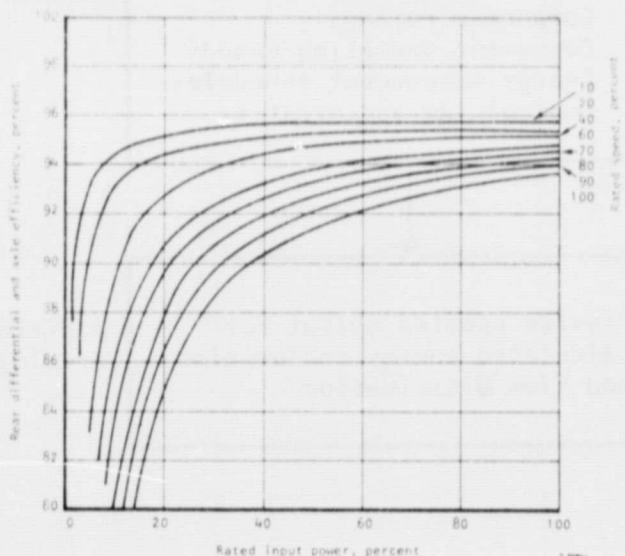
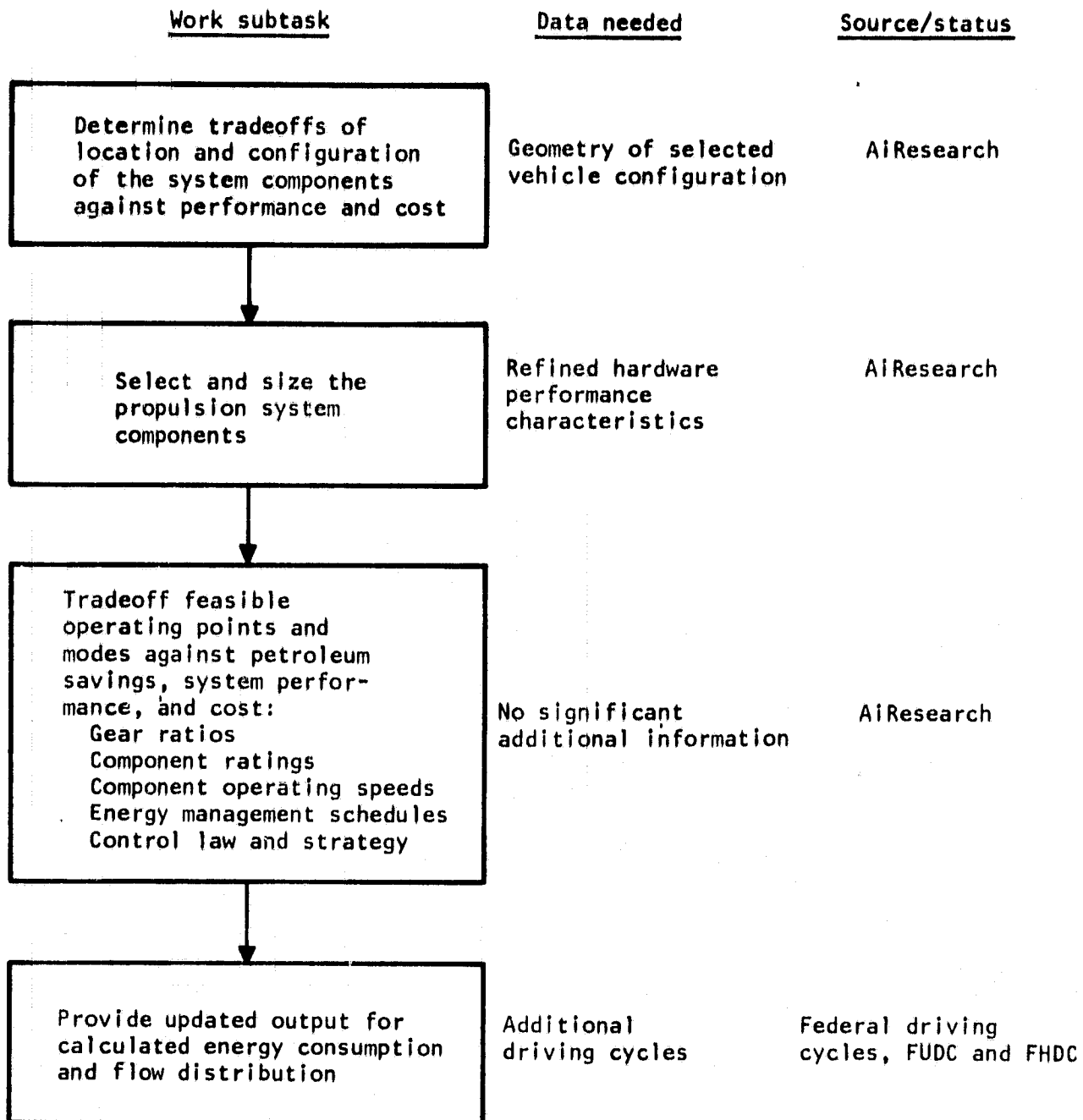
Major propulsion component	Computer description format
<u>Energy storage alternatives</u> (cont'd)	 <p>The graph shows Specific power (W/kg) on the y-axis (0 to 180) and Specific energy (W-hr/kg) on the x-axis (0 to 60). Two curves are shown: 'Charging' and 'Discharging'. The 'Charging' curve starts at approximately (10, 180) and decreases to (60, 0). The 'Discharging' curve starts at approximately (10, 100) and decreases to (60, 0). A small label 'S-46341' is located at the bottom right of the graph area.</p>
<u>Differential and axles</u>	 <p>The graph shows Rear differential and axle efficiency (percent) on the y-axis (80 to 100) and Rated input power (percent) on the x-axis (0 to 100). Multiple curves are shown, each representing a different rated speed. The curves generally show efficiency increasing with input power and then leveling off. A legend on the right side of the graph lists rated speeds: 10, 20, 40, 60, 70, 80, 90, and 100. A small label 'S-46254' is located at the bottom right of the graph area.</p>

Figure B-8.-- (Continued)

ORIGINAL PAGE IS
 OF POOR QUALITY



S46304

Figure B-9.--Task II flow diagram.

Task III, Conceptual Design

A work subtask flow chart for Task III is presented in fig. B-10. The interrelationship between each subtask, the data needed to perform the work, and the source and status of this data is shown. The overall objective of Task III is to describe the selected and optimized concept determined in Tasks I and II in sufficient detail that the selected system can be integrated into the vehicle at the component level.

Task IV, Development Plan

A flow diagram of the development plan of the selected and optimized propulsion system, previously determined and refined in Tasks I, II, and III is presented in fig. B-11. The objective of this task is to determine the cost and workload involved with the development of the selected system.

Task V, DOE Contractor's Coordination Conference

The work involved with program information dissemination and coordination conferences requires AIResearch to make two 15- to 20-min presentations of the program achievements in the Washington D.C. area to both government and industry personnel.

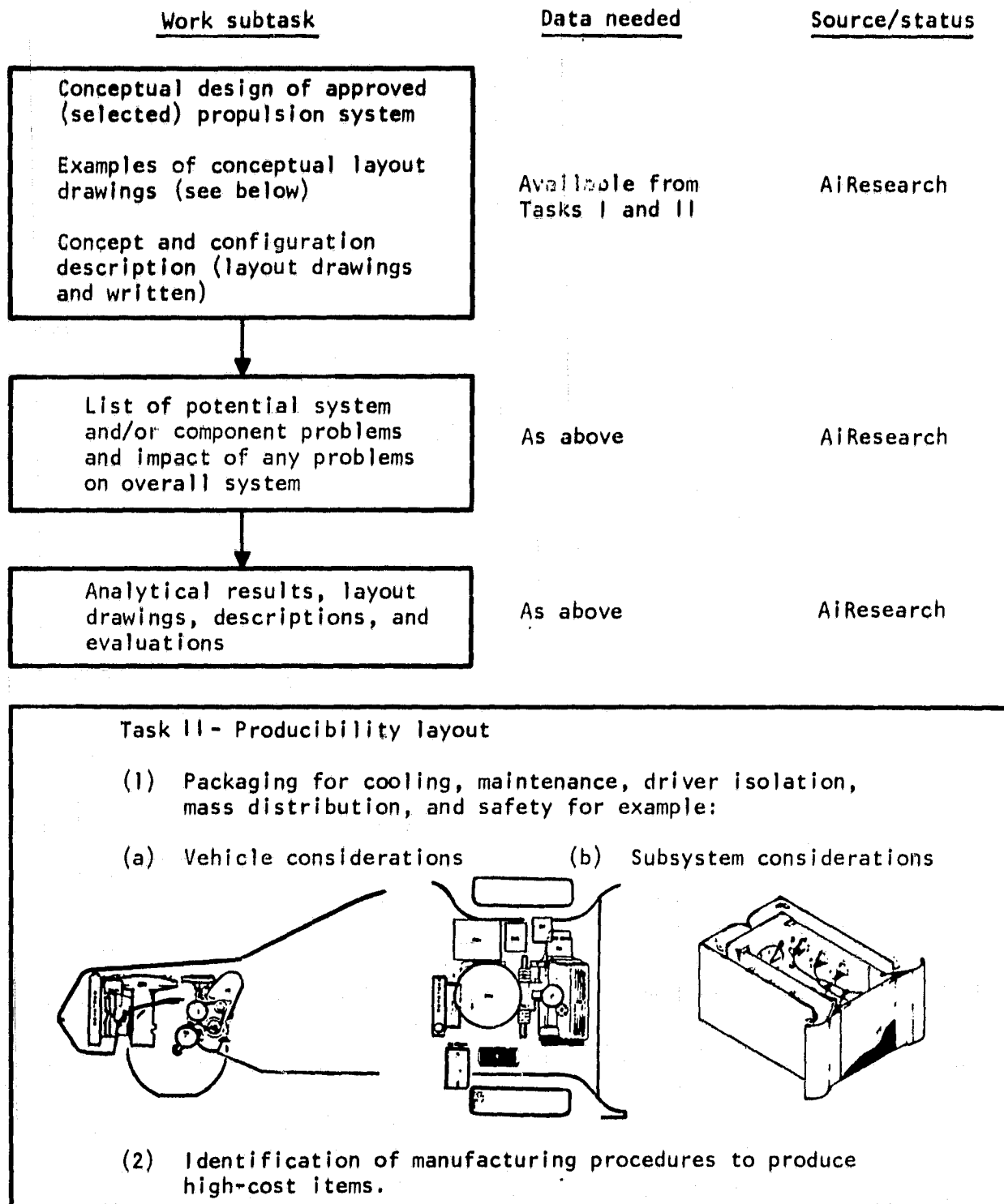
Task VI, Reporting

The following work subtasks constitute the formal reporting processes:

- (1) Monthly progress reports
- (2) Two informal reviews at NASA after completion of Tasks II and IV
- (3) One formal review at NASA that follows completion of Task III and that covers Tasks I, II, and III.

PROGRAM SCHEDULE

The 10-month program schedule shown in fig. B-12 includes amendments agreed to during the course of the work.



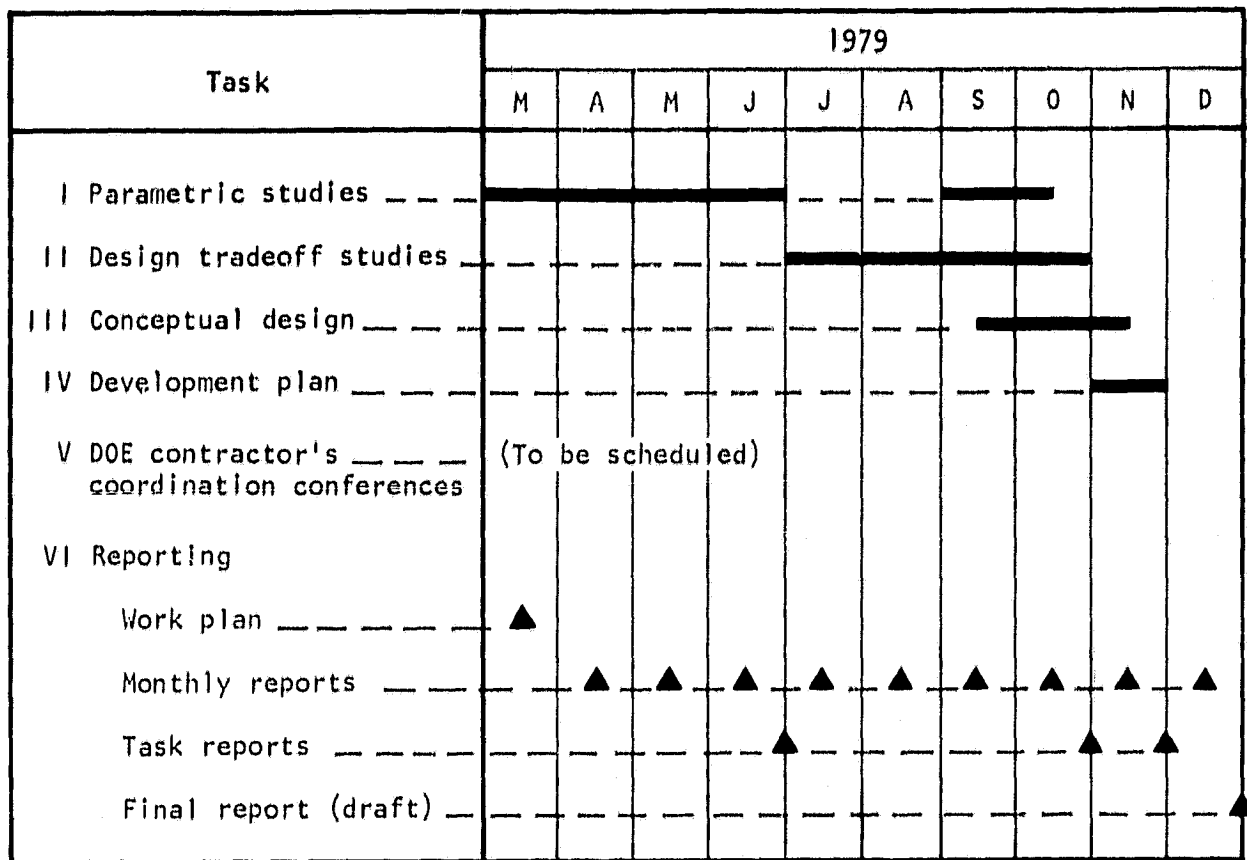
S 36530-A

Figure B-10.--Task III flow diagram.

<u>Work subtask</u>	<u>Data needed</u>	<u>Source/status</u>
<p>Work breakdown structure that includes:</p> <ul style="list-style-type: none"> (1) Tasks requiring major development effort (2) Analysis and design (3) Fabrication and test of a functional model (4) Fabrication and laboratory test of an engineering model of a advanced propulsion system (5) Fabrication and appropriate testing of a test bed vehicle incorporating the propulsion system to verify the integration and driver control of the system 	No significant additional data needed other than already available in Tasks I, II, and III	AIResearch
<p>Schedules, manpower requirements, materials, and facilities required to perform above tasks</p>	As above	AIResearch
<p>Twenty copies of this development plan to the NASA project manager</p>	As above	AIResearch

S-46269

Figure B-11.--Task IV flow diagram.



S 46270

Figure B-12.--Program schedule.

1. Report No. NASA CR-159771		2. Government Accession No.		3. Recipient's Catalog No.	
4. Title and Subtitle ADVANCED PROPULSION SYSTEM CONCEPT, FOR HYBRID VEHICLES				5. Report Date January 1980	
				6. Performing Organization Code 70210	
7. Author(s) L. V. Norrup and A. T. Lintz				8. Performing Organization Report No. 79-16430	
				10. Work Unit No.	
9. Performing Organization Name and Address AiResearch Manufacturing Company of California A Division of The Garrett Corporation 2525 W. 190th Street, Torrance, California 90509				11. Contract or Grant No. DEN 3-91	
				13. Type of Report and Period Covered Contractor Report	
12. Sponsoring Agency Name and Address Department of Energy Electric and Hybrid Vehicle Division Office of Transportation Programs				14. Sponsoring Agency Code DOE/NASA/0091-80/1	
15. Supplementary Notes Final Report. Prepared under interagency agreement EC-77-A-31-1044 Project Manager, F. Stenger, Electric and Hybrid Vehicle Project Office NASA Lewis Research Center, Cleveland, Ohio 44135					
16. Abstract The objective of this study was to evaluate a number of hybrid propulsion systems for application in several different vehicle sizes. A conceptual design was prepared for the most promising configuration. The program was divided into several tasks during which the various system configurations were parametrically evaluated and compared, design tradeoffs performed, and a conceptual design produced. Fifteen vehicle/propulsion system concepts were parametrically evaluated to select two systems and one vehicle for detailed design tradeoff studies. A single hybrid propulsion system concept and vehicle (five-passenger family sedan) were selected for optimization based on the results of the tradeoff studies. The final propulsion system consists of a 65-kW spark-ignition heat engine, a mechanical continuously variable traction transmission, a 20-kW permanent magnet axial-gap traction motor, a variable frequency inverter, a 386-kg lead-acid improved state-of-the-art battery, and a transaxle. The system was configured with a parallel power path between the heat engine and battery. It has two automatic operational modes: electric mode and heat engine mode. Power is always shared between the heat engine and battery during acceleration periods. In both modes, regenerative braking energy is absorbed by the battery. In the electric mode the battery (80% depth of discharge) provides an electric range of 218 km, when it is using petroleum at the rate of 30 km/liter. In the heat engine mode the mileage is 14 km/liter. The propulsion system has a life-cycle cost of \$0.054/km. The vehicle has a test weight of 2032 kg and can accelerate from 0 to 90 km/hr in 12 s. It has a top speed of 105 km/hr and a steady-state hill climbing capability of 90 km/hr on a four percent grade.					
17. Key Words (Suggested by Author(s)) Hybrid vehicle, battery-powered vehicle, hybrid propulsion system, traction motor, CVT			18. Distribution Statement Unclassified -- unlimited STAR category 85 DOE UC - 96		
19. Security Classif. (of this report) Unclassified		20. Security Classif. (of this page) Unclassified		21. No. of Pages 217	22. Price*

* For sale by the National Technical Information Service, Springfield, Virginia 22161